SINCLAIR KNIGHT MERZ

SKM

Australian Government

National Water Commission

NSW GOVERNMENT

Office of Water

Upper Macquarie Groundwater Model

PROJECT REPORT

Final

June 2010

Upper Macquarie Groundwater Model

PROJECT REPORT

Final

June 2010

FUNDING FOR THE PROJECT HAS BEEN PROVIDED BY A NATIONAL WATER COMMISSION GRANT TO THE NSW OFFICE OF WATER UNDER THE RAISING NATIONAL WATER STANDARDS PROGRAMME.

Sinclair Knight Merz
ABN 37 001 024 095
590 Orrong Road, Armadale 3143
PO Box 2500
Malvern VIC 3144 Australia
Tel: +61 3 9248 3100
Fax: +61 3 9248 3364
Web: www.skmconsulting.com

Contents

List of Figures

List of tables

Document history and status

Revision	Date issued	Reviewed by	Approved by	Date approved	Revision type
0	24/3/2010	B Barnett	B Barnett	24/3/2010	
1	3/06/2010	B Barnett	B Barnett	3/06/2010	Calibration revised, scenarios revised
2	15/06/2010	B Barnett	B Barnett	15/06/2010	

Distribution of copies

Revision	Copy no	Quantity	Issued to
0		1	R Brownbill, NOW
1		1	R Brownbill, NOW
2		1	R Brownbill, NOW

Printed:	28 January 2011
Last saved:	28 January 2011 12:20 PM
File name:	I:\VWES2\Projects\VW04680\Deliverables\Upper_Macquarie_Project_report_V3.docx
Author:	Vincent Puech,
Project manager:	Brian Barnett
Name of organisation:	Department of Water and Environment, NSW
Name of project:	Upper Macquarie Groundwater Model
Name of document:	Project Report
Document version:	Final (revision 2)
Project number:	VW04680

Executive Summary

The Upper Macquarie Aquifer is located in a narrow alluvial valley that follows the course of the Macquarie River. The geometry of the aquifer suggests that it is likely to be well connected hydraulically to the river. The Aquifer represents an important source of water for both municipal water supply and for agricultural purposes (predominantly irrigation). Groundwater abstraction has increased steadily in recent years and it is now in the order of 15 GL/year. The largest single abstraction is for the town water supply for the city of Dubbo and this amounts to about 2 to 3 GL/year in recent years. Groundwater levels have been observed to decline in monitoring wells in response to increased levels of abstraction. Observed declines in groundwater level have been most pronounced in the middle and downstream reaches where the largest extractions are located and where the valley is widest.

A three dimensional finite difference groundwater model was constructed in the Groundwater Vistas (version 5.37) modelling package using the USGS MODFLOW 2000 simulation code. The model includes three layers that represent the Upper and Lower Quaternary and deeper Tertiary aquifers. A fourth model layer has been included but this has been inactivated. The extent, shape and thickness of the layers have been defined by stratigraphic interpretations of bore logs and other data undertaken by Ann Smithson of the New South Wales Office of Water. The model stresses are applied using the MODFLOW RIV, EVT, RCH, WEL and GHB packages representing the interaction with the river, evapotranspiration, recharge, groundwater extraction and subsurface exchange of water with surrounding aquifers respectively.

Calibration was undertaken by matching model predicted groundwater levels to observed groundwater level time series data for the period from July 1980 to June 2008. The calibration process was assisted by the automated parameter estimation software PEST version 11 using pilot points and regularisation routines available in the PEST program. A total of 897 parameters (including 853 pilot points) were defined to calibrate the model and the resultant model includes spatial distribution arrays for the hydraulic conductivity and specific yield parameters. The calibrated model provides an effective representation of groundwater levels across the model domain and the scaled residual mean square (SRMS) of 3.4% is considered to be an acceptable calibration statistic.

A series of sixteen predictive scenarios were developed and run. The scenarios combine four different climate assumptions with four extraction regimes. In all cases extraction is assumed to be limited to the existing extraction wells and the rates assigned to each well have been estimated by scaling individual rates to achieve the desired extraction total for the scenario. In most scenarios the assigned extraction rate is not maintained for the duration of the model run as the model predicts substantial localised drawdown at some of the larger extraction well sites which leads to

de-saturation of individual model cells that contain the pumping wells. The principal areas of concern in this regard are in the vicinity of the Dubbo city water supply wells. The results suggest that with the current distribution of extraction wells the maximum possible extraction rate from the aquifer is likely to be about 15 GL/year. This outcome does not necessarily reflect the maximum sustainable yield of the aquifer since the model results are heavily influenced by the distribution of extraction wells assumed for the scenarios. A redistribution of extraction wells away from the existing Dubbo borefield would likely achieve a greater level of extraction.

The drying of model cells to the base of the aquifer is a modelling artefact and this situation would not arise in reality. However the fact that parts of the model are completed de-saturated in some of the predictive scenario runs indicates that the particular scenario is unsustainable and that at least partial de-saturation of the productive aquifers would occur at these locations in reality.

Future climate assumptions have little or no impact on the predicted groundwater responses to future extraction scenarios.

1. Introduction

1.1. Main Objectives

The Macquarie River is a typical westward flowing New South Wales river in the Murray Darling Basin with headwaters that lie in the Great Dividing Range. Average annual rainfall decreases toward the west and the upper catchment in the east produces the majority of the effective runoff. In the upper catchment the river flows through a narrow valley that does not have a well defined flood plain. Downstream of Wellington, the valley broadens and flattens allowing for irrigation development of agricultural land on the alluvial plains. A location map showing the surface extent of alluvial sediments (GMA boundary) is shown in Figure 1.

Irrigation development on the plains commenced on a large scale in 1965 following the construction of Burrendong Dam. River regulation provided by the dam allows for consistent year round flows and provides a level of protection against flooding.

Over the past 20 to 30 years irrigation activity in the Upper Macquarie valley, that part of the floodplain between Burrendong Dam (located about 20km upstream of Wellington) and Narromine, has fluctuated greatly in terms of net water use. Groundwater allocations have steadily risen over the period and it is likely that groundwater usage has, on average, followed this trend. Apart from irrigators, the Dubbo City Council remains a dominant water user of groundwater and river water for town water supply.

In an attempt to better understand and quantify the groundwater resource in this area and its interactions with the Macquarie River the New South Wales Office of Water commissioned Sinclair Knight Merz (SKM) to construct a numerical groundwater flow model of the Upper Macquarie Groundwater Management Area.

This report describes the construction and calibration of a MODFLOW groundwater flow model of the alluvial aquifers of the Upper Macquarie valley and its use as a predictive water resource management tool. It includes a detailed description of the hydrogeological conceptualisation on which the model is based and describes a series of 16 predictive model scenario runs. The 16 scenarios are a combination of 4 climatic scenarios (historic, dry, medium and wet) and four groundwater abstraction scenarios (no pumping, current development, maximum current development and full current entitlement). Scenarios were designed to assess groundwater responses to the applied extraction stresses within the next 50 years.

■ Figure 1 Location Map Showing the GMA Boundary

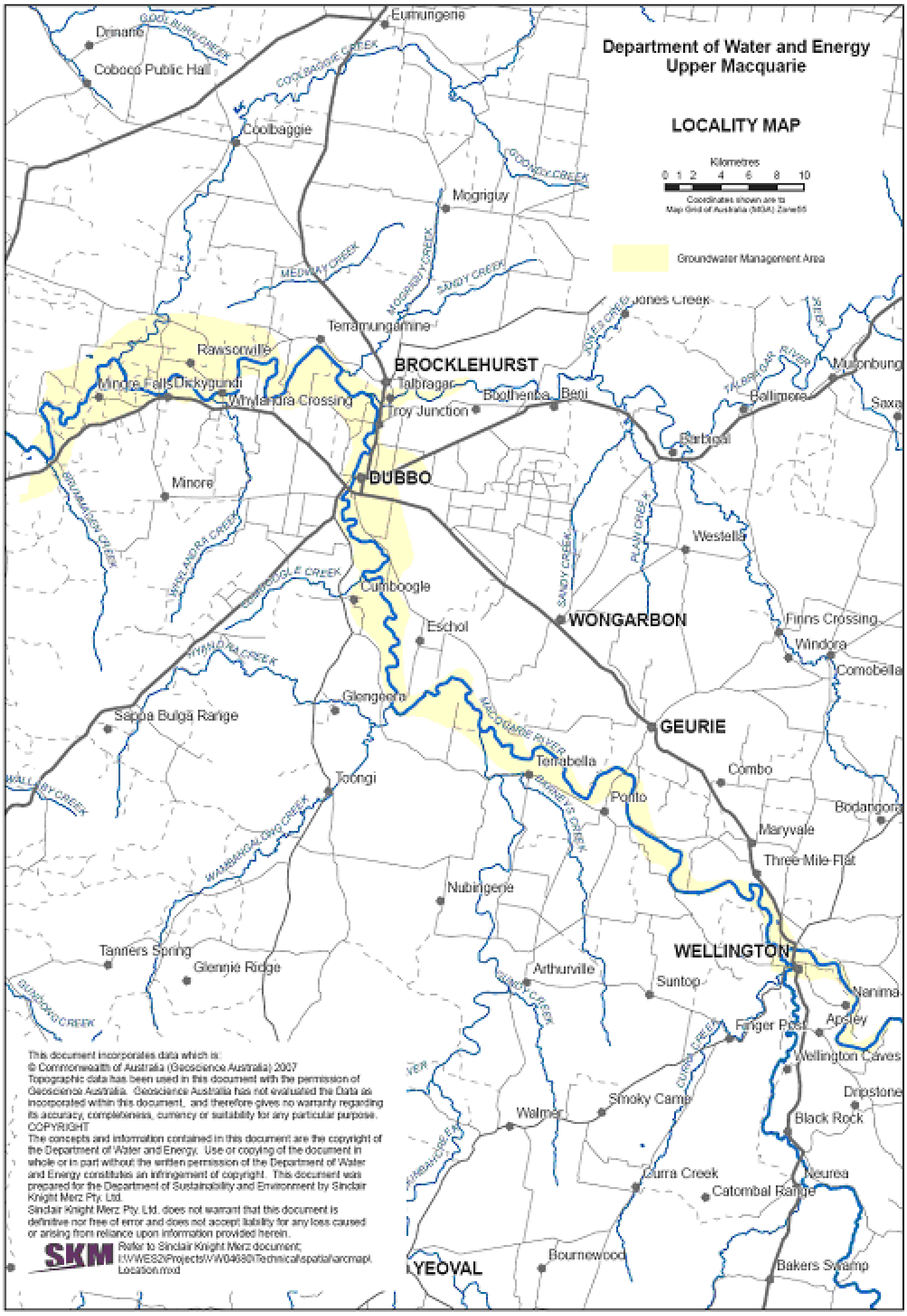

2. Description of Model Area

2.1. Physiography and Topography

The Upper Macquarie River valley is a relatively narrow alluvial filled valley surrounded by basement rocks that rise to levels in excess of 500 mAHD (some 250 m above the valley floor). The Macquarie River generally flows from south-east to north-west across the proposed model domain. It is regulated by the operation of Burrendong Dam which lies immediately upstream of the Upper Macquarie Groundwater Management Area (GMA). The river valley is relatively narrow and constrained in the region upstream of Wellington. Here the river flats are generally confined to narrow strips of alluvial material that follow the present-day course of the river.

The Bell River joins the Macquarie River from the South at Wellington. The Macquarie continues in a north-westerly direction and the river begins to meander through the gradually widening valley, in places up to several kilometres wide.

A few kilometres north of the city of Dubbo the Macquarie is joined by the Talbragar River where the river turns west and flows toward Narromine.

Within the study area the valley floor falls from about 275 mAHD at the upstream extremity of the GMA to an elevation of about 230 mAHD at the downstream limit of the study area. A topographic map of the study area is provided in Figure 2.

Figure 2. Topographical image of the Upper Macquarie River and surrounds

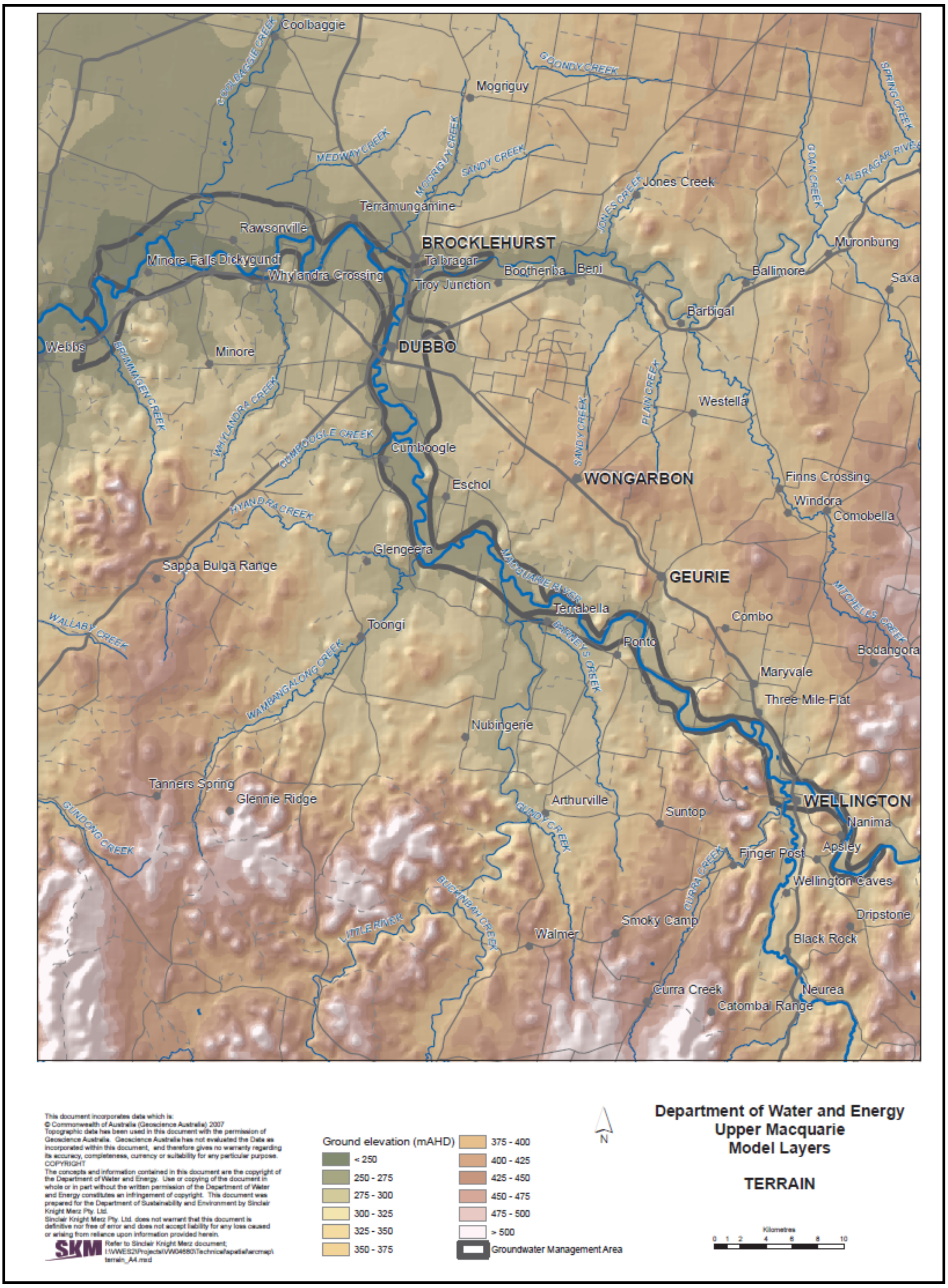

2.2. Climate

Climate data was sourced from the Bureau of Meteorology (BoM). Three weather stations were identified within the Upper Macquarie GMA (these are listed in Table 1). The Dubbo Airport and Wellington (Agroplow) stations provide long term climate observations whilst the Darling St. Station in Dubbo has been operational since 1994 and has proved useful in infilling missing data from the Airport station post 2000. Prior to 2000 the Dubbo Airport weather station is considered to provide a long record of accurate rainfall data (quality checked by BoM). The third station located at Wellington has very similar records to the Dubbo stations, as evidenced from the mean and standard deviation of records between 1900 and 1999 (refer to Table 1). In light of these observations the Dubbo Airport climate station was chosen for use across the entire Upper Macquarie GMA.

- **Table 1 Bureau of Meteorology climate stations within the Upper Macquarie GMA**

Station ID	Name	From	To	Mean Rainfall (1900-1999) (mm/month)	St. Dev Rainfall (1900-1999) (mm/month)
065012	Dubbo (Darling St)	Sep-1994	Present	na	na
065070	Dubbo (Airport)	Oct-1870	Present **	49.0	42.7
065034	Wellington (Agroplow)	Nov-1881	Present	51.4	43.2

***There are a large number of missing entries from Jan 2000 to present in station 065070. These were infilled by regression with 065012. Correlation between these two stations was found to be high with an R^2 value equal to 0.96.*

2.2.1. Rainfall

The Upper Macquarie GMA receives moderate rainfall with a long term average of 583 mm/yr (1871 to 2008) (refer to Figure 3). Through the period of record there have been a number of drier and wetter periods however the plot of cumulative residuals from the mean (Figure 4) indicates two key features. The first feature is an extended period of below average rainfall between 1895 and 1945. This was immediately followed by approximately 30 years of above average rainfall.

Since 2000 there has been a clear trend of below average rainfall. This is in line with much of South-East Australia and the southern parts of the Murray Darling Basin which have experienced drought conditions for the last decade. Prior to this period, between 1970 and 2000, measured rainfall remained reasonably close to the long term mean.

It is noted, that when viewed in a long-term historical sense, the rainfall pattern of the past decade does not seem extraordinary. However, climate science is in general agreement that the future climate in this area is likely to be warmer and drier than the historic average (CSIRO, 2007).

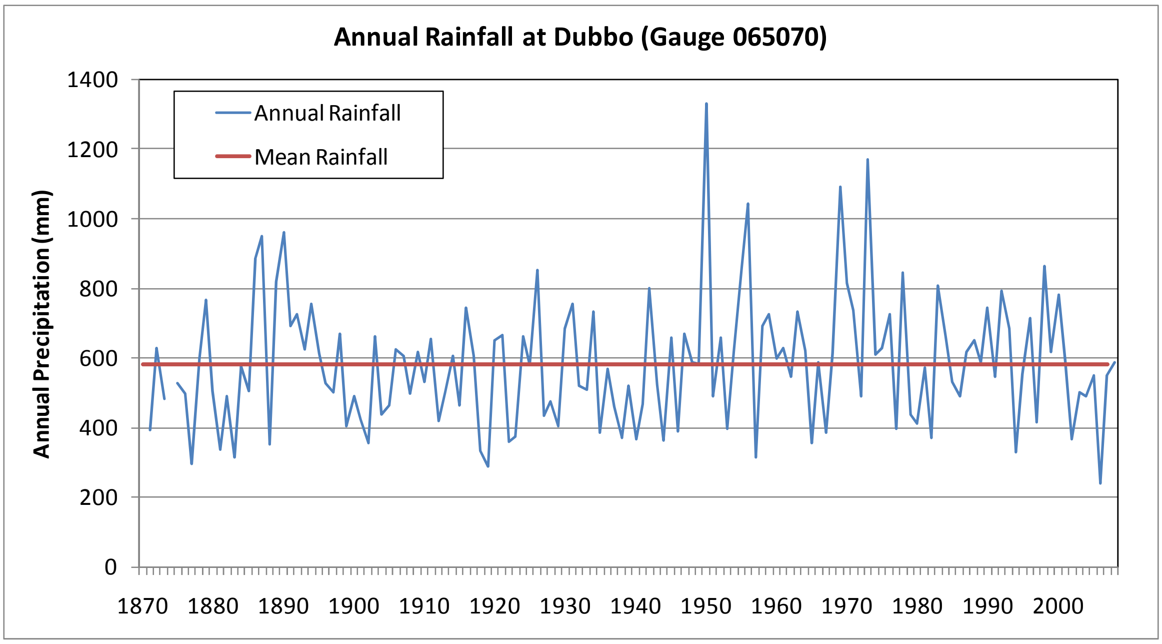

Figure 3 Annual rainfall at Dubbo (as recorded at BoM rain gauge 065012)

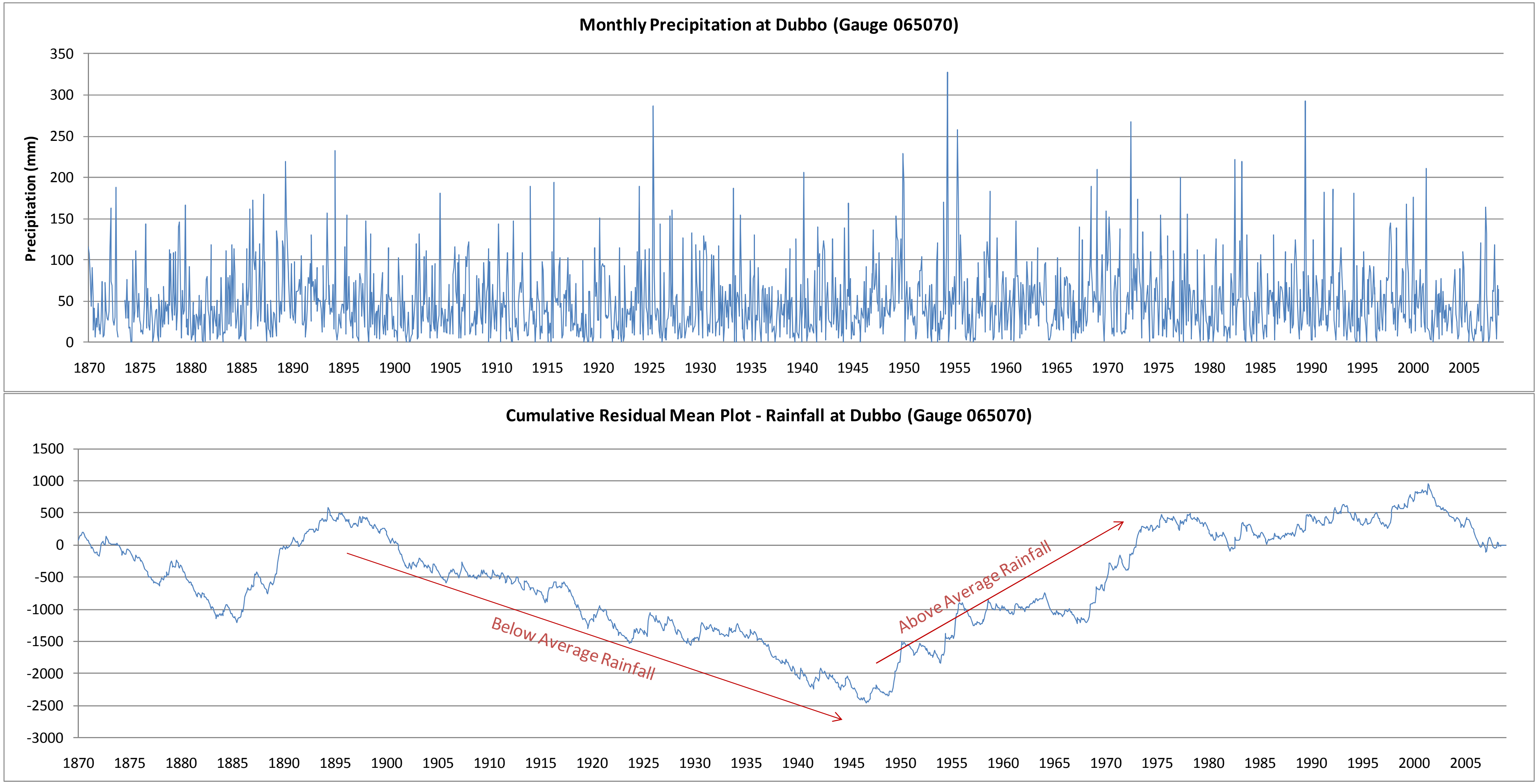

- **Figure 4 – Top, monthly precipitation recorded at Dubbo; Below, cumulative residuals from the mean for rainfall at Dubbo**

2.2.2. Evaporation

The only measured evaporation data available in the Upper Macquarie GMA are from site 065034 in Wellington. The seasonal pattern of evaporation is typical for the climate of South-Eastern Australia with generally hot-dry summers with high evaporation and cool-wet winters with low evaporation (Figure 5).

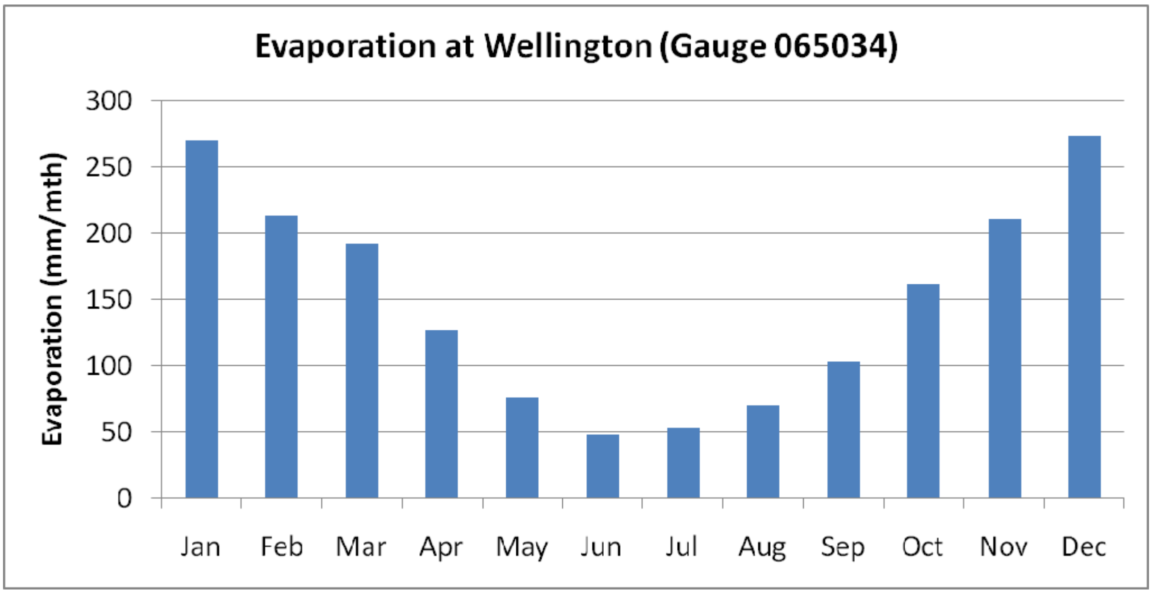

- **Figure 5 Average monthly pan evaporation as measured at Wellington**

2.3. Geology

The Upper Macquarie Alluvium GMA is defined by the distribution of high yielding unconsolidated alluvium associated with the Macquarie River between Wellington and Narromine. The alluvium represents sediments of Cainozoic age that have backfilled a riverine valley cut into the older landscape of the area. The Macquarie River transits three main geological provinces across the GMA area – these form the boundaries to the GMA:

1. The early to mid Palaeozoic rocks of the Lachlan Fold Belt (Great Dividing Range) upstream of Wellington;
2. Consolidated sediments of the late Palaeozoic to Mesozoic Gunnedah Basin, represented predominantly by the Triassic Napperby Formation; and
3. Sediments of the Mesozoic Surat Basin, represented by the Jurassic Pilliga Sandstone.

SKM

The unconsolidated sediments of the GMA are comprised of poorly sorted materials varying from gravel to clay and exhibiting substantial spatial variability. Generally, three main Cainozoic layers have been recognised, though their boundaries are sometimes hard to distinguish. A basal unit of quartzose sand and gravel with minor finer grained silt and clay. This is generally overlain by a layer of mottled polymictic gravel, sand, silt and clay. These are in turn overlain by a layer of finer grained silt and clay, usually about 5 to 15 metres thick. The upper fine grained unit increases in thickness with distance downstream within the GMA.

The Macquarie River meanders across the floodplain and has eroded a number of terraces reflecting recent changes in climate. This fluvial activity has caused the river to incise through the upper fine grained unit in places.

The geological description of the various layers is consistent with those for the Lachlan and Cowra Formations (identified in the Lachlan Valley to the south) and the Gunnedah and Narrabri Formations (identified in the Namoi Valley to the north).

At the western or downstream end of the GMA, palynology of the sediments underneath the Cainozoic alluvium indicates a Triassic age. This suggests that the incised valley has cut through the sediments of the Surat Basin.

2.4. Surface Hydrology

2.4.1. Gauging Stations & Weirs

There are four streamflow gauges on the Upper Macquarie River within the GMA. An additional two gauges are located on major tributaries (Talbragar River and Coolbaggie Creek). Figure 6 illustrates the location of these gauges. Table 2 provides location information for these gauges and additional gauges located upstream and downstream of the GMA. This data was sourced from the PINEENA database and was verified and updated with data from the HYDSYS database.

Flows in the Upper Macquarie are regulated to a large degree by releases from Burrendong Dam. However flows are also picked up from numerous tributaries. In addition there are also direct river diversions together with near stream groundwater pumping that both impact on river flows.

Hydrographs of river levels as recorded at the gauges are presented in Figure 7. The long-term hydrograph from downstream Burrendong Dam (421040) highlights a period of below average river levels since approximately 2002.

There is one weir located within the model domain at Dubbo and another immediately downstream of the model at Narromine. Both of these weirs were surveyed as part of this project and the results

SKM

have been incorporated into Table 2. The Dubbo weir is located approximately 6 km downstream of the Dubbo stream gauge, on the northern edge of the city.

Table 2 Gauging stations within the study area

Gauge ID	Gauge Name	Easting	Northing	Gauge Zero	Gauge Datum
421040	MACQUARIE RIVER AT D/S BURRENDONG DAM	695226	6387462	290.596	WCD
421003	MACQUARIE RIVER AT WELLINGTON	682506	6397922	278.584	AHD
421900	MACQUARIE RIVER AT WOLLOMBI (GEURIE)	659816	6413340	272.95*	AHD
421001	MACQUARIE RIVER AT DUBBO	650908	6428376	251.845	AHD
	Dubbo Weir	*650340*	*6428500*	*249.60***	*AHD*
421123	TALBRAGAR RIVER AT TALBRAGAR	*653387*	*6436685*	*NA*	*NA*
421055	COOLBAGGIE CREEK AT RAWSONVILLE	*637329*	*6442827*		
421127	MACQUARIE RIVER AT BAROONA	629651	6435306	231.726	AHD
421006	MACQUARIE RIVER AT NARROMINE	616803	6434585	235.839	AHD
	Narromine Weir	*625513*	*6434732*	*226.29***	*AHD*

*C-type benchmark surveyed prior to this project

** Weir crest elevation

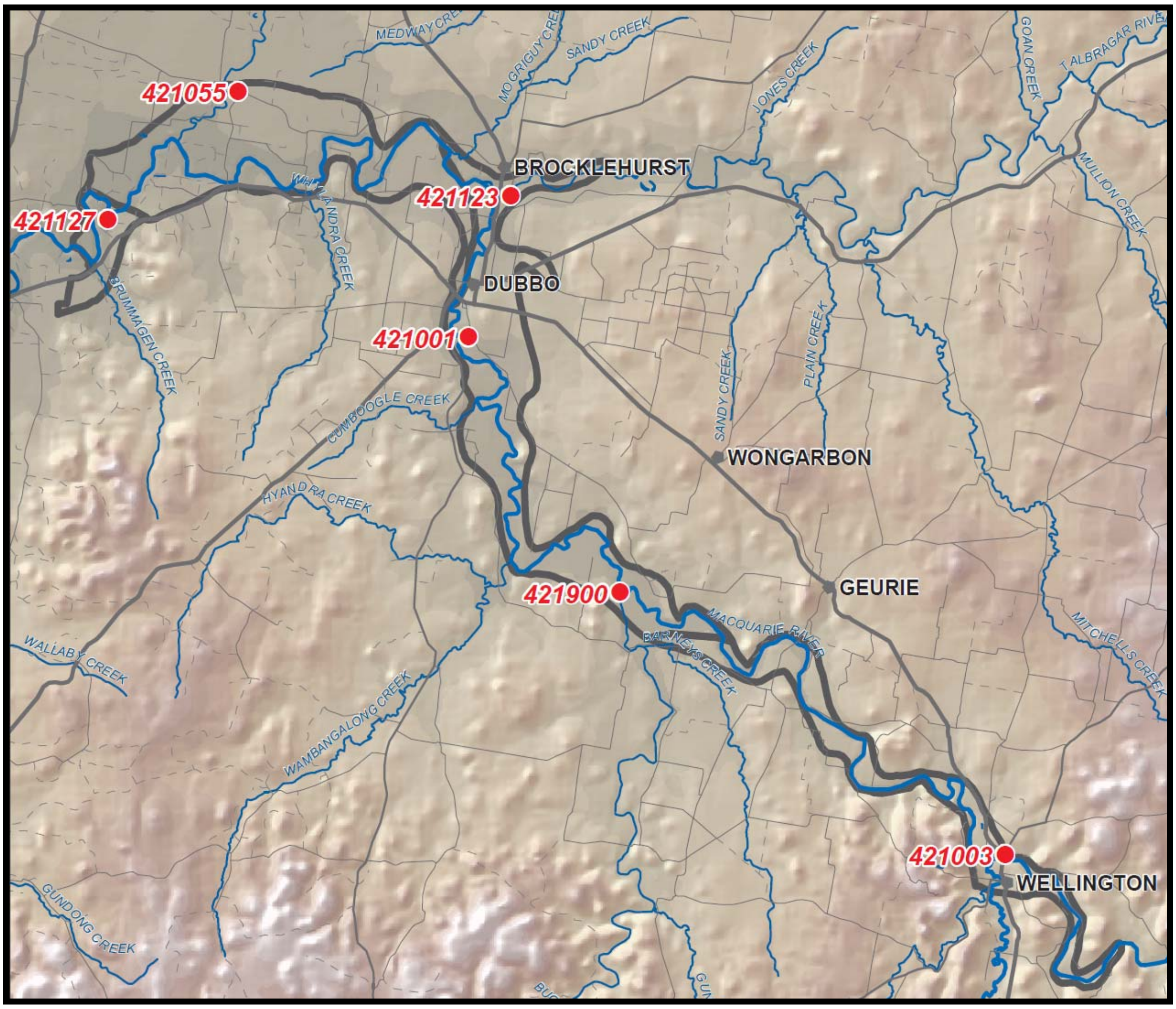

- **Figure 6. Map of key gauging stations within the study area**

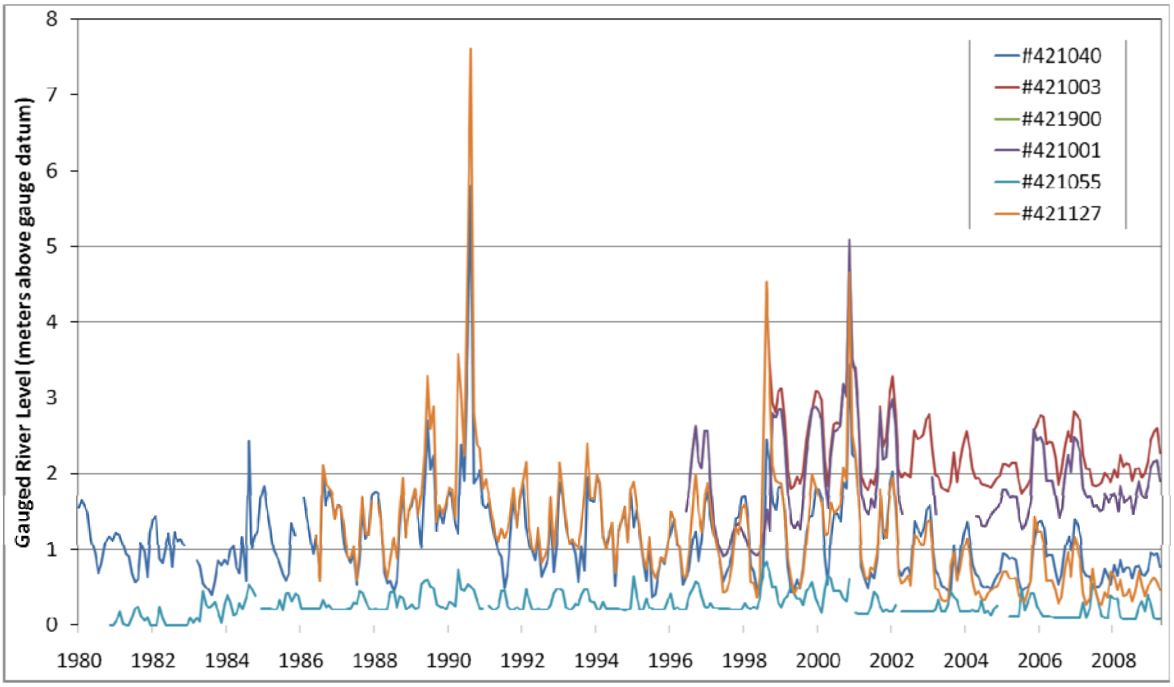

▪ **Figure 7. Hydrographs of river levels since 1980 in the Upper Macquarie**

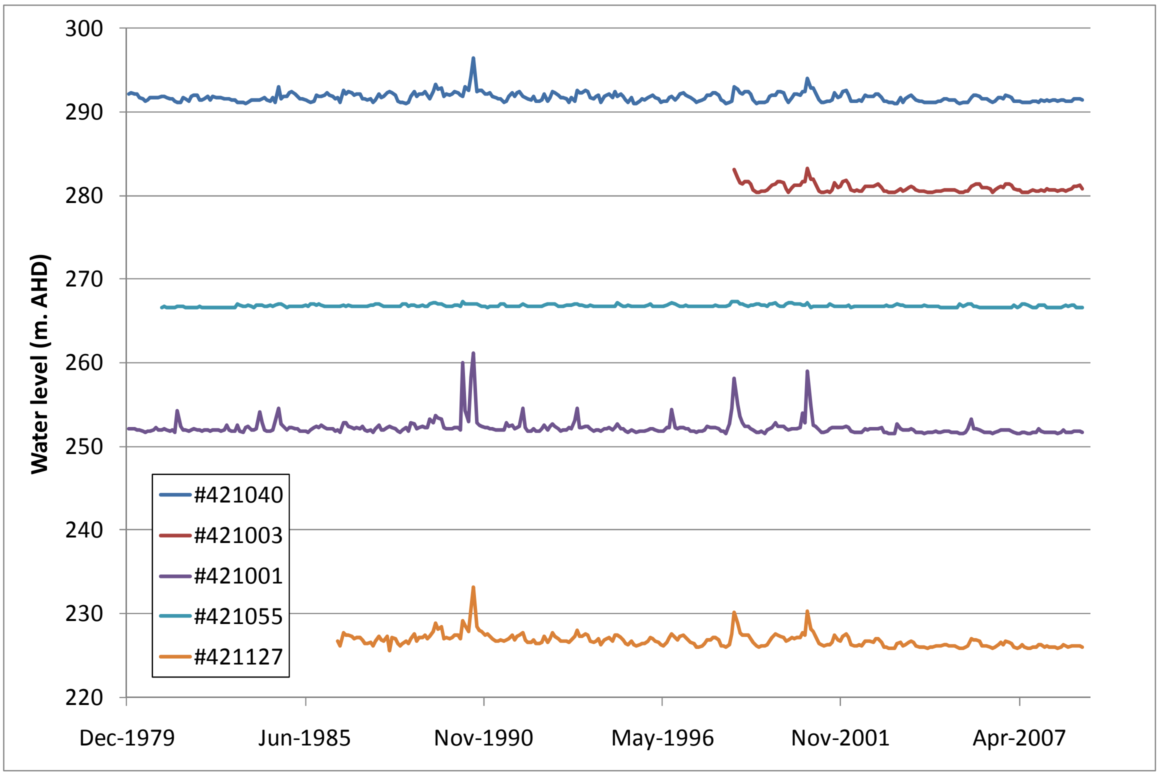

- **Figure 8. River levels at the Upper Macquarie's river gauges.**

2.4.2. IQQM River Model

There are three river gauges included in the existing IQQM model of the Upper Macquarie River as follows:

Macquarie River at Dubbo (421001)

Macquarie River at Baroona (421127)

Macquarie River at Narromine (421106)

These three gauges form the basis for defining reaches within the groundwater model that then report groundwater/surface water fluxes to the IQQM model.

2.4.3. Flooding

Across the Murray-Darling Basin, rainfall is distributed nearly uniformly across the year with a slight tendency towards higher falls from June to August. As a result there is no clearly defined flooding season. It is also recognised that flooding patterns have been significantly altered since the construction of Burrendong Dam in 1965.

Burrendong Dam was constructed with a conservation storage of 1,190 GL with an additional 490 GL of available storage for active flood retention. As a result the frequency of flooding has changed since 1965. Although the river is now highly regulated the history of flooding since regulation is reasonably well defined and provides a reasonable data set for defining appropriate model inputs to capture the groundwater impacts of flood inundation.

A further complicating factor is the various tributaries which can impact significantly on the spatial distribution of flooding across the valley. For example, SKM (1984) reports that major flooding occurred in 1955 during which time the flood waters were comparatively well confined in the area around Dubbo. However, five kilometres downstream where the Talbragar River enters, there was extensive over-bank flooding and associated inundation over a region up to 6 km wide.

The extent of flooding downstream of Burrendong Dam to Geurie is typically limited by the steeply rising valley floor. SKM (1984) reports that most flood events actually stay within the river channel and only three floods have been recorded to have broken over the banks, in 1926, 1955 and 1956. Downstream from Geurie the river valley is less steeply incised and over-bank flows are more common. In major flooding events, such as 1955, almost the entire GMA was inundated. A notable exception to this is the city of Dubbo where.only the western margins of the city were inundated.

In more recent years, significant floods were recorded on the Macquarie River in 1986 and in 1990. Many groundwater hydrographs, particularly upstream of Dubbo, exhibit a significant spike in water levels that coincide with the 1990 flooding event that suggests that this event resulted in substantial recharge to the aquifer.

2.5. Land use

Land in the Upper Macquarie GMA is primarily used for irrigated crops and pasture as well as non-irrigated winter cropping and dryland grazing. Above Wellington the confined valley is used predominantly for dryland grazing. The principal crops are sorghum, soybeans, sunflower and lucerne. Vegetables are grown on the river flats near Dubbo.

Figure 9 displays landsat imagery for the Upper Macquarie GMA. The landsat image can be used to infer landuse classes. In particular the irrigated areas show up as intense green whilst the urban area surrounding Dubbo also stands out as an area with increased vegetation compared to its general surroundings. In the model domain, irrigated zones cover an area of approximately 30 km^2. The landsat image dates from 2002, and is assumed to be representative of landuse during the calibration (1980-2008) and predictive model periods (2010 – 2060). In other words, no landuse change is allowed for in the model.

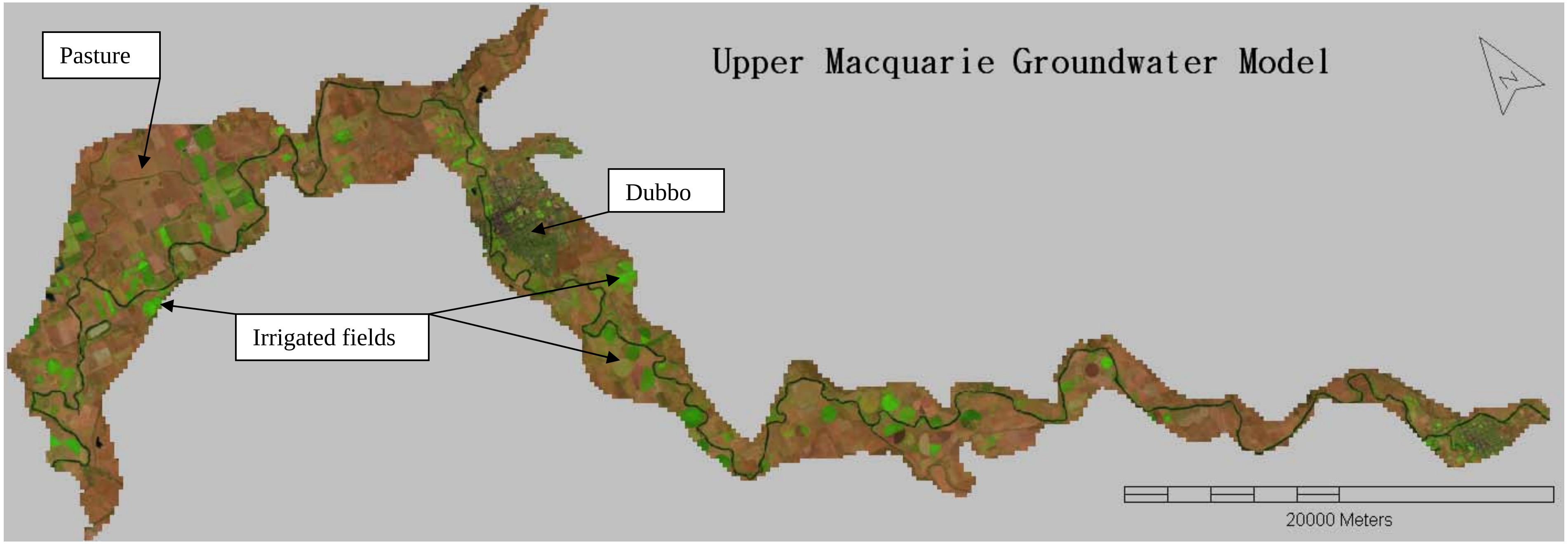

■ **Figure 9. Landsat imagery within the Upper Macquarie GMA. The map is presented in model coordinates (cf. Figure 20).**

2.6. Water Use

Both direct river diversions and groundwater abstractions occur in the Upper Macquarie. Water usage is primarily for irrigation but there are also lesser volumes used for commercial, municipal water supply and stock and domestic uses.

Figure 10 displays the available records of water usage and entitlements within the Upper Macquarie GMA. Surface water data is based on diversions from the river between Burrendong Dam and Narromine and is derived from various records and sources (*pers. comm*. Don Mampitiya, NOW, 29/07/2009). Surface water usage data is not a direct model input however it is used to estimate irrigation application volumes (refer to Section 3.6.2).

Groundwater usage has been metered since 1995/96 and the metered records are provided in Figure 10. Prior to this time there are no records of actual groundwater usage, however the usage volumes are considered to be relatively minor and therefore no groundwater usage prior to 1995 is included in the model (except for Dubbo city water supply)

Figure 11 displays the recorded water usage by the Dubbo City Council for the town water supply (both surface and groundwater) along with the respective entitlement volumes. This graph suggests that Dubbo City Council groundwater extraction has tended to decrease over the past 30 years. In contrast, there has been a definite increase in river water diversions, especially since 1999/2000 when diversions increased significantly to near the allocation limit of 8700 ML/yr. Figure 12 presents pie charts highlighting the proportion of water usage within the GMA for the Dubbo city water supply.

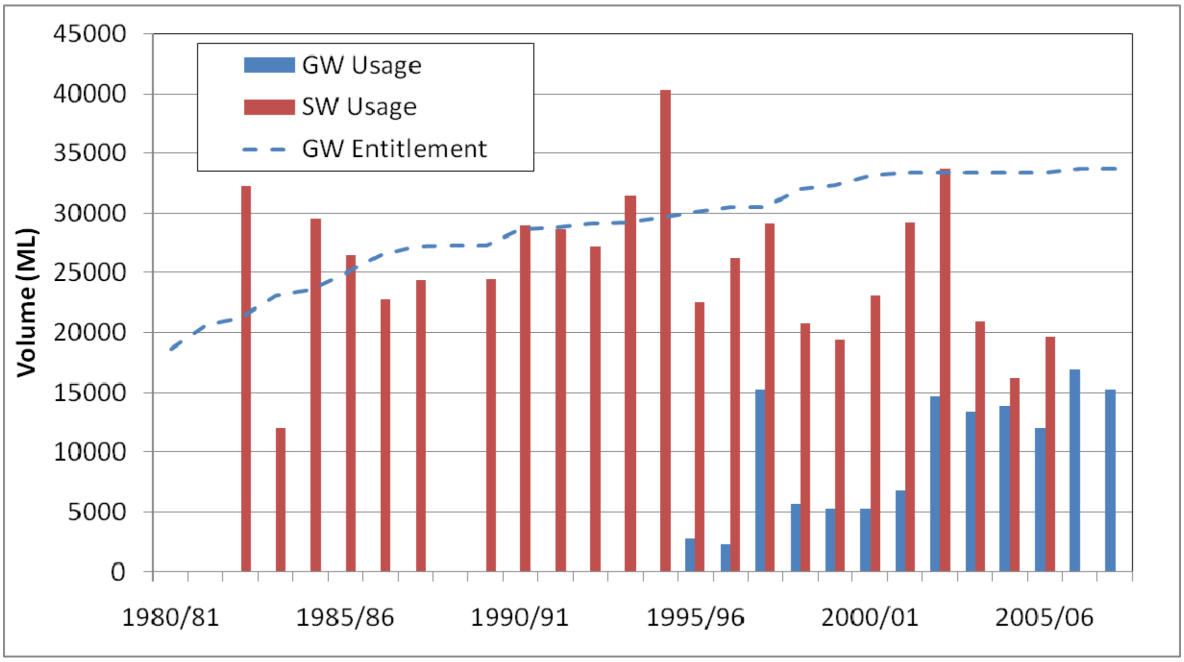

▪ **Figure 10. Recorded water usage within the Upper Macquarie GMA (ML/year)**

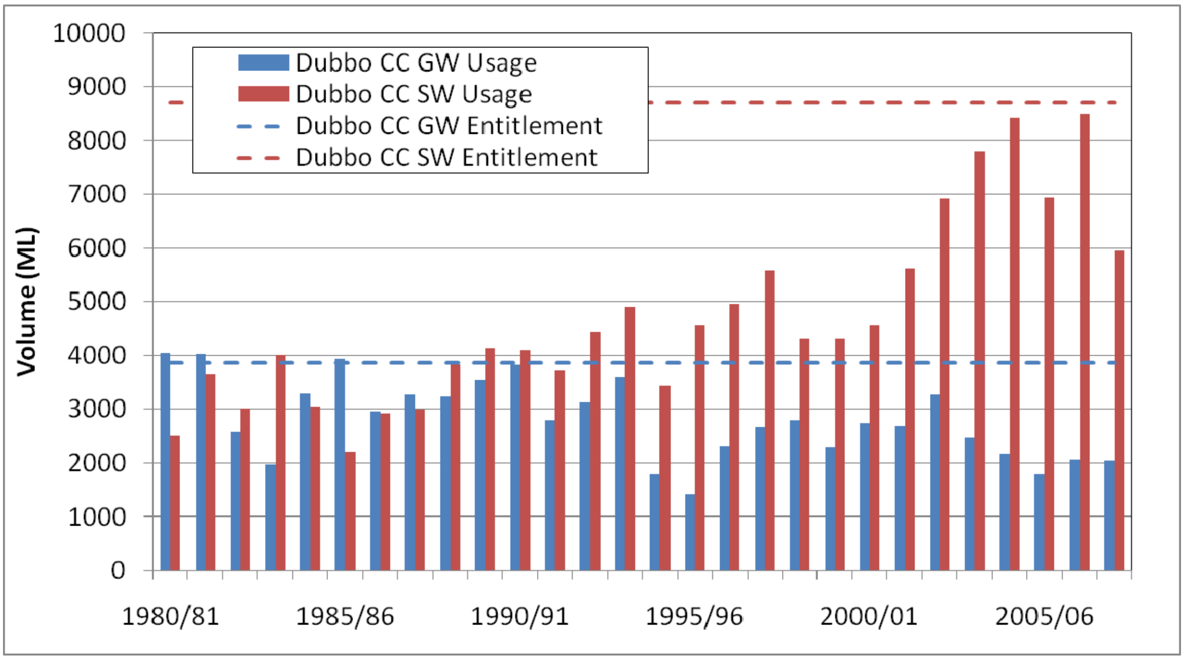

▪ **Figure 11. Recorded water usage for the Dubbo city water supply (ML/year)**

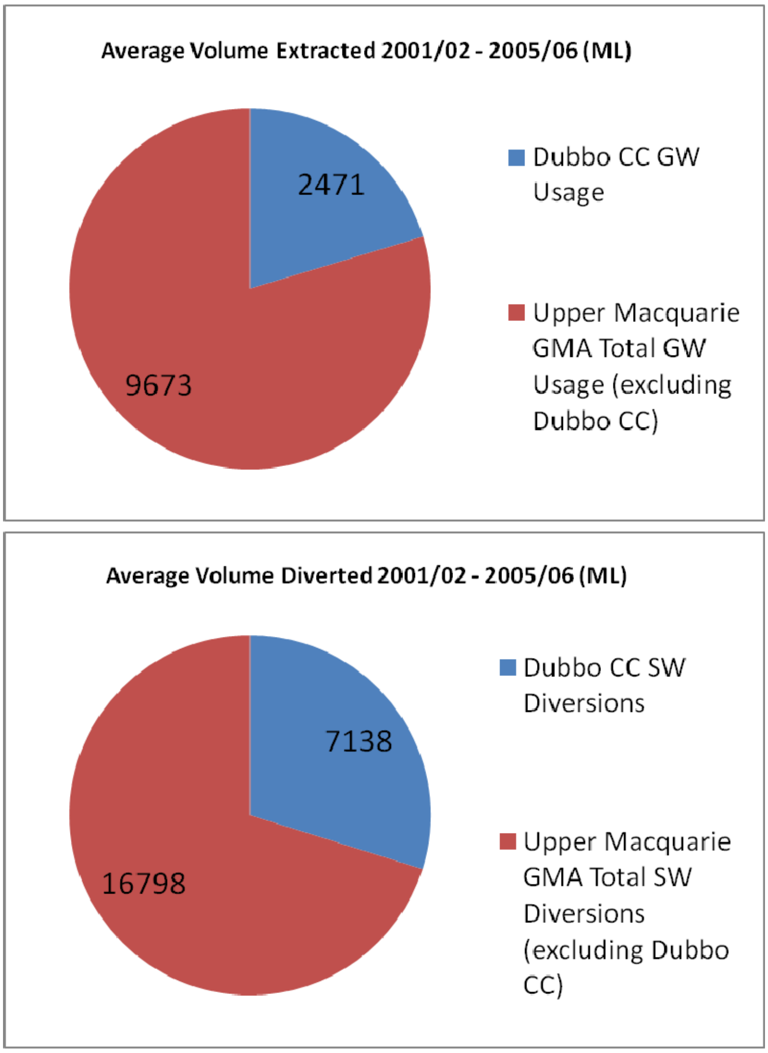

Figure 12. Pie charts showing the proportion of water used by the Dubbo City Council for town water supply.

2.7. Hydrogeology

The GMA has been subdivided into two main aquifers – a basal coarser Lower Aquifer (of Tertiary Age), overlain by a finer grained Quaternary Aquifer. The Lower Aquifer is generally more uniform in its grain size distribution, relative to the Upper Aquifer, though it is common for large lenses of clay to be present. The upper aquifer is more heterogeneous in its grain size distribution and its aquifer properties are quite variable (NOW, 2009).

The upper fine grained layer identified in bore logs represents the topmost part of the upper aquifer.

The Lower Aquifer is in contact with the underlying Napperby Formation along its entire length. Both Lower and Upper Aquifers lie laterally adjacent to the Pilliga Sandstone in the areas around Dubbo and further downstream. For present modelling purposes the Napperby Formation and the Pilliga Sandstone are assumed to be inactive.

There is a large number of groundwater monitoring bores within the Upper Macquarie GMA. These include a number of nested sites monitoring groundwater levels in both the upper and lower aquifers. Figure 13 presents a map showing the location of available monitoring bores in the GMA.

The groundwater system is typical of an alluvial valley. The groundwater in general flows towards the valley centre from the sides and down-gradient with the flow of the river.

Hydrographs for a selection of monitoring bores (many of which are nested) are presented in Figure 14 to Figure 16. The locations of the bores included in Figure 14 to Figure 16 are shown in Figure 13. Some of the key features of water level trends are summarised below:

- Many hydrographs, particularly upstream of Dubbo, include a spike in water levels in 1990. This is coincident with a flooding event that occurred in July-August 1990.

- Downstream of Dubbo, the peak in water levels in 1990 generally was not observed, however there was a significant but gradual increase in groundwater levels throughout 1990/91. This is likely to relate to the movement of water down the alluvial valley as the system returns to an equilibrium state.

All hydrographs indicate a declining trend in groundwater levels since approximately 2002.

Inspection of the water level trends over time as reported in Figure 14 to Figure 16, shows that there is reasonably good connection between the Lower and Upper Aquifers, especially in the upstream part of the GMA. For instance, water level data at three levels for bore 36380 (shown below in Figure 14) shows that presumed river recharge events result in groundwater peaks that are transmitted rapidly to all measured depths at this site. Similar observations can be made for bore 21498 Pipe 1 and 2 further downstream near Dubbo (refer to Figure 15). At this site, presumed pumping influences can be seen to affect both deep and shallow portions of the aquifer system.

However, a substantial pumping influence seen at bore 36443 Pipe 1, just upstream of Dubbo, is not reflected in other bores in the same area (see Figure 16). This indicates either a heterogeneous aquifer system or highly unconfined conditions with good interaction with the Macquarie River.

SKM

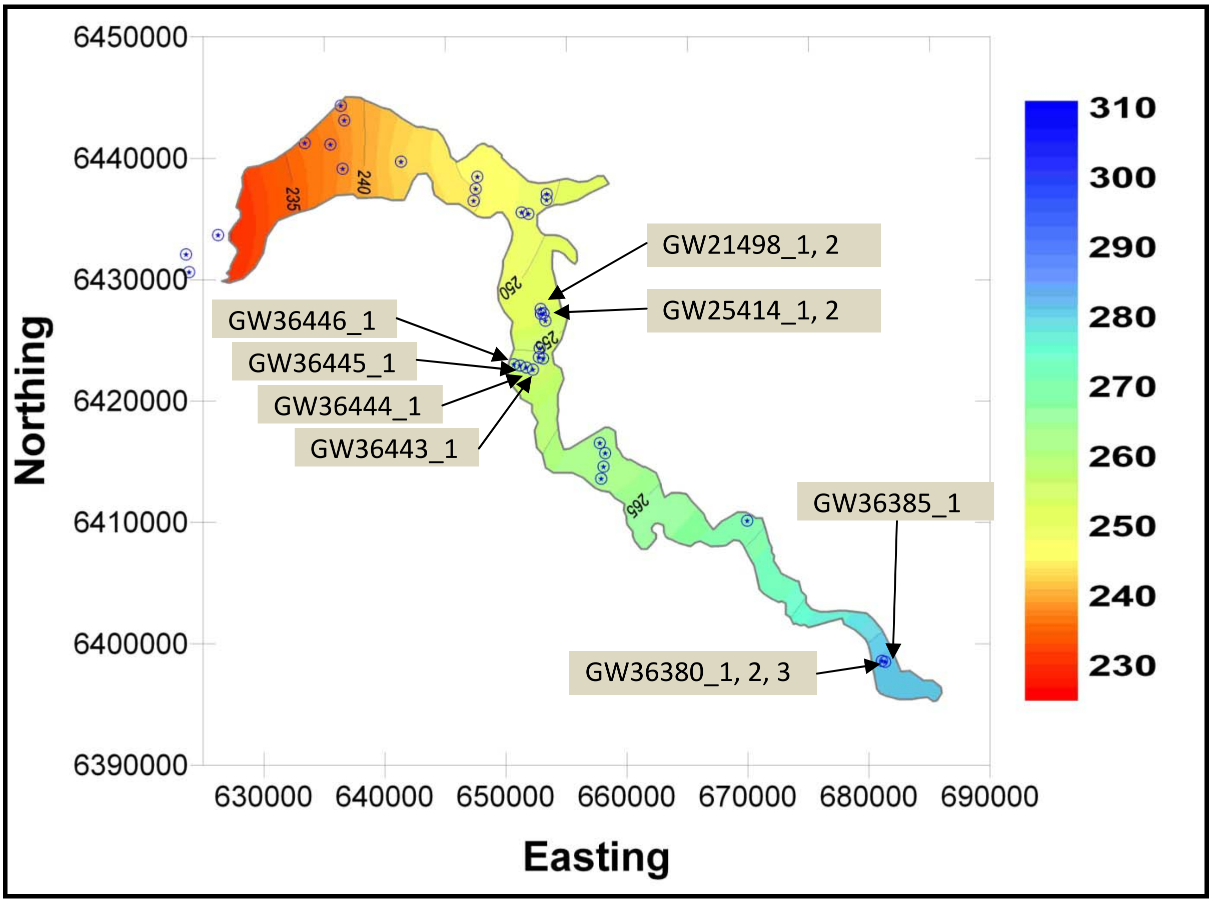

- **Figure 13. Location of monitoring bores (labelled bores are referenced in Figure 15, Figure 16 and Figure 17) and Watertable elevation in July 1980.**

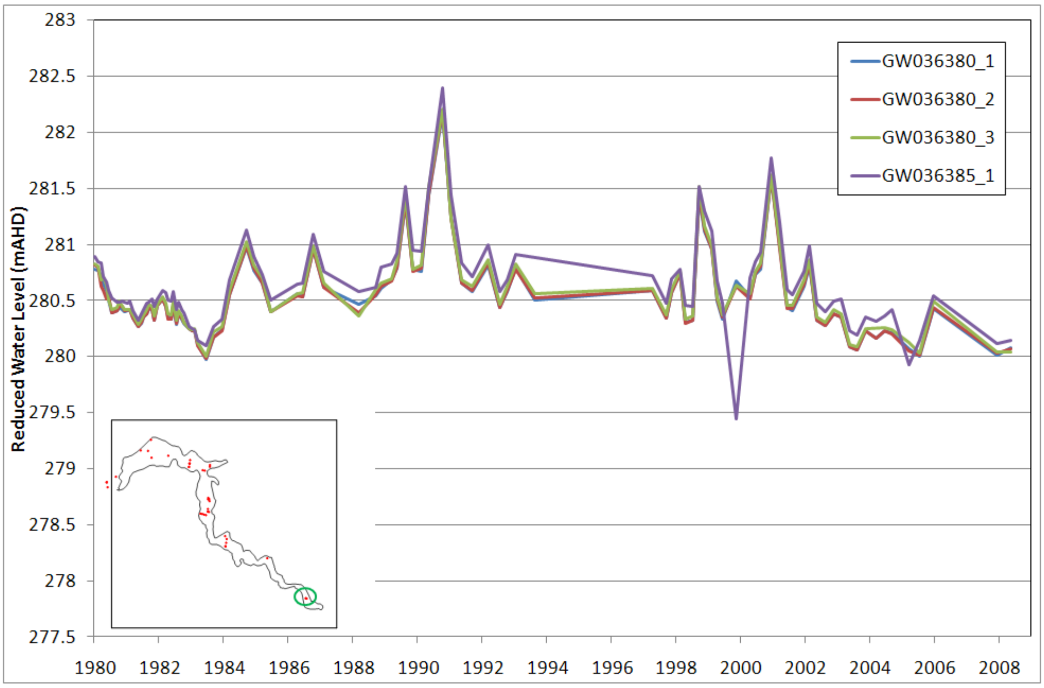

■ **Figure 14 Hydrographs for nested sites near Wellington**

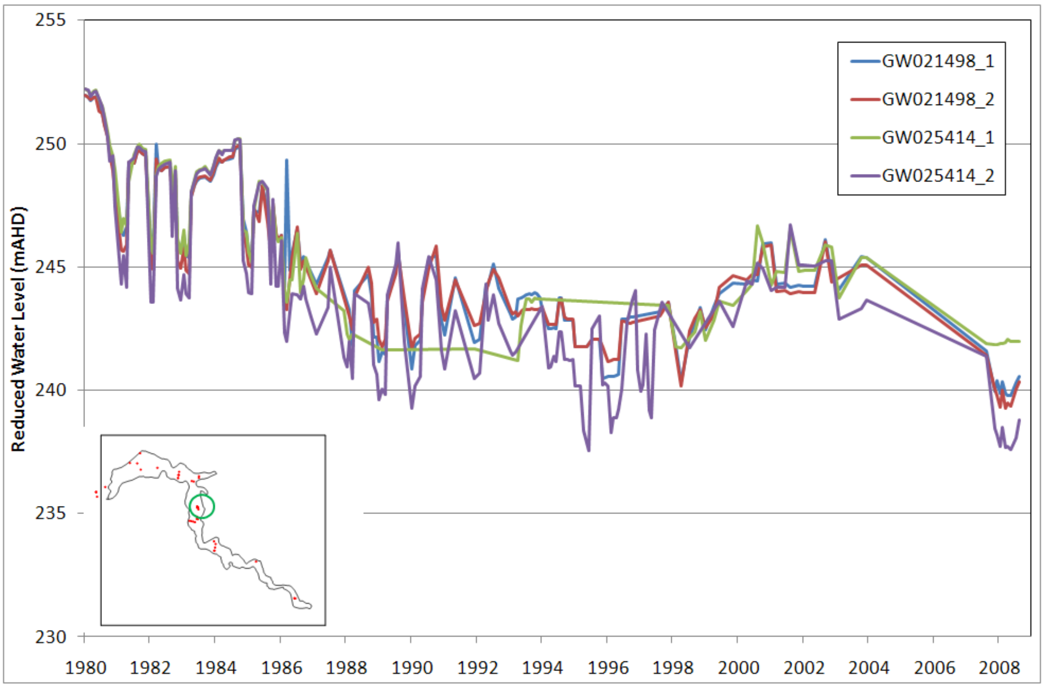

■ **Figure 15 Hydrographs of bores near Dubbo**

SKM

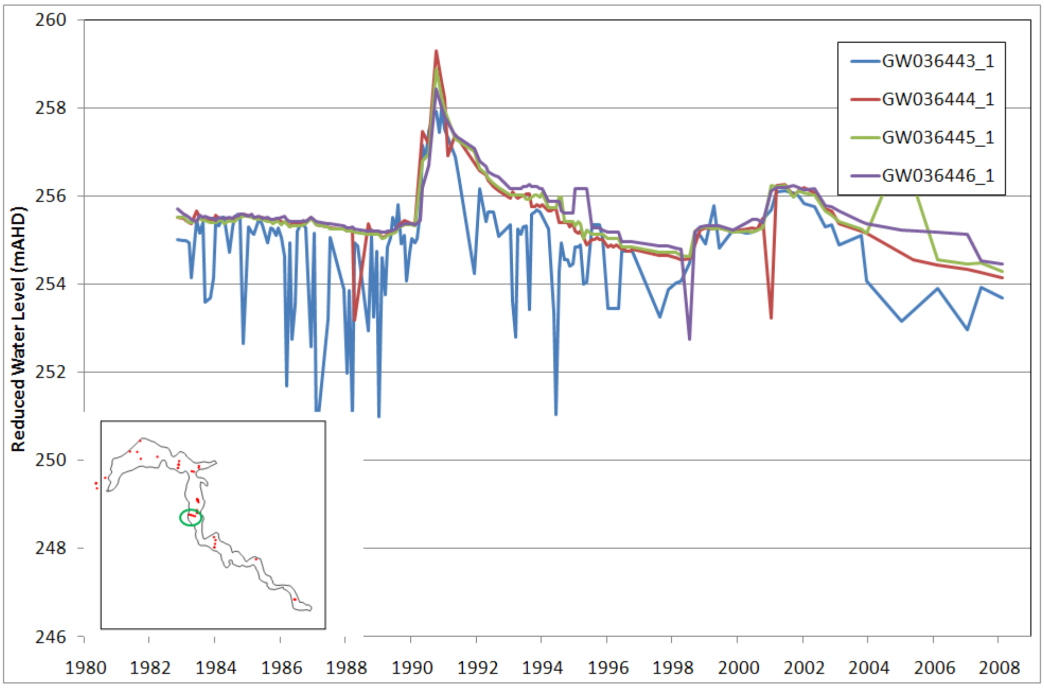

▪ **Figure 16 Hydrographs of bores upstream of Dubbo**

3. Groundwater Model Design

The groundwater model for the Upper Macquarie GMA was developed with the MODFLOW 2000 finite difference software code (Harbaugh et al., 2000) using the Groundwater Vistas (version 5) Graphical User Interface.

The packages used in this model to simulate the groundwater flow processes are listed hereunder;

- Basic (BAS),
- Output control (OC),
- Layer Property Flow (LPF) - *Groundwater flow package*
- Preconditioned Conjugate-Gradient (PCG) - *Solver*
- Discretisation (DIS),
- General Head Boundary (GHB),
- River (RIV),
- Recharge (RCH),
- Evapotranspiration (EVT),
- Well (WEL).

3.1. Conceptual Model

A conceptual model provides a simplified overview of a complex natural system. The Upper Macquarie groundwater model consists of four layers. The top three layers represent the Tertiary and Quaternary aquifers. The fourth layer represents the underlying bedrock. The quaternary aquifer was divided into two layers: the Upper and Lower Quaternary Aquifer. Layer 1 may be dry in places and therefore the second layer (Lower Quaternary Aquifer) can be confined in places and unconfined in others. The third layer (Tertiary Aquifer) is confined. The fourth layer remains inactive as the degree of connectivity between the alluvial sediments and the fractured rock aquifer has been assumed insignificant.

The active model domain is restricted to the mapped extent of alluvium within the Upper Macquarie valley (NOW, 2009) or the existing GMA boundary, whichever is greater. The alluvial extent represented in the model has been defined by Ann Smithson of the NSW Office of Water, and is provided in Figure 18.

The time varying stresses acting on the aquifer system and included in the model formulation are recharge from rainfall, irrigation and floods, and stream/aquifer interaction. In addition, evapotranspiration and groundwater pumping from the Quaternary and Tertiary aquifers are included in the model.

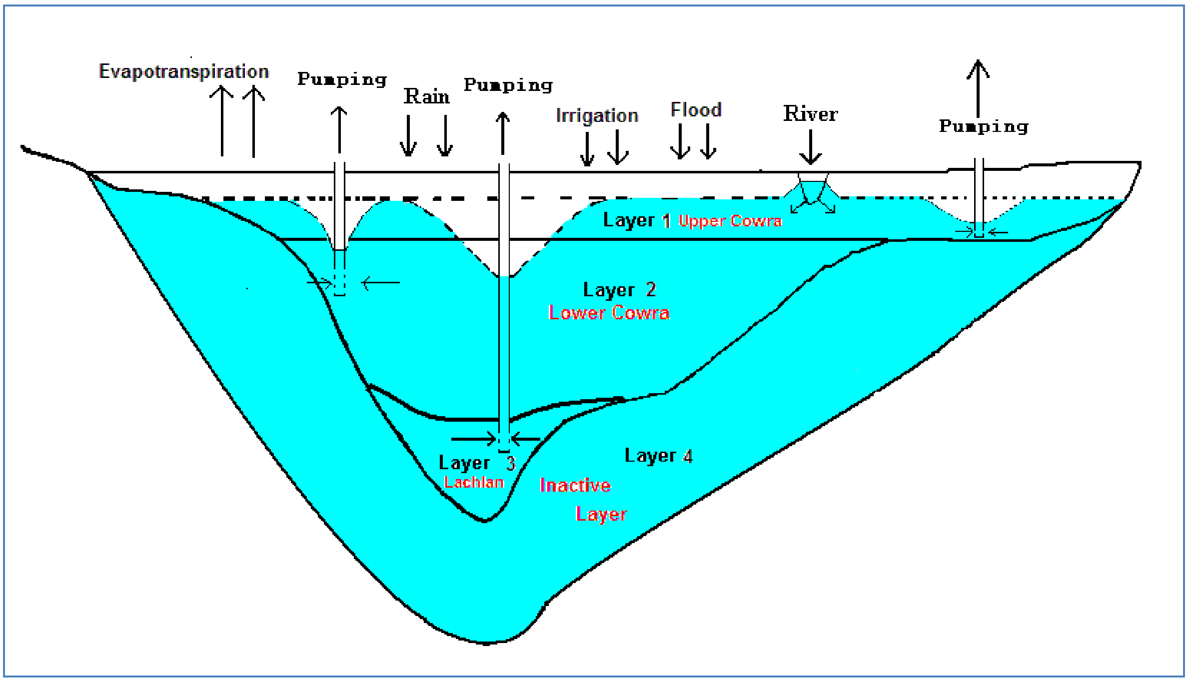

▪ **Figure 17. Conceptual Model for the Upper Macquarie GMA**

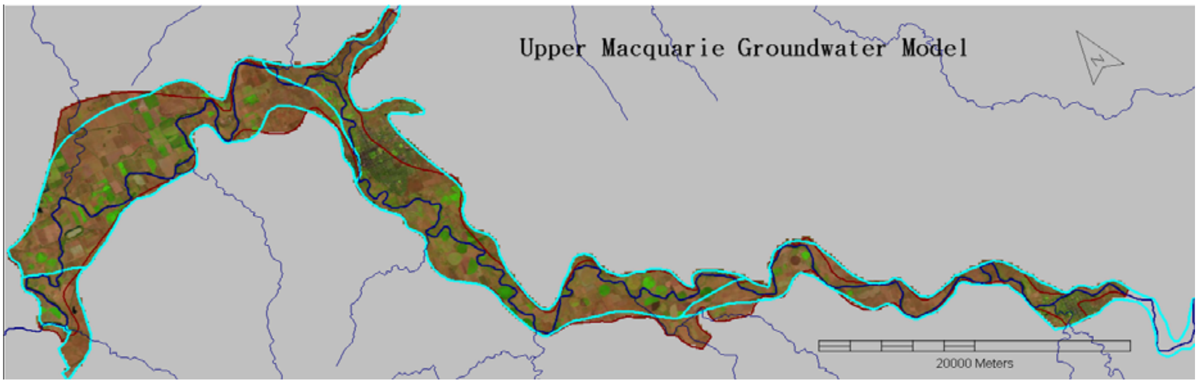

▪ **Figure 18. Model domain as defined by the greater of the extent of the alluvium (Maroon) or GMA boundary (aqua)**

3.2. Model Discretisation

Use of MODFLOW software requires discretisation of the model both spatially and temporally. Spatial discretisation is achieved by specifying an orthogonal set of rows and columns to form a mesh of rectangular shaped elements over the model area. A regular mesh has been adopted for this model with the understanding that it generally yields the most accurate form of the finite difference solution. The Upper Macquarie groundwater model was developed with a regular 200 by 200 m grid cell size (Figure 19). The grid cells falling outside the alluvial aquifer extents are designated as inactive.

In order to optimise MODFLOW models, it is required to minimise the grid size. To achieve this, the grid was rotated so that the general alignment of the Upper Macquarie Valley is parallel to a principal model coordinate (x axis). The model coordinates are obtained from MGA coordinates by translation and rotation as illustrated in Figure 20. The offset between MGA coordinates and the model coordinates is X = 623451.1 and Y= 6431976.2. The rotation of the grid is 325 degrees.

Model grid specifications are summarised in Table 3.

Note that some figures in the current report are presented in the model coordinates system as for example Figure 19 .

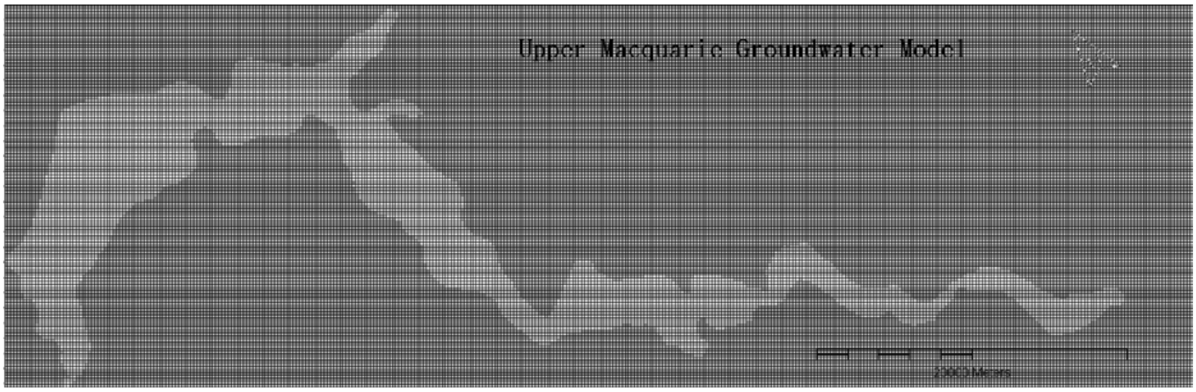

- **Figure 19. Model grid with 200 x 200m cells (the darker area represents the inactive area)**

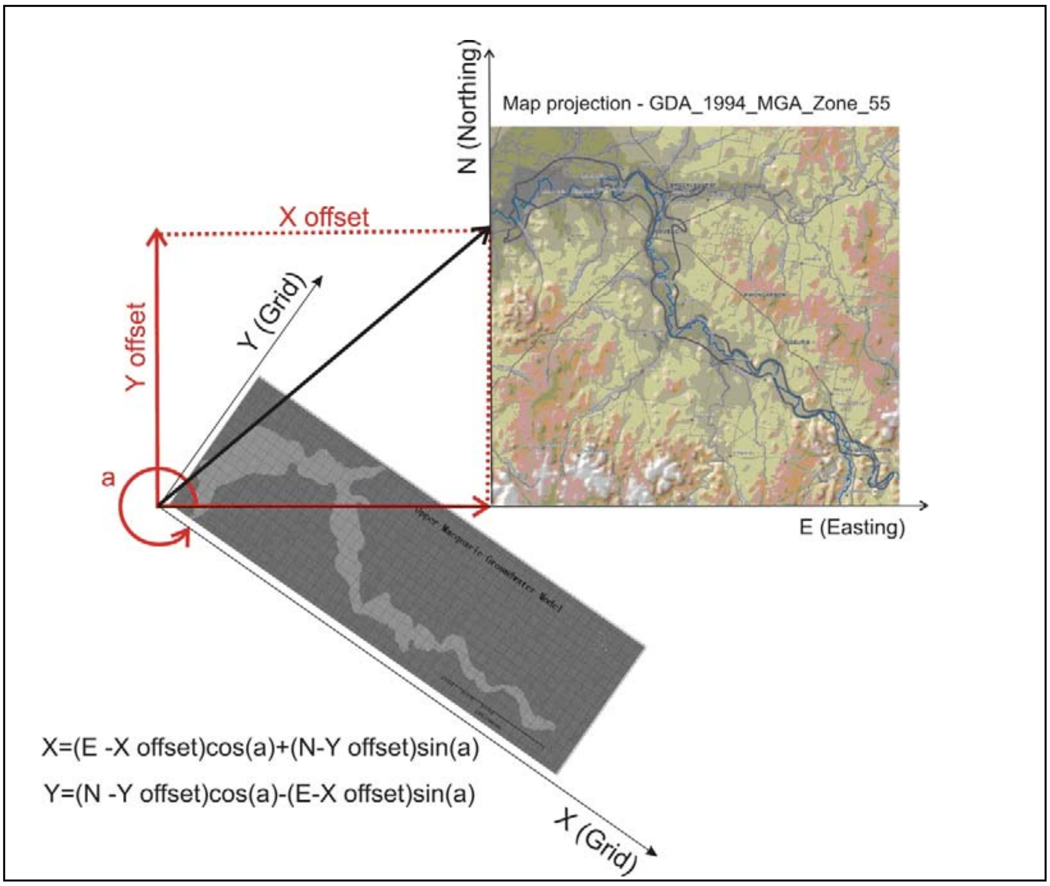

- **Figure 20. Coordinate transformation between site (map) coordinates and model coordinates.**

- **Table 3. Model grid specifications**

Lower Left Corner easting, northing	623451, 6431976 m AMG (GDA 1994 - MGA zone 55)
No of Layers	4 (3 actives & 1 inactive)
No of Rows	127
No of columns	384
Total Cells	195072
Total active cells	19302
Row width	200
Column width	200
Model dimension	25,000 m x 75,000 m
X offset	623451.0886
Y offset	6431976.235
Rotation (degree)	325

The model comprises four layers:

Layer 1 – Upper Quaternary Aquifer

Layer 2 – Lower Quaternary Aquifer

Layer 3 – Tertiary Aquifer

Layer 4 – Fractured Rock Basement (inactive layer)

The surface of the model is defined as a DTM derived from the Geoscience Australia nine second terrain model (Geoscience Australia, 2008). This model was supplemented with stream gauge elevations obtained from NSW Office of Water Pinneena Database version 9.2 and Geoscience Australia Geodata 3 (Geoscience Australia, 2006) stream alignments and recompiled to 100 m resolution.

The proposed model layers below ground are largely based on the work of Ann Smithson, NSW Office of Water (NOW, 2009). Model layer surfaces have been derived using an iterative finite difference surfacing utility that incorporates point data (bores and outcrop elevations) and linear data (contours and lineaments) to produce logical stratigraphic surfaces at 100 m grid cell resolution. The bore elevations were calibrated against the project terrain model to ensure consistency between all data sources. Descriptions are provided below (NOW, 2009).

BASEMENT ELEVATION - METHOD. The elevation of basement outcrop areas was established from the terrain model and geological map and incorporated into the analysis. Borehole data and digitized hand drawn contours supplied by the NOW and a paleo-valley alignment derived from the contours were also incorporated into the analysis.

LAYER 3 TOP ELEVATION. The elevation of the top of Layer 3 was compiled from bore analysis supplied by NOW. The model area was divided into a number of reaches aligned along the course of the river and each reach assigned an average elevation. The resultant surface was then compared to the basement to establish the extent and thickness of Layer 3.

LAYER 2 TOP ELEVATION. The elevation of the top of Layer 2 was compiled from the available bore data. The modelling technique extrapolates this surface out until it contacts the basement surface. This was then compared to the basement elevation and Layer 3 elevation to establish the thickness of Layer 2.

LAYER 1 THICKNESS. The thickness of Layer 1 was compiled as the difference between the ground elevation (as established from the terrain model) and the top of Layer 2, 3 or the basement, whichever was the shallowest.

Example cross-sections are provided in Figure 21. The thickness of all layers are presented in Figure 22.

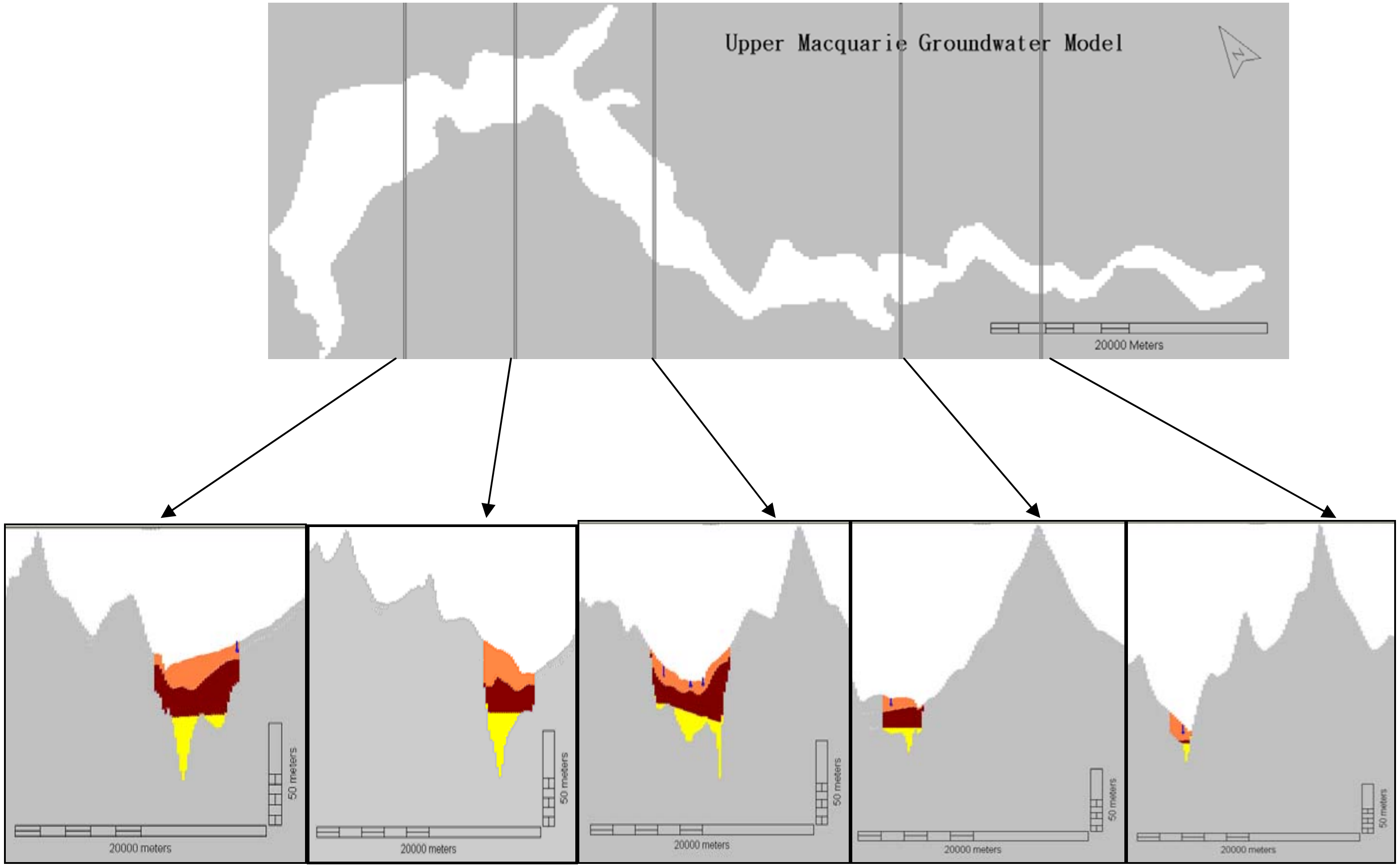

Figure 21. Cross-sections across the river valley highlighting the proposed layer structure

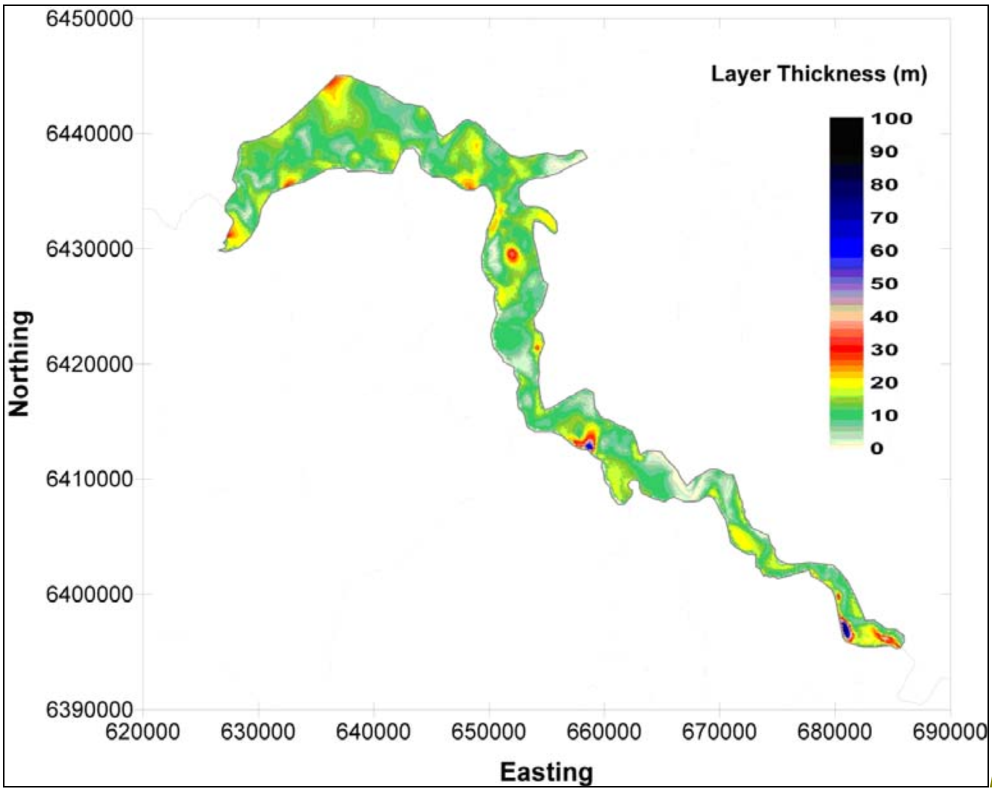

Layer 1

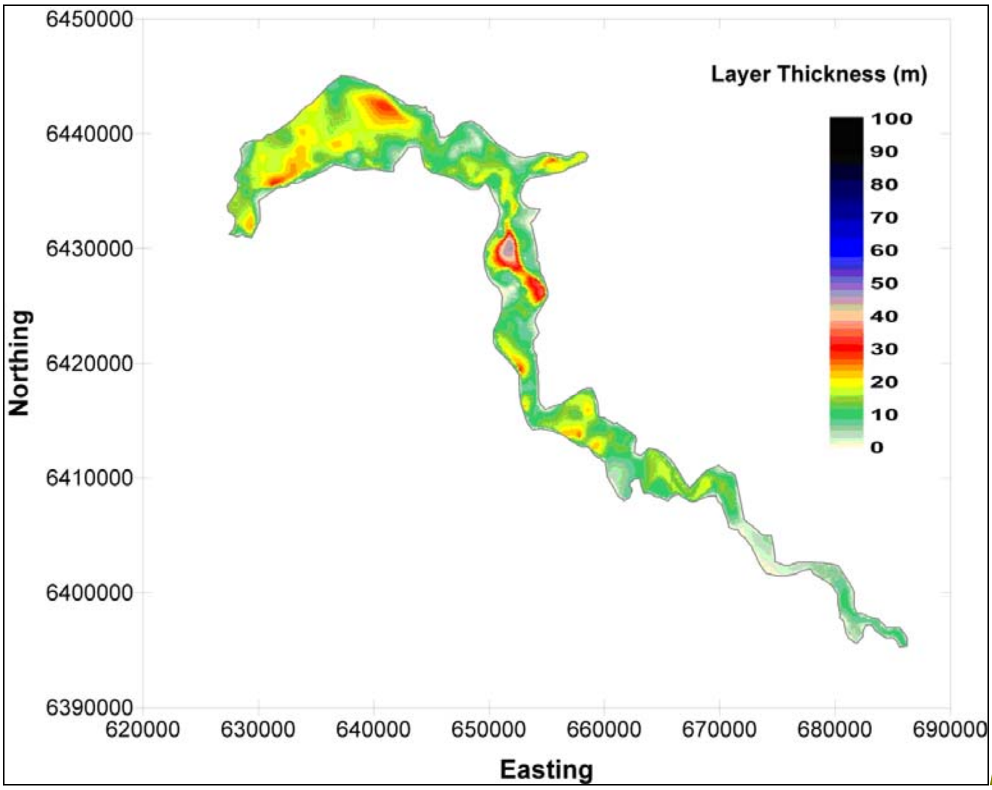

Layer 2

SKM

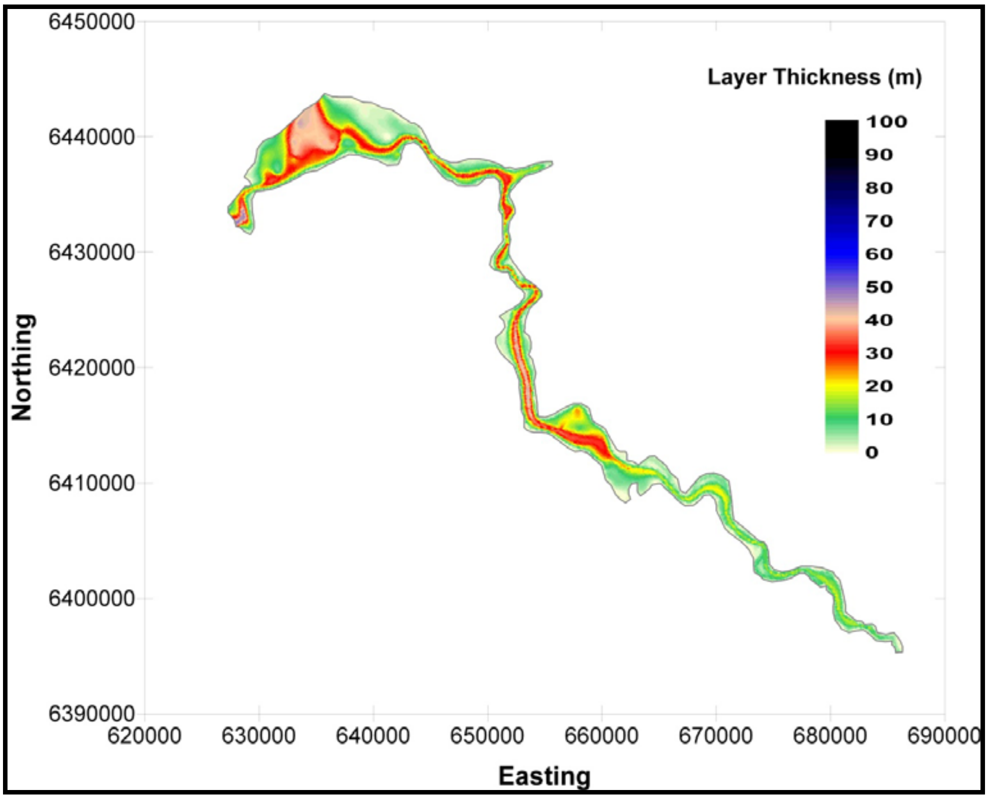

Layer 3

■ **Figure 22 Thickness of model layers (m)**

Transient simulation of a MODFLOW numerical model needs the calibration period to be discretised into several stress periods. Stress periods are periods within which the various model stresses are assumed to remain constant and for which data are available or can reasonably be inferred. Stress periods are further discretised into a number of time steps (calculation intervals), but in the current project, only one time step was used for each stress period. Time discretisation parameters are summarised in Table 4.

The calibration model was run on a monthly stress period from July 1980 to June 2008. The calibration period is divided in 336 stress periods. Each stress period was given a calendar month length varying from 28 to 31 days.

■ **Table 4. Time discretisation parameters for the Calibration Model**

Stress period length	1 month (form 28 days to 31 days)
No of stress periods	336
No of Time Steps	1
Start of calibration period	July 1980
End of calibration period	June, 2008
Calibration period length	28 years

Spatial and temporal discretisation details are read into the MODLFOW discretisation (DIS) package from the DIS file.

3.3. Initial heads

The MODFLOW numerical model requires the specification of initial heads for every active cell at the beginning of the model run. Initial conditions should closely match natural conditions existing at the start of the simulation.

Initial heads for the calibration model were obtained from measured groundwater levels in July 1980 in 38 water level observation wells located within the model domain. The data were obtained from the NSW Office of Water's Groundwater Data System (GDS).

The initial head data were interpolated using the Surfer™ software package to produce levels at each model cell. Initial heads are set to the same value for all layers as differences in heads between the various aquifers is not significant and does not need to be specified in the initial conditions assigned to the model. Contour maps showing the initial head distributions are shown in Figure 23. As already mentioned, Layer 1 remains dry in some areas and Layer 2 is partially saturated in such areas.

Initial heads are read into the basic package (BAS) in MODFLOW from the BAS file.

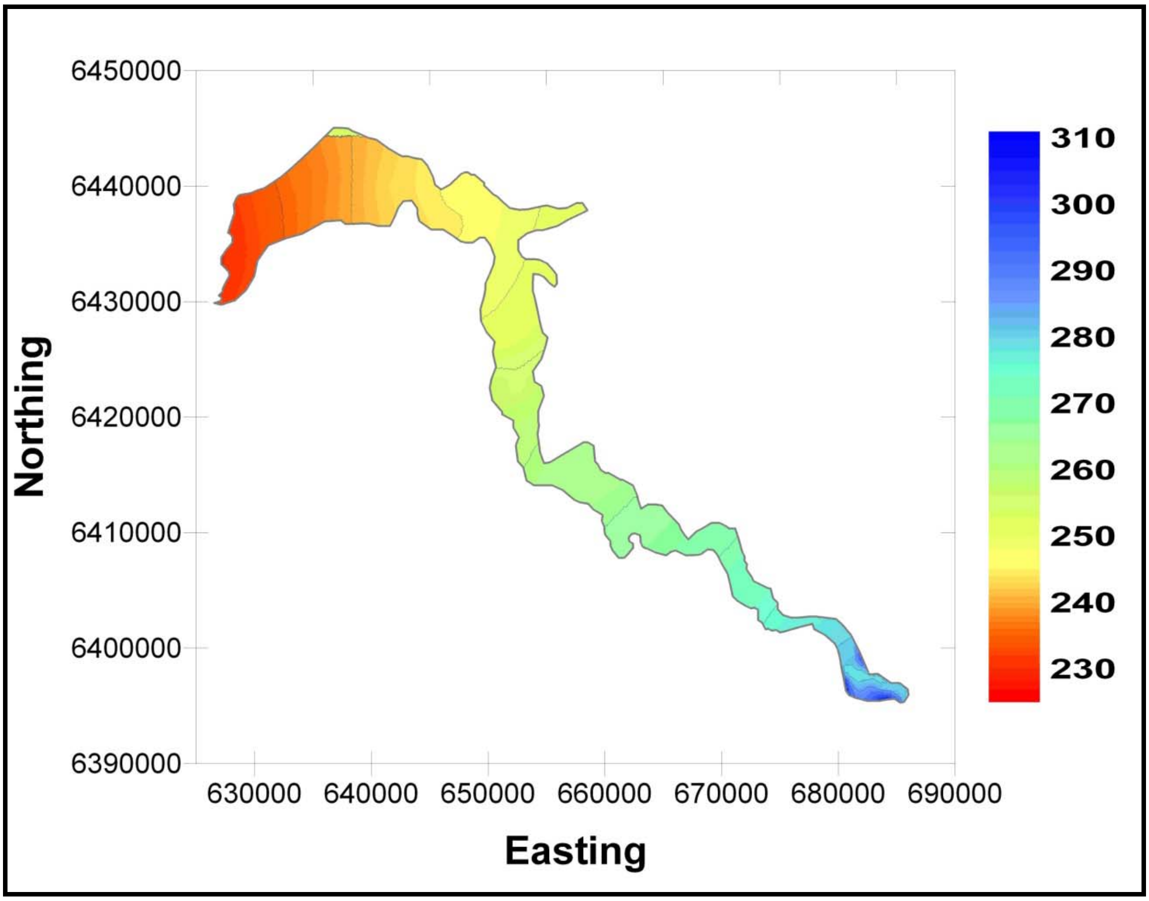

- **Figure 23. Initial heads in every layer of the Model.**

3.4. Aquifer parameters

Indicative hydraulic parameters (hydraulic conductivity and specific yield) for each layer were obtained from groundwater models developed in neighbouring regions which include the same geological units. Hydraulic parameters for Layers 1 and 2 (Upper and Lower Quaternary Aquifer) were derived from the Upper Lachlan Groundwater Model and the Lower Macquarie Groundwater Model. Hydraulic parameters for Layer 3 (Lachlan Formation Aquifer) were derived from the Mid Murrumbidgee and Upper Lachlan Groundwater Models.

The unconsolidated fine grained sediments constituting the Upper Quaternary Aquifer (Layer 1) have expected hydraulic conductivities ranging from 1 to 10 m/day. The initial estimation of this parameter for the calibration process was set at 5 m/day.

The gravel, sand, silt and clay of the Lower Quaternary Aquifer that constitute model Layer 2 have expected hydraulic conductivities ranging from 1 to 100 m/day. The initial estimation of Layer 2 horizontal hydraulic conductivity was set at 10 m/day for the calibration model.

Coarser unconsolidated deposits of the Tertiary alluvium (Layer 3) are expected to have hydraulic conductivities ranging from 10 to 200 m/day. Initial estimation of Layer 3 horizontal hydraulic conductivity was set at 10 m/day. Proposed initial model aquifers properties are summarised in Table 5.

For a model consisting of more than one layer a vertical hydraulic conductivity is also required for all but the lowermost layer. This parameter controls the leakage occurring between neighbouring layers. The initial estimate of vertical hydraulic conductivity for each layer was set at 0.2 m/day.

Specific Storage (Ss) is defined as the volume of water that a unit volume of aquifer releases from storage under a unit decline in hydraulic head due to aquifer compaction and water expansion. Aquifer compaction was considered negligible and the specific storage for confined layers was set to the value of water compressibility at 20°C : (5E-06 m^{-1}). The specific storage value was fixed and was not adjusted during calibrated.

Initial estimates of aquifer parameters specified were uniform across the model area. These initial parameter estimates were adjusted spatially during calibration of the model.

- **Table 5. Summary of model layers and initial estimates of aquifer properties**

Layer	Formation Represented	Lithological Summary	Hydraulic Conductivity	Vertical conductivity	Specific Yield	Specific storage
1	Quaternary Clay	Unconsolidated sediments, typically finer grained but highly heterogeneous.	5	0.2	0.1	Na
2	Quaternary Alluvium	Unconsolidated sediments. Polymictic gravels, sand, silt and clay	10	0.2	0.1	5 x 10-6
3	Tertiary Alluvium	Unconsolidated sediments, coarser grained aquifer, containing Quartzite gravel	15	0.2	Na	5 x 10-6
4	Basement	Fractured rock. Inactive in this project.	Na	Na	Na	Na

While the MODFLOW 2000 code allows for the rewetting of cells that have dried during a transient simulation, for improved calculation stability, the rewetting option was turned off.

Aquifer parameters are referenced in the Layer Property Flow (LPF) package in MODFLOW

SKM

3.5. Model boundaries

Boundary conditions control the location and rate at which water enters or leaves the model domain.

All contacts between the alluvium and basement rock were defined as 'No Flow' boundaries, thus assuming no interaction between the alluvial aquifers and the basement. The no flow boundary is defined by the inactive cells set all around the model domain. The basement layer has been incorporated in the model formulation to allow for its inclusion should it be required in the future.

The upstream and downstream model boundaries were defined by General Head Boundary conditions (GHB's). Additional GHB boundaries were placed where major tributaries enter the Upper Macquarie alluvium (four tributaries in total). All six GHB boundaries are displayed in Figure 24. Construction of the MODFLOW GHB input file requires, for each boundary cell, specification of a conductance term and a boundary head value. Six reaches of GHB cells are specified in each layer along the outflow boundary of the model. The boundary heads for the GHB cells were estimated by the river stage near the boundary. Initial value of conductance term used in these reaches was 2000 m^2/d.

All data relevant to this boundary are stored in the GHB package in MODFLOW.

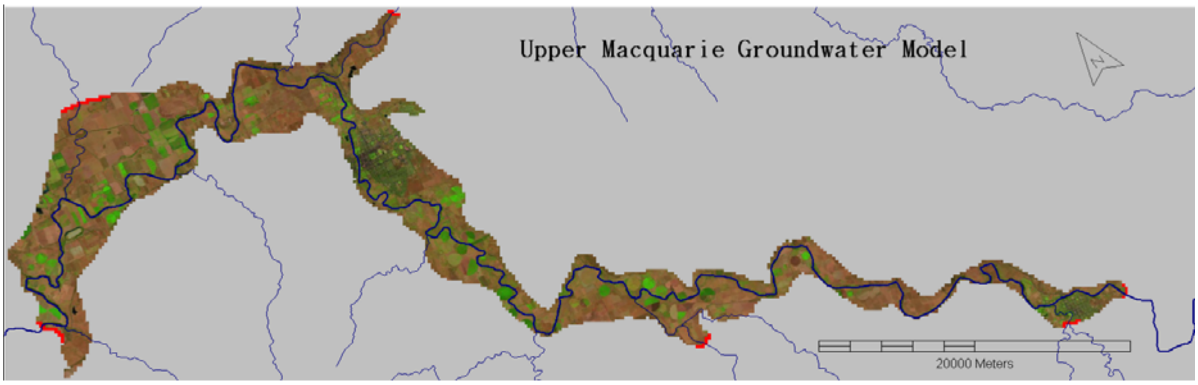

- **Figure 24. General Head Boundaries (red) defined in the Upper Macquarie Groundwater Model**

3.6. Recharge

Recharge was modelled with the MODFLOW recharge package. Recharge zones were defined for one part based on landuse (using the Landsat imagery previously shown in Figure 9 and Figure 18) and for the other part on eight regions defined arbitrarily for calibration purposes. Recharge zones fall into four broad categories, dry land (8 zones), irrigated land (8 zones), Hill-slope (6 zones) and superimposed onto dry land and irrigated zones, flood inundation recharge zone (8 zones). The zonation of recharge is represented in Figure 25.

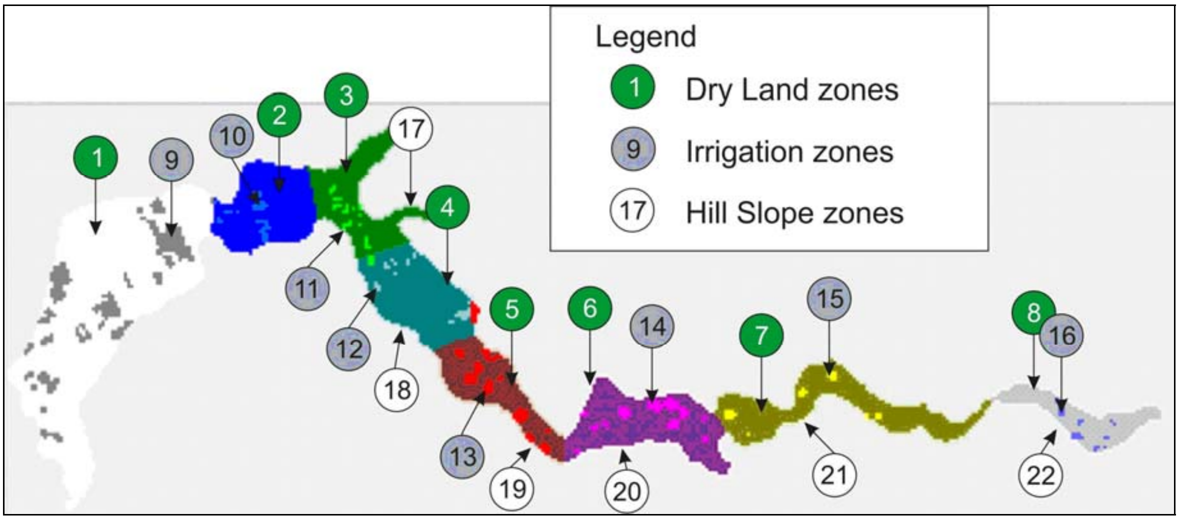

▪ **Figure 25 Model recharge zones**

▪ **Table 6 Recharge Factors**

		Recharge parameters bounds (initial value)				
Land use	**Zones**	R%	F%	I%	S%	**Recharge Formula**
Dry Land	1 to 8	1 -20 (5)*	1e-5 – 200 (5)			R% * Rain + F% * Flood
Irrigation	9 to 16	1 -20 (10)	1e-5 – 200 (5)	1 – 200 (10)		R% * Rain + F% * Flood + I% * Irrig
Hill slope	17 to 22				0.1 – 200 (100)	S% * Rain

* Values in brackets refer to the initial value adopted by the calibration model

3.6.1. Dryland Recharge

Recharge over non-irrigated land was modelled as a percentage of monthly rainfall. This percentage was determined during calibration for each of the eight regions. The rainfall time series used for the calibration model was that recorded at the Bureau of Meteorology's Dubbo climate station (065070) as previously presented in Figure 3.

SKM

The differences between the recharges rates applied to various parts of the model can be theoretically associated with uneven distribution of rainfall across the model area and with local variations in surface geology and soil type.

3.6.2. Irrigation Recharge

Irrigation recharge was assumed to occur each year in the eight months period from September to April. No irrigation was set from June to August. Irrigation recharge was applied in addition to rainfall recharge on areas that are irrigated (Figure 25).

The net volume of irrigation was approximated by the combined total volume of water diverted from the river and extracted from bores, excluding water used for the Dubbo city water supply. By dividing the total volume of water diverted by the approximate irrigated area (30 km^2), the annual irrigation rate per unit area of irrigated land was estimated. During the calibration process, an irrigation efficiency coefficient was determined that defines the ratio of applied irrigation to deep drainage and hence recharge.

The percentage of irrigation water recharging the watertable was refined during calibration but was initially estimated as 10% of the volume of water applied at the surface (with a minimal bound of 1% and a maximum of 20 %).

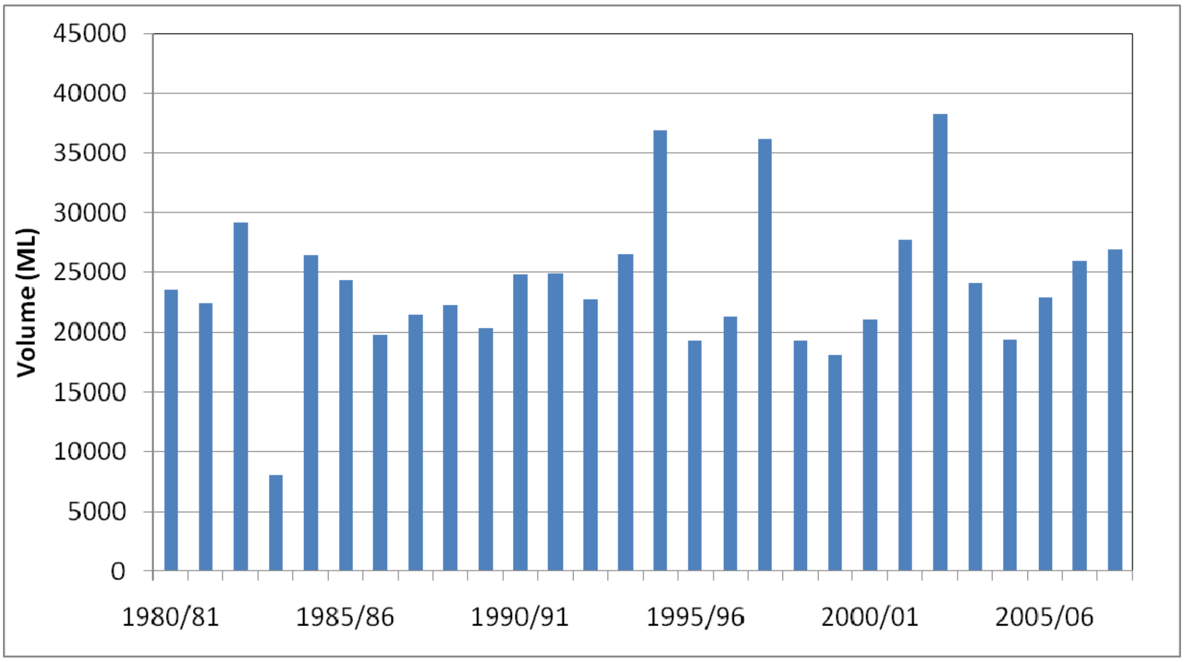

- **Figure 26. Total volume of water available for irrigation (river and bores) within the Upper Macquarie GMA**

3.6.3. Flood Inundation Recharge

Based on previous flood mapping work (SKM, 1984) it was assumed that major floods impact on the entire active model area.

The proposed method of applying flood inundation recharge was developed by NSW Office of Water and was used for the Lower Macquarie groundwater model as part of the Murray Darling Basin Sustainable Yields Project. Here, floods were simulated in the calibration run by adding 10 mm/day of recharge during a flood month, 1 mm/day and 0.2 mm/day respectively for the two months following the flood month. These rates were manipulated during the calibration process.

It was assumed that a flood occurs when the water level at Dubbo river Gauge (#421001) exceeds 8.0 meters. This occurred in April, July and August of 1990. The rate of flood recharge was also adjusted during calibration by a factor bounded between 10% and 200% of the assumed 10, 1,and 0.2 mm/day recharge for the three consecutive months for which inundation is modelled.

3.6.4. Hill-slope run-on

During calibration it was decided to increase recharge at the contact between the alluvial sediments and the outcropping bedrock. This was done to simulate the infiltration of runoff that originates from rainfall on the hills surrounding the aquifer. It represents the portion of runoff on the surrounding hills that does not directly enter the river system but instead recharges the aquifer where it flows onto the alluvium at the edge of the valley.

3.6.5. Recharge input file

The MODFLOW recharge file which combines dry land, irrigation, flood and hill-slope run-on recharge is generated by a Fortran application (Rech.exe) developed for this purpose. It calculates the recharge for each cell of the top active layer according to the formulae summarised in Table 7. It prepares the recharge package file (RCH) used by MODFLOW.

- **Table 7 Recharge calculation for each zone (R%,F%,I% and S% are the calibration factors defined for each recharge zone)**

Zone	Formula
1 to 8 (Dry land)	**R% * Rain + F% * Flood**
9 to 16 (Irrigation zone)	**R% * Rain + F% * Flood + I% * Irrig**
17 to 22 (Hill base)	**S% * Rain**

3.7. Evapotranspiration

Evapotranspiration (ET) was modelled using the MODFLOW EVT package. This package models level-dependent groundwater extraction directly from the groundwater system where shallow water tables exist. It does not include ET from the unsaturated zone, which is accounted for in the recharge rates.

The EVT package requires the definition of a maximum ET rate which is assumed to occur when the water table is at the ground surface. It also requires an extinction depth that defines the maximum water table depth for which evapotranspiration can occur. ET was modelled using an average monthly time series for the maximum ET rate repeated every year through the calibration period, as previously shown in Figure 5. In addition the maximum ET rate may be factored down from the measured pan evaporation rate to account for the non-linear relationship between plant water use and depth to water table (ie the relationship between plant water use and water table depth is not usually linear). An ET extinction depth of 2 m was applied across the active model domain.

ET being a minor contributor to the water balance, assumed values of maximum ET rate and extinction depth were applied and were not adjusted during the calibration process.

3.8. River / aquifer interaction

The influence of the Macquarie River is represented in the model by the MODFLOW river package (RIV) which allows for mass transfer between the groundwater and the river.

MODFLOW (McDonald and Harbaugh, 1988) simulates leakage between a river and the aquifer as a vertical flow through the riverbed. The rate of leakage is controlled by the head difference between the river stage and the water table and by the conductance term. The river conductance term is used to represent the presence of river bed sediments which may inhibit the movement of water between the river and aquifer.

For calibration purposes, the river was divided into 8 segments (Figure 27) matching the 8 dryland recharges zones (Figure 25). The river conductance term for each of the 8 sections, initially set to 2000 m^2/day, was modified during calibration to achieve the best fit with near river monitoring bores. Bounds for river conductance were set at 10000 and 5000.

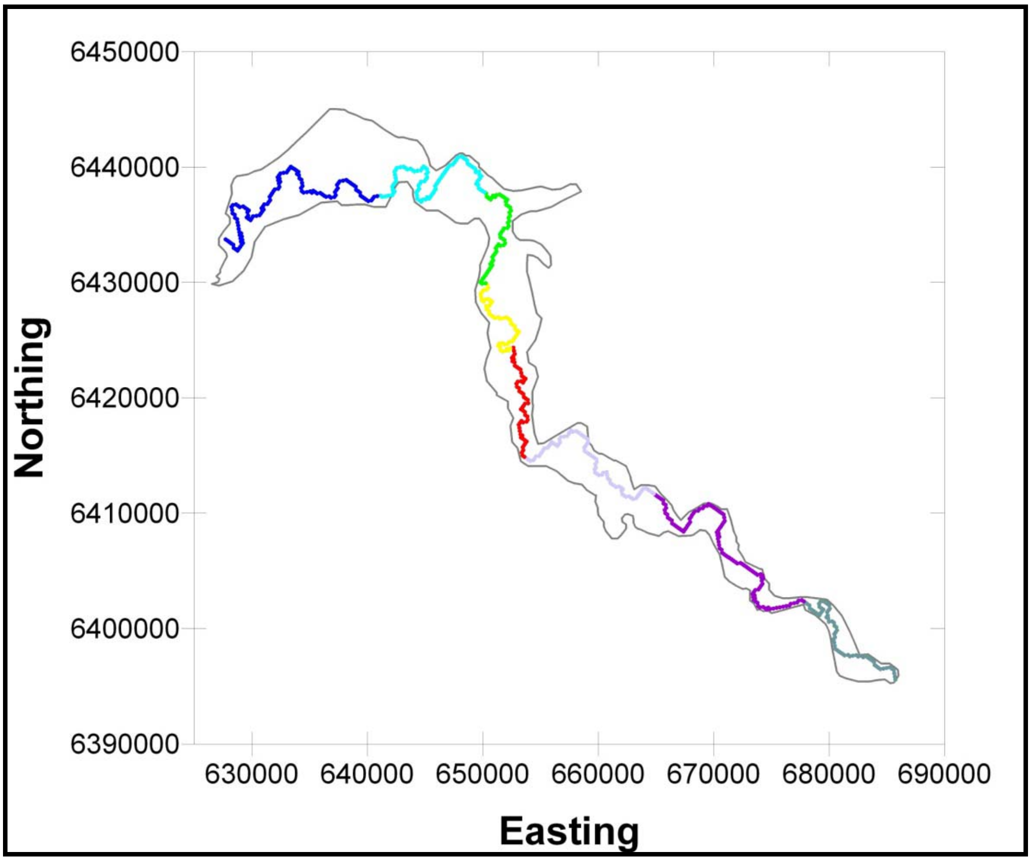

Figure 27. River reaches in which conductance term is assumed constant. The river consists of 8 sections numbered 1 to 8 from west to east.

During the calibration period, river levels at each of the gauges used historic river level data as previously presented in Figure 7.

3.8.1. Estimating river elevation between gauges

The commonly accepted approach for estimating the river elevation between river gauges is to use a simple linear interpolation method. However, this has proven to become problematic as rivers very rarely have a constant gradient and therefore linear interpolation can lead to large errors in river stage elevation particularly where there are large distances between river gauges.

The Upper Macquarie River is a good example of this where the river gradient is variable but more importantly the distances between gauges is commonly in the 10's of kilometres. However, improvements in river elevation definition in the model can be achieved through the use of a digital terrain model. Herein, we use the assumption that the river bed elevation is linked to topography.

The process for defining the river elevation is based on the following assumptions:

Assumption 1 – The river elevation approximately follows the digital terrain model

Assumption 2 – At any section across the river valley, the river is the lowest point in the terrain

The method used to define the river stage and river bottom is summarised by the following steps (also shown diagrammatically in Figure 28):

1) The ‘top of layer 1’ elevation is extracted for each river cell based on the DTM
2) The river cells are ordered from the upstream end of the model to the downstream end of the model and plotted to create a long section of the dtm elevation along the river
3) Given the cell elevation is based on a 200 m by 200 m average, the cell elevations do not always decrease downstream (i.e. if we linked the river elevation directly to the dtm we would get parts of the river flowing uphill, obviously an unrealistic result). Therefore we create a ‘reference elevation’ which is based on the dtm but always ensures that the elevation is decreasing downstream (or at least remains level).
4) The river gauges and weirs are inserted as fixed reference points for the creation of a river bed and river stage levels.
5) The ‘reference elevation’ is adjusted downward such that it fits the gauge zero elevations at each river gauge. This defines the river bed elevation for each modelled river cell which remains fixed in the model for all stress periods.
6) The river stage is then defined as a height above the river bed based on the gauge data. This is calculated for each stress period in the model run.

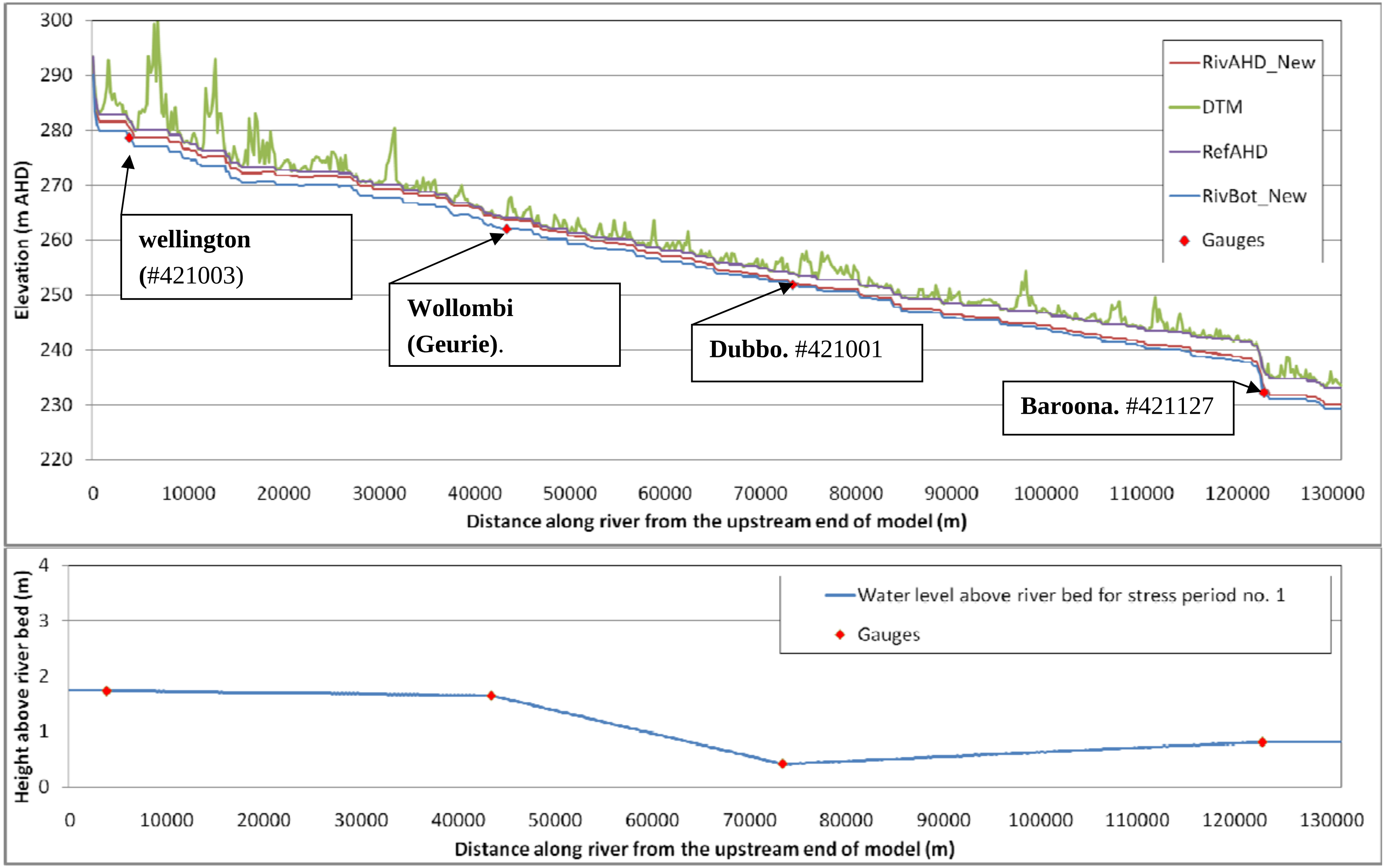

- **Figure 28 Example of process for defining the river elevation in the Upper Macquarie Groundwater Model**

3.9. Groundwater Abstractions & Surface Water Diversions

Surface water diversions are not explicitly modelled in groundwater models, however they are implicitly accounted for through the river definition process. As the river is defined by recorded water level elevations, this process implicitly accounts for the impacts of river diversions on the river flow and river stage.

Groundwater extractions were explicitly modelled through the adoption of the MODFLOW WELL package. Recorded annual usage for each bore in the GMA has been supplied by NSW Office of Water. The spatial distribution of these bores is shown in Figure 29 and their combined extraction volumes are shown Figure 10.

Among the 256 abstraction bores located in the model domain, only 109 have recorded abstraction data. The volume of abstraction for the 147 other bores was assumed to be zero. Half of the total volume abstracted is sourced from only nine bores. 60 bores have a yearly abstraction less than 1000 ML/year. Figure 10 and Figure 11 illustrate the abstraction volumes used in the calibration model.

A list of all active abstraction bore is given in Appendix A. The list includes pumping rates, and screen elevations.

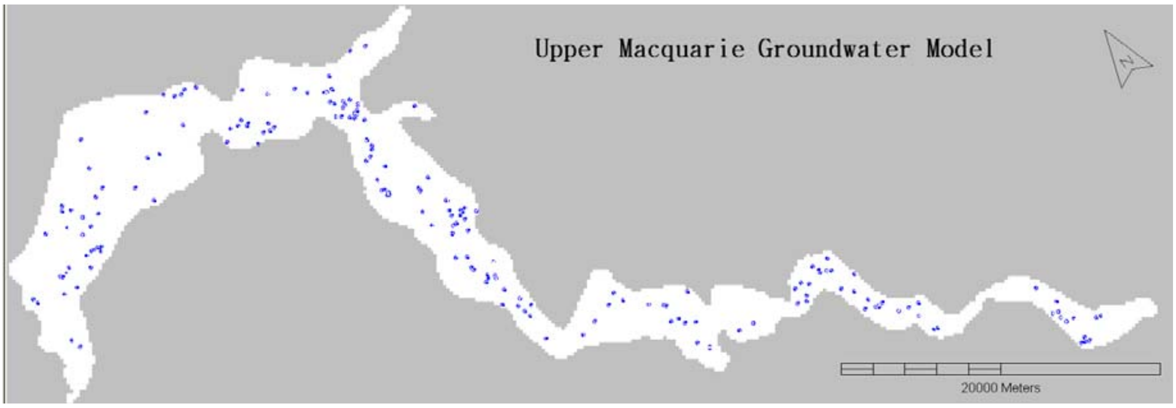

- **Figure 29. Distribution of extraction bores across the Upper Macquarie model**

3.10. Solver

The 'Pre-conditioned Conjugate Gradient' (PCG2) is used as the mathematical solver in this model. The parameter settings for the package are shown in Table 8.

- **Table 8. Parameter settings in the PCG2 solver package**

Maximum Outer Iterations	100
Maximum Inner Iterations	50
Head Change Criterion for convergence	0.0001
Residual Criterion for Convergence	1
Relaxation Parameter	0.97
Matrix Preconditioning Method	Cholesky
Maximum Bound on Eigenvalue	2
Damping Factor	0.5
Max number of convergence	100

4. Model Calibration

Calibration of groundwater models is a process in which important model parameters are adjusted, within realistic limits, to produce the best match between simulated and observed data. The process begins with an initial estimate of parameters (such as hydraulic conductivity, storativity, recharge rates and boundary conditions) for each active cell in the model grid. In the current model, the calibration process was assisted by the automated parameter estimation software PEST version 11 (Doherty, 2003).

During calibration, the current MODFLOW Model was controlled by PEST through the MSDOS command line and therefore outside the Groundwater Vistas interface. This approach, which allows more flexibility, was dictated by the fact that the recharge input file is prepared by an independent Fortran application that could not be managed within GW Vistas interface.

The calibration model was run on a monthly stress period from July 1980 to June 2008. The calibration period is divided into 336 stress periods. Each stress period was given a calendar month of between 28 and 31 days. Only one time step was used for each stress period. The LPF flow package was used during calibration and the calculations were processed by a modified version of the PCG solver provided by NSW Office of Water. The modified solver accepts a solution if convergence is not achieved after a specified number (100) of iteration. No verification period was allowed for.

A total of 897 parameters (including 853 pilot points) were defined to calibrate the model. As such a vast number of parameters inevitably generate significant levels of non uniqueness. Non uniqueness can be limited and reduced by creating links between the parameters through the process of Regularisation. Regularisation was undertaken by a PEST utility accessed within the Groundwater Vistas software. In order to retain acceptable calculation times required for PEST to estimate each parameter, the 897 parameters were reduced to a set of 255 ‘super parameters’. This process, named Singular Value Decomposition (SVD) was also conducted by routines from the PEST utilities suite (Christenson and Doherty, 2008).

The major focus of the calibration was to achieve an accurate match between the model predicted groundwater levels and recorded hydrographs as defined by the Scaled Root Mean Square (SRMS) error. The PEST processing aims to minimise an objective function which in the case of the current project was defined by two terms; the first being the variation between observed water level records and calculated heads (SRMS) and the second being the variation between consecutive readings of observed water level and model predicted variation in water levels at these times. The second term forces PEST to seek to reproduce the water level variation amplitude as much as trying to minimise the difference between average observed and calculated values.

Calibration is generally considered to be acceptable when the SRMS is less than 5% (MDBC, 2001).

4.1. Observation Bores

Records of groundwater levels from a total of 38 observation bores were used to define the objective function for PEST. Hydrographs at the observation bores are presented previously in this report (cf. Figure 14 to Figure 16). The number of observation bores and actual observation used in the calibration process are presented in Table 9. The locations of the observation bores are illustrated in Figure 30 to Figure 32

Some locations have nested bores with screens located in different formations i.e. in the Quaternary and Tertiary aquifers. From the 38 Observation bores, 5 are located in model Layer 1, 24 are located in model Layer 2, and 9 are in Layer 3. During calibration every observation was given the same weight. A summary of observation data is given in Appendix B.

- **Table 9.Distribution of calibration observations data**

Layer	Number of bores	Number of observations	% of total
1	5	490	9
2	24	2901	56
3	9	1803	35
total	38	5194	100

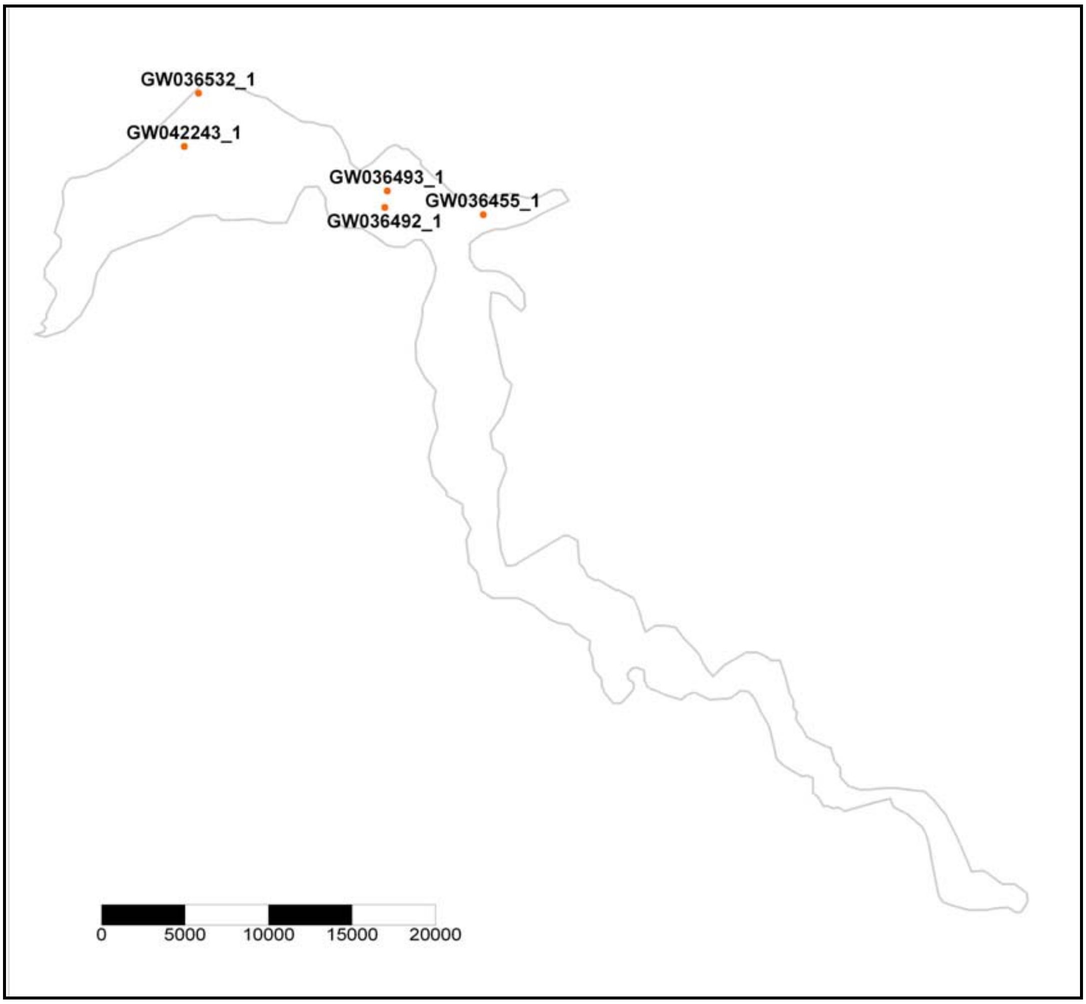

- **Figure 30 Observation wells in Layer 1**

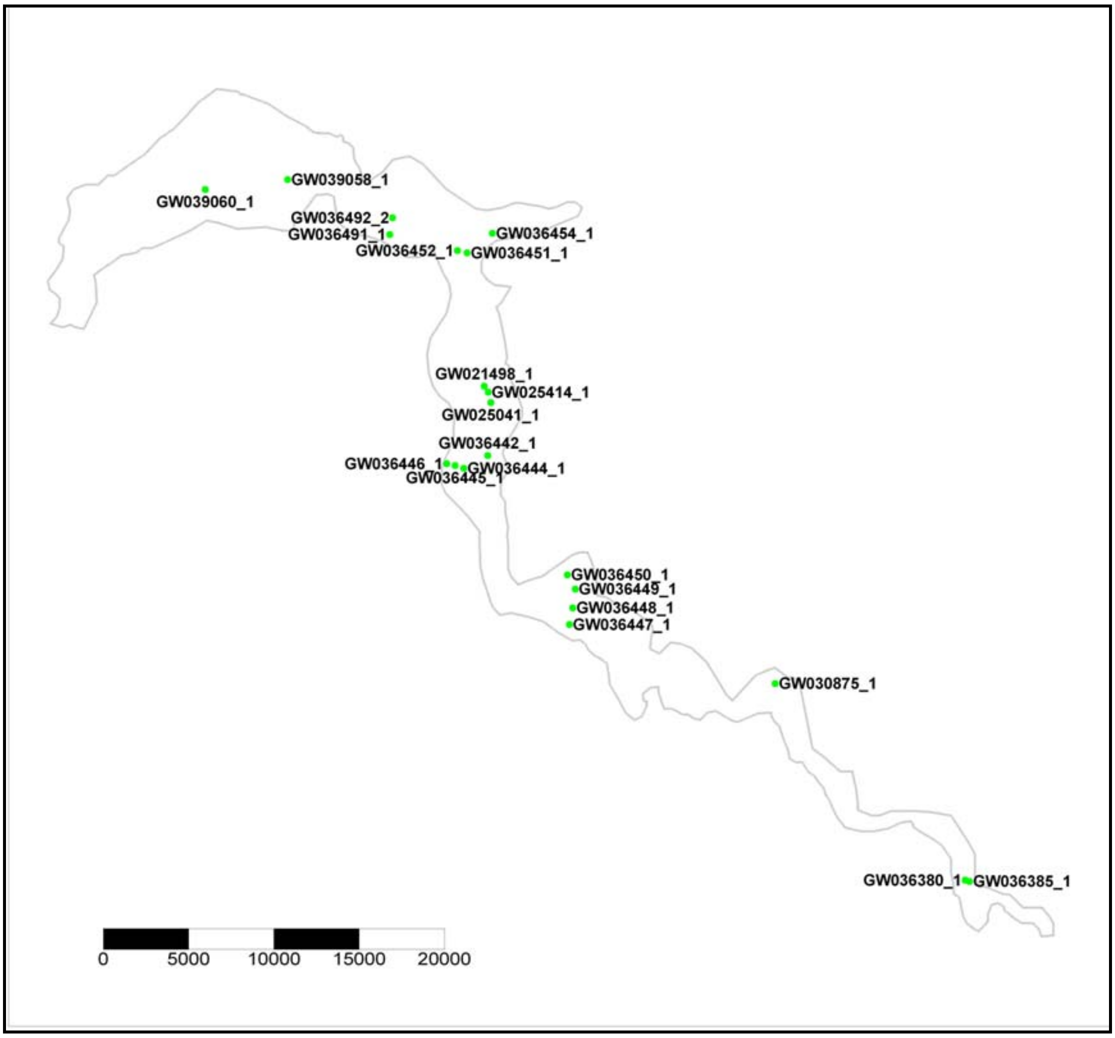

- **Figure 31 Observation wells in Layer 2**

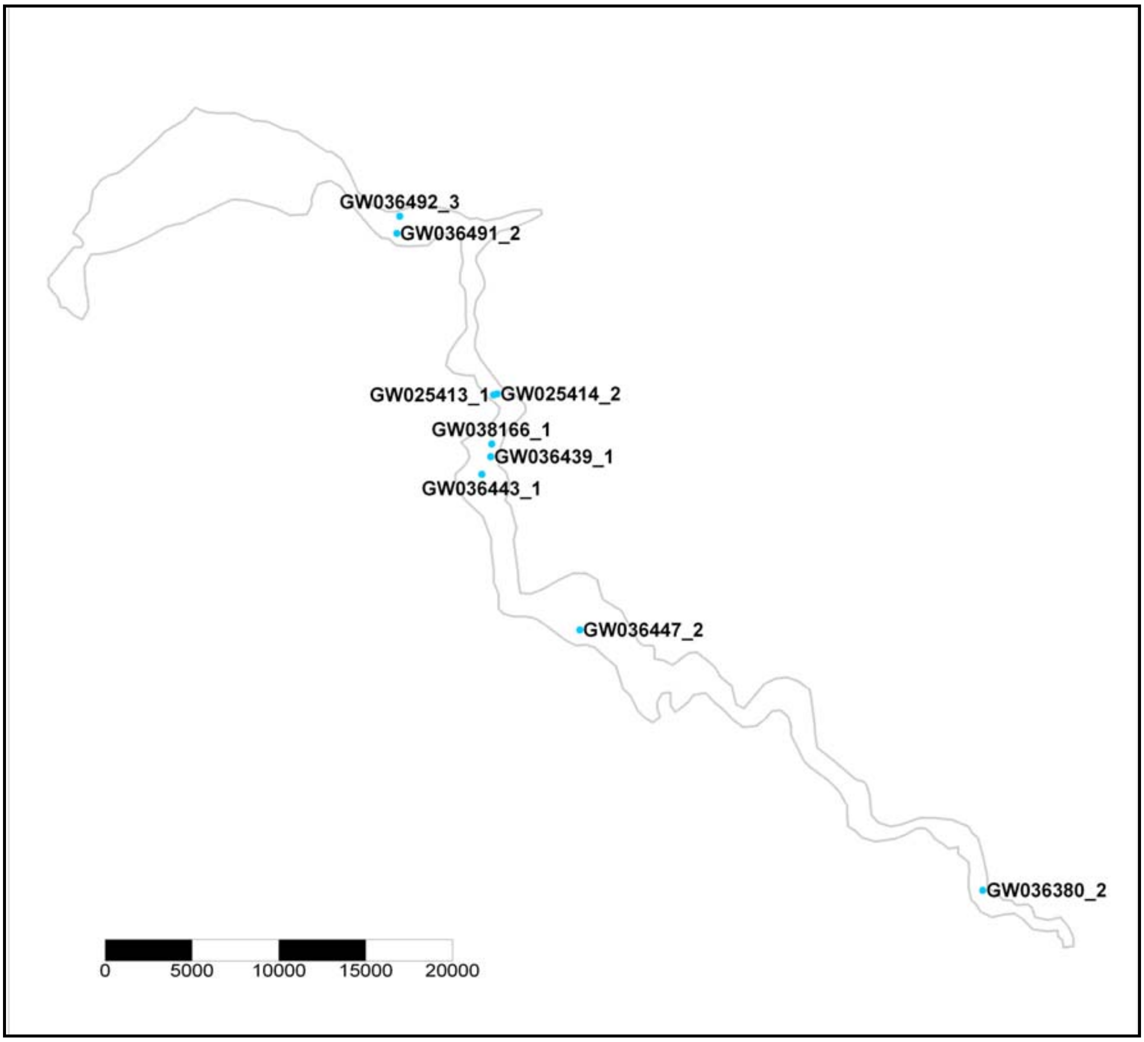

- **Figure 32 Observation wells in Layer 3**

4.2. PEST Calibration

4.2.1. Calibrated parameters

A total of 897 parameters were defined to calibrate the model. The breakdown of the parameters is given in Table 10.

Table 10. Parameters for calibration

Category	Layer	Number of parameters
Horizontal conductivity: Kx	**1, 2 & 3**	**312**
Vertical conductivity : Kz	**1, 2 & 3**	**312**
Specific Yield: Sy	**1, 2**	**229**
Recharge parameters	**1**	**30**
GHB Conductance	**1, 2 & 3**	**6**
River Conductance	**1, 2**	**8**
TOTAL		***897***

The detail for each category is described in the following chapters.

4.2.2. Pilots points

The calibration process for parameter fields such as the hydraulic conductivities and specific yield are processed by the 'pilot points' methodology. Through this process, PEST estimates the parameter value at each pilot point and generates a continuous spatial distribution for that parameter for the whole model area by interpolation (kriging) between the pilot points.

A total of 119 pilot points were distributed across model Layer 1 as shown in Figure 33. The pilot points were distributed in a manner aimed at evenly covering the whole model area. The arrangement was made denser between observation bores and scarcer at locations where no information is available to describe the aquifer's behaviour.

The same distribution of pilot points was used in Layers 2 and 3. Nevertheless due to their smaller extent of the deeper layers, the number of pilot points in deeper layers is reduced to 111 in Layer 2 and 83 for Layer 3.

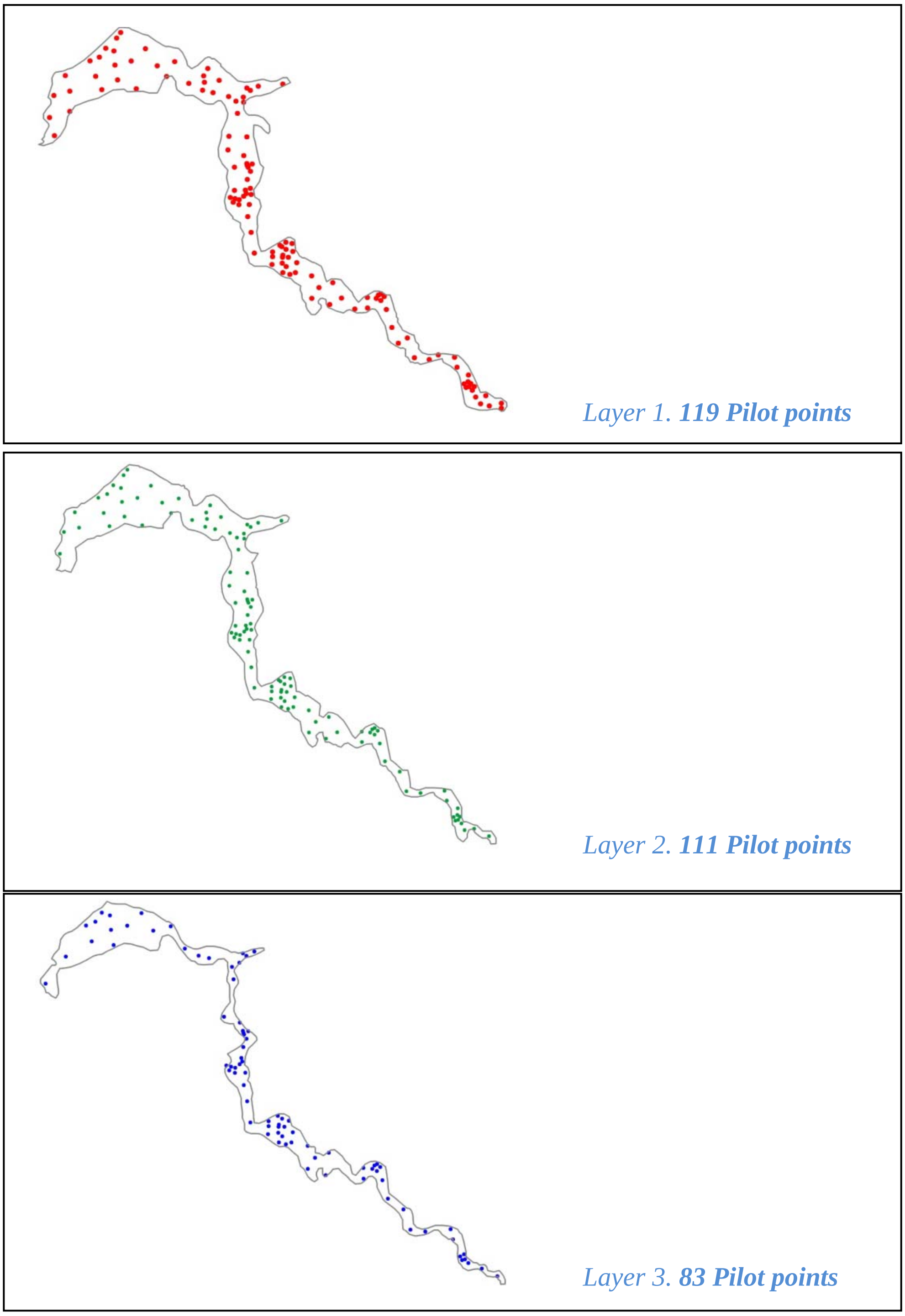

- **Figure 33 PEST Pilot points distribution.**

4.3. PEST Results

4.3.1. Hydraulic Conductivities

During the PEST calibration process the values of hydraulic conductivities were bounded between values reported in Table 11 in order to prevent PEST adopting values that are outside the acceptable limits (with regard to the hydrogeological conceptualisation) for this parameter.

Horizontal hydraulic conductivities

- **Table 11 Horizontal hydraulic conductivity bounds for PEST**

Zone	Layer	Initial	Lower bound	Upper bound
Kx	**1**	**5**	**1**	**20**
Kx	**2**	**10**	**1**	**100**
Kx	**3**	**15**	**5**	**200**

Figure 34 shows the distribution of horizontal hydraulic conductivity obtained in each model layer after PEST calibration process.

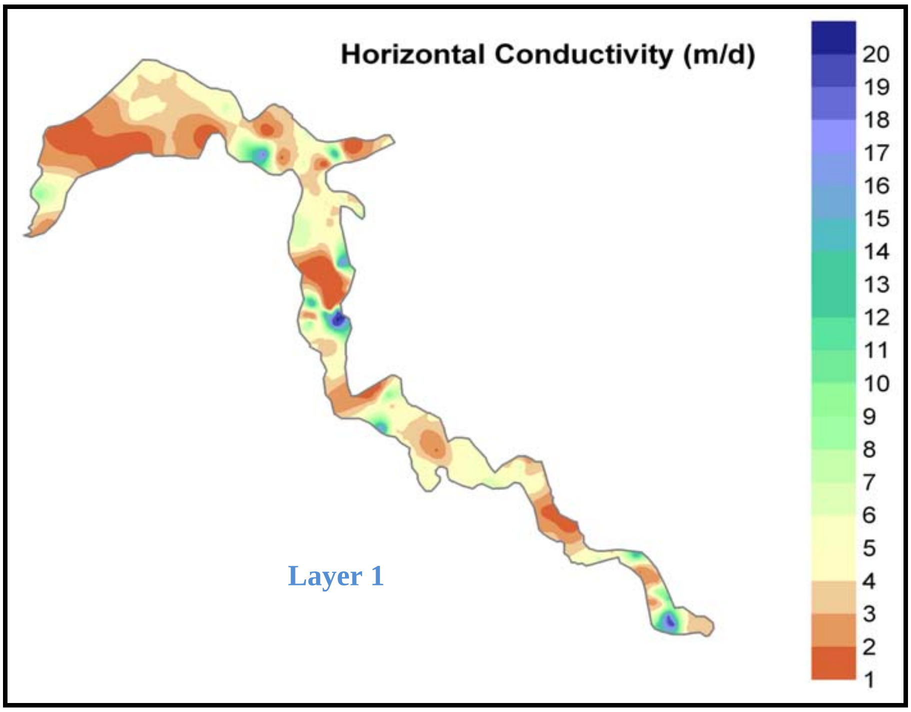

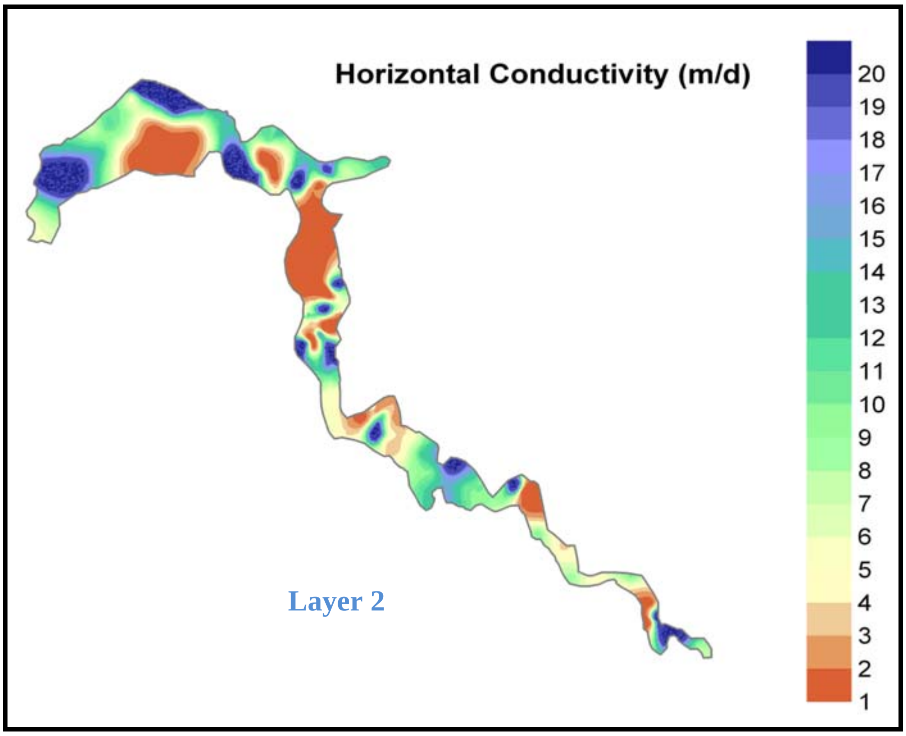

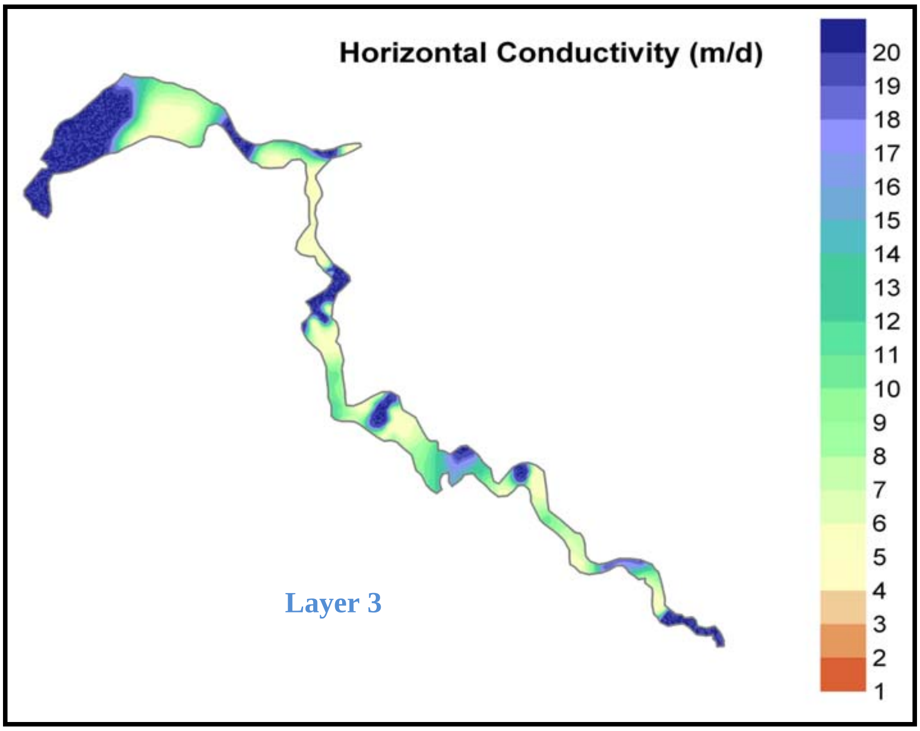

- **Figure 34. Horizontal hydraulic conductivities (m/day).**

Vertical hydraulic conductivities

Table 12 summarises the vertical hydraulic conductivity bounds used for PEST calibration and Figure 35 shows the distribution of vertical hydraulic conductivity obtained in each model layer after PEST calibration process.

- **Table 12 Vertical hydraulic conductivity bounds for PEST**

Zone	Layer	Initial	Lower bound	Upper bound
Kz	**1**	**0.2**	**0.02**	**20**
Kz	**2**	**0.2**	**0.02**	**20**
Kz	**3**	**0.2**	**0.02**	**20**

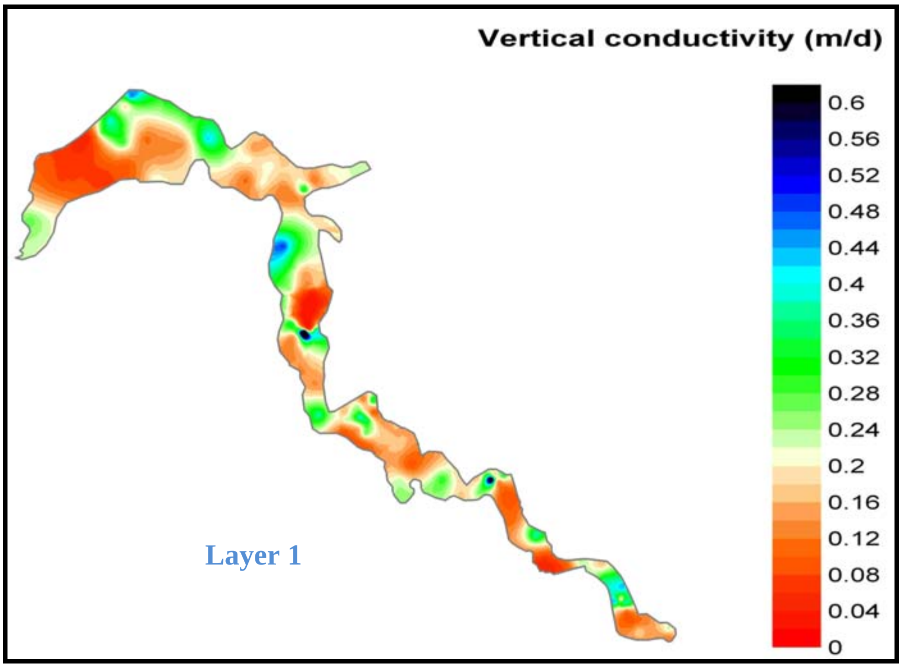

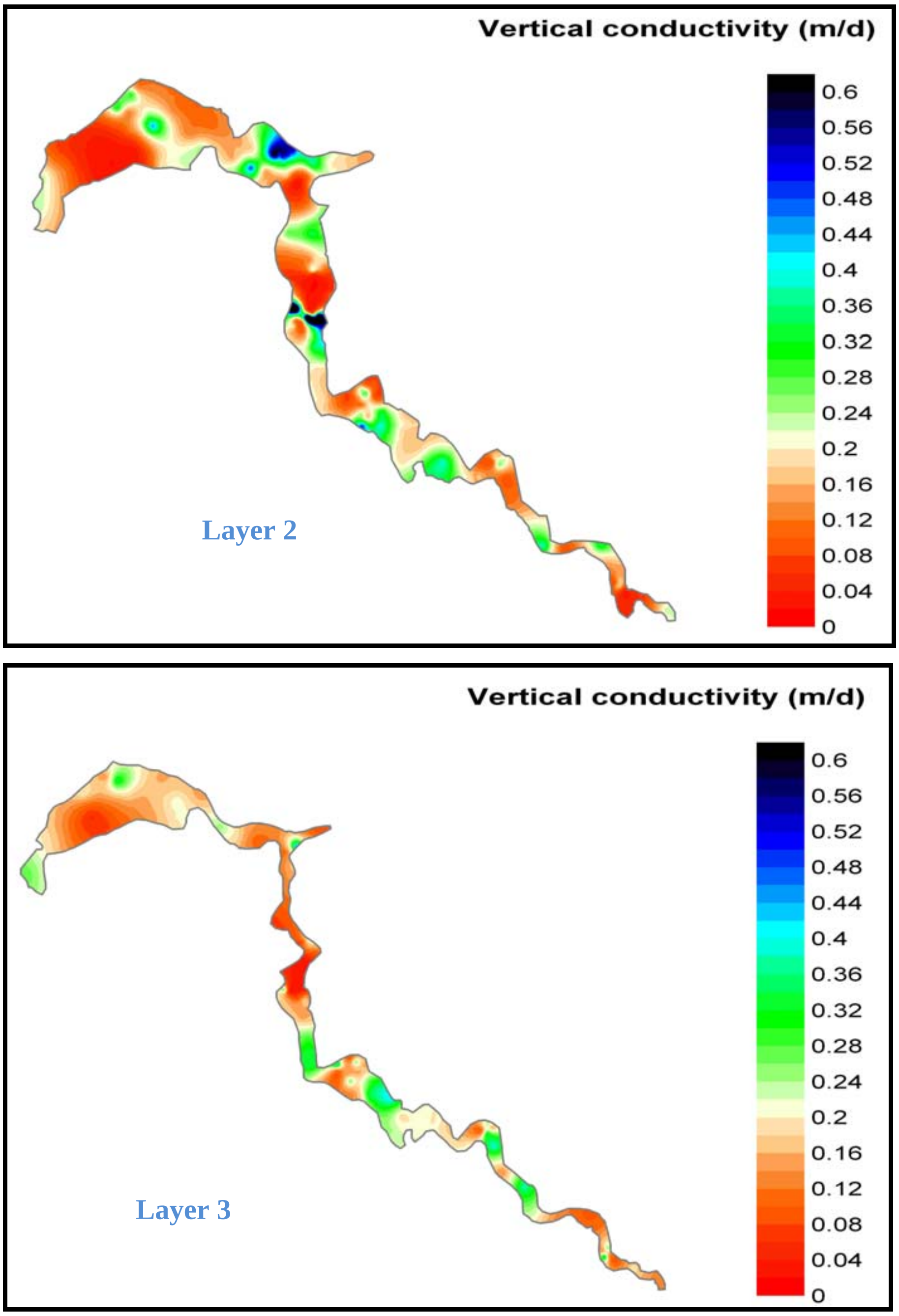

- **Figure 35. Vertical hydraulic conductivity (m/day).**

4.3.2. Specific Yield

Table 13 summarises specific yield bounds used for PEST calibration and Figure 36 shows the distribution of specific yield obtained in each model layer after PEST calibration process.

.

▪ **Table 13 Specific Yield Bounds for PEST**

Zone	Layer	Initial	Lower	Upper
Sy	**1**	0.1	0.01	0.4
Sy	**2**	0.1	0.01	0.4

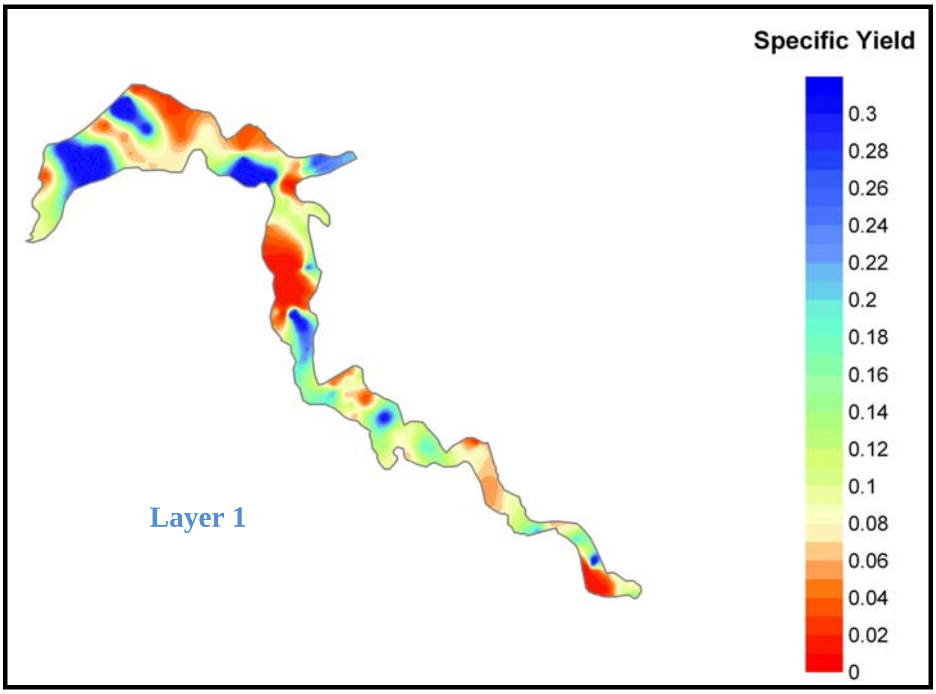

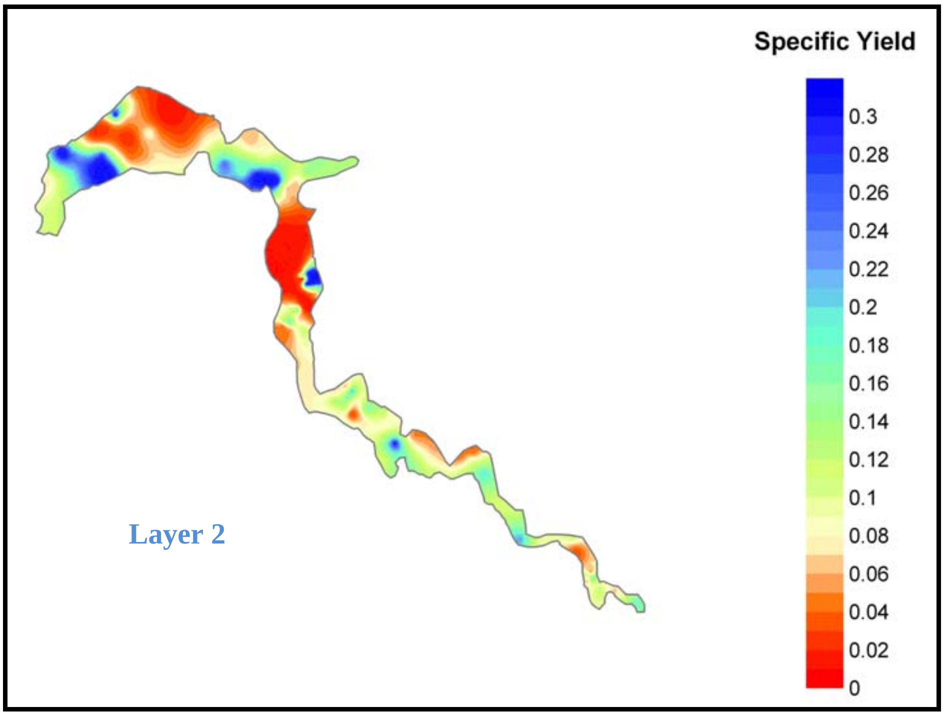

■ **Figure 36. Specific yield as calibrated by PEST.**

4.3.3. Recharge coefficients

Recharge coefficients are defined as the percentage of rainfall that would recharge the aquifer for each of the recharge zones detailed in chapter 3.6. These parameters were bound by values reported in Table 14 to Table 17. Recharge is the most sensitive parameter and it is the main driver of the calibration process. The PEST Regularisation process was adopted to maintain homogeneity between neighbouring values. Nevertheless in the upstream part of the model, PEST required high values of recharge to match calculated and observed heads. In the downstream part of the model PEST required the lowest allowed rate of recharge to get the best fit between observed and calculated heads. This behaviour may indicate actual variation in recharge rate along the Macquarie alluvial basin, but it could also possibly indicate that the model recharge rate is compensating for inaccuracies or omissions in the model. Factors such as observation measurement error, either in observed groundwater or river stage elevation, or limitations in the conceptual model may contribute to model inaccuracy. Table 14and Table 15 present the dryland recharge and irrigation recharge factors respectively.

- **Table 14 : Dryland recharge**

Zone	Initial	Lower bound	Upper bound	Sensitivity Rank	% of rainfall
1	**5**	**1**	**20**	*9*	**1**
2	**5**	**1**	**20**	*2*	**1**
3	**5**	**1**	**20**	*3*	**1**
4	**5**	**1**	**20**	*8*	**20**
5	**5**	**1**	**20**	*24*	**1**
6	**5**	**1**	**20**	*59*	**3.4**
7	**5**	**1**	**20**	*120*	**1**
8	**5**	**1**	**20**	*65*	**20**

- **Table 15 : Irrigation recharge**

Zone	Initial	Lower bound	Upper bound	Sensitivity rank	% of diverted water
9	**10**	**1**	**20**	*19*	**1**
10	**10**	**1**	**20**	*22*	**1**
11	**10**	**1**	**20**	*88*	**1**
12	**10**	**1**	**20**	*77*	**1**
13	**10**	**1**	**20**	*62*	**1**
14	**10**	**1**	**20**	*116*	**1.15**
15	**10**	**1**	**20**	*523*	**2.3**
16	**10**	**1**	**20**	*505*	**12.1**

The calibrated flood factors presented in Table 16 are generally low downstream and higher upstream illustrating the fact that flood events have a more noticeable effect on the groundwater levels for the upstream bores than they have downstream.

- **Table 16 : Flood inundation recharge**

Zone	Initial	Lower bound	Upper bound	Sensitivity rank	% of Flood
1 & 9	**5**	**1E-5**	**200**	*91*	**1**
2 & 10	**5**	**1E-5**	**200**	*53*	**1.4**
3 & 11	**5**	**1E-5**	**200**	*11*	**5.3**
4 & 12	**5**	**1E-5**	**200**	*93*	**0.9**
5 & 13	**5**	**1E-5**	**200**	*141*	**8.9**
6 & 14	**5**	**1E-5**	**200**	*512*	**15.6**
7 & 15	**5**	**1E-5**	**200**	*631*	**5.3**
8 & 16	**5**	**1E-5**	**200**	*530*	**18.3**

The hill slope run on recharge factors are presented Table 17. Again, in the upstream recharge regions (particularly in Zone 22) PEST required as much recharge as possible to optimise the match between observed and calculated hydrographs. Nevertheless the calibration is not sensitive to the parameter for Zone 22 and despite PEST requiring as much water as possible, the impact on hydrographs is limited.

- **Table 17 : Hill slope run on**

Zone	Initial	Lower bound	Upper bound	Sens. rank	% of rainfall
17	**100**	**0.1**	**200**	*1*	**35.9**
18	**100**	**0.1**	**200**	*41*	**0.6**
19	**100**	**0.1**	**200**	*4*	**4.6**
20	**100**	**0.1**	**200**	*45*	**22**
21	**100**	**0.1**	**200**	*209*	**4**
22	**100**	**0.1**	**200**	107	**42**

4.3.4. River conductance term

The river was divided into eight segments of similar length. The river conductance term for each of the eight segments was modified during calibration to achieve the best fit with near river monitoring bores.

River conductance is shown to have a relatively low sensitivity ranking suggesting the model calibration is not strongly influenced by the value of this parameter. A relatively high lower bound was adopted (1000) for this parameter to try to avoid drying of cells near the river that host extraction wells.

Regularisation of the river conductance was applied to achieve as much homogeneity of conductance along the river as possible. The calibrated river cell conductance terms and their sensitivity rankings are presented in Table 18.

- **Table 18 Calibrated River Conductance Terms**

Reach	Sensitivity rank	Lower Bound	Upper Bound	Calibrated Value
1	*86*	1000	5000	**1000**
2	*90*	1000	5000	**1000**
3	*67*	1000	5000	**3440**
4	*42*	1000	5000	**1000**
5	*66*	1000	5000	**1340**
6	*85*	1000	5000	**1000**
7	*76*	1000	5000	**1000**
8	*113*	1000	5000	**1000**

4.3.5. GHB conductance term

The GHB conductance term has little influence on the calibration as illustrated by the low sensitivity of the calibration to this parameter. The calibrated GHB conductance terms and their sensitivity rankings are presented in Table 19.

- **Table 19 Calibrated River Conductance Terms**

Reach	Head	Lower Bound	Upper bound	Sen. rank	Cond
1	229	*1000*	*5000*	*717*	**1000**
2	238.6	*1000*	*5000*	*481*	**1540**
3	250	*1000*	*5000*	*224*	**1940**
4	272	*1000*	*5000*	*318*	**1000**
5	289	*1000*	*5000*	*482*	**1310**
6	288	*1000*	*5000*	*891*	**1000**

4.4. Model sensitivity

Immediately after it calculates the Jacobian matrix (the Jacobian matrix being composed of the derivatives of each “model-generated observation” with respect to each parameter), PEST writes composite parameter sensitivities to a “parameter sensitivity file” with the extension “.sen”.

The relative composite sensitivity of a parameter is obtained by multiplying its composite sensitivity by the magnitude of the value of the parameter. It is thus a measure of the composite changes in model outputs that are incurred by a fractional change in the value of the parameter.

It is important to note that composite sensitivities recorded in the parameter sensitivity file are sensitivities “as PEST sees them”. In the current model all parameters are log-transformed and sensitivity is expressed with respect to the log of the parameters.

However, the calculated sensitivities allow parameters to be ranked according to their effect on the objective function. The most sensitive parameters (highest values of sensitivity) have the greatest impact on the calibration if its value were to be modified. Table 20 lists the 25 most sensitive parameters. The four most sensitive parameters are within the recharge group emphasizing the importance of this parameter in the model calibration.

- **Table 20 The 25 most sensitive model parameters.**

Param	Group*	Initial_Value	Sensitivity	Rank
fslope3	rch	100	1.04E-02	1
prain2	rch	5	4.02E-03	2
prain3	rch	5	3.43E-03	3
fslope5	rch	100	2.34E-03	4
kpl2p27	kp	10	2.22E-03	5
kzl2p27	kz	0.2	2.17E-03	6
kpl1p37	kp	5	1.94E-03	7
prain4	rch	5	1.87E-03	8
prain1	rch	5	1.59E-03	9
kpl2p47	kp	10	1.59E-03	10
fflood3	rch	5	1.49E-03	11
kpl2p46	kp	10	1.26E-03	12
spl1p34	sp	0.1	1.18E-03	13
kpl2p37	kp	10	1.15E-03	14
kpl3p37	kp	10	1.15E-03	15
kpl1p42	kp	5	1.13E-03	16
kpl1p53	kp	5	1.03E-03	17
kpl1p33	kp	5	9.99E-04	18
firrig1	rch	10	9.96E-04	19
kpl1p46	kp	5	9.61E-04	20
kpl2p36	kp	10	9.49E-04	21
firrig2	rch	10	9.48E-04	22
kpl1p44	kp	5	9.43E-04	23
prain5	rch	5	9.39E-04	24
kpl3p47	kp	10	9.17E-04	25

* rch is recharge, kp is horizontal hydraulic conductivity, kz is vertical hydraulic conductivity and sp is specific yield

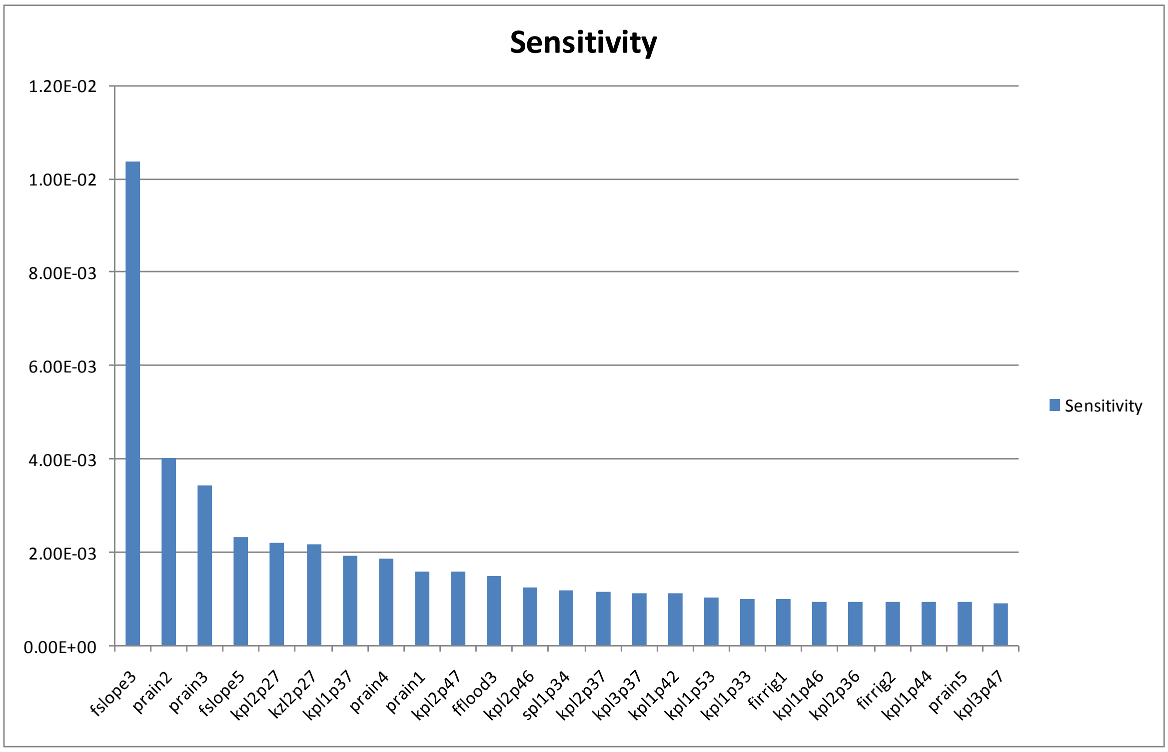

- **Figure 37 The 25 most sensitive parameters with relative sensitivity**

4.5. Calibration statistics

Modelling guidelines (MDBC, 2000) recommend evaluation of the success of calibration using both qualitative (visual comparison) and quantitative (statistical) terms. The discussions in the preceding sections provided a qualitative assessment of the calibration. Quantitative measures assessing calibration usually involve mathematical and graphical comparisons between measured and simulated aquifer heads and the calculation of statistics regarding residuals. The two plots presented in Figure 38 provide a comparison between the observed target water levels and corresponding model simulated water levels. The first of these plots is a scattergram of observed heads and corresponding model simulated heads. A 45° line through the origin represents a perfect calibration with a coefficient of determination of one (R2 = 1). The extent of scatter about this line is regarded as a measure of how good the model calibration is. Some minor discrepancies between the observed and simulated aquifer heads are noticeable, which are not uncommon in a model of this magnitude.

The other plots Figure 39 and Figure 40 presents the probability distribution of residuals or errors (the difference between observed and simulated heads) and the sorted absolute value of the residuals. A positive residual indicates an overestimate by the model whereas a negative residual is an underestimate. In summary, nearly 70% of the simulated heads are underestimated and 30% are overestimated. Though, 60% of the calculated head are within a meter from the observed head and 85% are within 2m.

There are several other error statistics commonly used to evaluate the comparison between observed and simulated values of head (Anderson and Woessner, 1992). The most common statistic values are summarised in Table 21. The mean error (ME) or mean sum of residuals (MSR) is the average of the differences between observed and simulated heads. However, a zero value of MSR does not necessarily indicate a perfect match between observed and simulated heads because positive and negative errors can average to zero. The root mean square (RMS), which is calculated by taking the square root of the average of the squared differences between observed and simulated heads, is a more useful statistic because it evaluates the spread of the errors by approximating the standard deviation of the errors. Modelling guidelines (MDBC, 2000) rate RMS as the best error measure if errors are normally distributed. The scaled root mean square (SRMS) is another error measure commonly used. It is defined as the ratio of RMS to the range of head measurement expressed as a percentage. A SRMS value less than 5% indicates that errors are only a small part of the overall model response (MDBC, 2000).

At the end of the calibration process the normalised SRMS error was 3.5%. Figure 38 displays the observed heads plotted against their calculated equivalent.

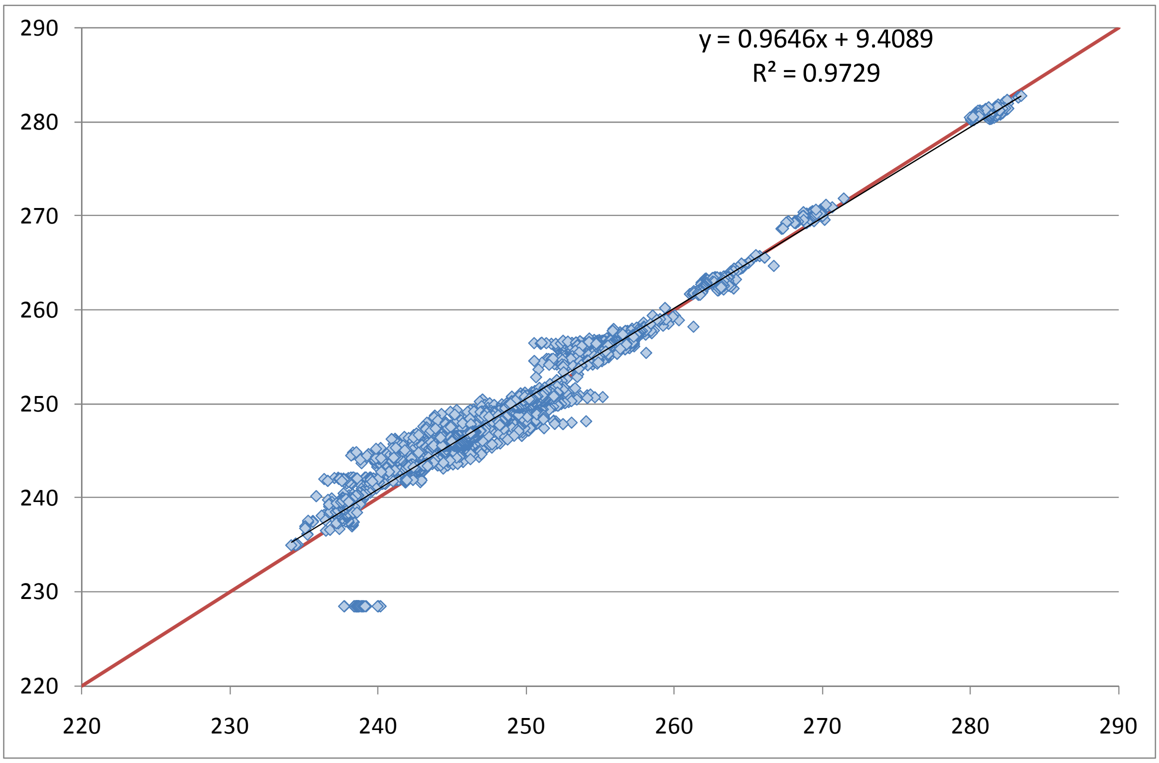

- **Figure 38. Observed versus Calculated heads**

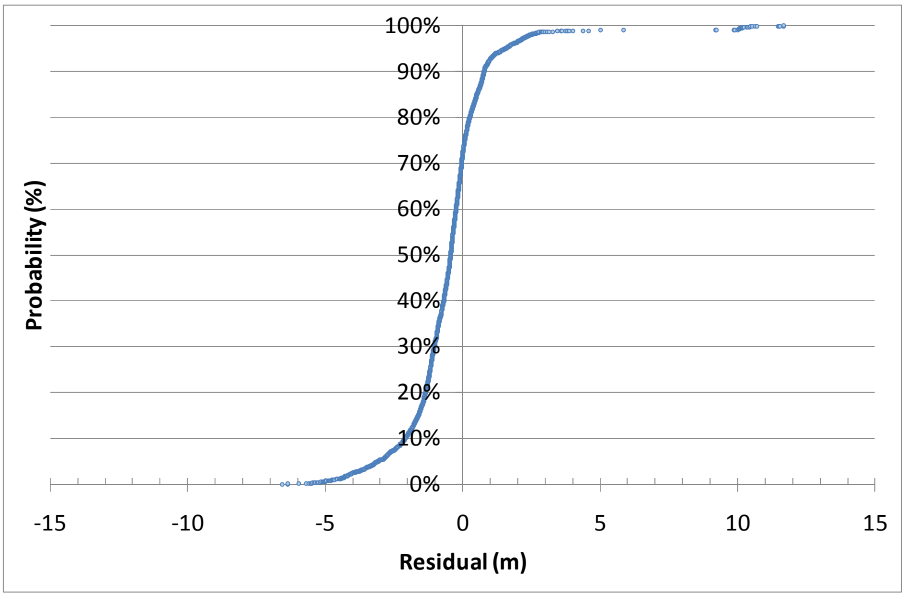

- **Figure 39. Sorted residual**

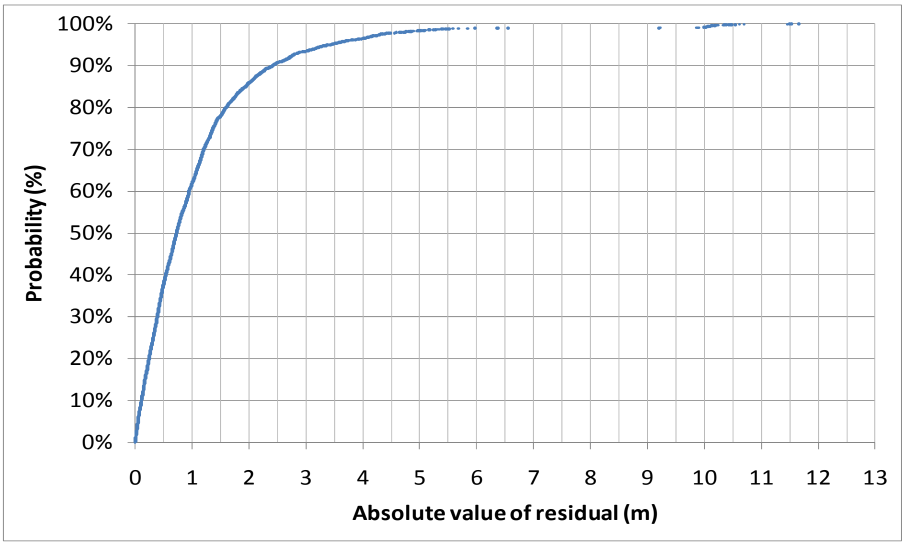

- **Figure 40. Sorted absolute residual**
- **Table 21. Calibration statistics**

Statistic	*unit*	*Value*
Number of Observations		4761
Average Observed Head	m	251.8
Maximum Observed Head	m	283.4
Minimum Observed Head	m	234.1
Range of Observed Heads	m	49.3
Sum of Squares	m^2	14534
Mean Sum of Squares	m^2	3.05
Root mean Square	m	1.75
Scaled Root Mean Square	%	**3.55**
Sum of residuals	%	-2357
Mean Residual	m	-0.5
Coefficient of determination		0.97

4.5.1. Hydrographs

A selection of representative calibration hydrographs for each layer is shown in Figure 41 to Figure 43 below. Hydrographs for all observation bores are reported in Appendix C.

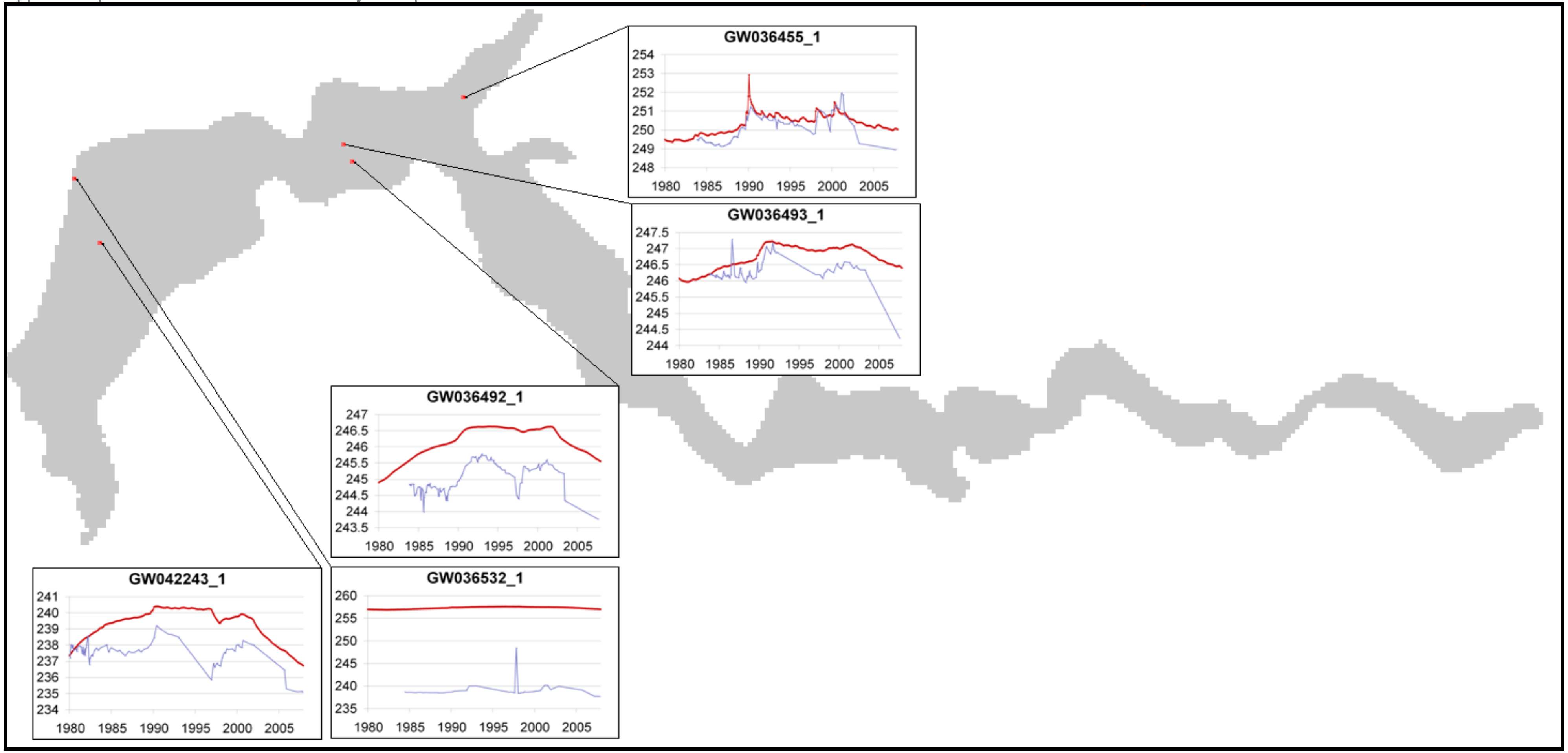

▪ **Figure 41 A Selection of Calibration Hydrographs in Layer 1**

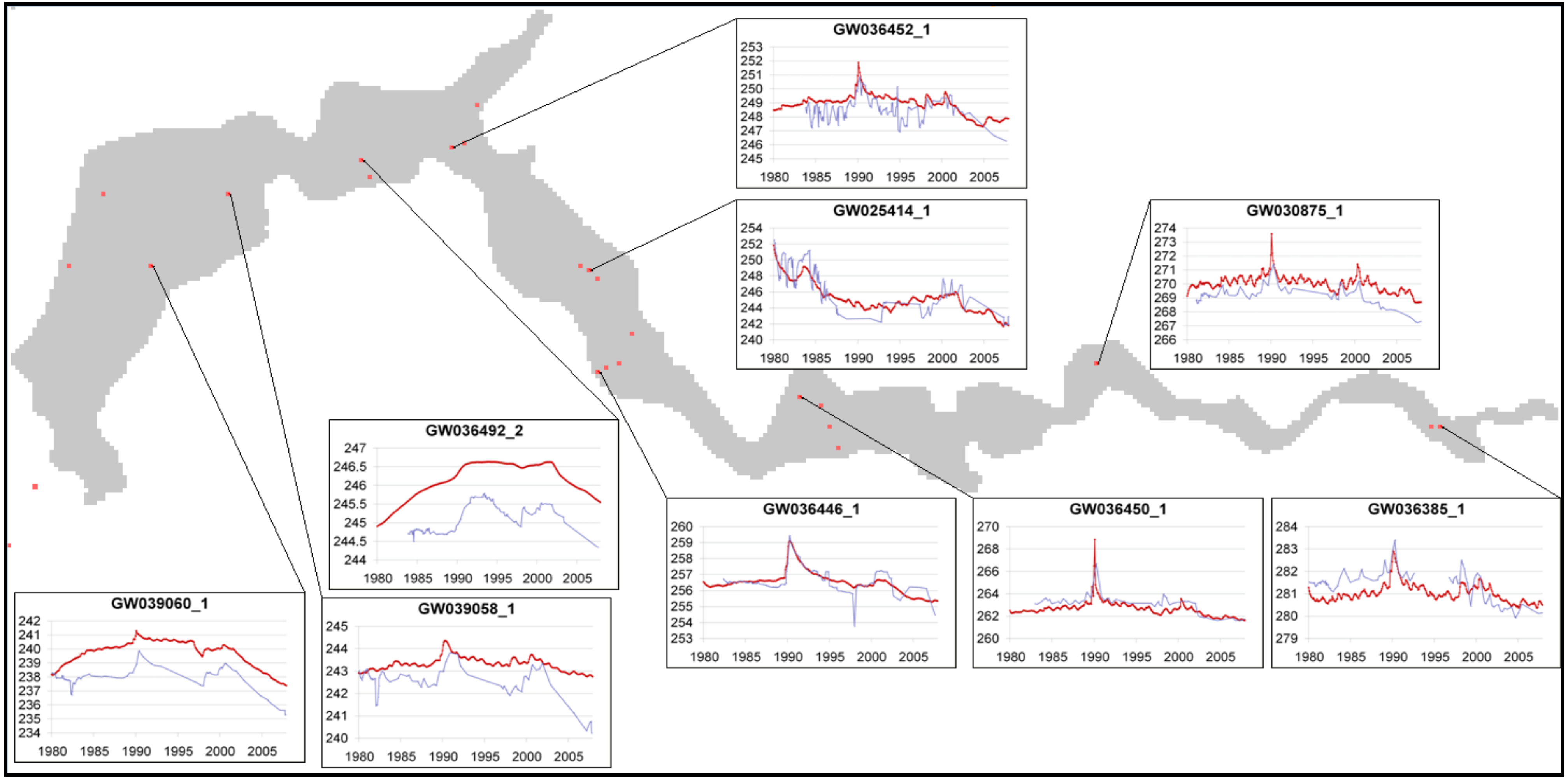

- **Figure 42 A Selection of Calibration Hydrographs in Layer 2**

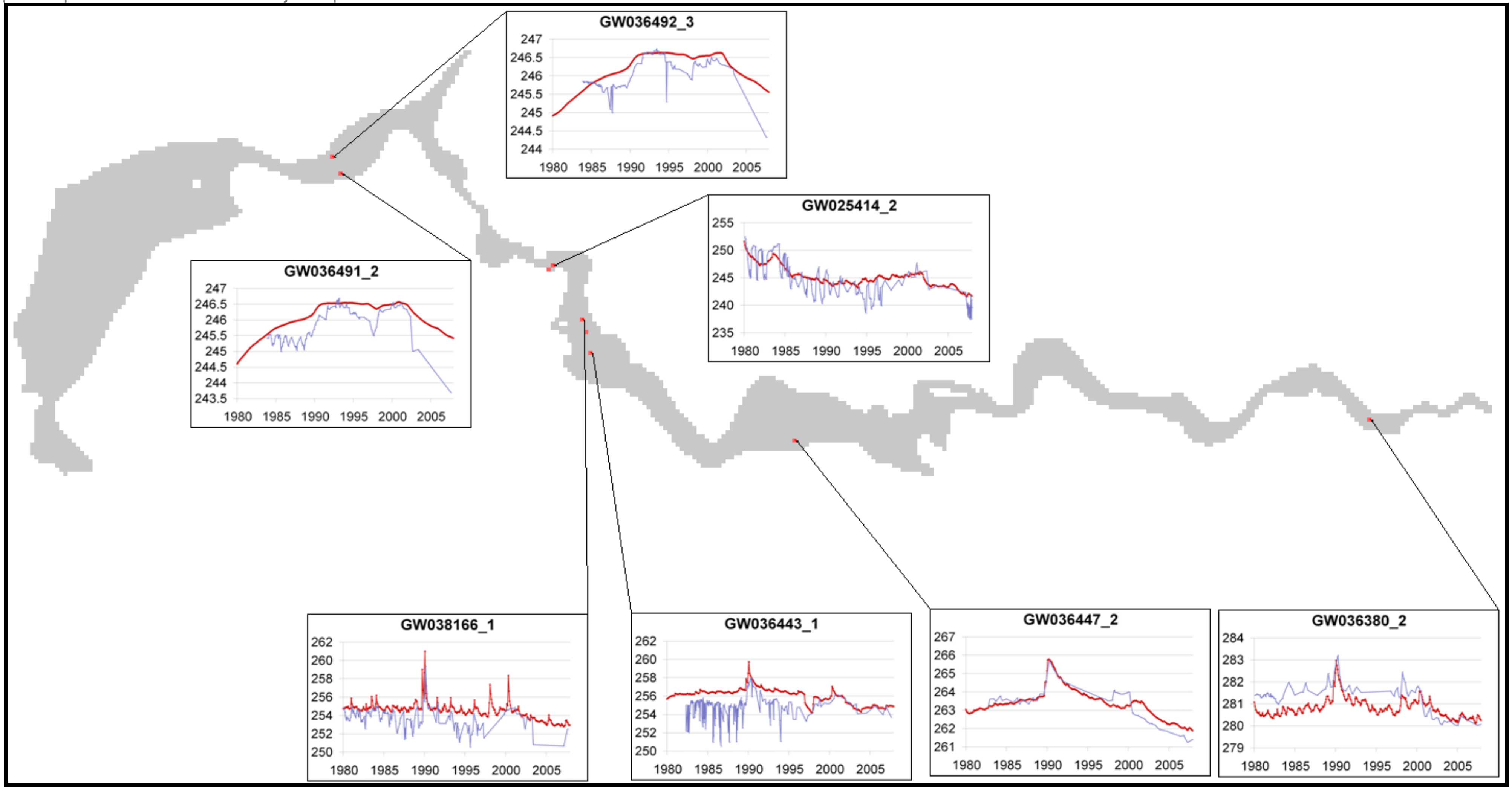

- **Figure 43 A Selection of Calibration Hydrographs in Layer 3**

4.5.2. Mass Balance

Yearly average water fluxes for the 28 years of the calibration period are presented graphically in Figure 44 and Figure 45. Figure 44 shows the annual average mass balance for each model layer with fluxes into and out of the model and between model layers shown in GL/year. Figure 45 shows the model mass balance in terms of average annual fluxes and also presents the time series plots for all fluxes for the calibration model. The mass balance illustrates that recharge and river leakage are the dominant contributors to the fluxes into the model. The flux through the General Head Boundaries (GHB's) is relatively small in comparison. The fluxes to and from storage illustrate a small imbalance with the Storage In flux being 0.8 GL/year greater than Storage Out. This suggests that there is a small net decline in groundwater level throughout the simulation run. It is assumed that this drawdown is in response to the gradual increase in groundwater pumping during the course of the calibration period.

Flows out of the model are dominated by the extraction wells and discharge to the river. The GHB and ET (evapotranspiration) fluxes are relatively small in comparison.

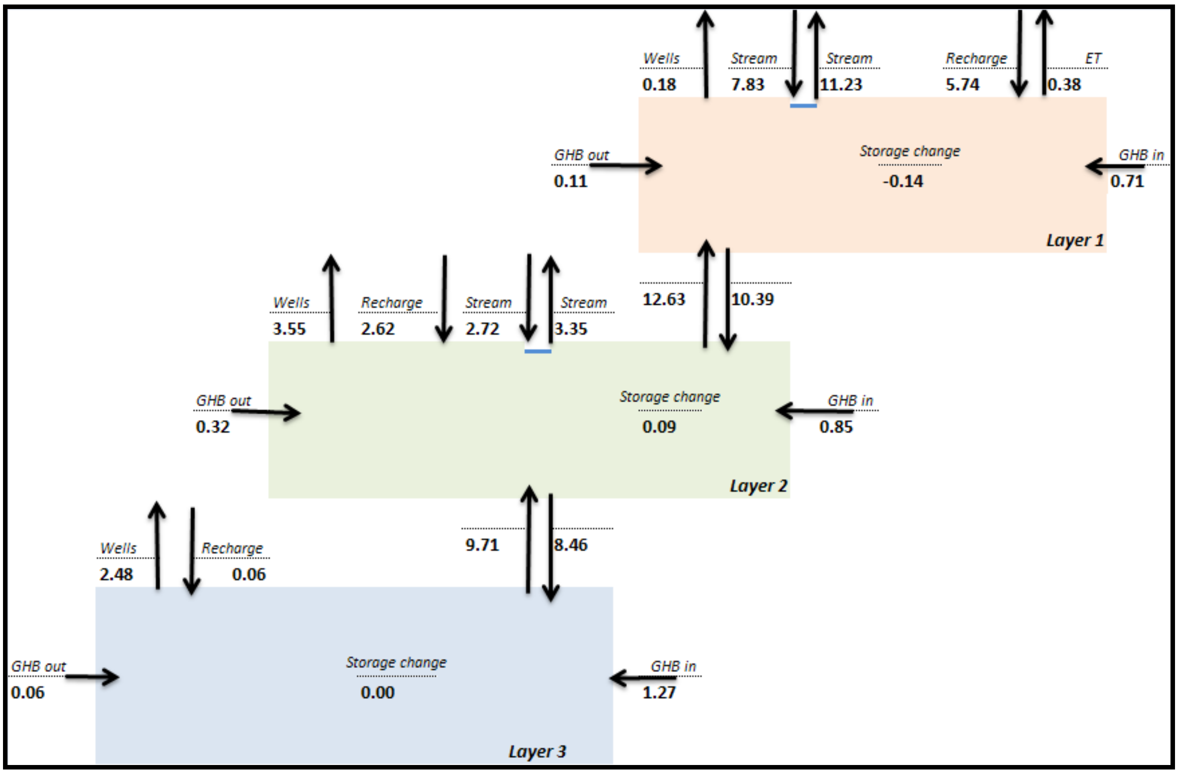

▪ **Figure 44 Average annual water balance for individual layers (Units GL/year)**

▪ **Table 22 Recharge breakdown**

Zone	Recharge (GL/year)	Recharge without flood component (GL/year)	flood (GL/year)
Dryland	***5.84***	***5.42***	*0.42*
Irrigation	***0.85***	***0.81***	*0.04*
Hill_slope	***1.72***	***1.72***	*0*
Total	*8.41*	*7.95*	*0.46*

Mass Balance Summary

FLOW IN	Storage	River_Leakage			GHBs	Recharge	Total IN
(GL/year)	10.8		10.5		2.8	8.4	32.6
FLOW OUT	Storage	Wells	River_Leak	ET	GHBs		Total Out
(GL/year)	10.8	6.2	14.6	0.4	0.5		32.6

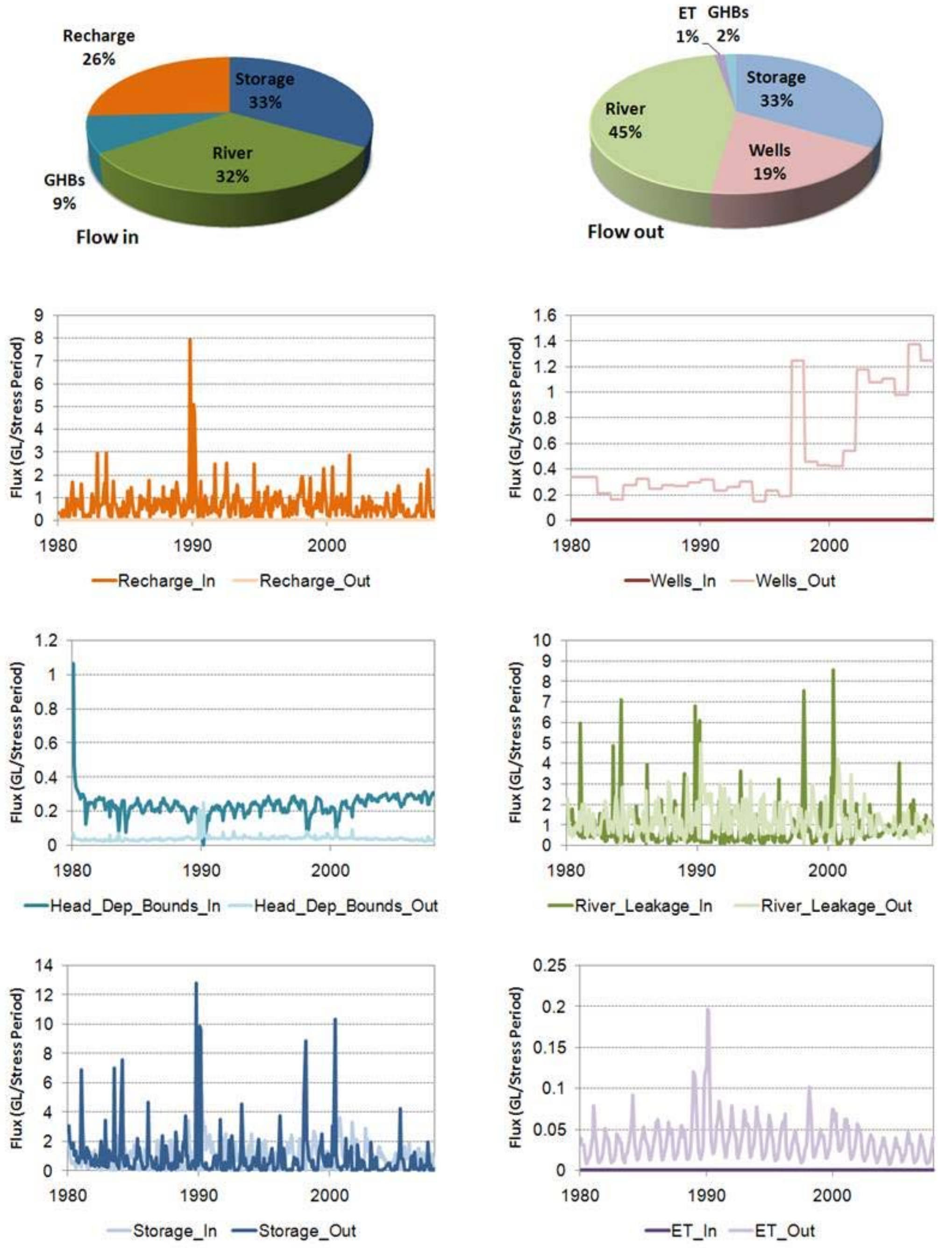

Figure 45 Mass balance for the whole model

4.6. Discussion

A consistent issue was apparent in almost all of the model calibration runs undertaken during the course of the project. This was a reduction in modelled well extraction rate due to the drying of model cells that host high yielding extraction wells. This problem was particularly apparent in the region of the model that corresponds to the Dubbo City water supply borefield and occurred even in those wells extracting water from model Layer 3 (the effective basal model layer). The phenomenon arises in the model because the MODFLOW re-wetting function has been de-activated to assist with numerical stability. In fact it is a modelling artefact and in many cases it would not be possible for the aquifer to dry or become de-saturated to the base of alluvium. In reality as water levels drop in an aquifer due to pumping the aquifer becomes partially saturated if the groundwater heads drop below the aquifer top. If extraction continues unabated the loss of saturated thickness of the aquifer leads to a loss of well productivity and wells are unable to maintain production at previous levels. Furthermore as the water levels decline the extraction pump operation is compromised and the pump will fail if water levels fall to the level of the pump intake. In other words declining groundwater levels and loss of saturated aquifer thickness leads to a decline in groundwater extraction rates that prevent the aquifer from drying completely.

The final calibrated model has been modified slightly to ensure that the aquifer does not dry and turn wells off during the calibration period. These modifications largely revolved around deepening well screens to ensure that they extract water from model Layer 3. These modifications were successful in maintaining the desired pumping rates for the duration of the model run.

Even though the modelled impacts are not necessarily real, the fact that the calibration model consistently includes drying of cells in the area of the Dubbo City water supply borefield suggests that the actual historic extraction in this region is close to the maximum that can be sustained. It is noted that the model is reasonably well calibrated in this location and hence predicted water levels are close to those measured in observation wells (refer to Group 4 Wells in Figure 43). As a result it must be assumed that water levels have declined below the top of Layer 3 in localised areas near the individual production wells. In other words it is likely that partial de-saturation of the Tertiary Aquifer has occurred in the past. This conclusion should be tested by gathering additional data on the Dubbo City water supply to:

- Confirm the groundwater extraction rates for individual wells included in the simulation,
- Review the model layer structure in this region to confirm the elevation of the top of the Lachlan Formation in the model (Model Layer 3) is consistent with local bore log information
- Determine whether there is any evidence that pumping rates have been reduced in particular bores due to excessive drawdown and loss of productivity.

5. Predictive Model Scenarios

5.1. Scenarios approach

A series of 16 predictive model scenarios have been formulated and run over a fifty years timeframe starting from June 2010. All scenarios start with initial conditions defined by water levels calculated at the end of the model calibration period (June 2008). There is a gap of two years (June 2008 to June 2010) between the end of calibration and the start of the scenarios for which no significant changes in groundwater level are assumed. The models are used to assess the potential impacts likely to arise under various future climate and groundwater extraction assumptions as follows.

The scenarios are a combination of four climate scenarios (historic, climate and future dry, medium and wet climate change assumptions) and four different levels of groundwater abstraction:

- Pre-development (no pumping)
- Current development (average of the last five years i.e. 11.4 GL/year)
- Current development (maximum annual extraction rate in the last five years i.e. 16.9 GL/year).
- Full current entitlement (i.e. 33.5 GL/year)

The combination makes a total of 16 scenarios as summarised in Table 23.

Scenarios rely on outputs from the IQQM River Model to define the river boundary conditions. The climate scenarios considered for this study are those developed by the CSIRO in the Murray Darling Basin Sustainable Yields Project (SKM, 2008). The climate assumptions relate to the 10th and 50th, 90th percentile rainfall outcomes for a number of different global climate model runs. The historic rainfall (Scenario 1a to 1d) is based on records from July 1956 to June 2006 at BOM station #065034 (Wellington).

Data for the rainfall recharge and river boundary condition were supplied by the NSW Office of Water. Table 24 shows an analysis of the four climate assumptions used in the scenarios. The table shows a comparison between the average annual rainfall for all climate assumptions and the corresponding average annual model recharge for all climate assumptions. It can be seen that the scenarios cover a range of model recharge rates between 88% and 112% of the historic recharge.

A comparison between the average river stage for the scenarios is presented in Table 25. This table shows the average river stage at station 421001 in Dubbo for the various different climate assumptions used in the scenarios.

Table 23 Scenarios construction summary

Scenario	Climate	Pumping	River Model Scenario
1a	historic	No pumping	A0
1b	historic	Current pumping - Average (= 11.4GL/Year)	A0
1c	historic	Current pumping - maximum (= 16.9 GL/Year)	A0
1d	historic	Full current entitlement (= 33.5 GL/year)	A0
2a	dry	No pumping	C0H_10
2b	dry	Current pumping (average)	C0H_10
2c	dry	Current pumping (maximum)	COH_10
2d	dry	Full current entitlement	COH_10
3a	medium	No pumping	C0M_50
3b	medium	Current pumping (average)	C0M_50
3c	medium	Current pumping (maximum)	COM_50
3d	medium	Full current entitlement	COM_50
4a	wet	No pumping	C0H_90
4b	wet	Current pumping (average)	C0H_90
4c	wet	Current pumping (maximum)	COH_90
4d	wet	Full current entitlement	COH_90

Table 24 Climatic scenarios comparison and corresponding model recharge

RAINFALL Scenarios	Historic (1)	Dry (2)	Medium (3)	Wet (4)
Average rainfall (mm/year)	**646.2**	**574.5**	**636.8**	**721.4**
Proportion of historic rainfall	*100.0%*	*88.9%*	*98.6%*	*111.7%*
Corresponding average RECHARGE scenarios				
	Historic	Dry	Medium	Wet
Dryland (GL/year)	6.30	5.61	6.21	7.02
Irrigation (GL/year)	0.79	0.74	0.78	0.85
Hill_slope (GL/year)	1.94	1.72	1.91	2.17
Total (GL/year)	**9.03**	**8.07**	**8.90**	**10.04**
Proportion of historic scenario	*100.0%*	*89.4%*	*98.6%*	*111.2%*

- **Table 25 Comparison of average river stage (station 421001 at Dubbo) for the different climate assumptions.**

	Historic (1)	Dry (2)	Medium (3)	Wet (4)
Average river stage (m)	**0.77**	**0.67**	**0.74**	**0.85**
proportion to historic scenario	*100.0%*	*86.8%*	*96.0%*	*110.6%*

5.2. Results

5.2.1. Limitation to Groundwater Extraction

During the scenarios, abstraction rates occasionally exceeded the amount that could be provided by the model and forced some cells to dry up shutting down abstraction at that location. Because the MODFLOW re-wetting option has been de-activated wells that are shut down due to de-saturation are never returned to service during the remainder of the model run. This limitation has significant impacts on calculated hydrographs and the resulting mass balances. It is an indication that rates assumed for the scenario are not sustainable and would lead to partial de-saturation of the Quaternary and Tertiary Aquifers.

Figure 46 to Figure 48 present time series of the targeted and actual modelled pumping rates. It shows that in scenario 1b the modelled pumping rate is that same as the target rate. In scenario 1c, some cells dry up reducing slightly the pump rate from a targeted 16.9 GL/year to an actual 16.4 GL/year. The location of drying cells for scenario 1b is illustrated in Figure 49. It shows that the drying issues occur mainly around Dubbo where there is a high density of abstraction bores. The problem is even more pronounced for scenario 1d, with higher pumping rates. Due to the drying up of some cells, the model pumping rate is reduced to an average of 29 GL/year instead of the targeted 33.5 GL/year. Figure 50 illustrates that for the scenario 1d, the drying also occurs mainly around Dubbo.

The result suggests that there is only limited capacity to increase groundwater extraction in the region of Dubbo and that continued high level extractions from this area of the aquifer may not be sustainable in the long term. Alternative options for obtaining groundwater for the Dubbo City water supply may involve drilling of wells some distance from the city to help to distribute the pumping over a wider area and thereby reduce the localised impacts associated with closely spaced extraction wells.

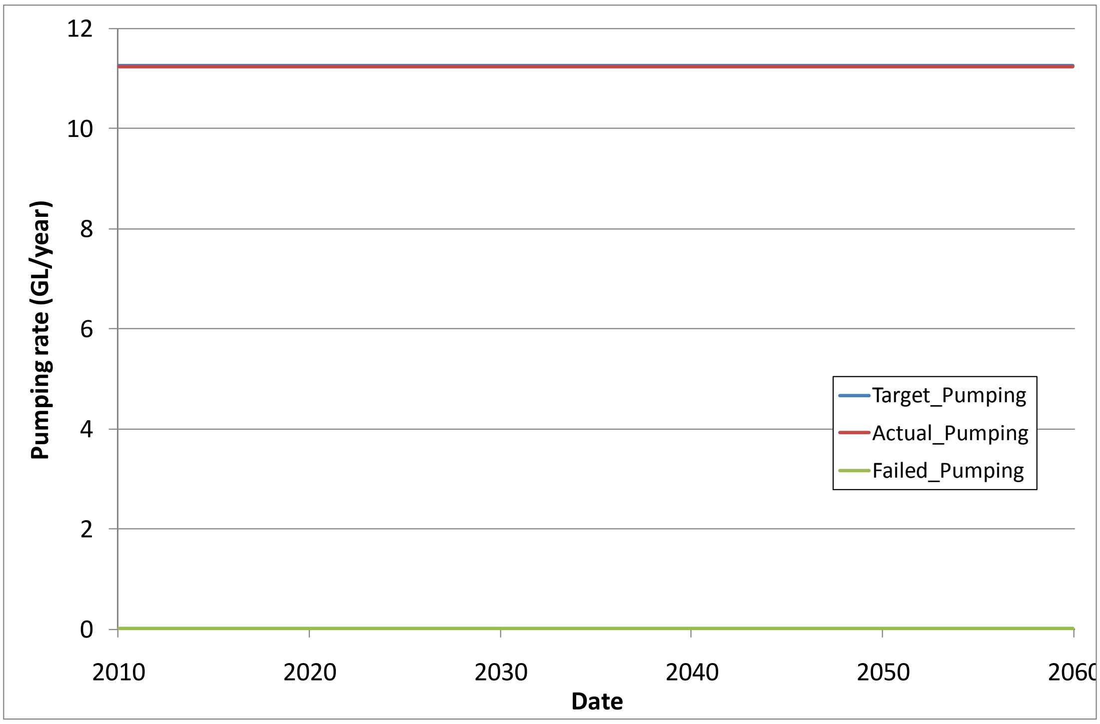

▪ **Figure 46 comparison of Targeted and actual abstraction for Scenario 1b**

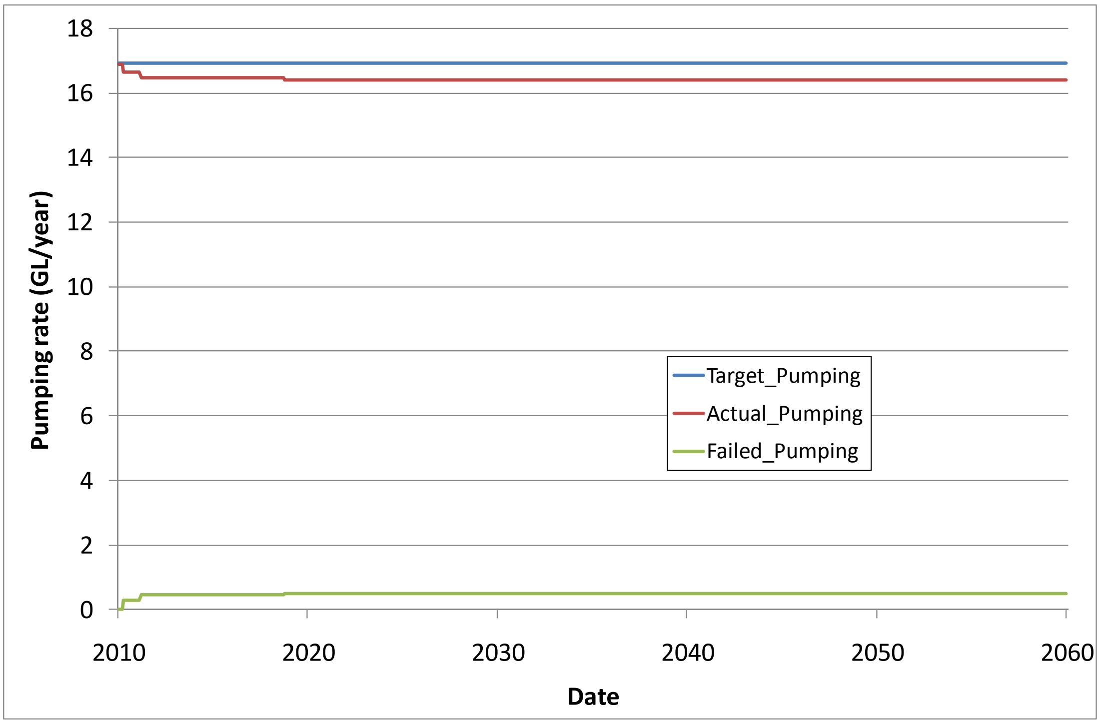

▪ **Figure 47 comparison of Targeted and actual abstraction for Scenario 1c**

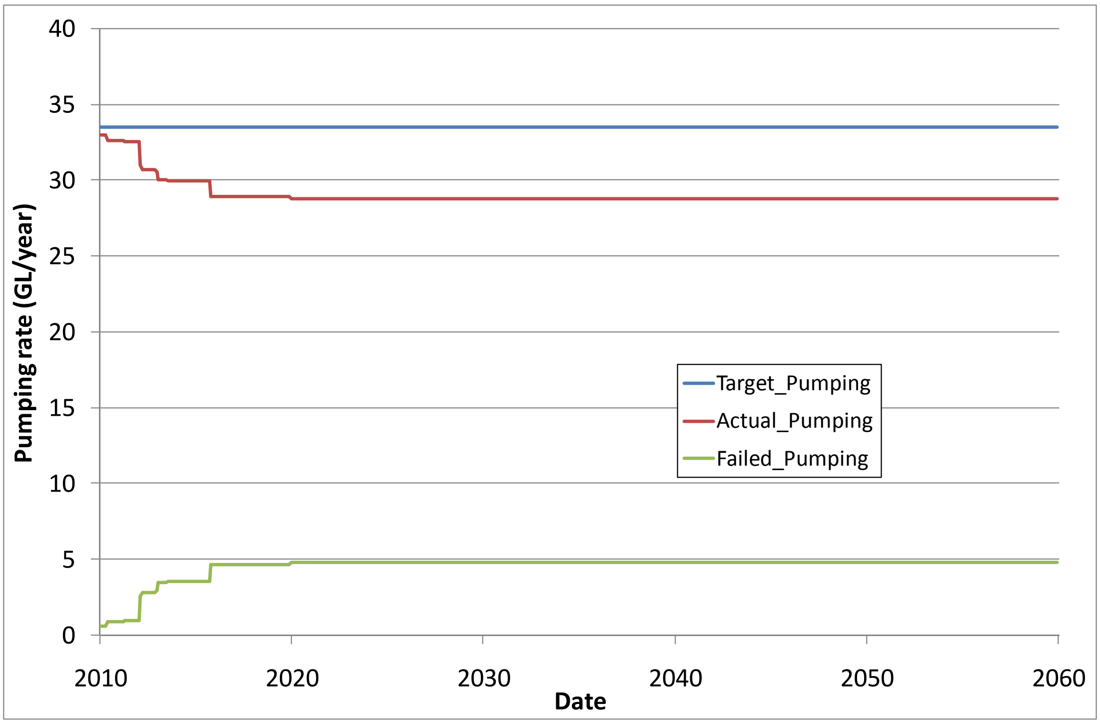

▪ **Figure 48 Comparison between targeted and actual abstraction for Scenario 1d**

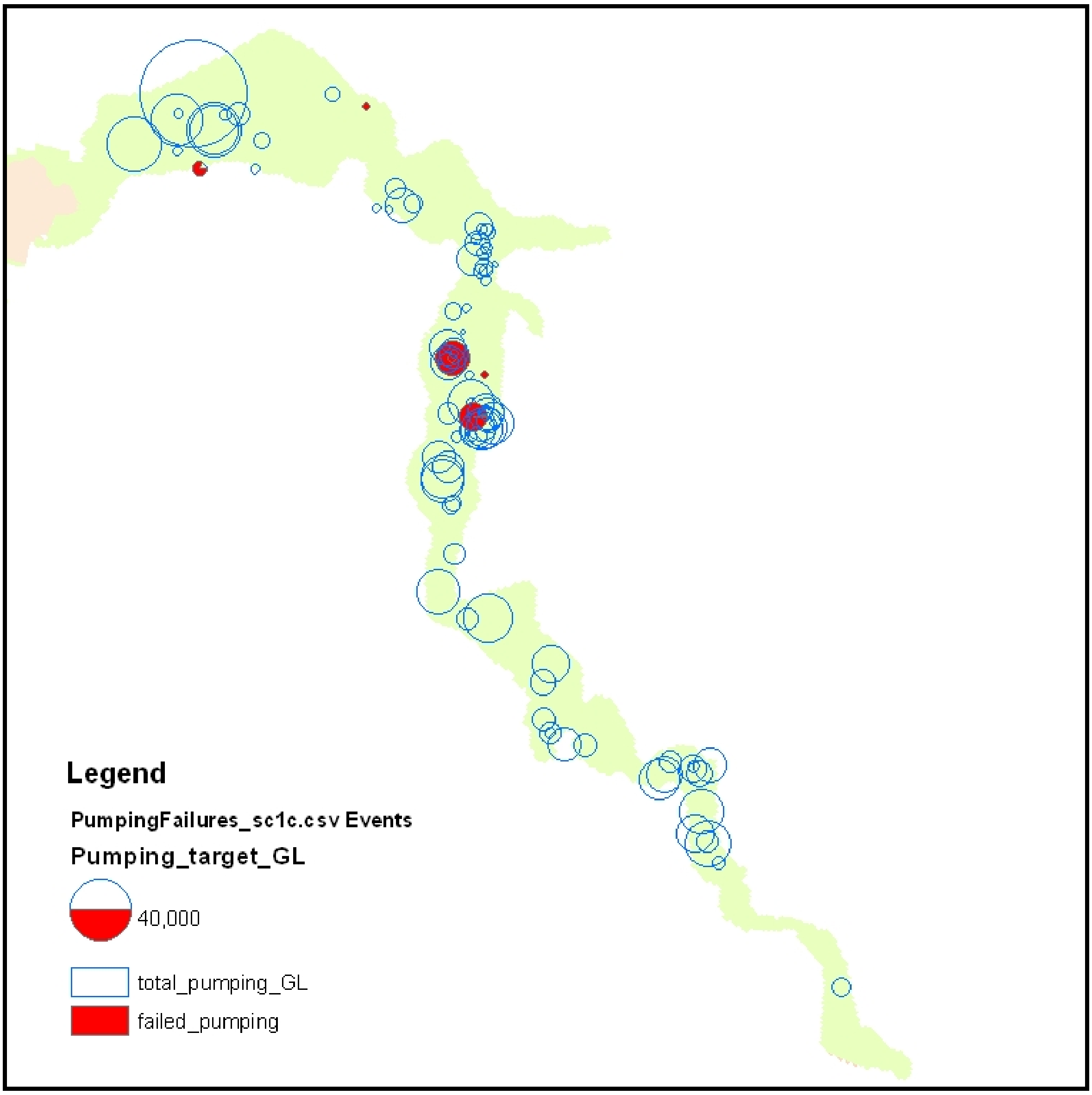

▪ **Figure 49 Pumping target for Scenario 1c and failed pumping due to drying up of cells**

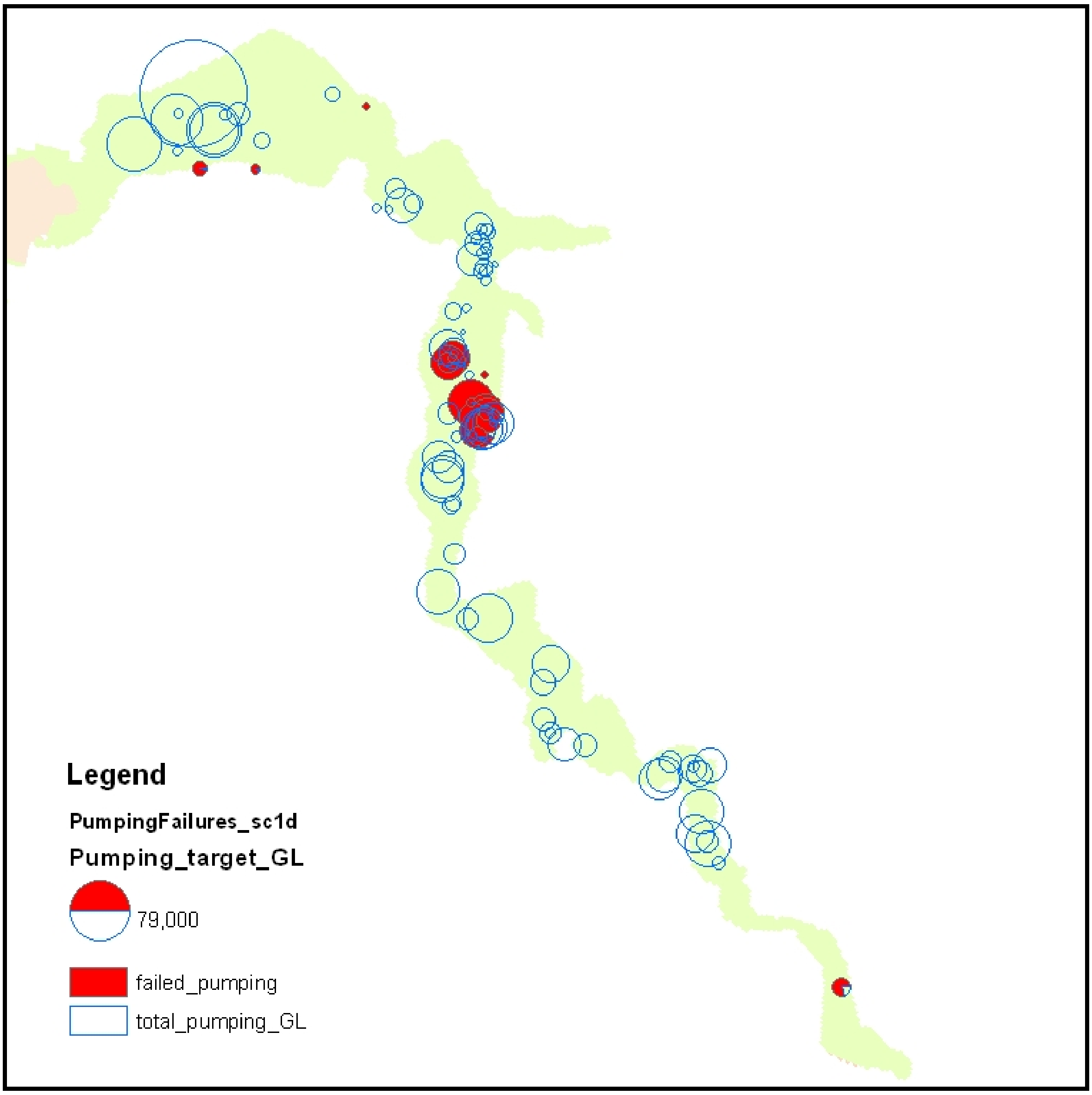

- **Figure 50 Pumping target for Scenario 1d and failed pumping due to drying up of cells**

5.2.2. Groundwater Hydrographs

Figure 51 to Figure 56 present a representative selection of hydrographs for each of the scenarios. Figure 51 to Figure 53 show the hydrographs for Scenarios 1a to 1d. These scenarios are based on historic climate with various levels of groundwater extraction. Results suggest that groundwater extraction has a profound influence on the predicted groundwater levels throughout the model domain.

Figure 54 to Figure 56 present the representative hydrographs for Scenarios 1b, 2b, 3b and 4b. Here the impact of the various climate change assumptions can be seen. In all of the ‘b’ scenarios the extraction rate is defined as 11.4 GL/year being the average of the last five years of measured groundwater extraction. Figure 54 to Figure 56 therefore illustrate the influence of future climate variability on the predicted groundwater levels in the aquifer. It is interesting to note that the climate variability has a more pronounced influence on groundwater levels in the downstream part of the aquifer compared to regions further upstream. This phenomenon is probably related to the width of the valley and hence the surface area on which the recharge fluxes are applied.

Hydrographs at the representative sites for Scenarios 2, 3 and 4 for all pumping assumptions (a, b, c and d) are presented in Appendix F

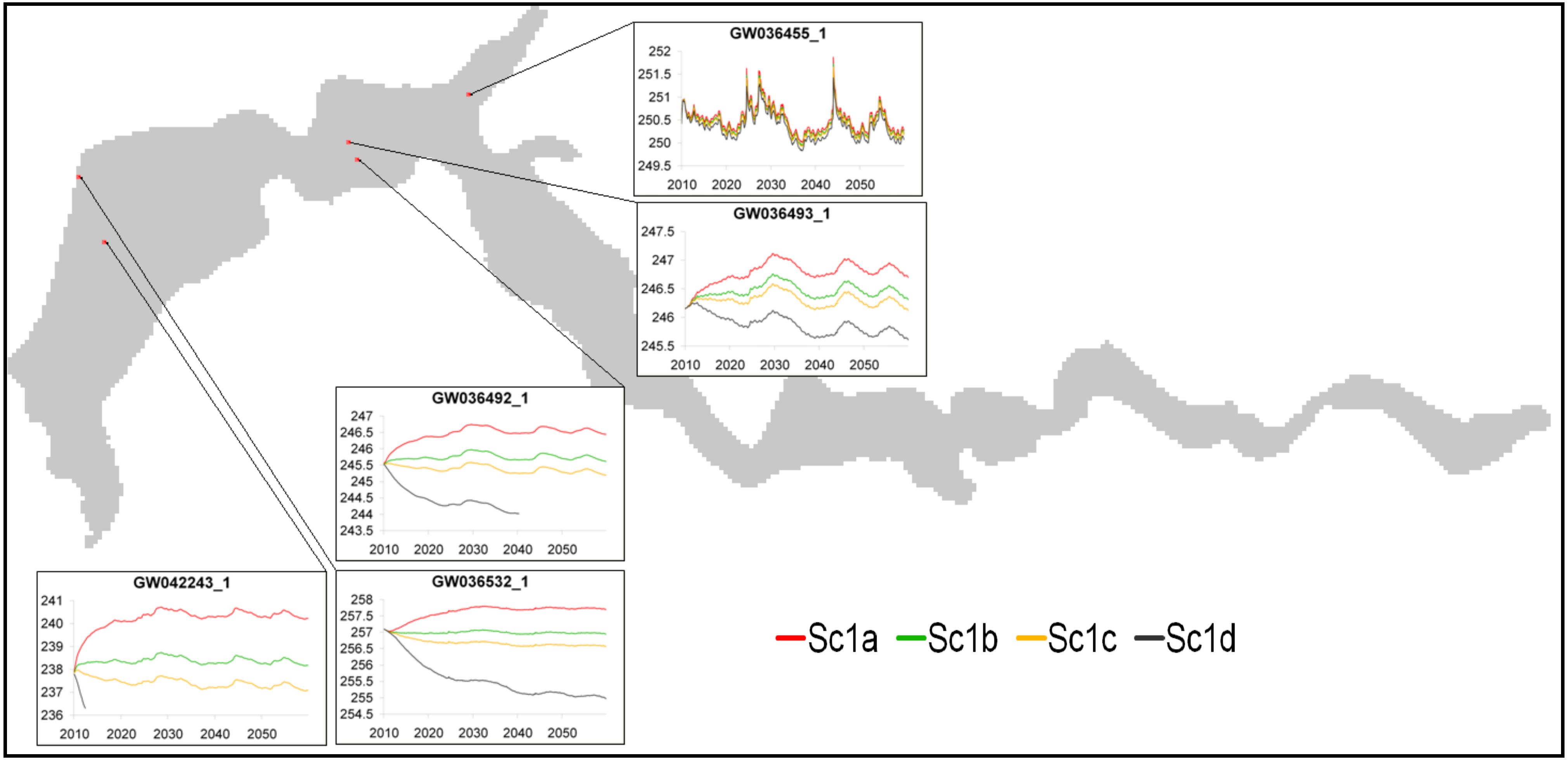

- **Figure 51 Hydrograph in Layer 1 (Blank if it's a dry cell) for scenario 1a,1b,1c,1d**

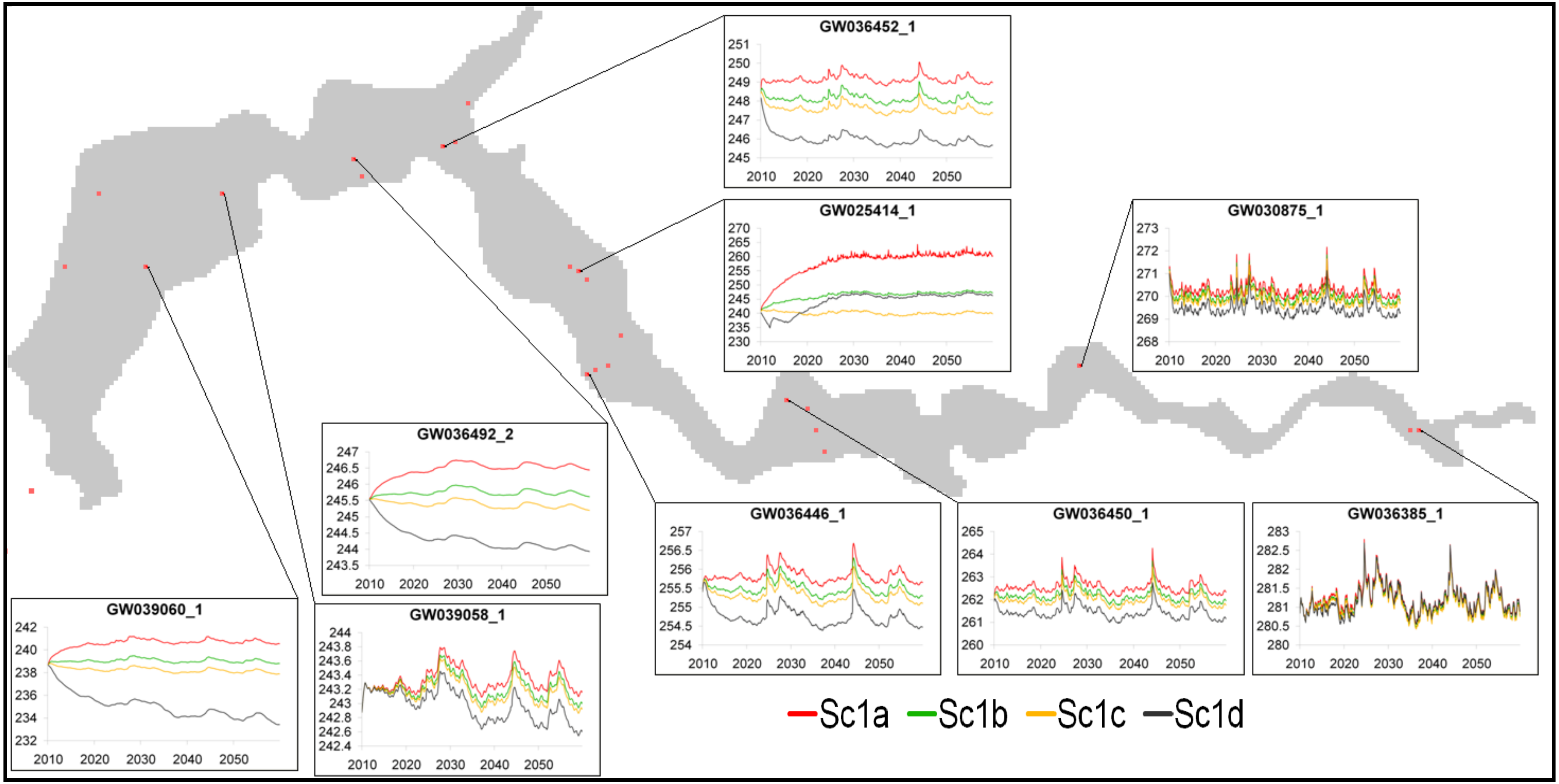

Figure 52 Selection of representative hydrographs in Layer 2 for scenario 1a,1b,1c,1d

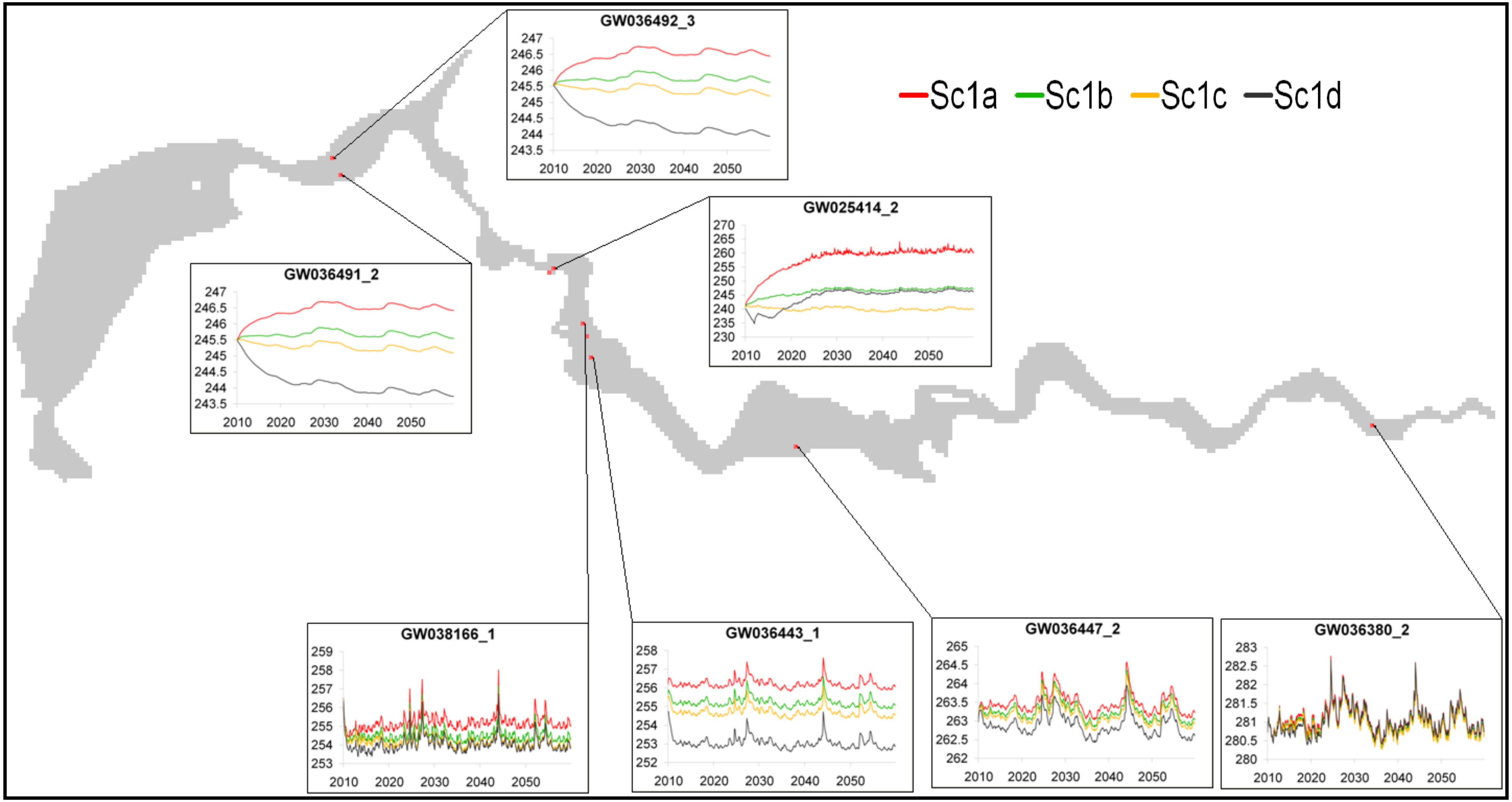

- **Figure 53 Hydrographs in Layers 3 for scenario 1a,1b,1c,1d**

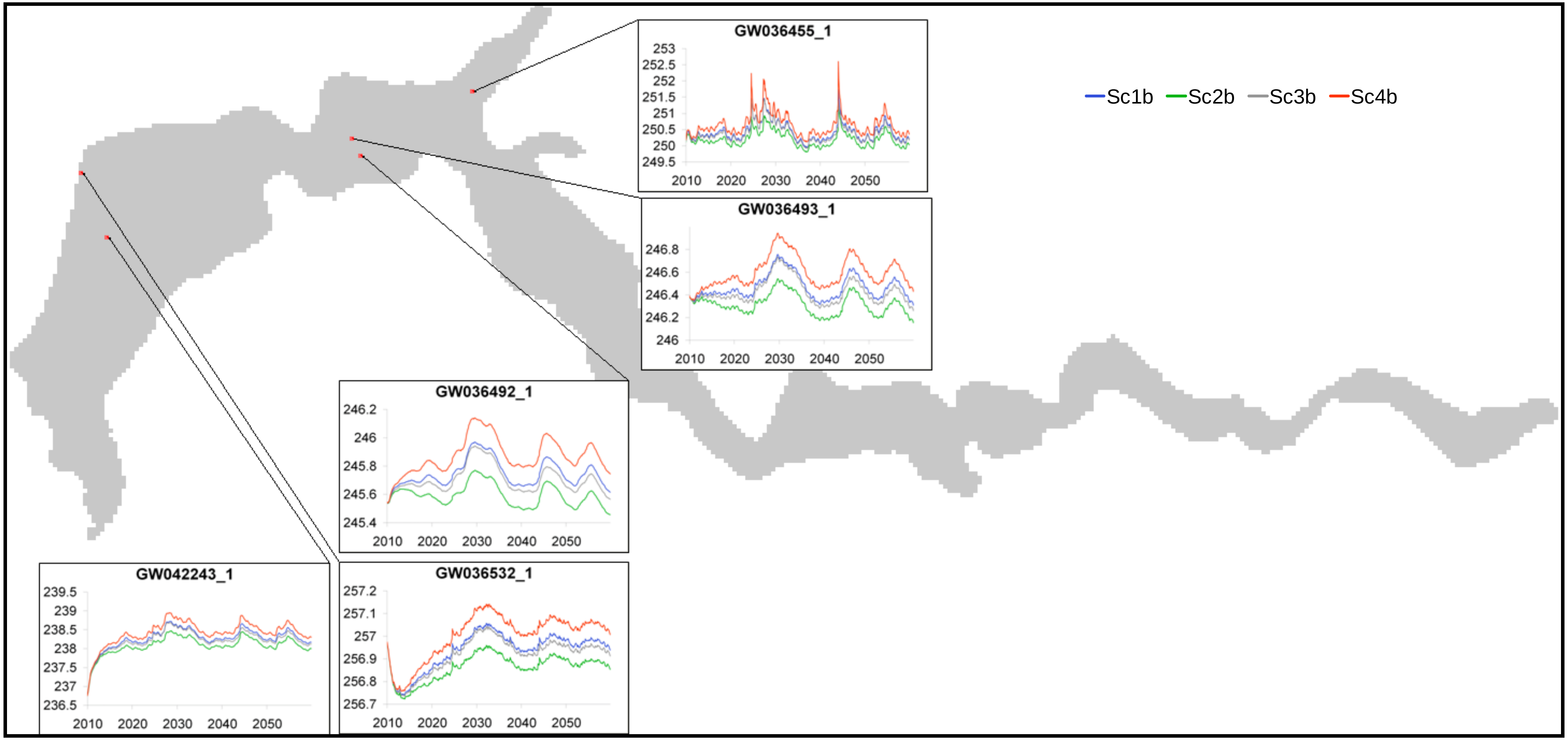

Figure 54 Hydrographs in layer 1 for scenario 1b, 2b, 3b and 4b.

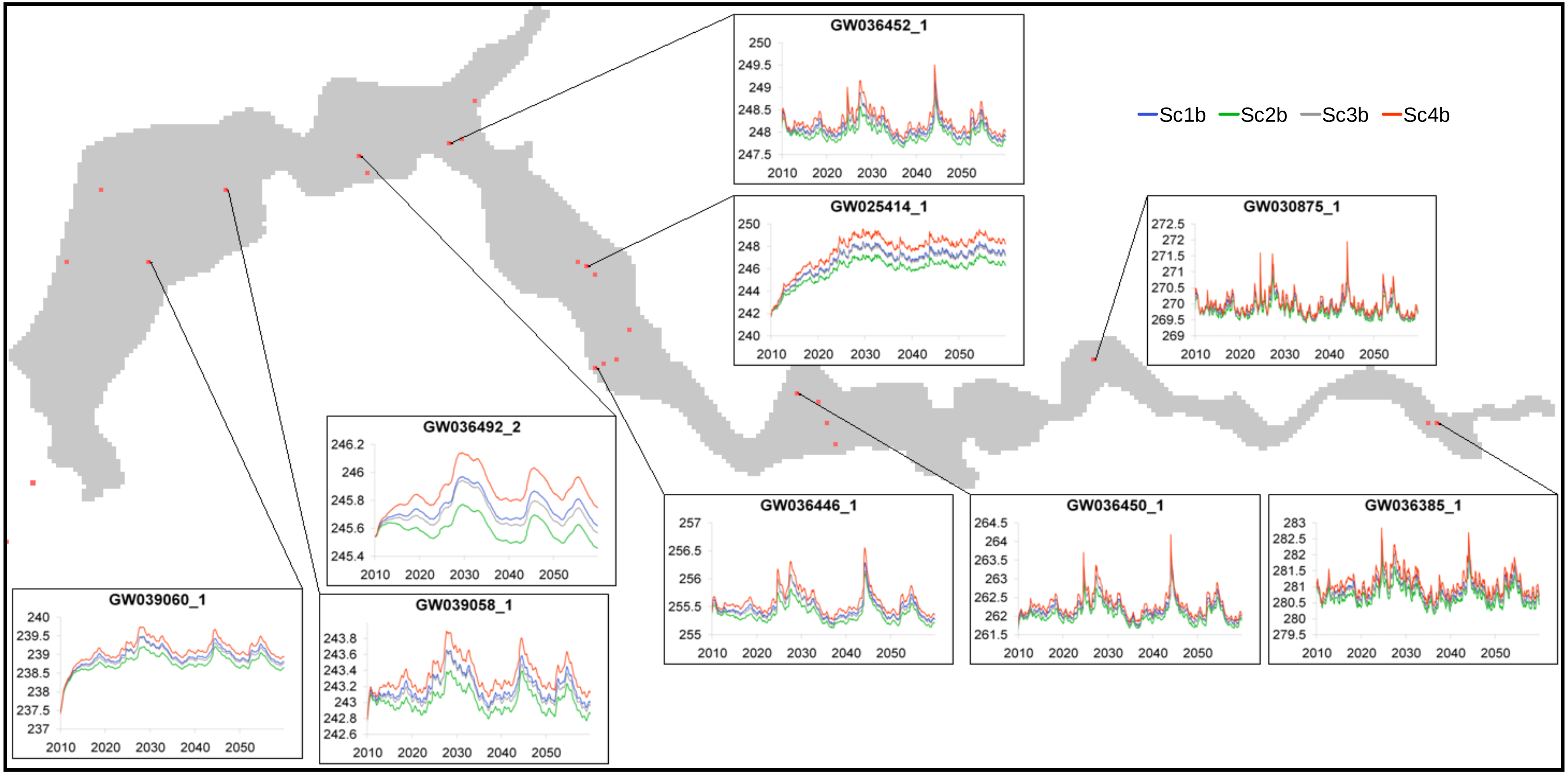

▪ **Figure 55 selection of representative Hydrographs in layer 2 for scenario 1b, 2b, 3b and 4b**

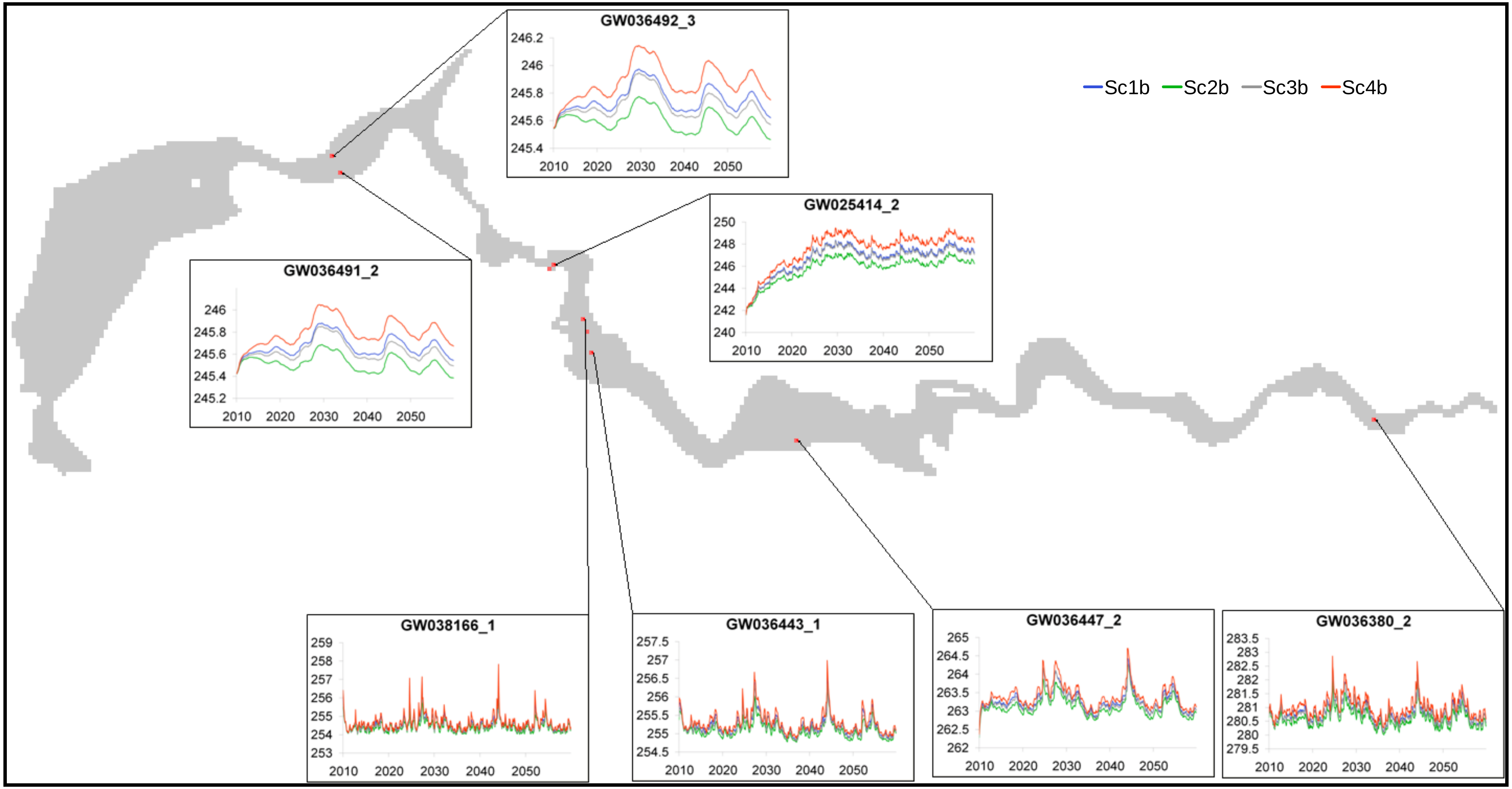

■ **Figure 56 Hydrographs in layer 3 for scenario 1b, 2b, 3b and 4b**

5.2.3. Groundwater Level Changes

Figure 57 presents the change of the water table elevation between the last time step (June 2060) and the Initial condition (June 2010). Negative changes indicate a declining water table while positive changes show an increase of the water table elevation. As mentioned above, the progressive shutting down of wells due to over abstraction and drying of productive cells in the model, creates a false impression of water level recovery in the Dubbo region particularly obvious in Scenario 1d.

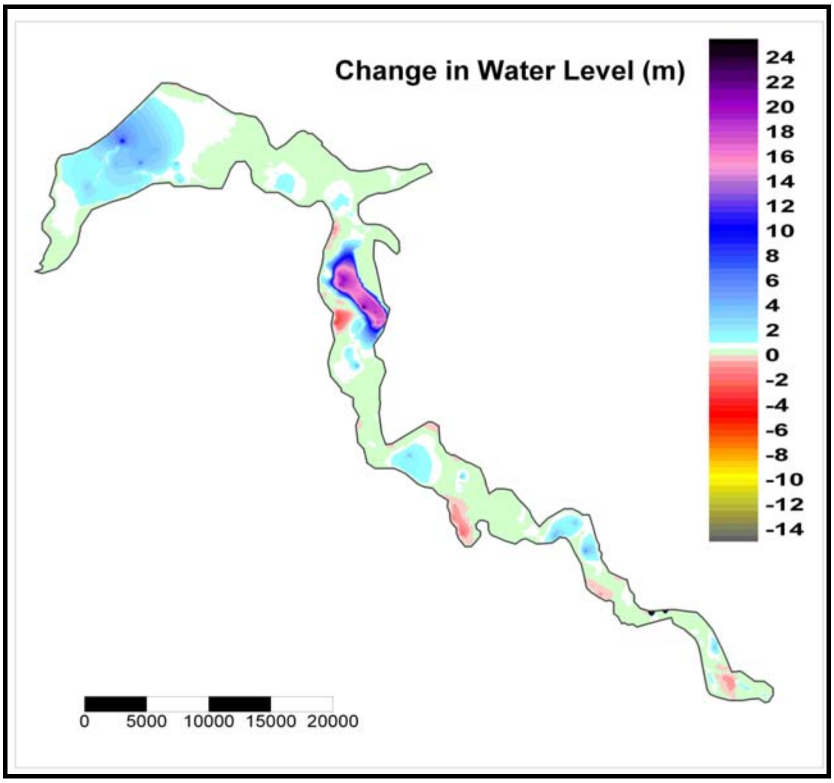

Scenario 1a

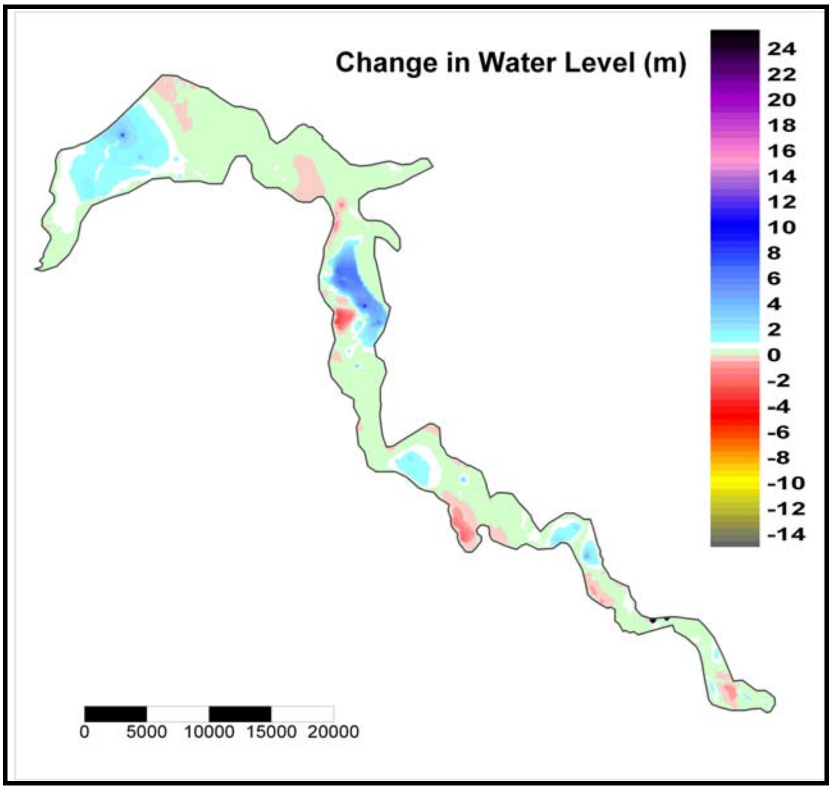
Change in Water Level (m)
24
22
20
18
16
14
12
10
8
6
4
2
0
-2
-4
-6
-8
-10
-12
-14
0 5000 10000 15000 20000

Scenario 1b

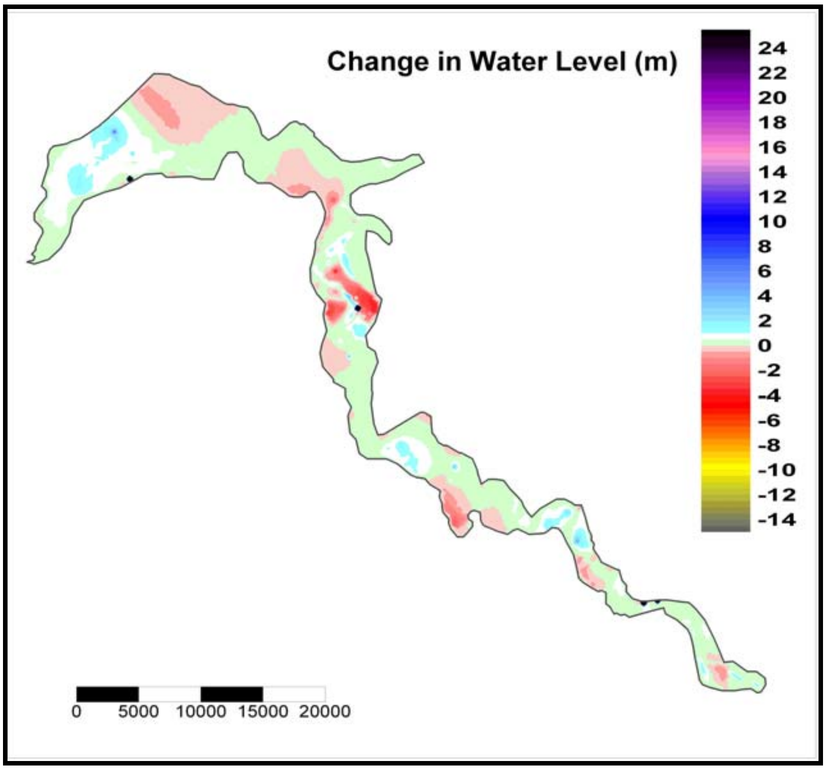
Change in Water Level (m)
24
22
20
18
16
14
12
10
8
6
4
2
0
-2
-4
-6
-8
-10
-12
-14
0 5000 10000 15000 20000

Scenario 1c

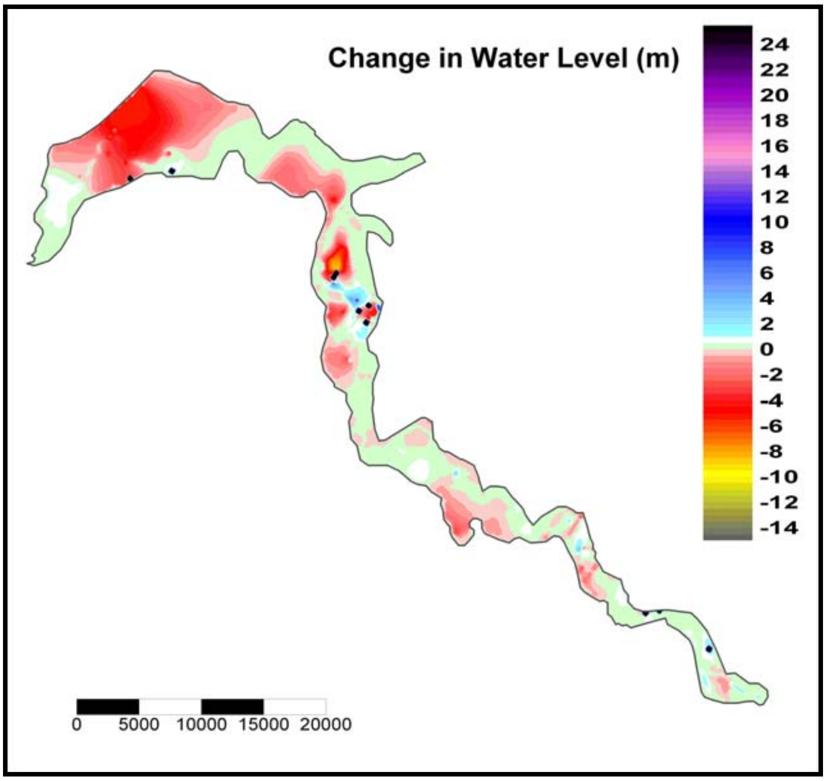

Scenario 1d

- **Figure 57 Predicted change in groundwater head for scenarios 1a, 1b, 1c and 1d (in metres)**

Note: The increases of water level in the Dubbo Region for scenario 1b to 1d are due to the progressive shutting down of abstraction wells when the cell in which they are located dry up.

5.2.4. Mass Balance

Mass balance details for all scenarios are given in Appendix D. A summary of the annual average mass balances for all scenarios is shown in Table 26.

Table 26 Annual Average Mass Balance for all Scenarios (GL/year)

	Flux IN				Flux OUT				
Scenario	Storage	River_Leakage	GHBs	Recharge	Storage	Wells	River_Leakage	ET	GHBs
Sc 1a	8.79	8.90	2.63	9.23	10.08	0.00	18.48	0.36	0.62
Sc 1b	8.80	14.49	2.75	9.03	9.28	11.26	13.76	0.33	0.44
Sc 1c	9.07	18.48	2.79	9.02	9.16	16.71	12.81	0.32	0.38
Sc 1d	10.17	28.53	3.07	9.00	9.48	29.55	11.15	0.30	0.29
Sc 2a	7.37	7.67	2.86	8.09	8.46	0.00	16.68	0.32	0.52
Sc 2b	7.65	14.17	2.94	8.09	8.02	11.26	12.90	0.30	0.38
Sc 2c	7.97	18.19	3.00	8.08	7.92	16.71	12.00	0.29	0.33
Sc 2d	9.33	27.93	3.32	8.06	8.41	29.36	10.37	0.26	0.25
Sc 3a	8.26	8.02	2.72	8.91	9.43	0.00	17.57	0.35	0.57
Sc 3b	8.53	14.36	2.80	8.91	9.00	11.26	13.60	0.32	0.43
Sc 3c	8.82	18.35	2.85	8.90	8.87	16.71	12.66	0.31	0.37
Sc 3d	9.96	28.37	3.13	8.88	9.24	29.51	11.01	0.29	0.28
Sc 4a	9.66	8.69	2.51	10.01	10.93	0.00	18.92	0.39	0.64
Sc 4b	9.95	14.79	2.59	10.01	10.53	11.26	14.70	0.37	0.50
Sc 4c	10.19	18.71	2.63	10.01	10.38	16.71	13.67	0.35	0.43
Sc 4d	11.17	28.87	2.88	9.98	10.60	29.70	11.93	0.33	0.33

The information presented in Table 26 can be used to compare the different fluxes in the different scenarios to illustrate the manner in which the model's water balance changes as groundwater extraction changes. One of the most interesting issues is to determine the impact that increased groundwater extraction is likely to have on the flow in the Macquarie River. This information can be obtained by calculating the differences in river fluxes between each pumping scenario and the non-pumping scenario for the different climate assumptions. For each scenario the difference in baseflow (River Out Flux in Table 26) and difference in river leakage to groundwater (River In Flux in Table 26) are estimated and added to get the total predicted loss of river flow. Figure 58 shows the results of this analysis.

It can be seen that there is almost a linear relationship between the loss of river flow and the extraction rate. The percentage of the groundwater extraction obtained from loss of river flow (ie a combination of loss of base flow and increased river bed leakage to groundwater) is presented in Figure 59. Here it can be seen that a substantial proportion (80 to 90%) of the volume of the water extracted as groundwater is actually sourced from the river.

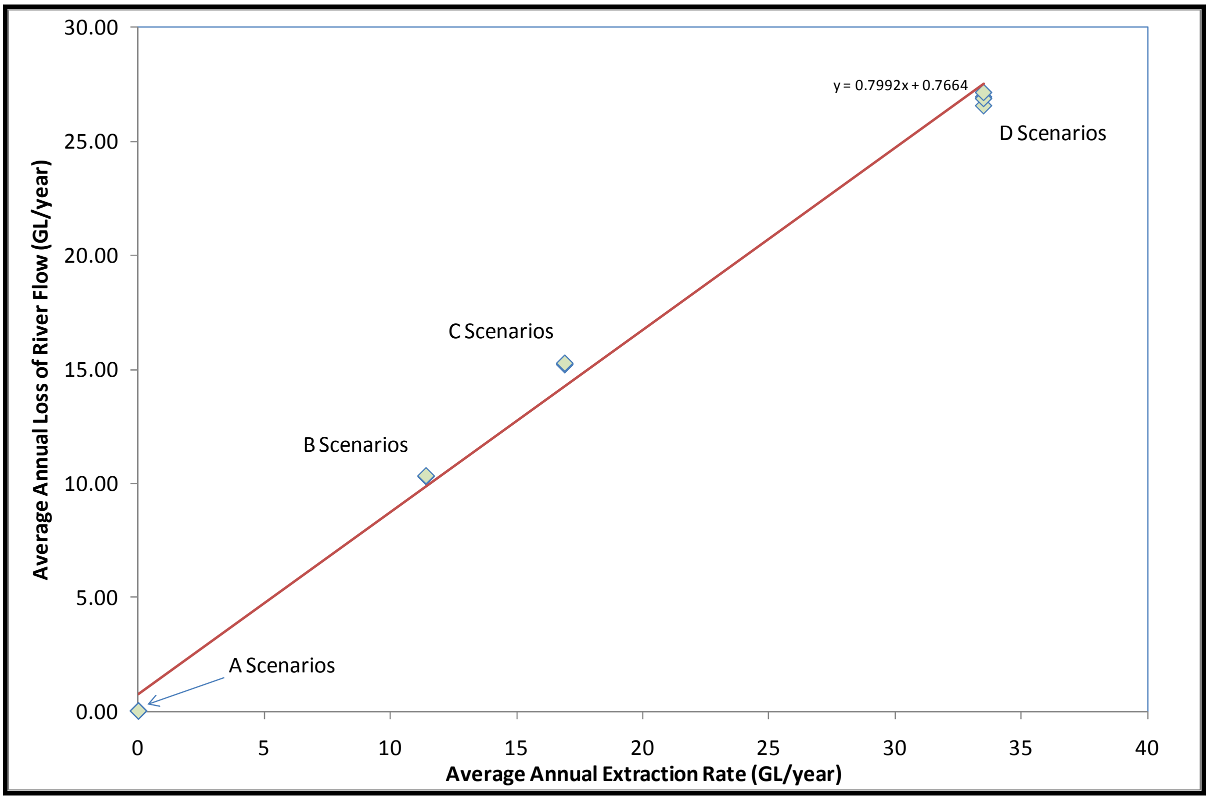

- **Figure 58 Relationship between extraction rate and loss of river flow**

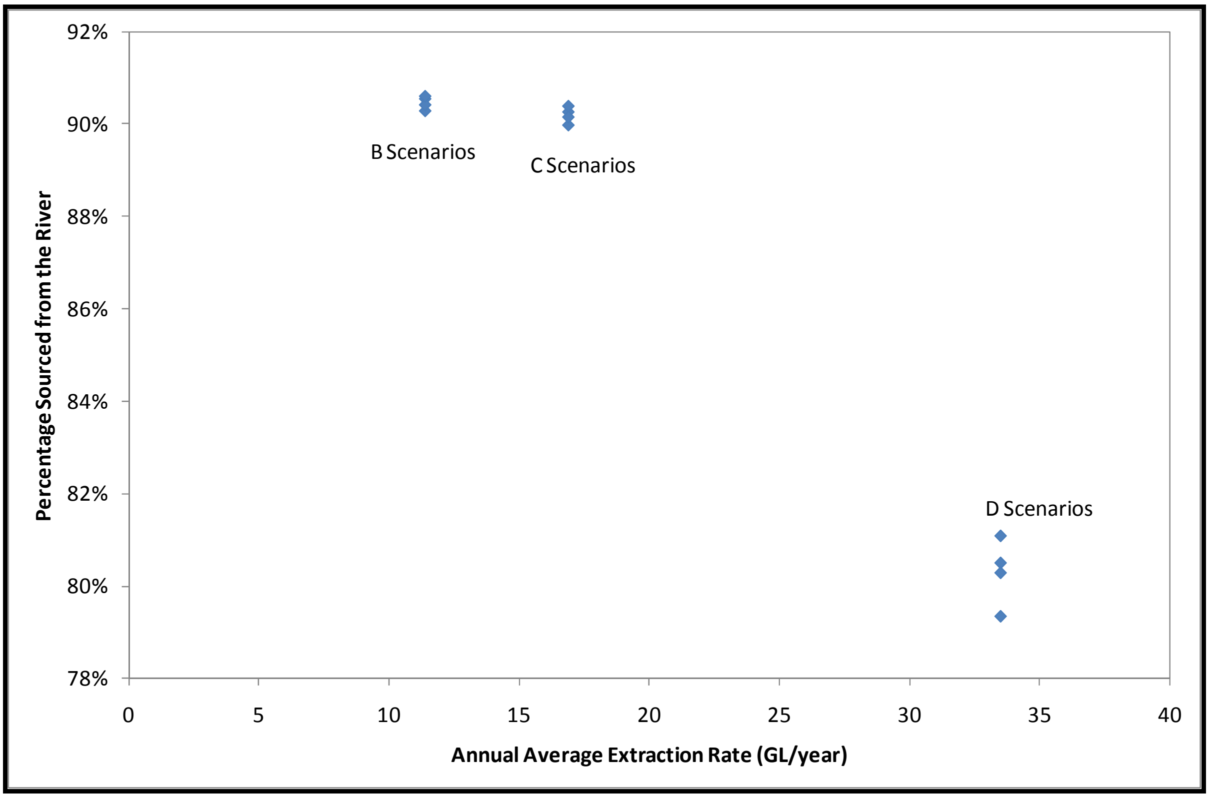

- **Figure 59 Proportion of groundwater extraction sourced from river flow reduction**

6. Conclusions

A three dimensional finite difference groundwater flow model was constructed in the Groundwater Vistas modelling package using the USGS MODFLOW 2000 simulation code. The model includes layers that represent (from top to bottom) the Upper Quaternary, the Lower Quaternary and the confined Tertiary Aquifer. A fourth model layer that can be used to represent basement has been included in the model formulation but this layer has been de-activated at this stage. The extent, shape and thickness of the layers have been defined by stratigraphic interpretations of bore logs and other data undertaken by Ann Smithson of the New South Wales Office of Water. The MODFLOW RIV, EVT, RCH, WEL and GHB packages have been used to represent the interaction with the river, evapotranspiration, recharge, groundwater extraction and exchange of groundwater with surrounding aquifers respectively.

Calibration was undertaken by matching model predicted groundwater levels to observed groundwater level time series data for the period from July 1980 to June 2008. The calibration process was assisted by the automated parameter estimation software PEST version 11 using pilot points and regularisation routines available in the PEST program. A total of 897 parameters (including 853 pilot points) were defined to calibrate the model and the resultant model includes spatial distribution arrays for the hydraulic conductivity and specific yield parameters. The calibrated model provides an effective representation of groundwater levels across the model domain and the normalised RMS error of 3.4% is considered to be an acceptable calibration statistic.

The calibration process has resulted in a ranking of all calibration parameters according to calibration sensitivity. Recharge scaling factors and hydraulic conductivity parameters were shown to be the most sensitive. In other words variation in these particular parameters will result in bigger variations in key model outcomes (predicted groundwater levels) compared to similar variation in other model parameters.

It was noted during calibration that many of the model runs were influenced by groundwater extractions being automatically terminated by Modflow due to de-saturation of aquifer cells that host individual extraction wells. Most of the aquifer de-saturation and reduction in extraction appeared to occur in the region of the Dubbo City water supply wells. While it was considered important to adjust the model so that the measured extraction rates are sustained in the calibration period it is apparent that the model is finely balanced in that the measured extraction rates and drawdown observed around the Dubbo City borefield is close to that which will lead to de-saturation of aquifer cells in the model. It is assumed that in reality the recent extraction from the Dubbo City borefield is close to the maximum that can be sustained in the short term and that there is no guarantee that such levels of extraction are sustainable in the long term.

A series of sixteen predictive scenarios were developed and run over a 50 year time frame. The scenarios combine four different climate assumptions with four extraction regimes. In all cases extraction is assumed to be limited to the existing extraction wells and the rates assigned to each well have been estimated by scaling individual rates to achieve the desired extraction total for the scenario. In most scenarios the assigned extraction rate is not maintained for the duration of the model run as the model predicts substantial localised drawdown at some of the larger extraction well sites which leads to de-saturation of individual model cells that contain the pumping wells. The principal areas of concern in this regard are in the vicinity of the Dubbo City water supply wells. The results suggest that with the current distribution of extraction wells the maximum possible extraction rate from the aquifer is likely to be about 15 GL/year. This outcome does not necessarily reflect the maximum sustainable yield of the aquifer as a whole since the model results are heavily influenced by the distribution of extraction wells assumed for the scenarios. A redistribution of extraction wells away from the existing highly producing wells (eg those in the Dubbo City borefield) would likely achieve a greater level of sustainable extraction.

While the turning off of extraction wells due to cell drying is a model artefact that would not occur in practice. It is assumed that wells would progressively decline in output as de-saturation of the aquifer progresses. Complete de-saturation of aquifer cells in the model is believed to be an indicator that the aquifer is being over-stressed in these locations. This conclusion is drawn from the fact that the model is reasonably well calibrated in most heavily developed areas and the fact that the model predicts dramatic declines in groundwater heads suggests that partial de-saturation of productive aquifers is likely to occur and indeed would lead to declining well productivity in these regions.

Comparisons between modelling scenarios with different climate assumptions illustrates that fact the model outcomes are more dependent on the assumed extraction regime than on the future climate. Some influence due to climate variability is apparent in the model result. The degree to which the assumed climate influences predicted water levels in the model is greater in the downstream part of the model domain where the valley is wider and the recharge fluxes are applied over a greater area than in the upstream part of the aquifer.

The changes in model water balance arising from increasing levels of groundwater extraction have been interrogated to determine the water balance components that are changed to account for increased levels of groundwater extraction. The model results suggest that the river fluxes are substantially altered by increasing groundwater extraction and as much as 90% of groundwater pumping is sourced from a combination of reduced river baseflow and increased river bed leakage to groundwater.

7. Reference

Anderson, M. P. and Woessner, W. W. (1992). *Applied Groundwater Modeling*. Academic Press, San Diego.

CSIRO., 2007. Climate Change in Australia – Technical Report 2007. ISBN 9781921232947 (PDF)

Doherty, J., 2003. Groundwater model calibration using pilot points and regularisation. *Ground Water*. 41 (2): 170-177.

Christensen, S. and Doherty, J., 2008. Predictive error dependencies when using pilot points and singular value decomposition in groundwater model calibration. *Advances in Water Resources*. 31, 674-700.

Geoscience Australia, 2006. Geodata Topo 250k, Series 3 (June 2006)

Geoscience Australia, 2008. Geodata 9 Second DEM, Third Edition (July 2008)

Middlemis. H., 2000. Murray-Darling Basin Commission Groundwater Flow Modelling Guidelines. Produced by Aquaterra Consulting for the MDBC.

NOW (2009). Groundwater Status Report for the Upper Macquarie GMA. Report in preparation by Ann Smithson, New South Wales Office of Water.

SKM., 1984. Macquarie Valley Flood Plain Atlas. June 1984. Report prepared for the Water Resources Commission of NSW.

Appendix A Active abstraction bores used in the GW model.

Average rate is the total abstraction volume for the 28 years of the calibration period divided by 28.

License_nb	Bore_ID	Easting	Northing	Row	Column	Layers	Average_Rate(ML/Year)
80BL007326	GW059002	661703	6409725	109	221	1-2	7.60
80BL009381	GW800419	663816	6409536	104	230	2	24.20
80BL013101	GW060187	632964	6439037	71	19	1-2	4.35
80BL017907	GW005581	656747	6415225	101	185	1-2	151.49
80BL018315	GW062412	651134	6434871	36	106	1-2-3	42.22
80BL019034	GW039541	653282	6421131	86	154	1-2	13.38
80BL019070	GW039464	646945	6436719	41	83	2	5.75
80BL100431	GW800010	654018	6426510	62	141	2	315.12
80BL100432	GW800311	654431	6426104	63	144	2-3	516.79
80BL101250	GW019575	651203	6435795	32	103	1-2	24.45
80BL106337	GW021320	652978	6426957	63	136	2	620.70
80BL107398	GW060177	646554	6436879	41	81	1	56.99
80BL109155	GW025415	651342	6429150	59	123	2-3	367.26
80BL109156	GW060182	651365	6429424	58	122	2	276.22
80BL109157	GW800544	650930	6429650	58	120	2	408.39
80BL109158	GW800402	651180	6428841	61	123	2	360.48
80BL110005	GW023042	661218	6410410	108	217	1-2	43.36
80BL114945	GW059324	651084	6436750	29	100	1-2	19.52
80BL115119	GW802467	654137	6425739	65	144	2-3	104.81
80BL116543	GW053389	650787	6429311	60	120	2	1.68
80BL116544	GW801180	654051	6418347	96	165	2	47.93
80BL117174	GW008436	636275	6439794	59	31	2	49.11
80BL117345	GW060283	651691	6435325	33	107	1-2	15.10
80BL117925	GW062071	653363	6428634	55	133	2	1.86
80BL119631	GW802848	652606	6424838	73	140	1-2	3.21
80BL119718	GW800103	647109	6437179	38	82	1-2-3	24.30
80BL120283	GW059133	653280	6426152	66	139	2-3	41.00
80BL120497	GW801334	652018	6434426	36	110	1-2	7.24
80BL120565	GW800102	651631	6436558	28	103	1-2	24.70
80BL121759	GW053950	653650	6416074	106	170	1-2	132.29
80BL124008	GW025021	652361	6422439	84	146	2-3	142.35
80BL124564	GW047000	633011	6438636	73	21	2	23.20
80BL125099	GW055777	652528	6423114	80	145	1-2	71.77
80BL126215	GW026826	637962	6438632	59	41	2	13.13
80BL126663	GW800615	651889	6434582	35	110	1-2	14.92
80BL127327	GW008445	660650	6412452	101	209	1-2	26.27
80BL127363	GW800696	633538	6436904	78	28	2	4.10
80BL128563	GW039385	643273	6441915	30	53	2-3	10.71
80BL130389	GW004972	668705	6409763	89	250	2-3	38.76
80BL131052	GW802330	660876	6413558	96	207	1-2	23.05
80BL131704	GW059177	653900	6425619	66	143	2	44.64
80BL131736	GW025021	636895	6443050	44	24	1-2-3	5.53
80BL131761	GW024654	635132	6438608	67	29	2-3	60.95
80BL131780	GW024654	637991	6436968	65	46	2	4.89
80BL131978	GW801009	652445	6434944	32	111	1	2.03
80BL131979	GW063683	651483	6432070	47	115	2	0.93
80BL131981	GW047823	650864	6429664	58	119	2-3	0.29

80BL131982	GW025939	650867	6429663	58	119	2-3	2.96
80BL131984	GW800863	651574	6430744	52	119	2	0.32
80BL131987	GW037824	651728	6434307	37	110	1-2	11.63
80BL132367	GW060612	645188	6436434	47	77	2	4.60
80BL132483	GW802192	651073	6436042	32	102	1-2	2.14
80BL132516	GW034236	651239	6436656	29	101	1-2	5.50
80BL134020	GW008387	670477	6409487	85	258	2	33.37
80BL134021	GW028007	655645	6414934	105	181	1-2	16.49
80BL134025	GW047969	681193	6399625	94	330	1-2	18.45
80BL135231	GW016617	632795	6436144	84	27	2	1.61
80BL138679	GW801008	651831	6426034	70	134	1-2	19.81
80BL142509	GW028685	645868	6436488	45	79	2	0.64
80BL150719	GW039353	634865	6436240	77	35	2	1.53
80BL154184	GW047943	652513	6428434	59	130	2	0.54
80BL236310	GW800885	641232	6442129	35	44	2-3	3.85
80BL236312	GW060001	653763	6425159	68	144	2	15.31
80BL236485	GW060749	652163	6433859	37	113	2	0.68
80BL236540	GW801287	668363	6408649	94	251	2	117.77
80BL236588	GW021295	635591	6439588	62	28	2	20.66
80BL236655	GW029828	630913	6436734	87	17	2	237.07
80BL236874		668570	6408955	92	251	2	52.17
80BL237100	GW060290	651777	6435630	31	106	1	8.92
80BL237141	GW042707	671073	6406119	97	270	1-2-3	115.88
80BL237285	GW030948	650790	6431721	50	113	1-2	2.00
80BL237286	GW020647	651485	6432073	47	115	2	3.28
80BL237335	GW060178	671139	6407434	91	266	2-3	149.17
80BL237342	GW802114	633525	6440334	64	18	2-3	654.11
80BL237607	GW062188	672740	6404820	97	280	1	11.06
80BL238258	GW062342	671848	6405836	96	274	1	22.16
80BL238359	GW030933	653395	6425103	70	143	1-2	3.71
80BL238380		653728	6419098	93	161	1	0.43
80BL238763	GW060482	650692	6430348	56	117	2	0.04
80BL238862	GW800338	633011	6438636	73	21	2	143.68
80BL239439	GW063091	654198	6426159	63	143	2	4.78
80BL239504		633409	6436926	79	27	2	4.50
80BL239733		651899	6423519	81	141	2	43.47
80BL241079		653656	6425514	67	143	2	42.32
80BL241151		645950	6437785	39	76	1	6.57
80BL241534	GW800085	635133	6438604	67	29	2	75.69
80BL241650		653926	6426563	62	141	2	20.06
80BL241798		670962	6410108	81	258	1	27.23
80BL242418	GW800896	661721	6409756	109	221	1	14.45
80BL242470	GW801002	653858	6425774	66	143	2	20.56
80BL242490	GW800199	671871	6405748	96	274	1	51.96
80BL242607		632963	6439049	71	19	1	0.71
80BL242959		650780	6431730	50	113	1	2.14
80BL243075		670109	6409826	84	255	2	1.07
80BL243157		670078	6409659	85	255	2	11.63
80BL243660		652410	6422226	84	147	2	15.56
80BL243971		653223	6420983	87	154	1	2.18
80BL244787		651603	6436686	27	102	1	1.21

Appendix B Observation Bores

Work_No	EAST	NORTH	Readings	From	To	Layer	Scr_Fr	Scr_To	Bore_Depth	RLNS
GW021498_1	652883.1	6427575	250	1973	2008	2	39.6	51.8	74.7	275.751
GW025041_1	653261.1	6426614	248	1973	2008	2	23.5	25.9	25.9	262.521
GW025413_1	652903.2	6427174	259	1973	2008	3	33.5	45.7	64.6	269.314
GW025413_2	652903.2	6427174	251	1973	2008	3	48.8	61	64.6	269.314
GW025414_1	653113.4	6427233	195	1973	2008	2	22.9	29	61	268.16
GW025414_2	653113.4	6427233	248	1973	2008	3	36.6	54.9	61	268.16
GW030875_1	669939.3	6410143	84	1981	2008	2	15	18	18	280.64
GW036380_1	681069.6	6398580	101	1980	2008	2	17.5	22.5	42	291.87
GW036380_2	681069.6	6398580	101	1980	2008	3	29.3	32.4	42	291.87
GW036385_1	681329.4	6398514	101	1980	2008	2	19.5	24.5	27	293.943
GW036439_1	652744.5	6423603	245	1982	2008	3	37.5	44.2	37.5	263.9
GW036442_1	653083.1	6423506	154	1982	2008	2	18	21	27.5	265.193
GW036443_1	652232.3	6422595	246	1982	2008	3	18	51.5	51.5	266.056
GW036444_1	651685.5	6422757	152	1982	2008	2	16	19	23	264.51
GW036445_1	651164.8	6422919	153	1982	2008	2	21	24	30	267.04
GW036446_1	650669.3	6423019	154	1982	2008	2	15.4	17.4	23.3	267.18
GW036447_1	657871.7	6413605	65	1983	2008	2	29	32	51	273.027
GW036447_2	657871.7	6413605	65	1983	2008	3	51	71.5	51	273.027
GW036448_1	658070.1	6414588	65	1983	2008	2	27	37	42	273.63
GW036449_1	658218.2	6415695	65	1983	2008	2	27	33	36	273.862
GW036450_1	657760.8	6416534	64	1983	2008	2	23	29	32	272.81
GW036451_1	651875.5	6435414	159	1983	2008	2	19.5	23.5	27.5	259.67
GW036452_1	651301.3	6435546	136	1984	2008	2	24	30	34	261.41
GW036454_1	653359.4	6436562	136	1984	2008	2	25.9	32	35	262.727
GW036455_1	653393	6437055	136	1984	2008	1	20	22	24	263.409
GW036491_1	647334.5	6436498	135	1984	2008	2	32.5	36.5	55	267.49
GW036491_2	647334.5	6436498	135	1984	2008	3	43.5	49.5	55	267.49
GW036492_1	647506	6437481	135	1984	2008	1	12	16.5	37.5	259.582
GW036492_2	647506	6437481	135	1984	2008	2	19.5	24	37.5	259.582
GW036492_3	647506	6437481	135	1984	2008	3	31.5	34	37.5	259.582
GW036493_1	647651.2	6438464	92	1984	2008	1	15	17	22.8	258.49
GW036519_1	623850.3	6430621	73	1984	2008	2	24	27	53	244.27
GW036532_1	636361.4	6444320	47	1984	2008	1	22	26	73.5	260.152
GW038166_1	652808	6424342	193	1974	2008	3	28.9	34.9	35	265.863
GW039058_1	641355.8	6439724	203	1970	2008	2	15.2	21.3	21.9	254.49
GW039060_1	636527.7	6439144	214	1969	2008	2	17.1	22.3	22.3	251.55
GW039061_1	633385.8	6441249	229	1969	2008	2	15.2	17.6	17.7	248.069
GW042243_1	635506.4	6441129	114	1968	2008	1	0	14.9	14.9	249.327

Appendix C Calibration Hydrographs

Legend for all hydrographs is as follow:

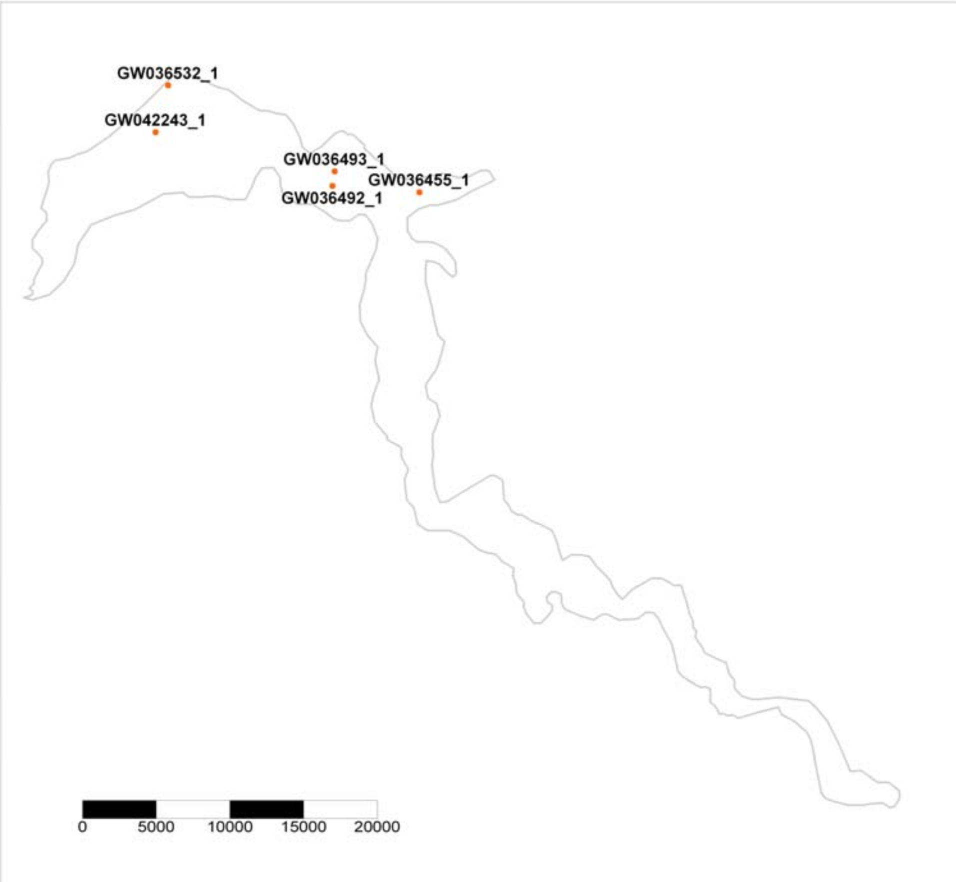

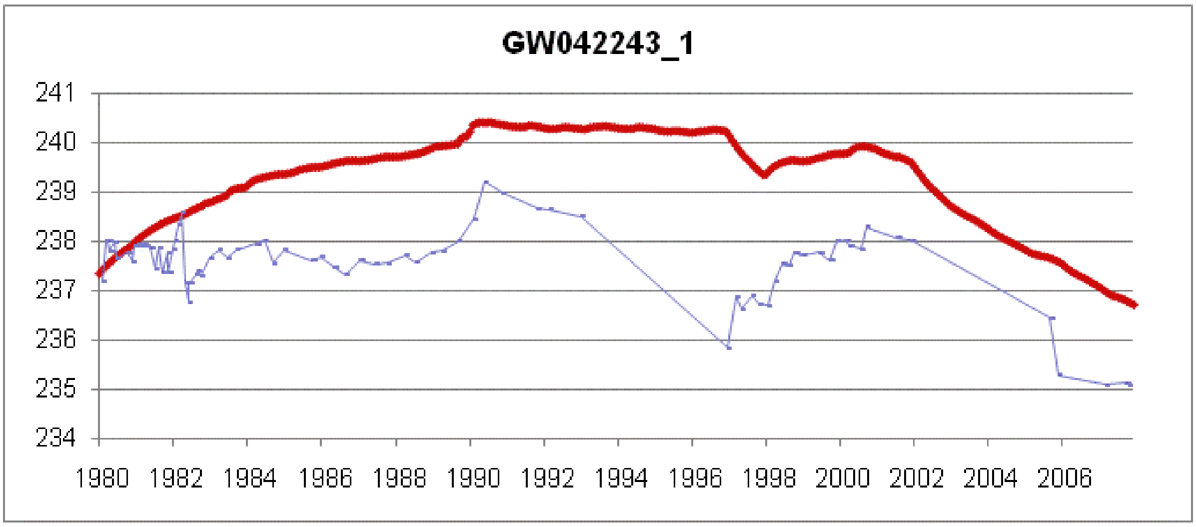

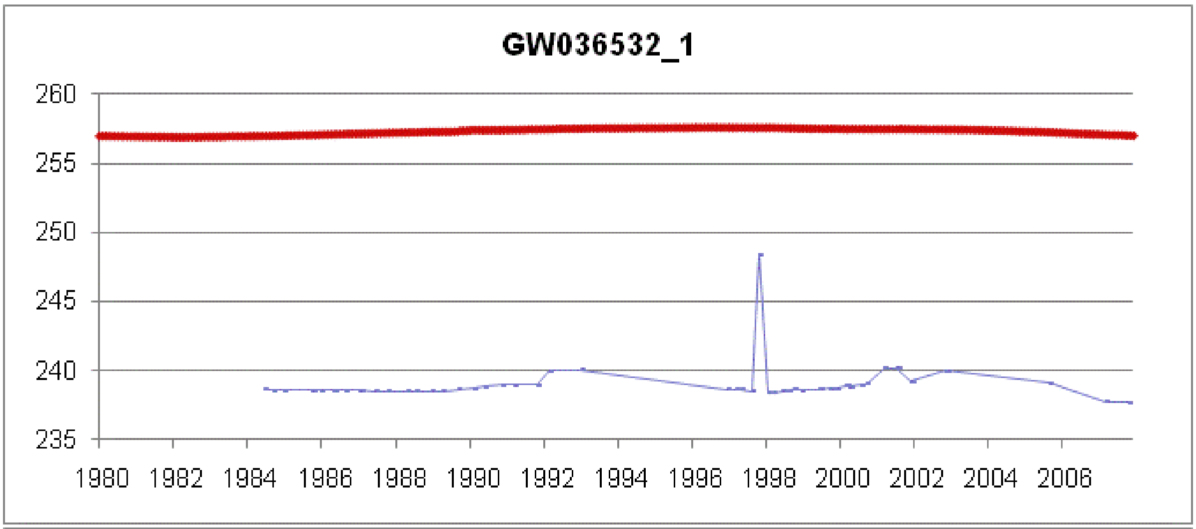
GW036532_1
260
255
250
245
240
235
1980 1982 1984 1986 1988 1990 1992 1994 1996 1998 2000 2002 2004 2006

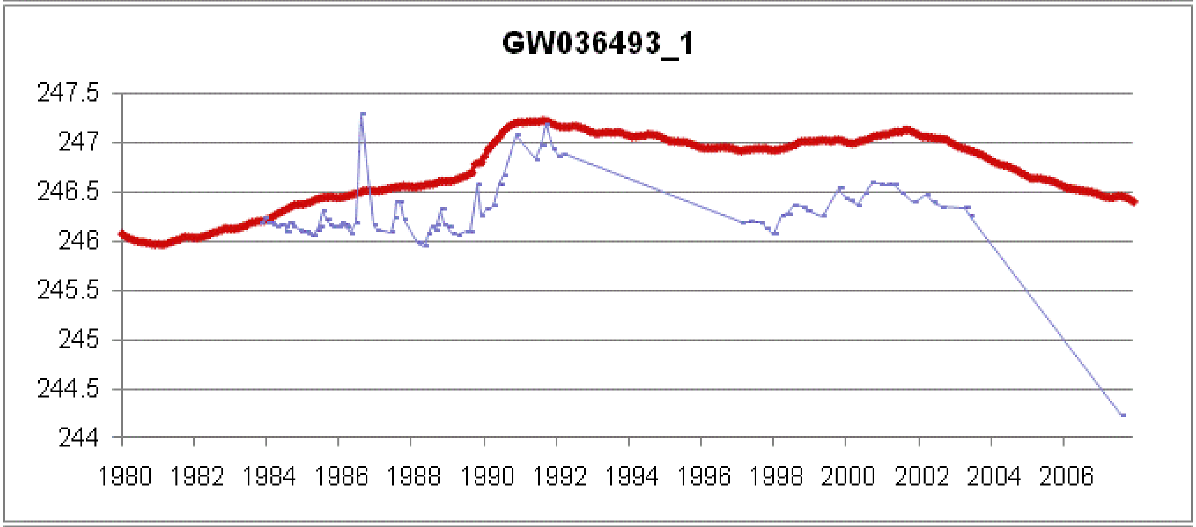
GW036493_1
247.5
247
246.5
246
245.5
245
244.5
244
1980 1982 1984 1986 1988 1990 1992 1994 1996 1998 2000 2002 2004 2006

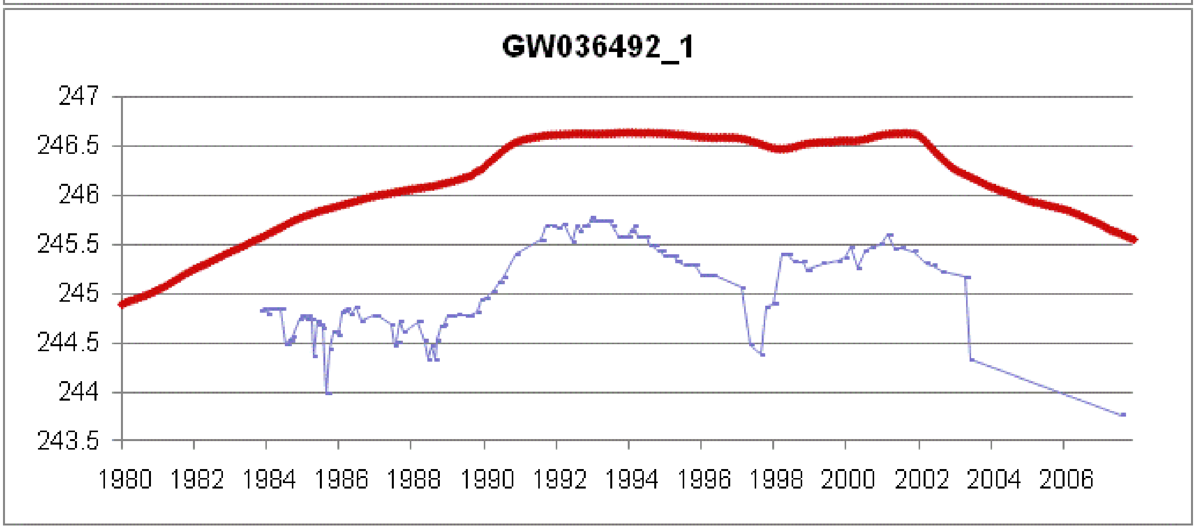
GW036492_1
247
246.5
246
245.5
245
244.5
244
243.5
1980 1982 1984 1986 1988 1990 1992 1994 1996 1998 2000 2002 2004 2006

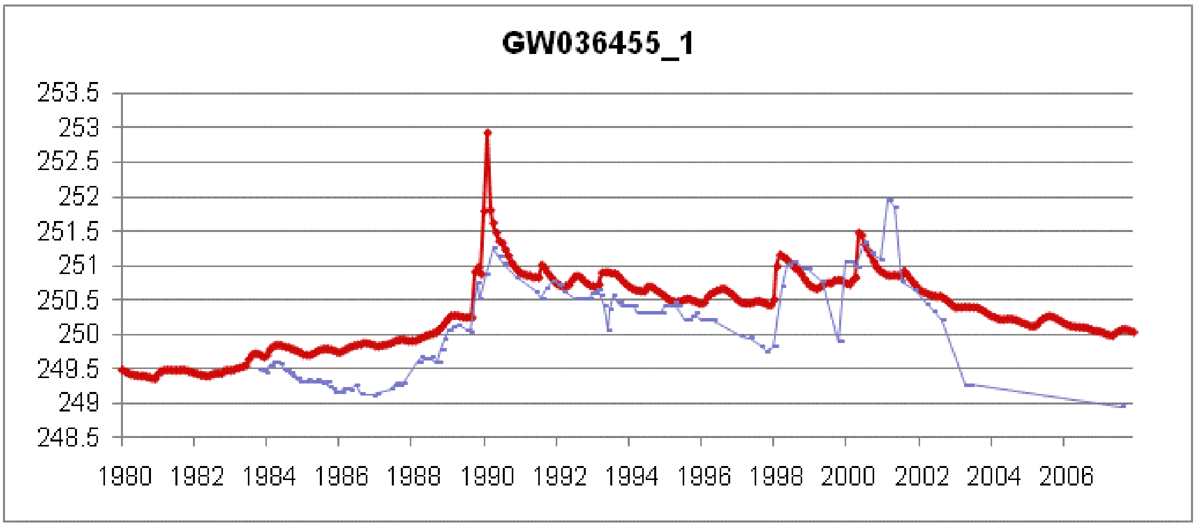
GW036455_1
253.5
253
252.5
252
251.5
251
250.5
250
249.5
249
248.5
1980 1982 1984 1986 1988 1990 1992 1994 1996 1998 2000 2002 2004 2006

Layer 2

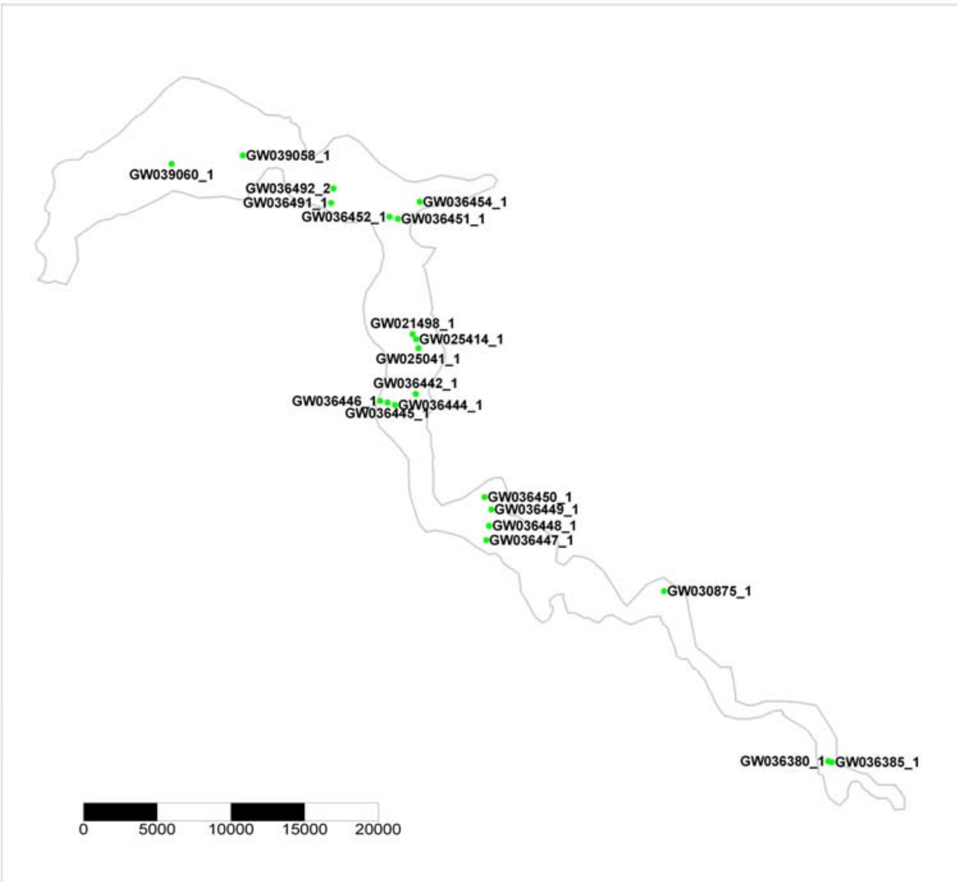
GW039058_1
GW039060_1
GW036492_2
GW036491_1
GW036452_1
GW036451_1
GW036454_1
GW021498_1
GW025414_1
GW025041_1
GW036442_1
GW036446_1
GW036445_1
GW036444_1
GW036450_1
GW036449_1
GW036448_1
GW036447_1
GW030875_1
GW036380_1
GW036385_1
0 5000 10000 15000 20000

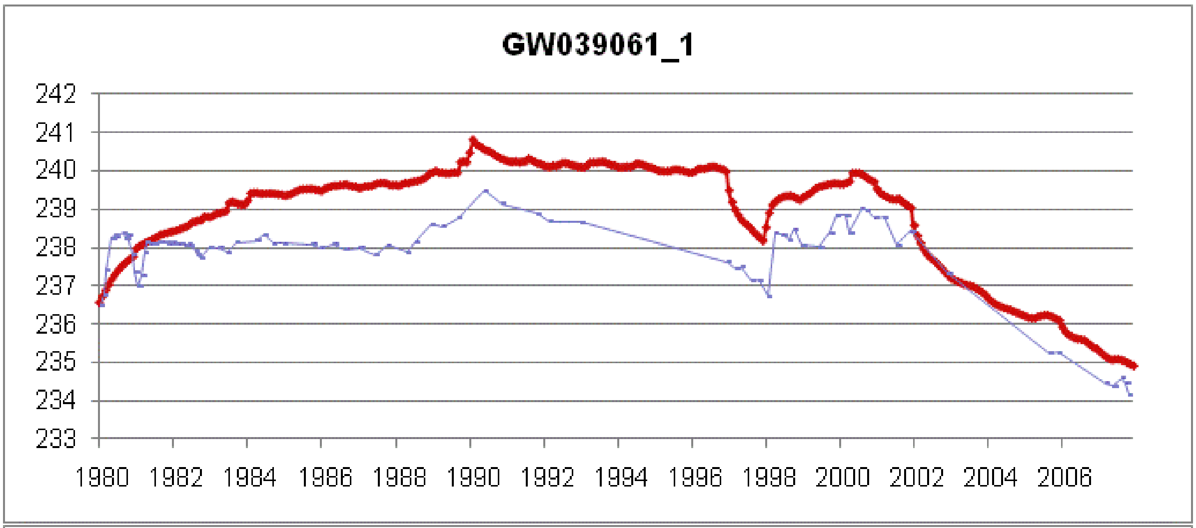
GW039061_1
242
241
240
239
238
237
236
235
234
233
1980 1982 1984 1986 1988 1990 1992 1994 1996 1998 2000 2002 2004 2006

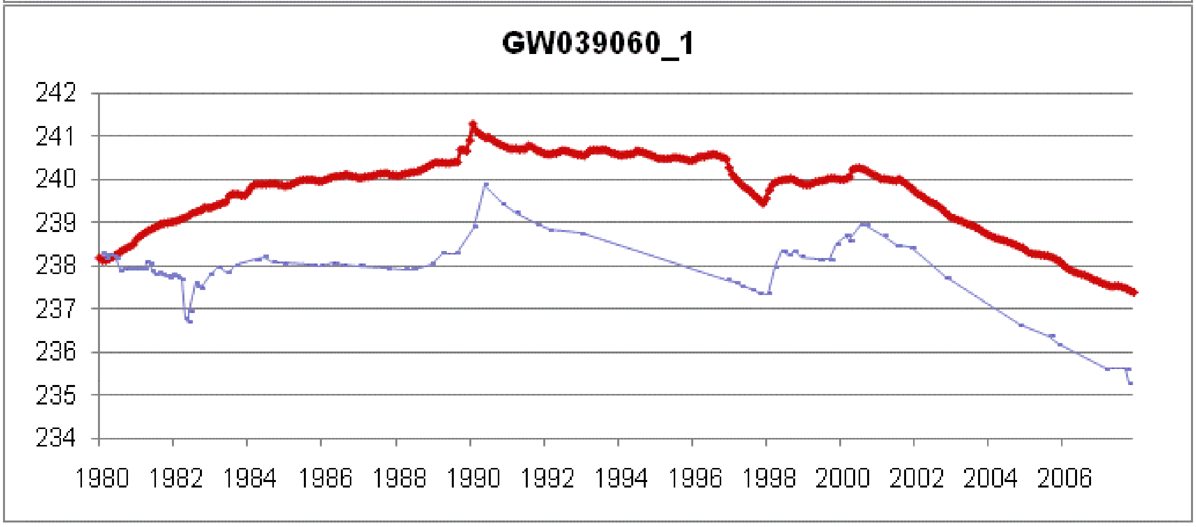
GW039060_1
242
241
240
239
238
237
236
235
234
1980 1982 1984 1986 1988 1990 1992 1994 1996 1998 2000 2002 2004 2006

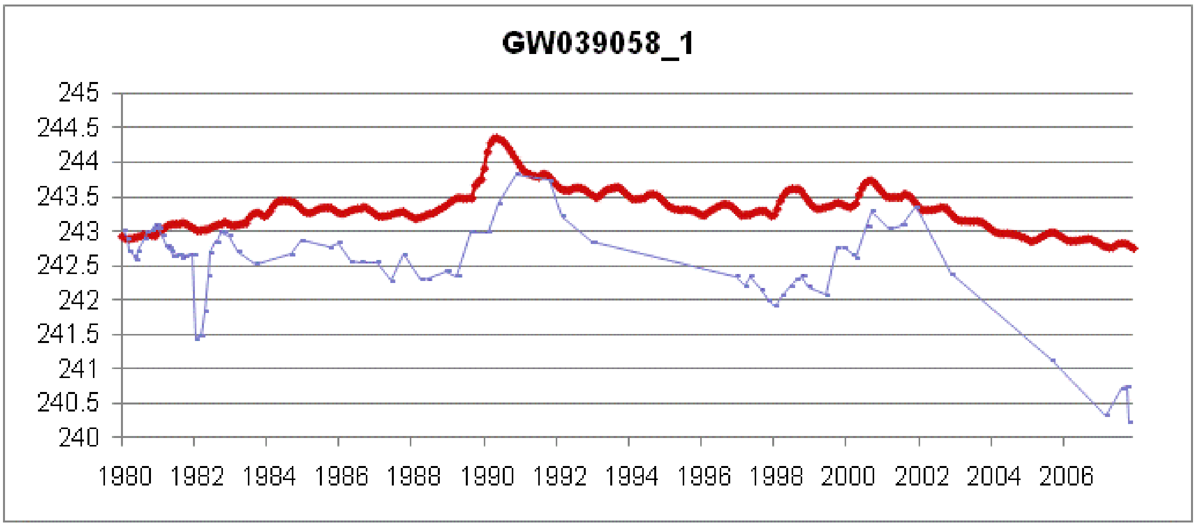
GW039058_1
245
244.5
244
243.5
243
242.5
242
241.5
241
240.5
240
1980 1982 1984 1986 1988 1990 1992 1994 1996 1998 2000 2002 2004 2006

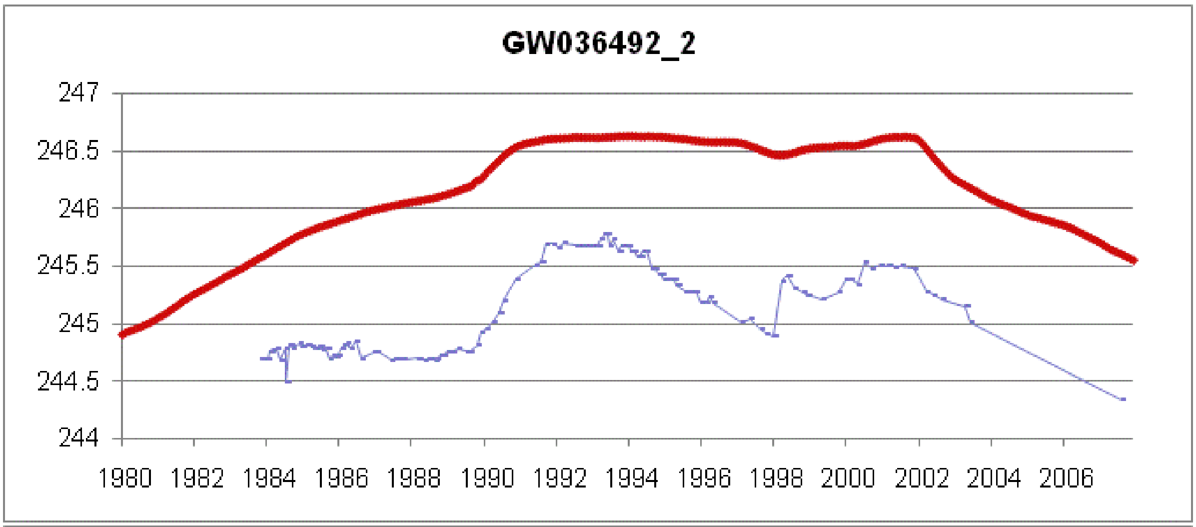
GW036492_2
247
246.5
246
245.5
245
244.5
244
1980 1982 1984 1986 1988 1990 1992 1994 1996 1998 2000 2002 2004 2006

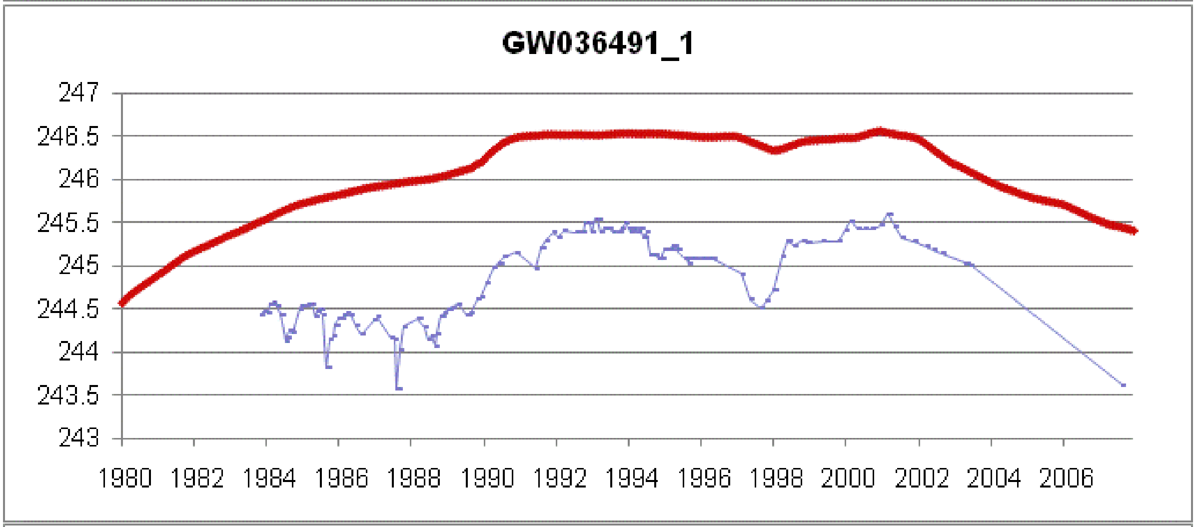
GW036491_1
247
246.5
246
245.5
245
244.5
244
243.5
243
1980 1982 1984 1986 1988 1990 1992 1994 1996 1998 2000 2002 2004 2006

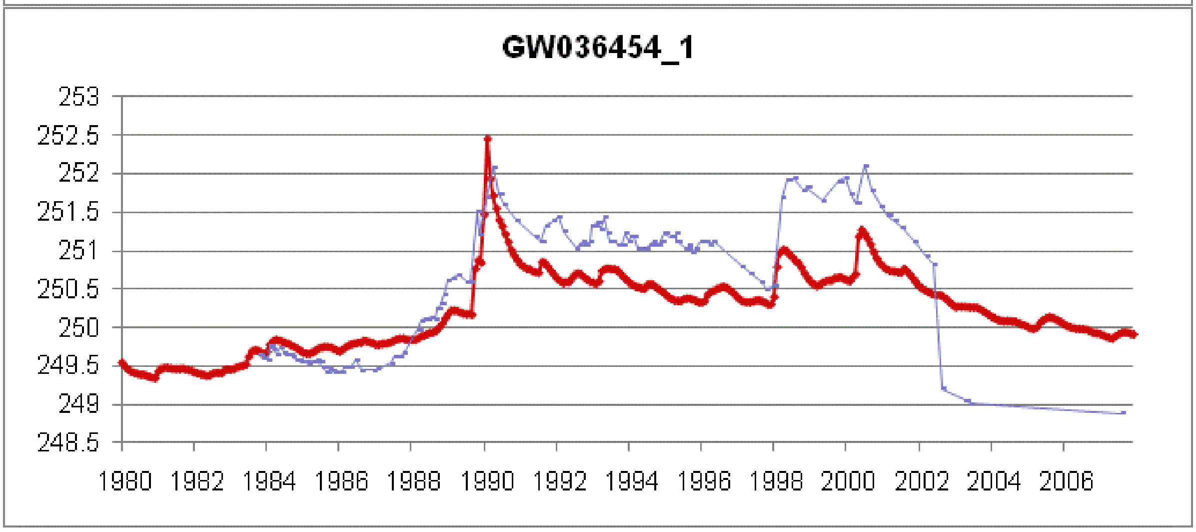
GW036454_1
253
252.5
252
251.5
251
250.5
250
249.5
249
248.5
1980 1982 1984 1986 1988 1990 1992 1994 1996 1998 2000 2002 2004 2006

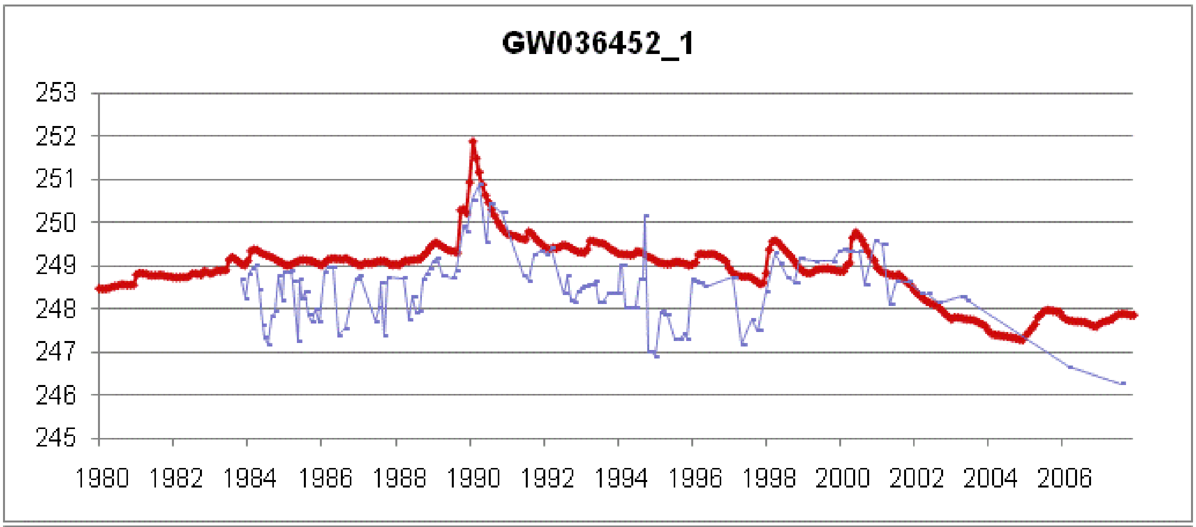
GW036452_1
253
252
251
250
249
248
247
246
245
1980 1982 1984 1986 1988 1990 1992 1994 1996 1998 2000 2002 2004 2006

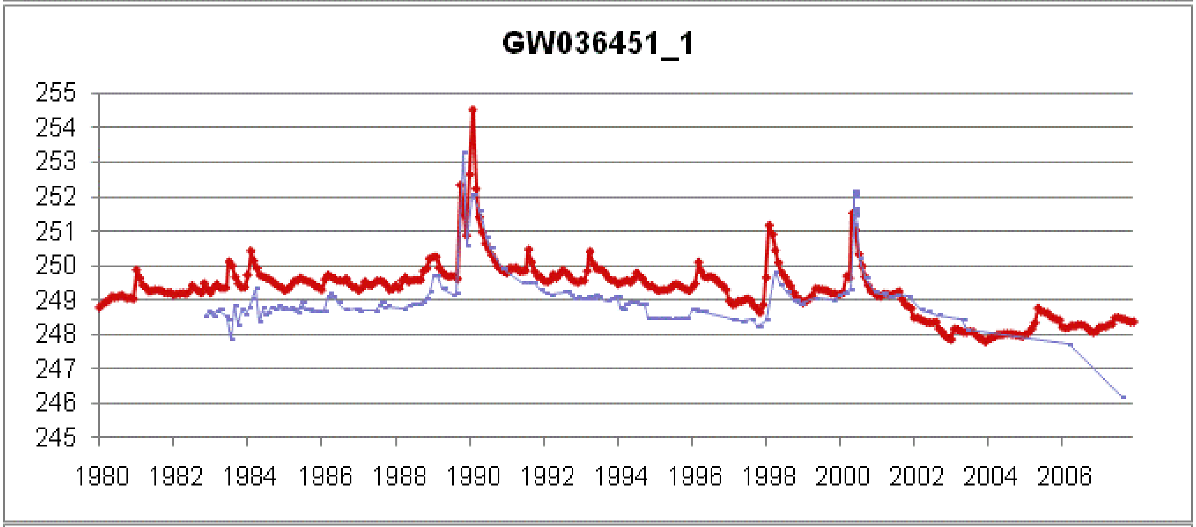
GW036451_1
255
254
253
252
251
250
249
248
247
246
245
1980 1982 1984 1986 1988 1990 1992 1994 1996 1998 2000 2002 2004 2006

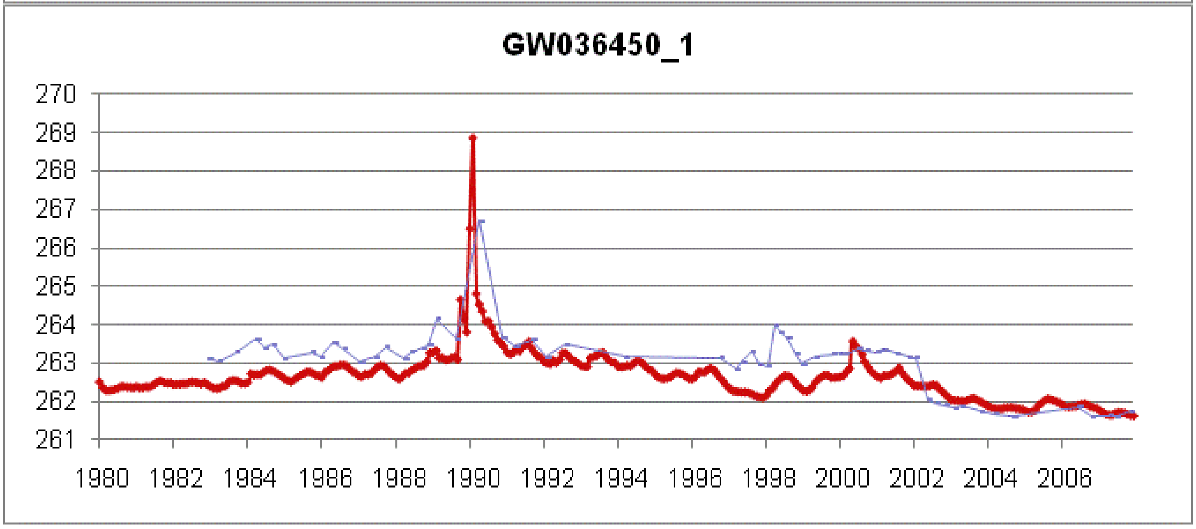
GW036450_1
270
269
268
267
266
265
264
263
262
261
1980 1982 1984 1986 1988 1990 1992 1994 1996 1998 2000 2002 2004 2006

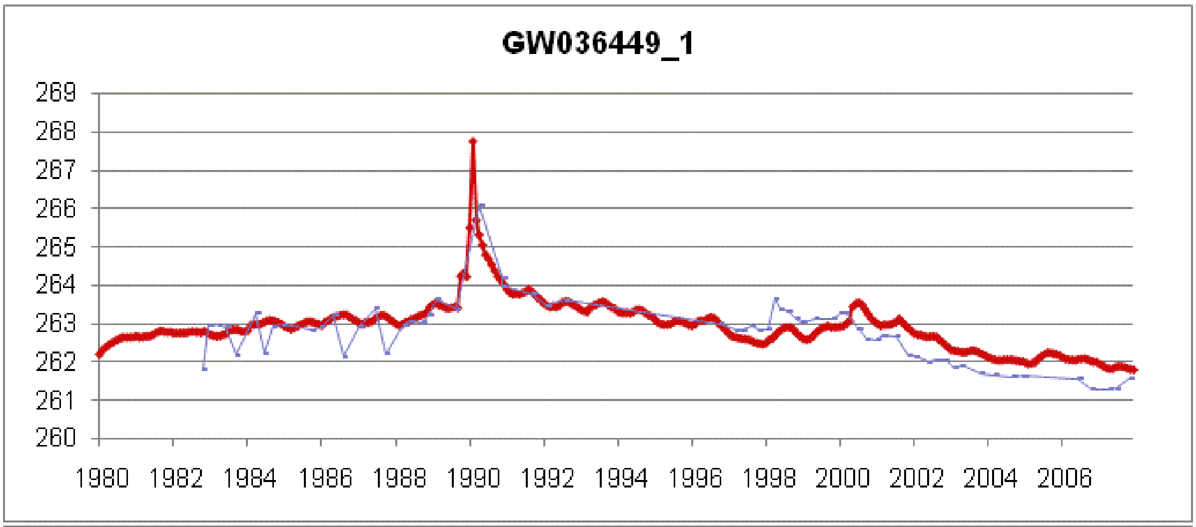
GW036449_1
269
268
267
266
265
264
263
262
261
260
1980 1982 1984 1986 1988 1990 1992 1994 1996 1998 2000 2002 2004 2006

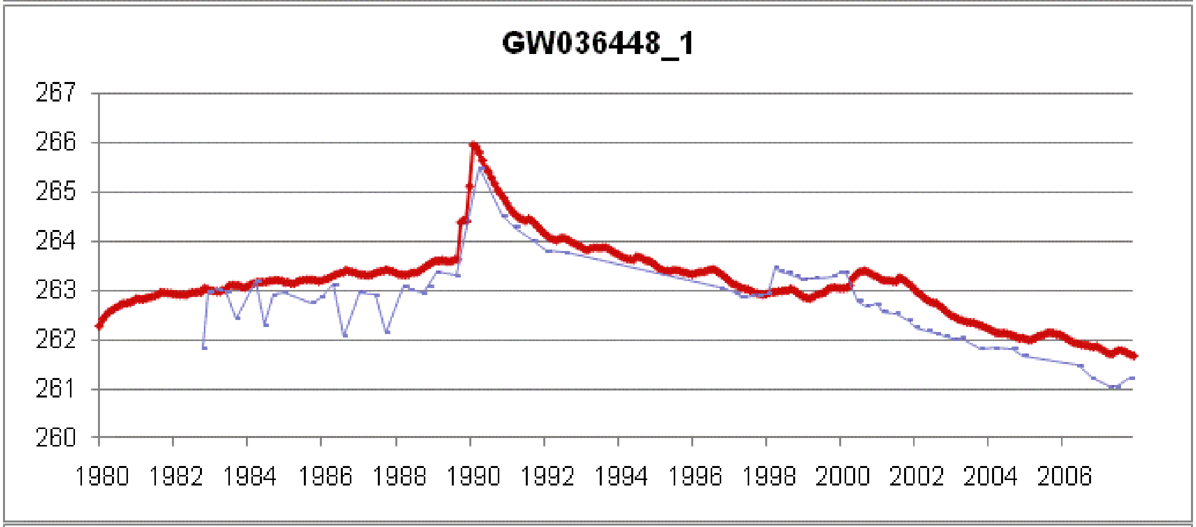
GW036448_1
267
266
265
264
263
262
261
260
1980 1982 1984 1986 1988 1990 1992 1994 1996 1998 2000 2002 2004 2006

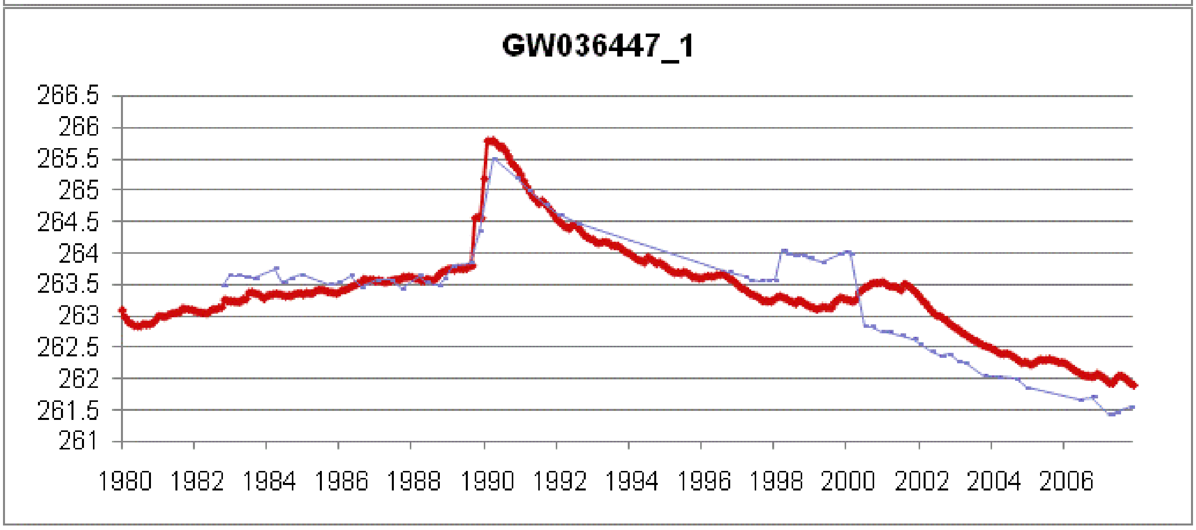
GW036447_1
266.5
266
265.5
265
264.5
264
263.5
263
262.5
262
261.5
261
1980 1982 1984 1986 1988 1990 1992 1994 1996 1998 2000 2002 2004 2006

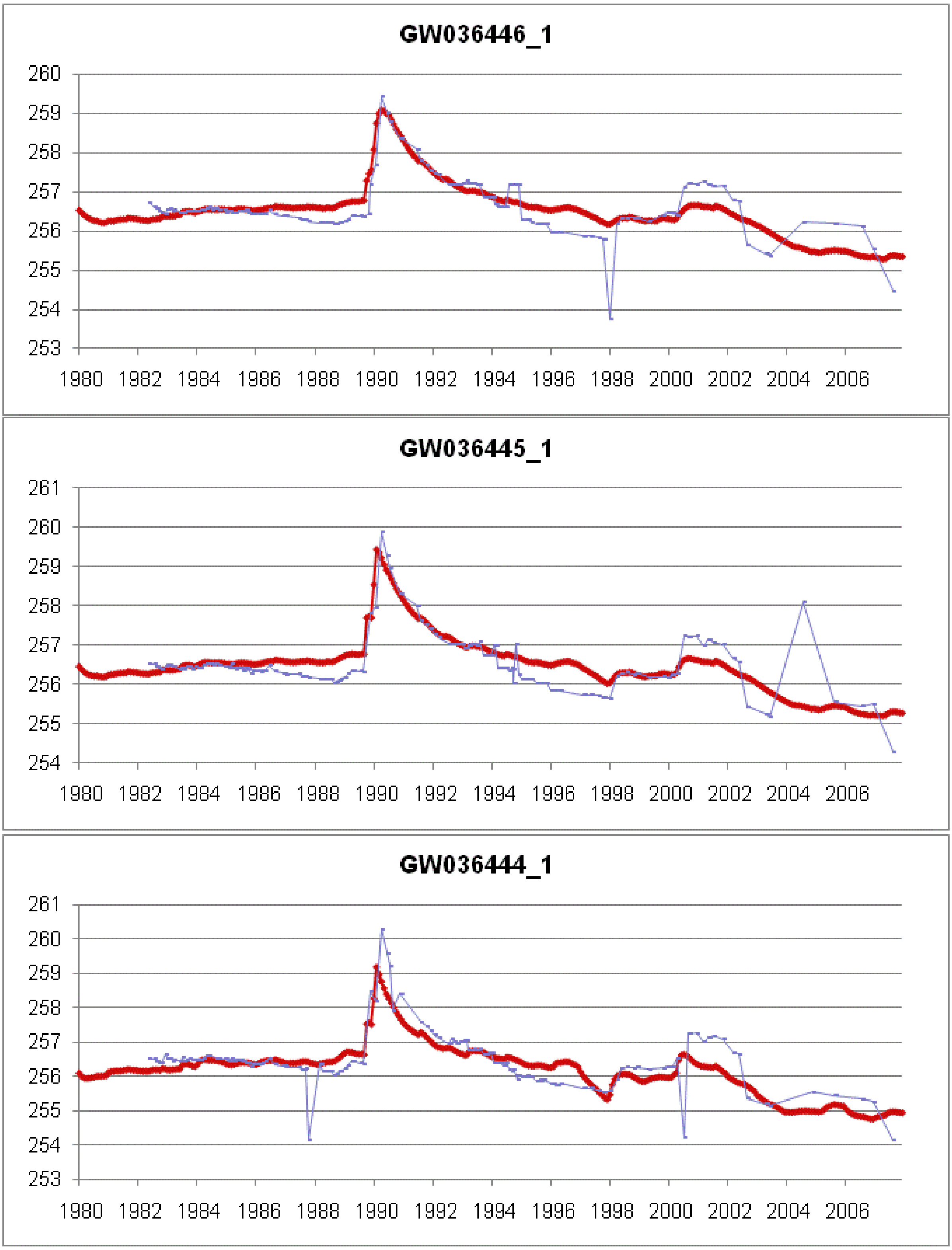
GW036446_1
260
259
258
257
256
255
254
253
1980 1982 1984 1986 1988 1990 1992 1994 1996 1998 2000 2002 2004 2006
GW036445_1
261
260
259
258
257
256
255
254
1980 1982 1984 1986 1988 1990 1992 1994 1996 1998 2000 2002 2004 2006
GW036444_1
261
260
259
258
257
256
255
254
253
1980 1982 1984 1986 1988 1990 1992 1994 1996 1998 2000 2002 2004 2006

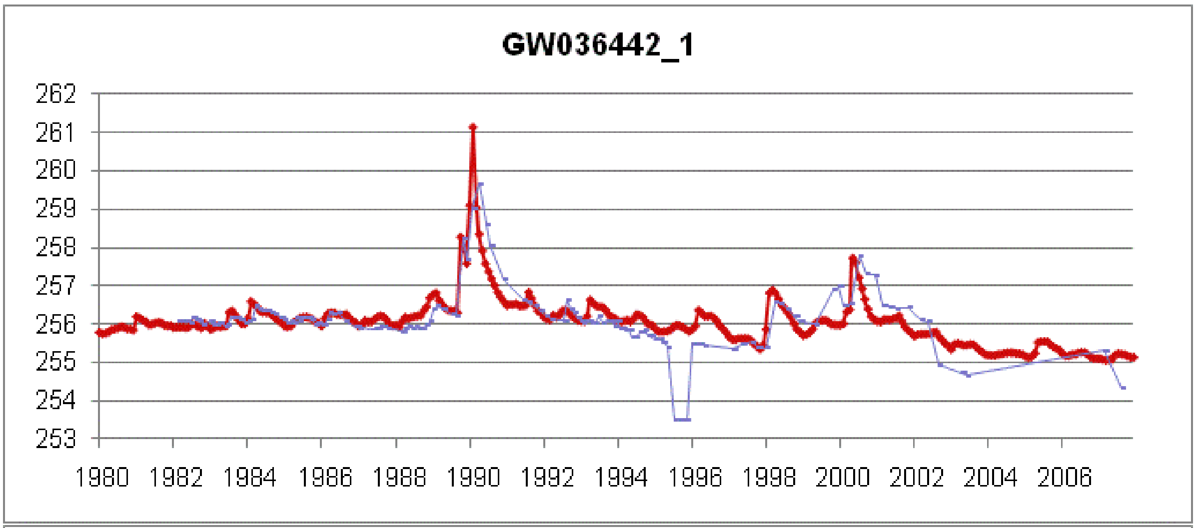
GW036442_1
262
261
260
259
258
257
256
255
254
253
1980 1982 1984 1986 1988 1990 1992 1994 1996 1998 2000 2002 2004 2006

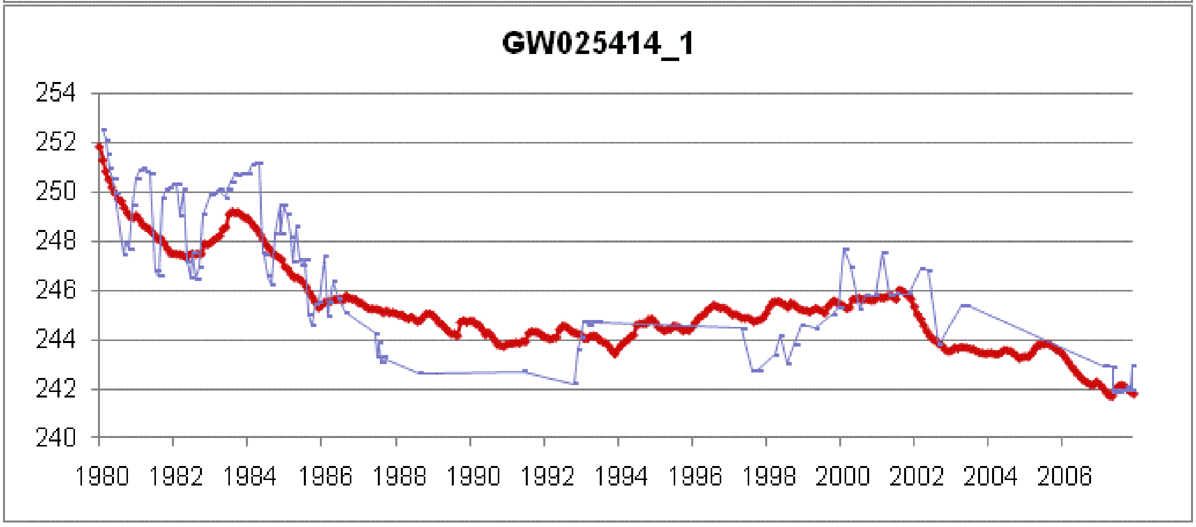
GW025414_1
254
252
250
248
246
244
242
240
1980 1982 1984 1986 1988 1990 1992 1994 1996 1998 2000 2002 2004 2006

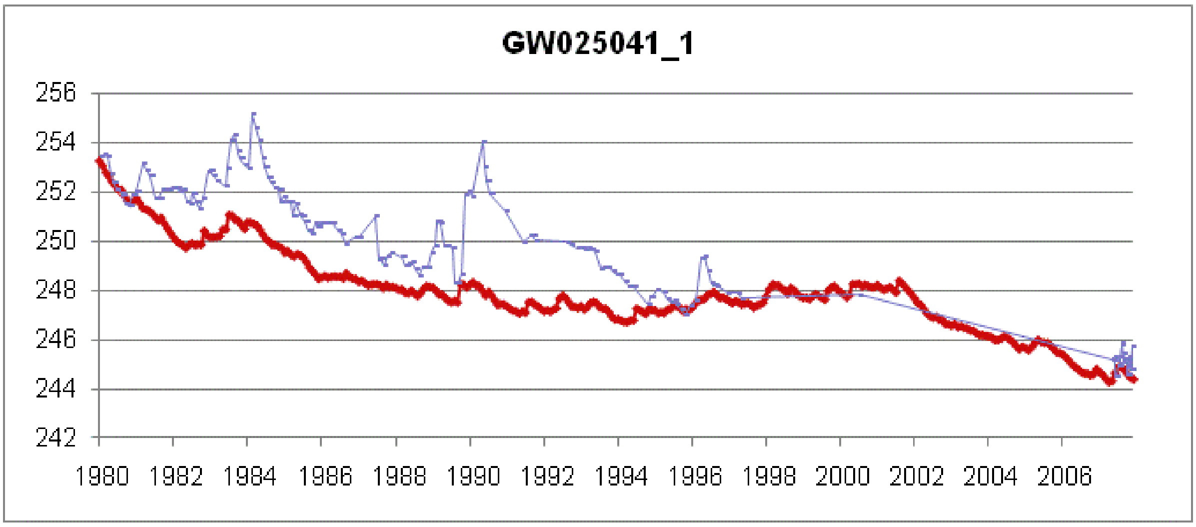
GW025041_1
256
254
252
250
248
246
244
242
1980 1982 1984 1986 1988 1990 1992 1994 1996 1998 2000 2002 2004 2006

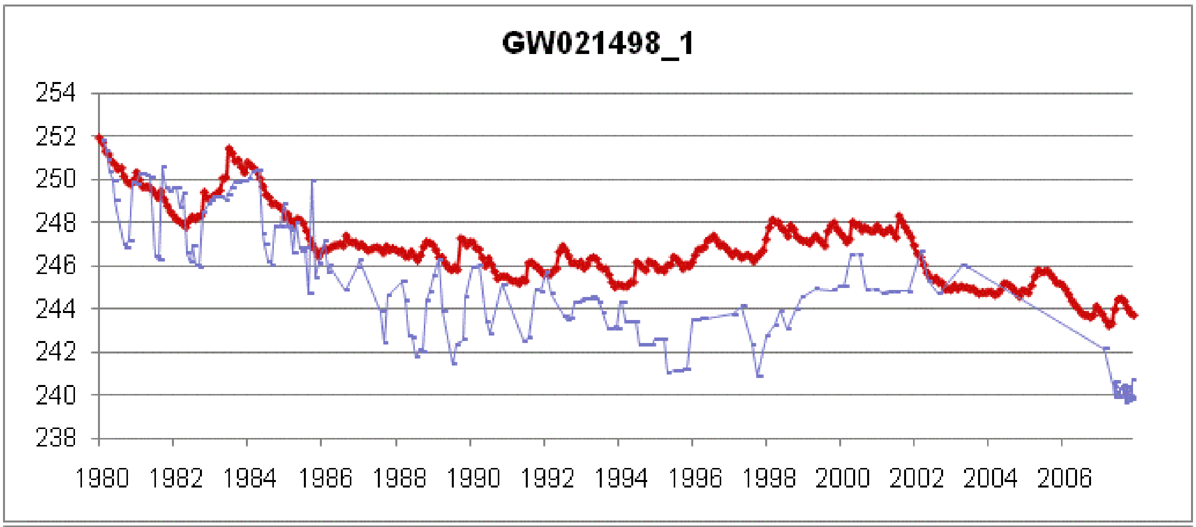
GW021498_1
254
252
250
248
246
244
242
240
238
1980 1982 1984 1986 1988 1990 1992 1994 1996 1998 2000 2002 2004 2006

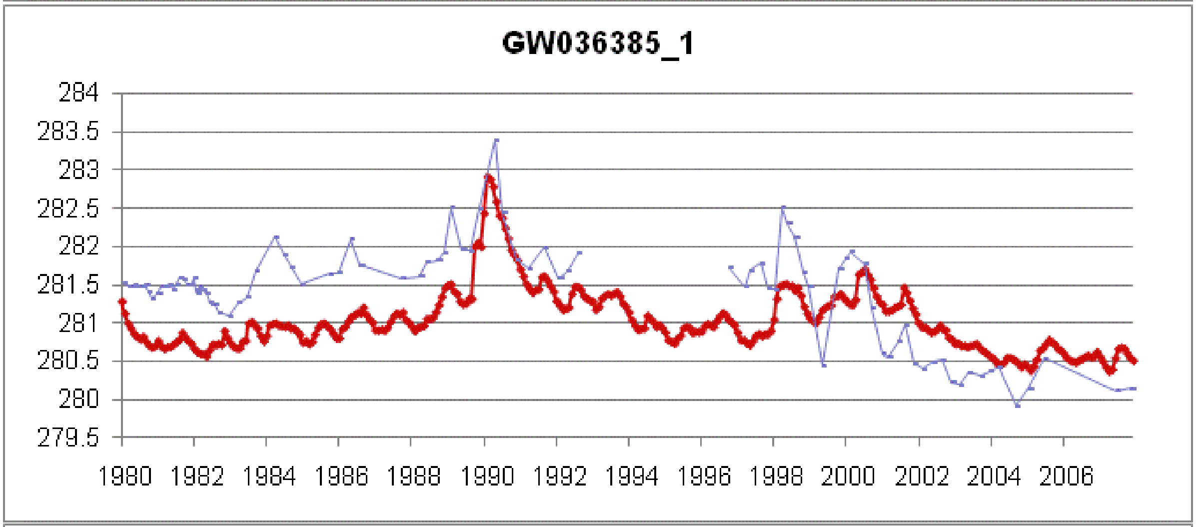
GW036385_1
284
283.5
283
282.5
282
281.5
281
280.5
280
279.5
1980 1982 1984 1986 1988 1990 1992 1994 1996 1998 2000 2002 2004 2006

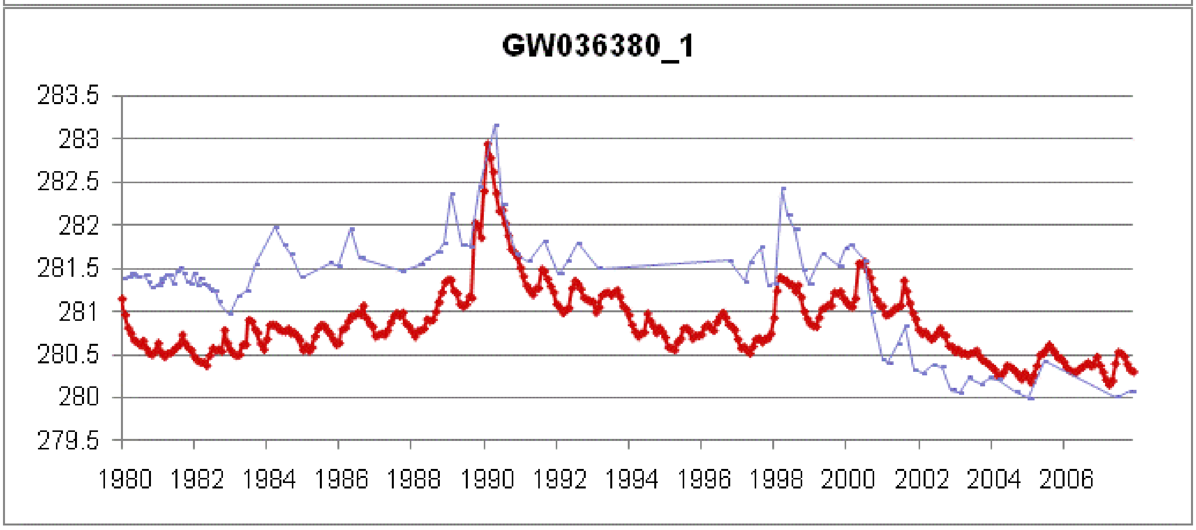
GW036380_1
283.5
283
282.5
282
281.5
281
280.5
280
279.5
1980 1982 1984 1986 1988 1990 1992 1994 1996 1998 2000 2002 2004 2006

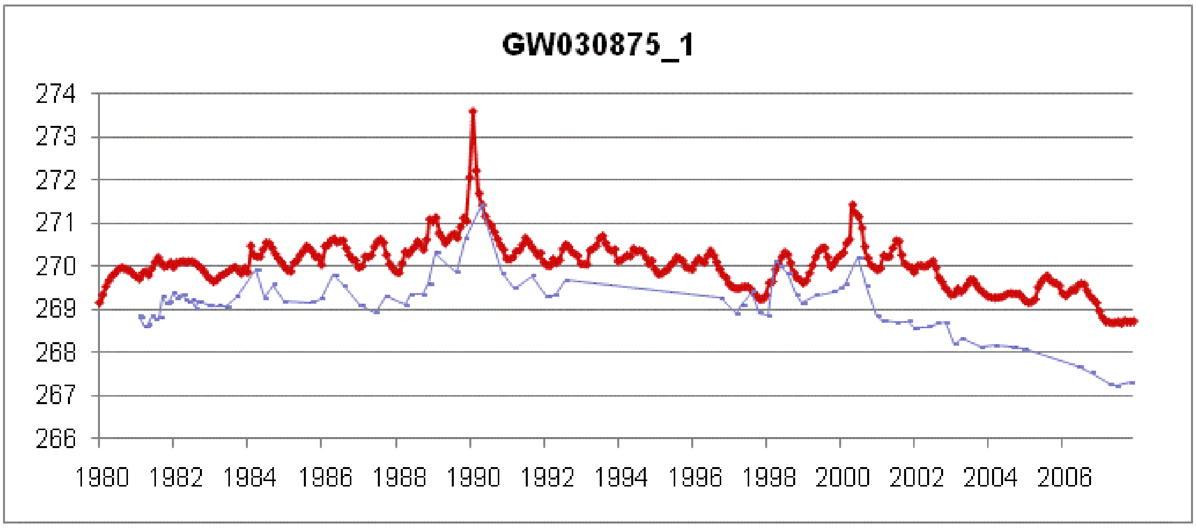
GW030875_1
274
273
272
271
270
269
268
267
266
1980
1982
1984
1986
1988
1990
1992
1994
1996
1998
2000
2002
2004
2006

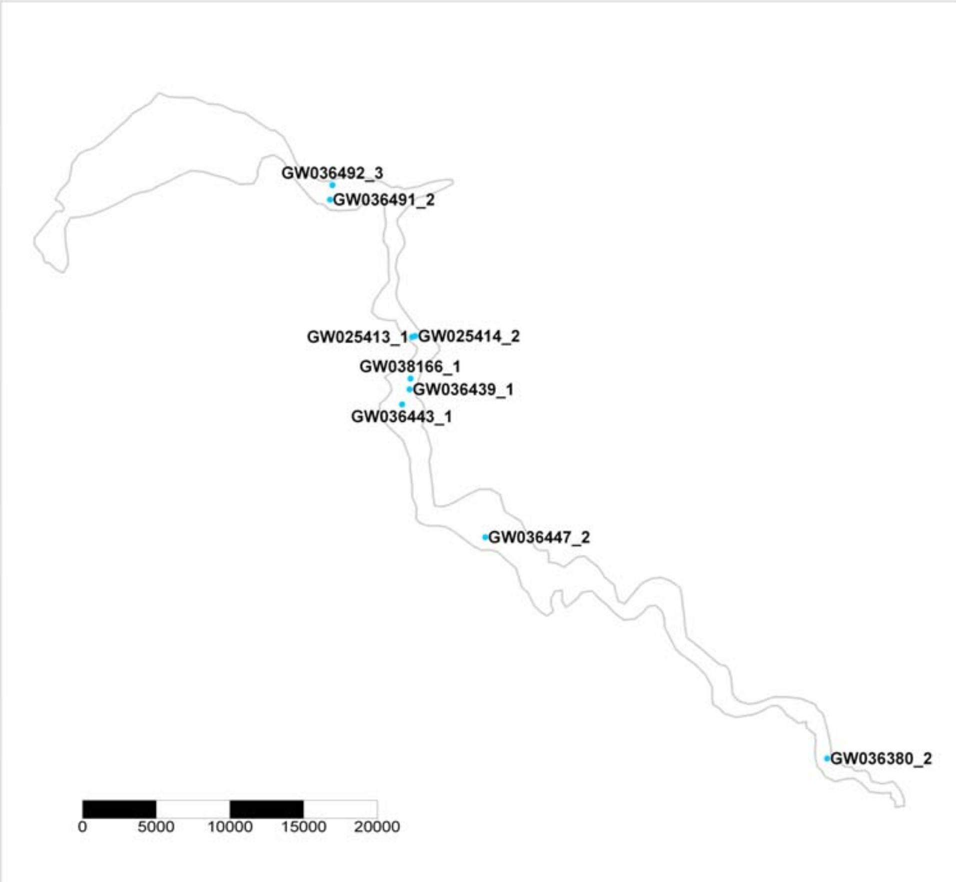
GW036492_3
GW036491_2
GW025413_1
GW025414_2
GW038166_1
GW036439_1
GW036443_1
GW036447_2
GW036380_2
0
5000
10000
15000
20000

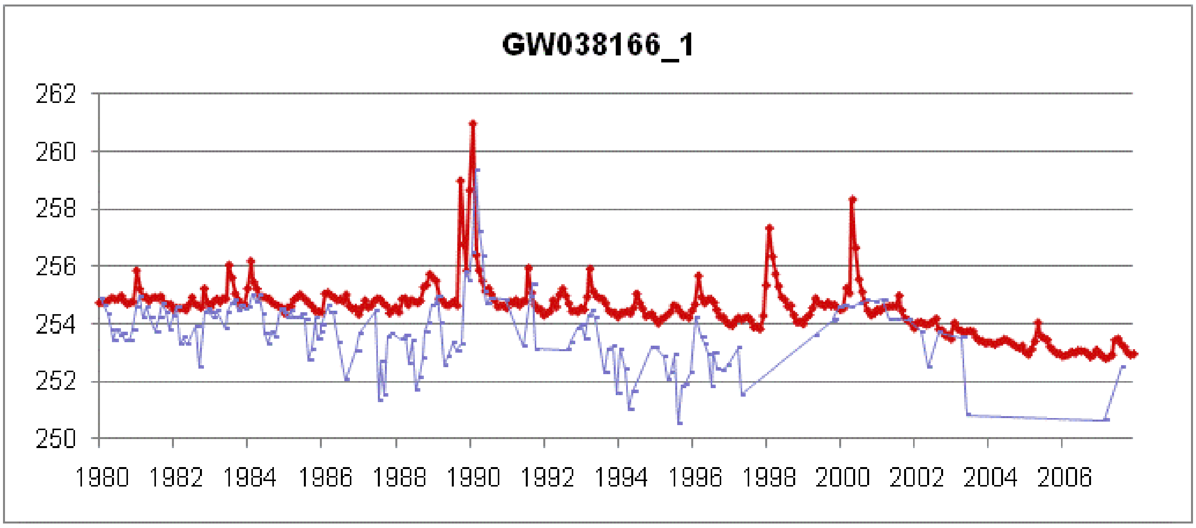
GW038166_1
262
260
258
256
254
252
250
1980
1982
1984
1986
1988
1990
1992
1994
1996
1998
2000
2002
2004
2006

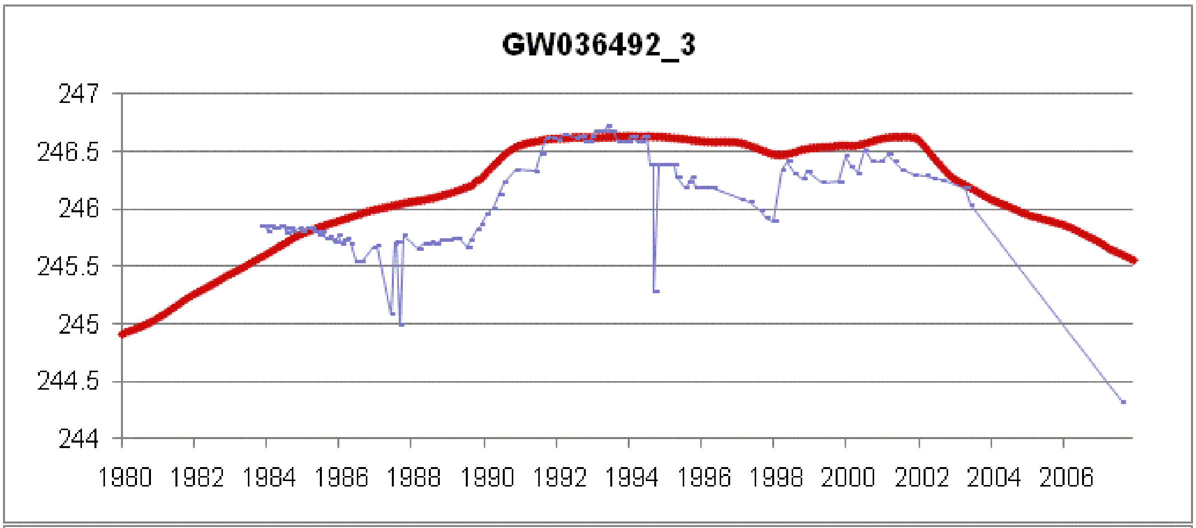
GW036492_3
247
246.5
246
245.5
245
244.5
244
1980 1982 1984 1986 1988 1990 1992 1994 1996 1998 2000 2002 2004 2006

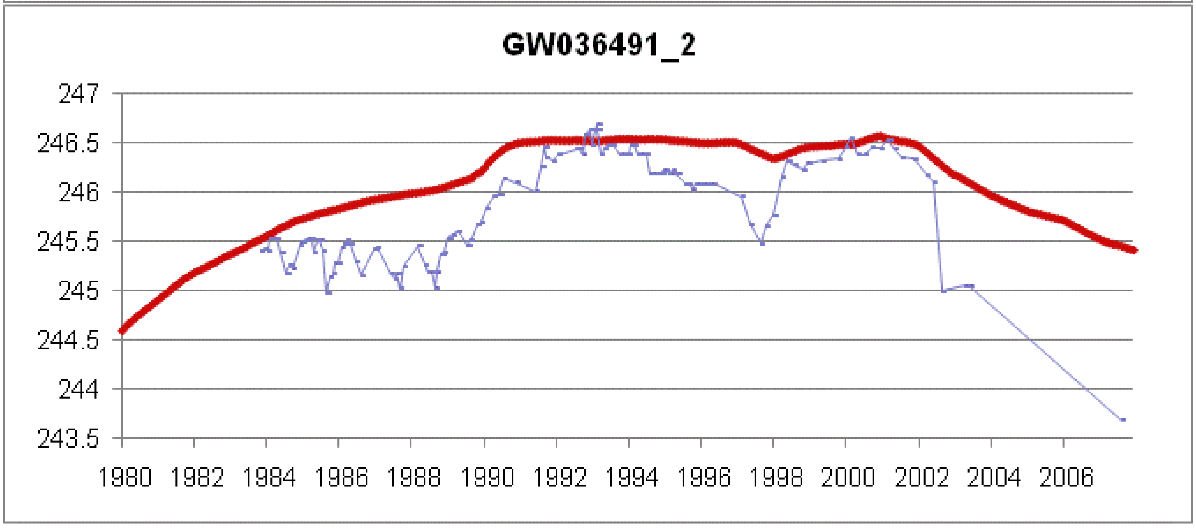
GW036491_2
247
246.5
246
245.5
245
244.5
244
243.5
1980 1982 1984 1986 1988 1990 1992 1994 1996 1998 2000 2002 2004 2006

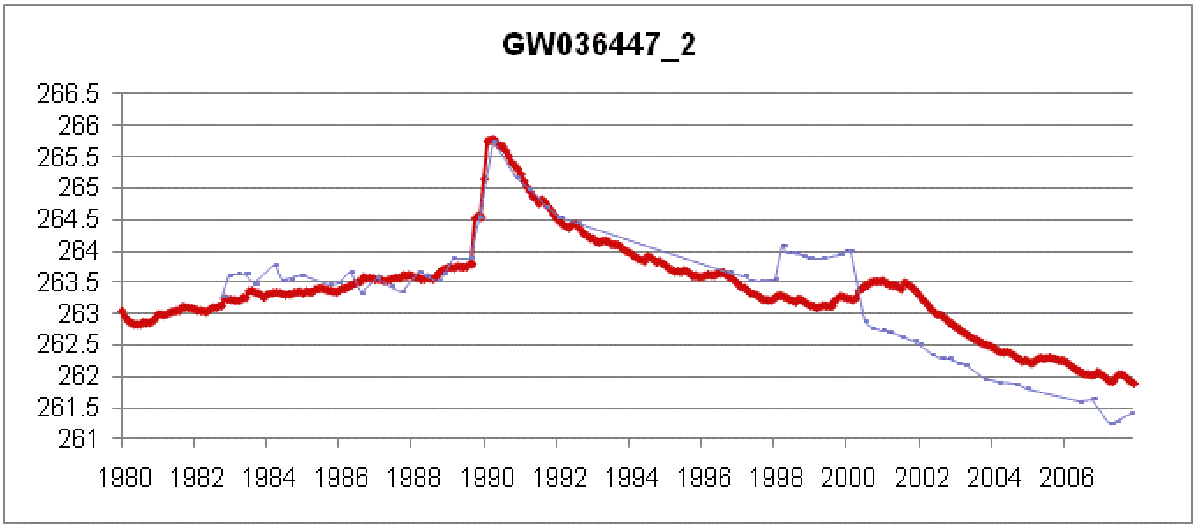
GW036447_2
266.5
266
265.5
265
264.5
264
263.5
263
262.5
262
261.5
261
1980 1982 1984 1986 1988 1990 1992 1994 1996 1998 2000 2002 2004 2006

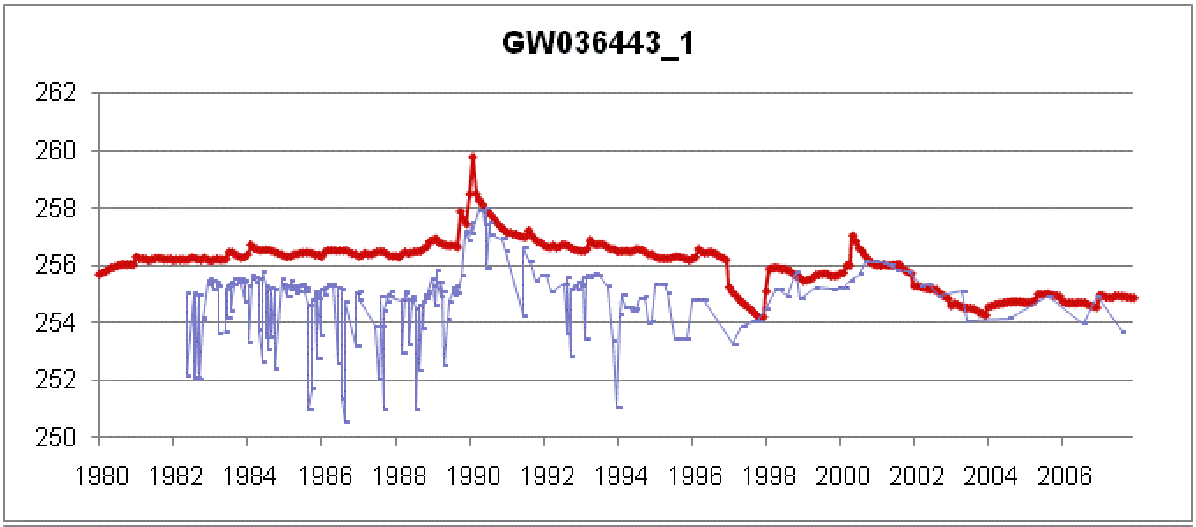
GW036443_1
262
260
258
256
254
252
250
1980 1982 1984 1986 1988 1990 1992 1994 1996 1998 2000 2002 2004 2006

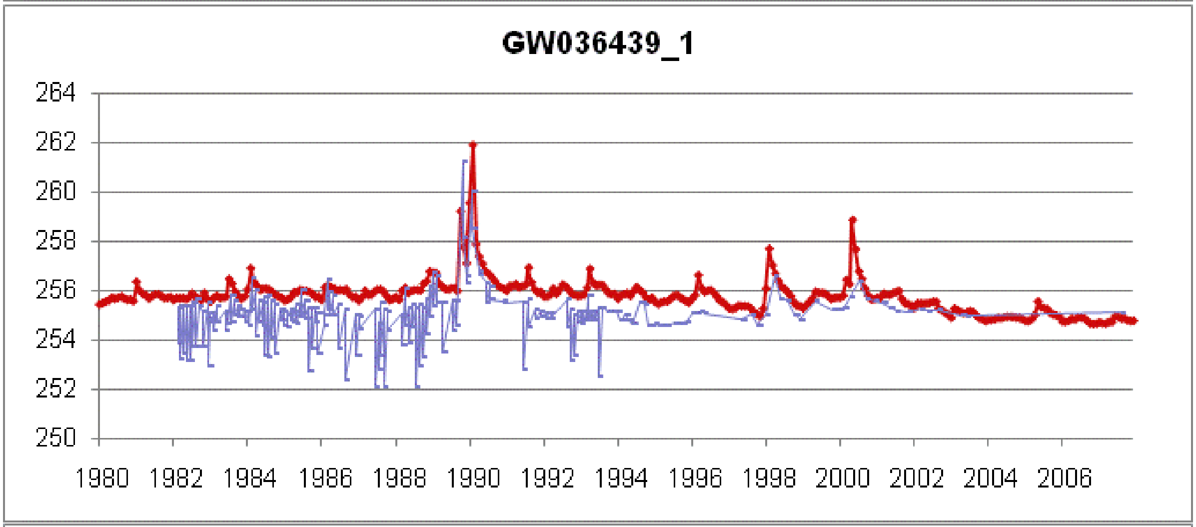
GW036439_1
264
262
260
258
256
254
252
250
1980 1982 1984 1986 1988 1990 1992 1994 1996 1998 2000 2002 2004 2006

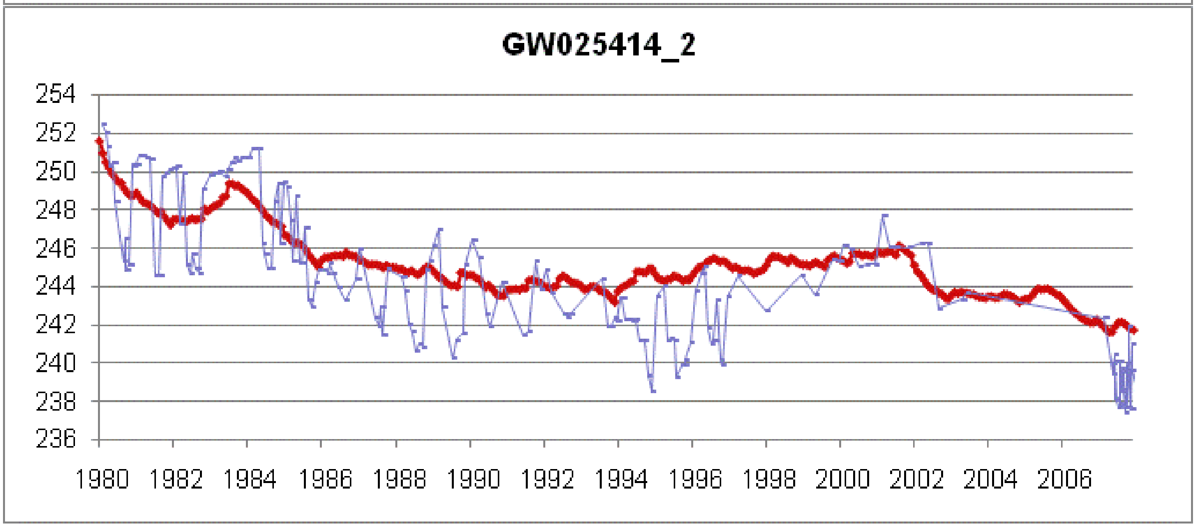
GW025414_2
254
252
250
248
246
244
242
240
238
236
1980 1982 1984 1986 1988 1990 1992 1994 1996 1998 2000 2002 2004 2006

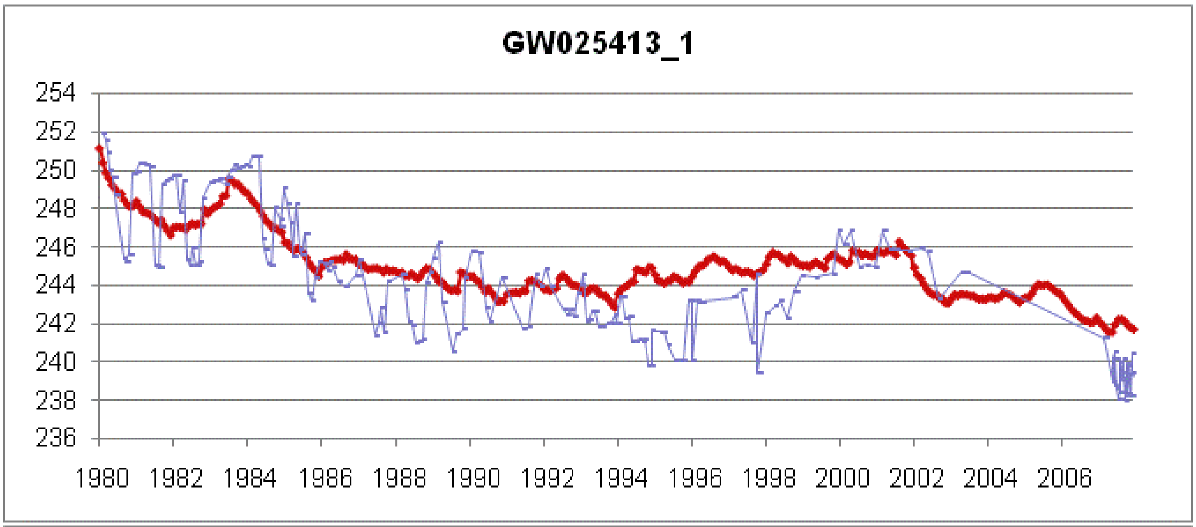
GW025413_1
254
252
250
248
246
244
242
240
238
236
1980 1982 1984 1986 1988 1990 1992 1994 1996 1998 2000 2002 2004 2006

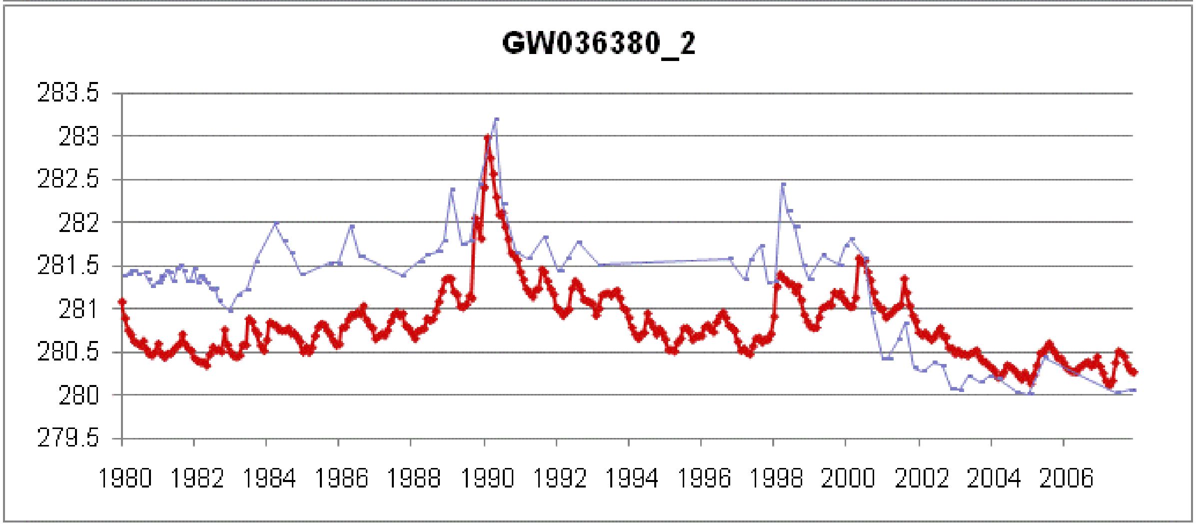
GW036380_2
283.5
283
282.5
282
281.5
281
280.5
280
279.5
1980 1982 1984 1986 1988 1990 1992 1994 1996 1998 2000 2002 2004 2006

Appendix D Mass Balance

Scenario 1a

Mass Balance Summary

FLOW IN	Storage		River_Leakage		GHBs	Recharge	Total IN
(GL/year)	8.8		8.9		2.6	9.2	29.5
FLOW OUT	Storage	Wells	River_Leakag	ET	GHBs		Total Out
(GL/year)	10.1	0.0	18.5	0.4	0.6		29.5

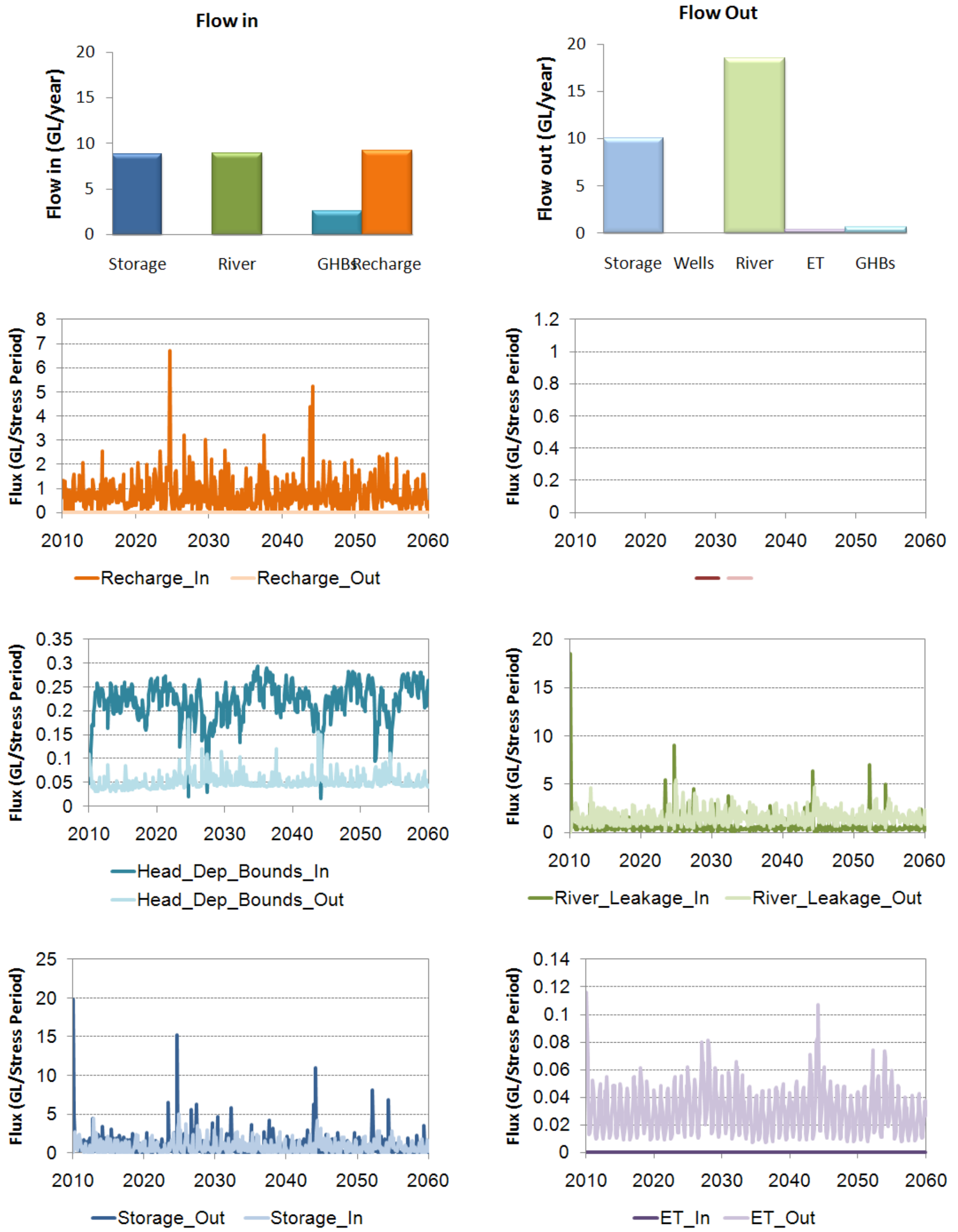

Scenario 1b

Mass Balance Summary

FLOW IN	Storage		River_Leakage		GHBs	Recharge	Total IN
(GL/year)	8.8		14.5		2.7	9.0	35.1
FLOW OUT	Storage	Wells	River_Leaka	ET	GHBs		Total Out
(GL/year)	9.3	11.3	13.8	0.3	0.4		35.1

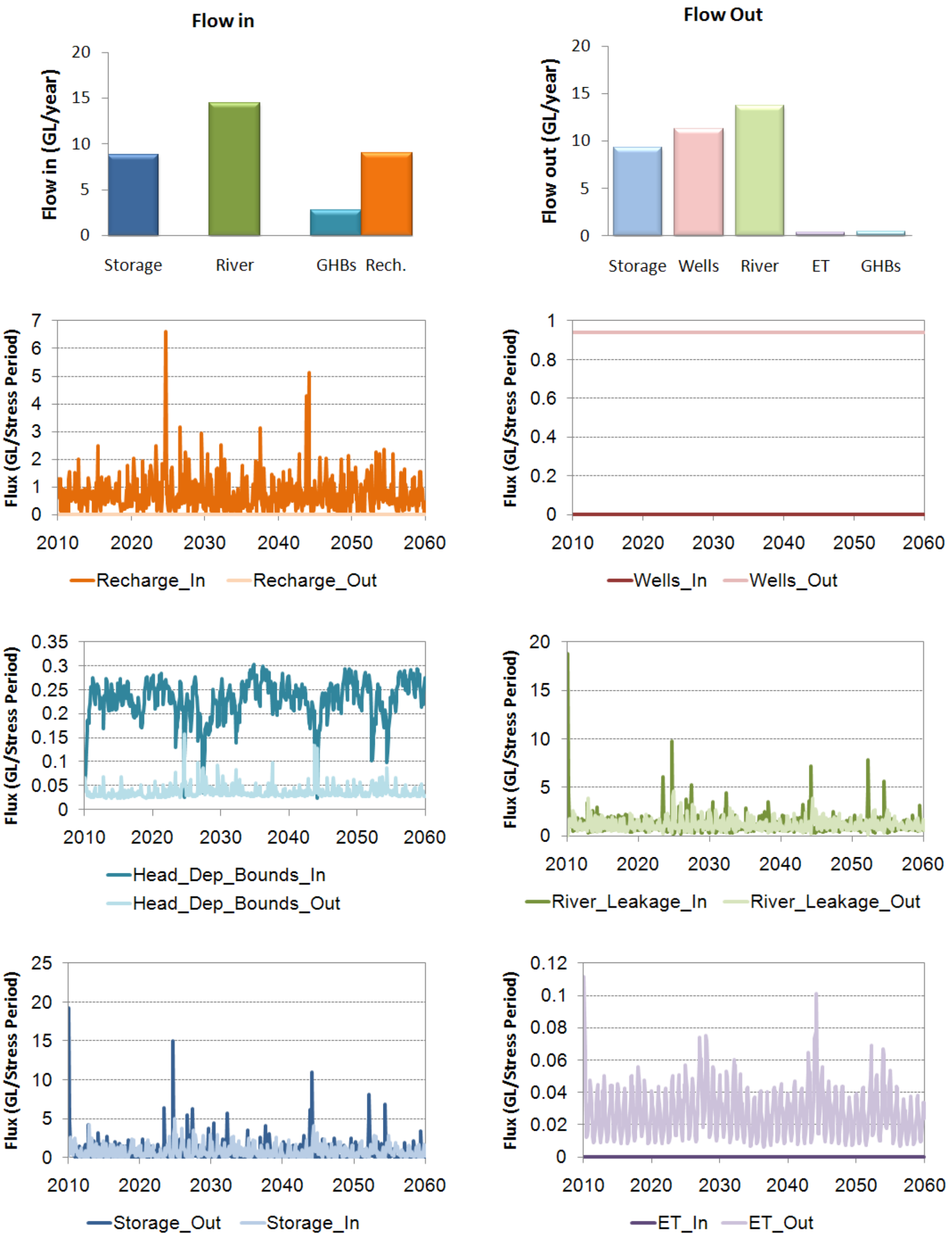

Scenario 1c

Mass Balance Summary

FLOW IN	Storage		River_Leakage		GHBs	Recharge	Total IN
(GL/year)	9.1		18.5		2.8	9.0	39.4
FLOW OUT	Storage	Wells	River_Leaka	ET	GHBs		Total Out
(GL/year)	9.2	16.7	12.8	0.3	0.4		39.4

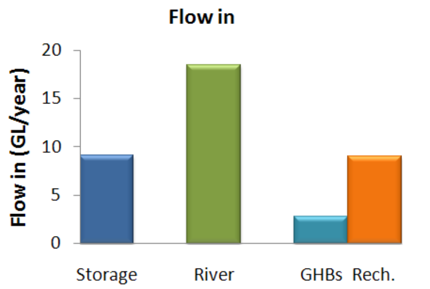

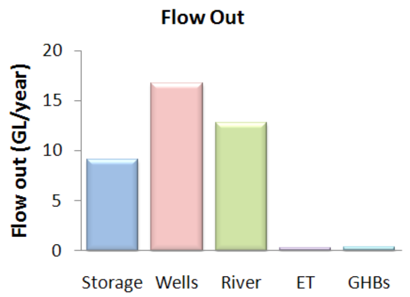

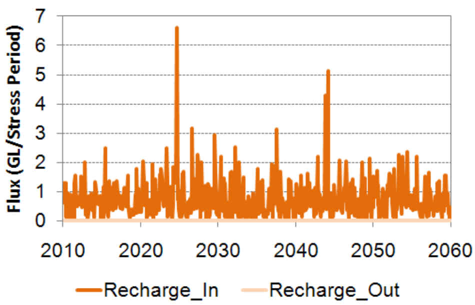

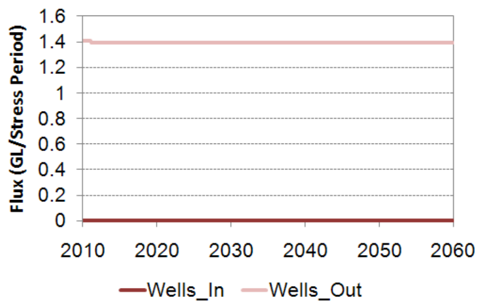

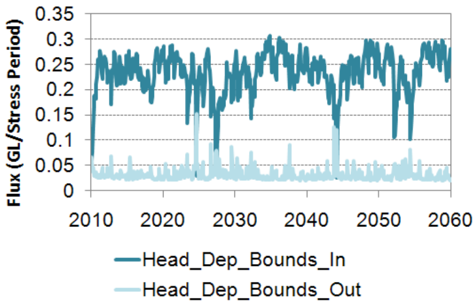

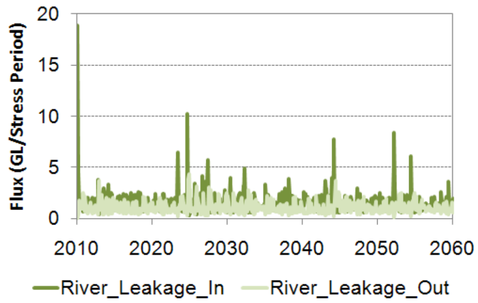

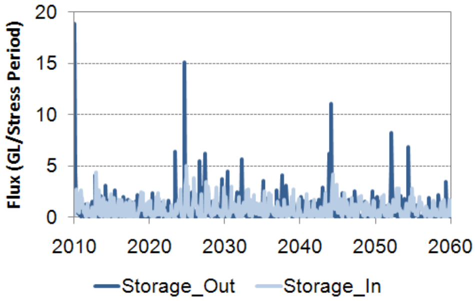

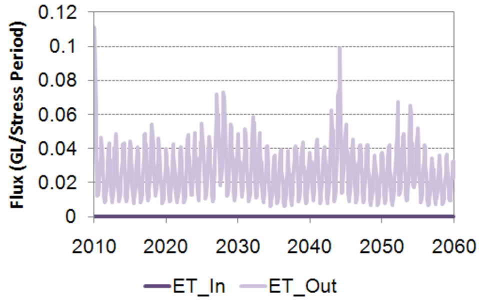

Scenario 1d

Mass Balance Summary

FLOW IN	Storage		River_Leakage		GHBs	Recharge	Total IN
(GL/year)	10.2		28.5		3.1	9.0	50.8
FLOW OUT	Storage	Wells	River_Leakag	ET	GHBs		Total Out
(GL/year)	9.5	29.6	11.1	0.3	0.3		50.8

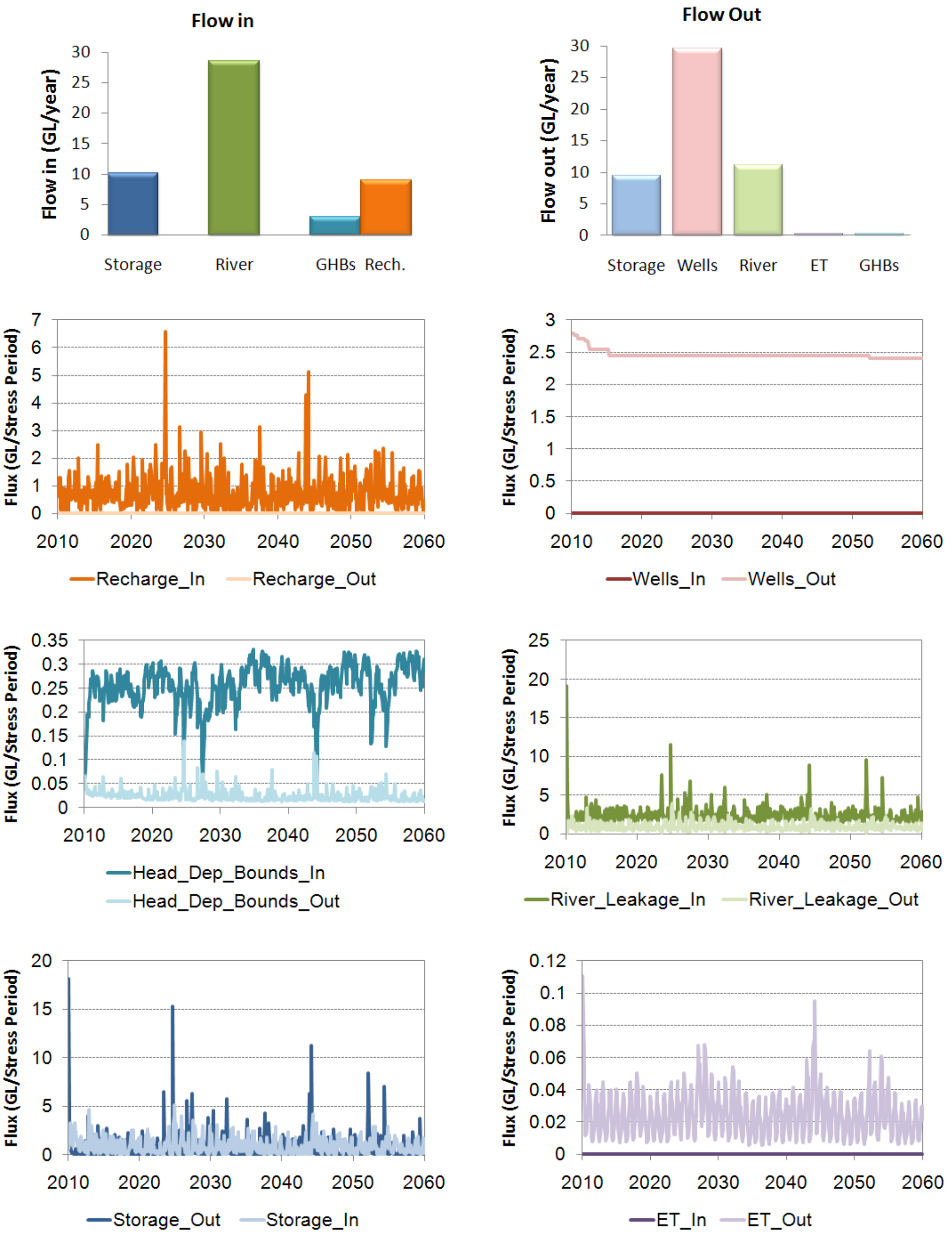

Scenario 2a

Mass Balance Summary

FLOW IN	Storage		River_Leakage		GHBs	Recharge	Total IN
(GL/year)	7.4		7.7		2.9	8.1	26.0
FLOW OUT	Storage	Wells	River_Leakage	ET	GHBs		Total Out
(GL/year)	8.5	0.0	16.7	0.3	0.5		26.0

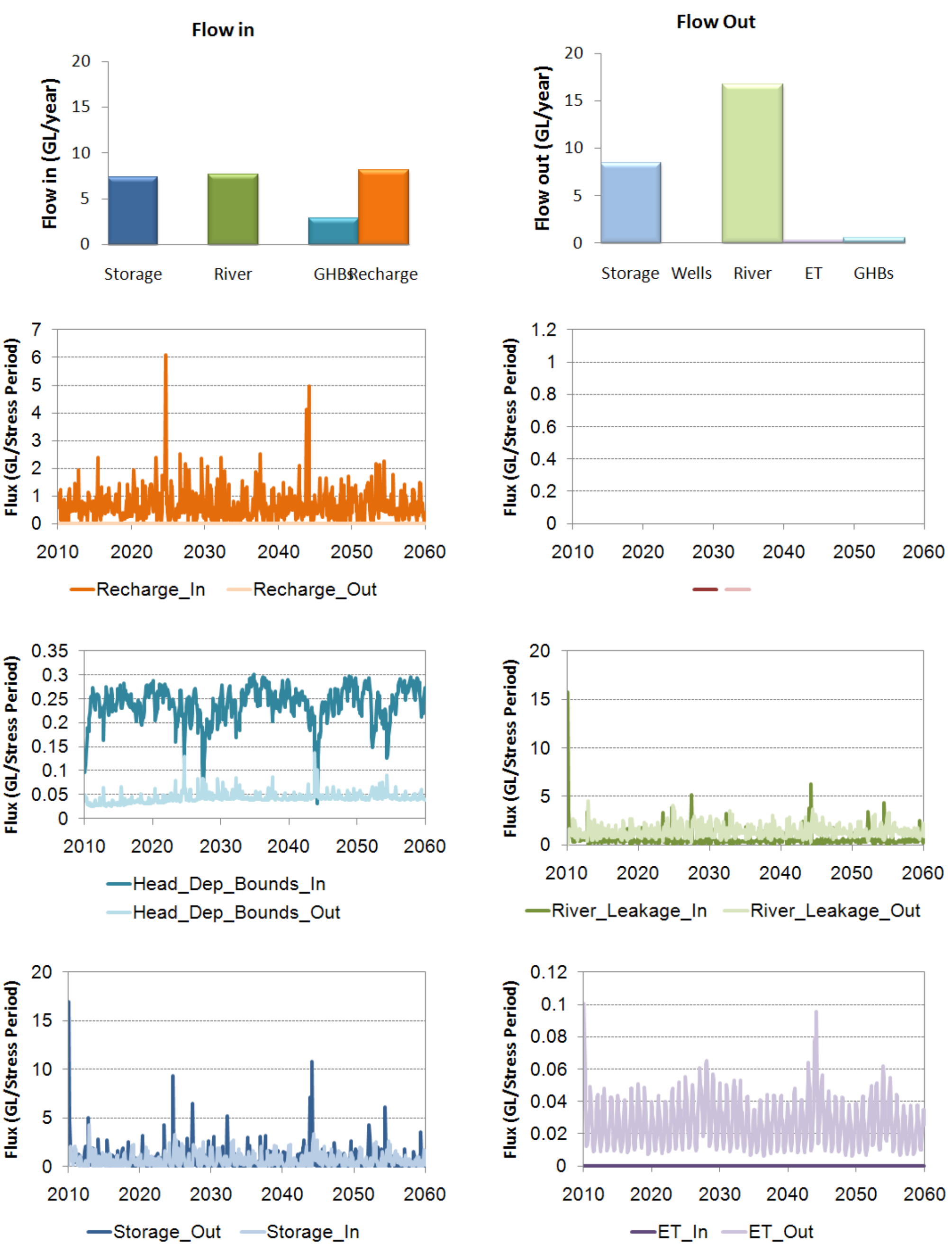

SINCLAIR KNIGHT MERZ

Scenario 2b

Mass Balance Summary

FLOW IN	Storage		River_Leakage		GHBs	Recharge	Total IN
(GL/year)	7.6		14.2		2.9	8.1	32.9
FLOW OUT	Storage	Wells	River_Leaka	ET	GHBs		Total Out
(GL/year)	8.0	11.3	12.9	0.3	0.4		32.9

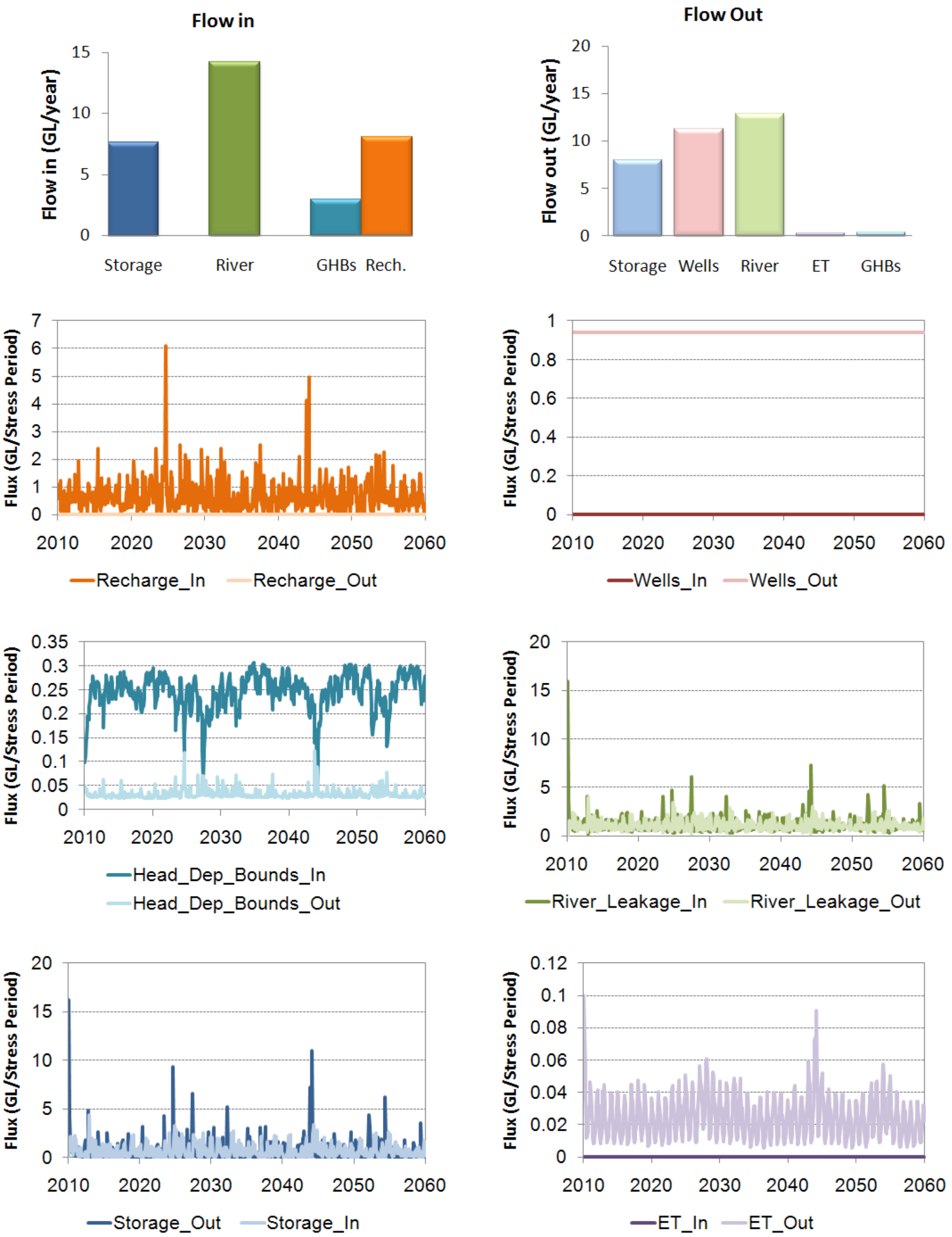

Scenario 2c

Mass Balance Summary

FLOW IN	Storage		River_Leakage		GHBs	Recharge	Total IN
(GL/year)	8.0		18.2		3.0	8.1	37.2
FLOW OUT	Storage	Wells	River_Leakag	ET	GHBs		Total Out
(GL/year)	7.9	16.7	12.0	0.3	0.3		37.2

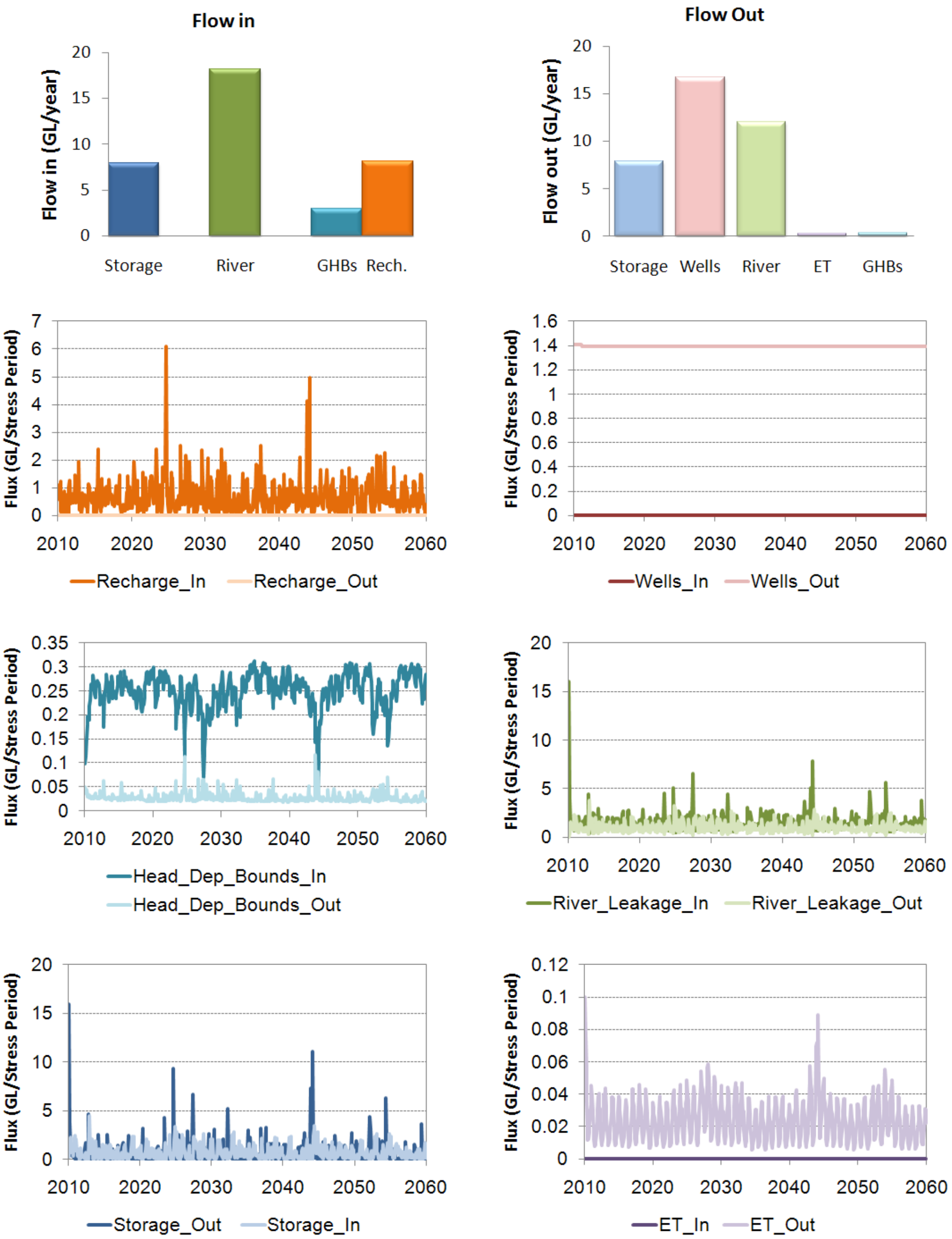

Scenario 2d

Mass Balance Summary

FLOW IN	Storage		River_Leakage		GHBs	Recharge	Total IN
(GL/year)	9.3		27.9		3.3	8.1	48.6
FLOW OUT	Storage	Wells	River_Leakag	ET	GHBs		Total Out
(GL/year)	8.4	29.4	10.4	0.3	0.3		48.6

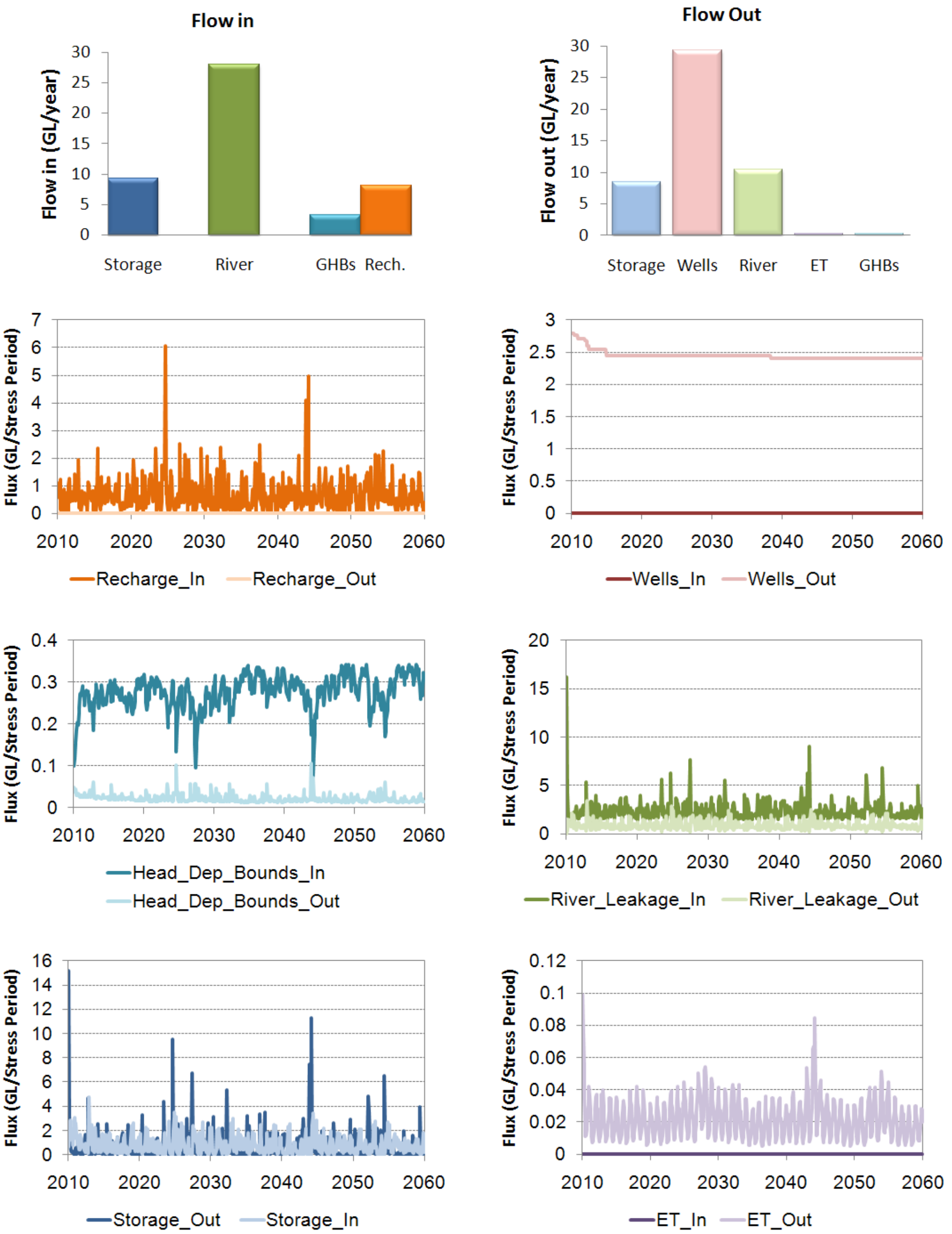

Scenario 3a

Mass Balance Summary

FLOW IN	Storage		River_Leakage		GHBs	Recharge	Total IN
(GL/year)	8.3		8.0		2.7	8.9	27.9
FLOW OUT	Storage	Wells	River_Leakag	ET	GHBs		Total Out
(GL/year)	9.4	0.0	17.6	0.3	0.6		27.9

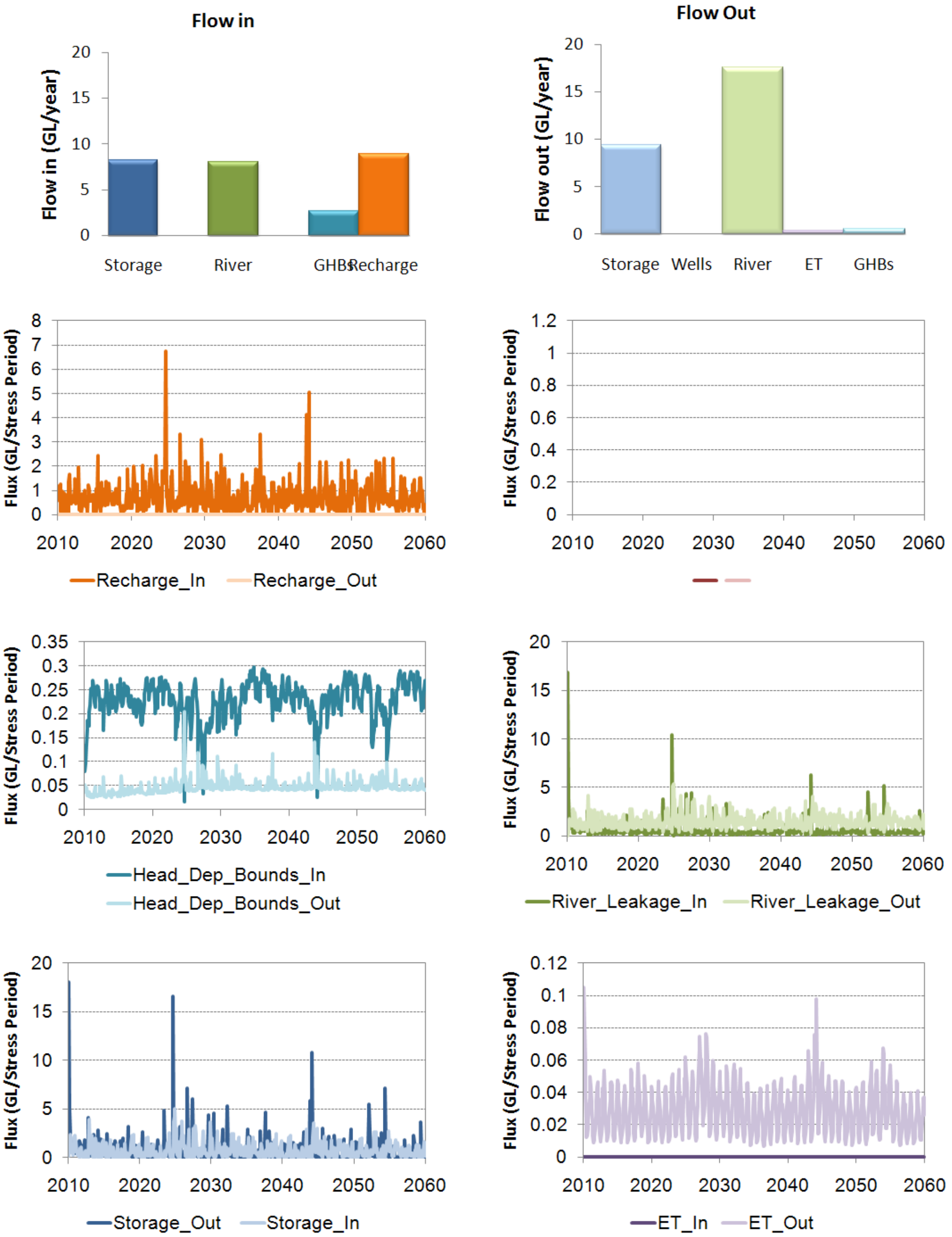

Scenario 3b

Mass Balance Summary

FLOW IN	Storage		River_Leakage		GHBs	Recharge	Total IN
(GL/year)	8.5		14.4		2.8	8.9	34.6
FLOW OUT	Storage	Wells	River_Leakag	ET	GHBs		Total Out
(GL/year)	9.0	11.3	13.6	0.3	0.4		34.6

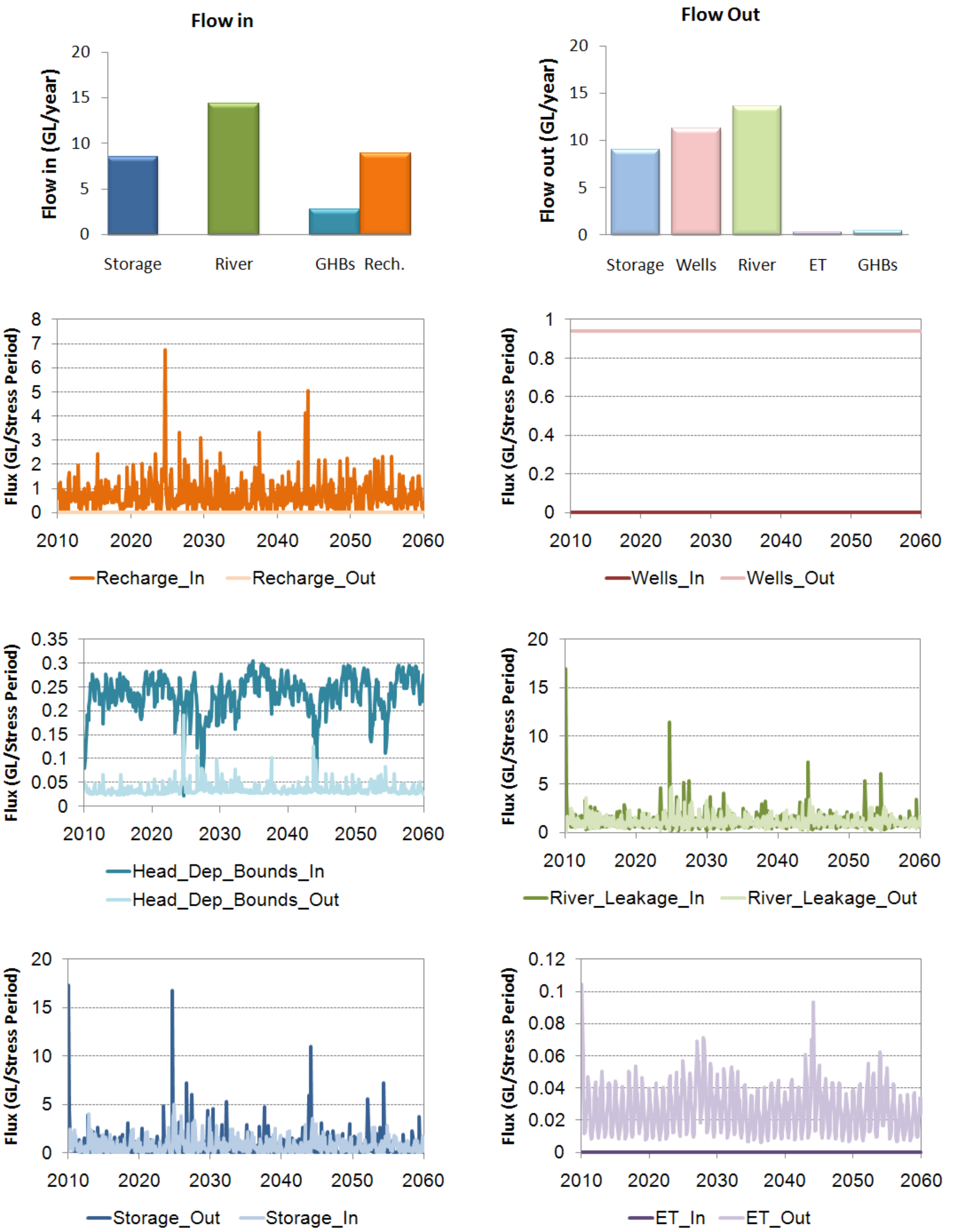

Scenario 3c

Mass Balance Summary

FLOW IN	Storage		River_Leakage		GHBs	Recharge	Total IN
(GL/year)	8.8		18.4		2.9	8.9	38.9
FLOW OUT	Storage	Wells	River_Leakag	ET	GHBs		Total Out
(GL/year)	8.9	16.7	12.7	0.3	0.4		38.9

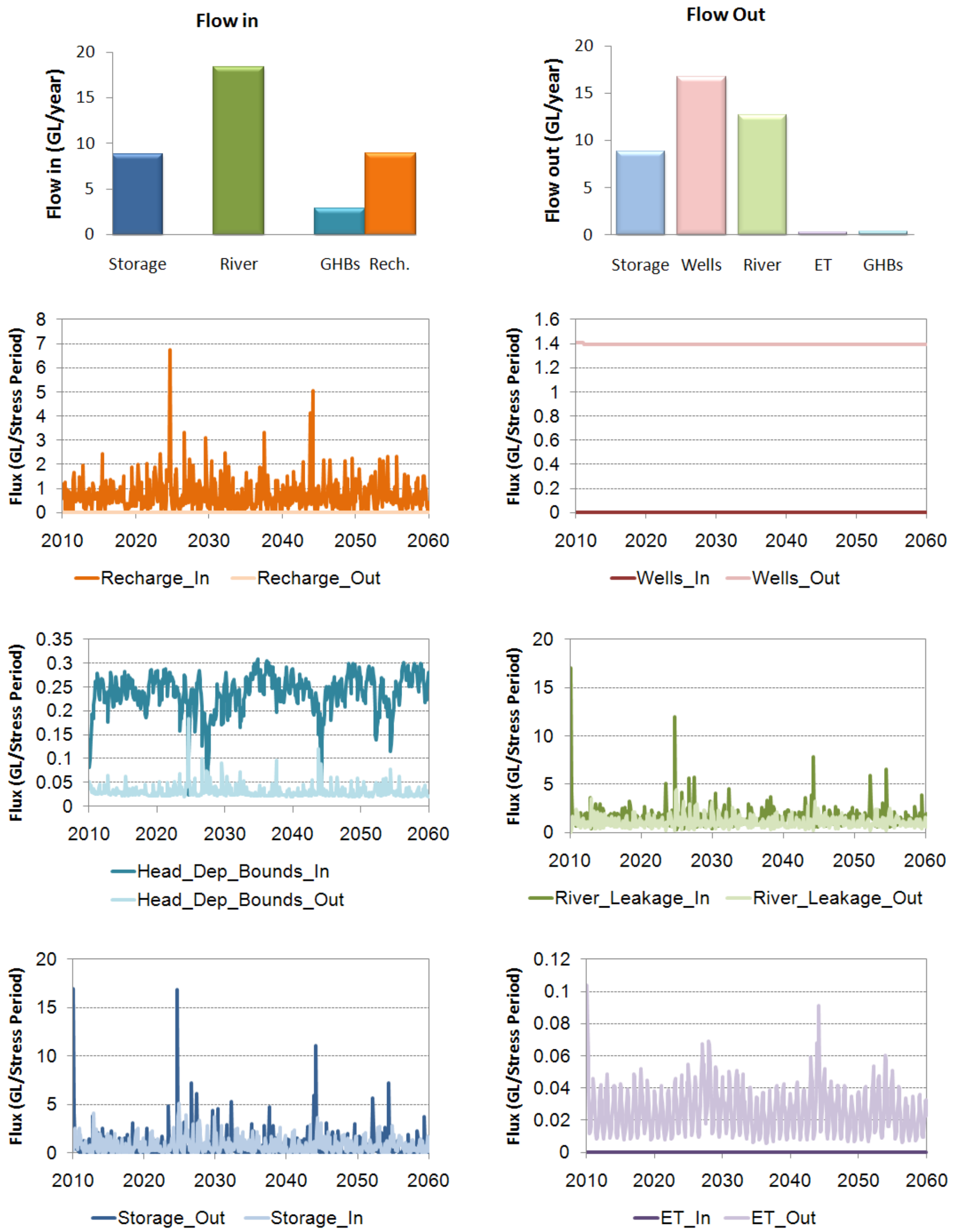

Scenario 3d

Mass Balance Summary

FLOW IN	Storage		River_Leakage		GHBs	Recharge	Total IN
(GL/year)	10.0		28.4		3.1	8.9	50.3
FLOW OUT	Storage	Wells	River_Leaka	ET	GHBs		Total Out
(GL/year)	9.2	29.5	11.0	0.3	0.3		50.3

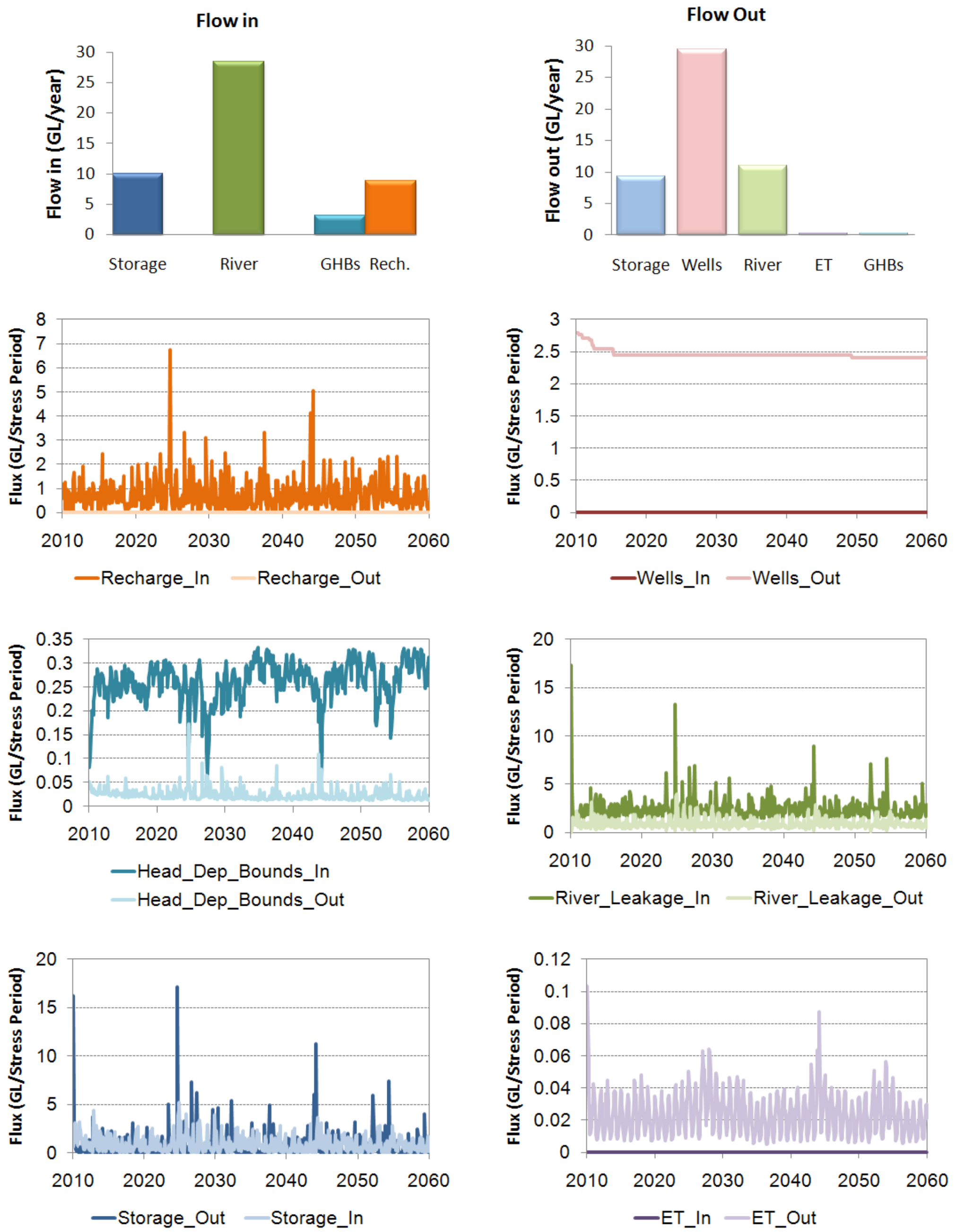

Scenario 4a

Mass Balance Summary

FLOW IN	Storage		River_Leakage		GHBs	Recharge	Total IN
(GL/year)	9.7		8.7		2.5	10.0	30.9
FLOW OUT	Storage	Wells	River_Leaka	ET	GHBs		Total Out
(GL/year)	10.9	0.0	18.9	0.4	0.6		30.9

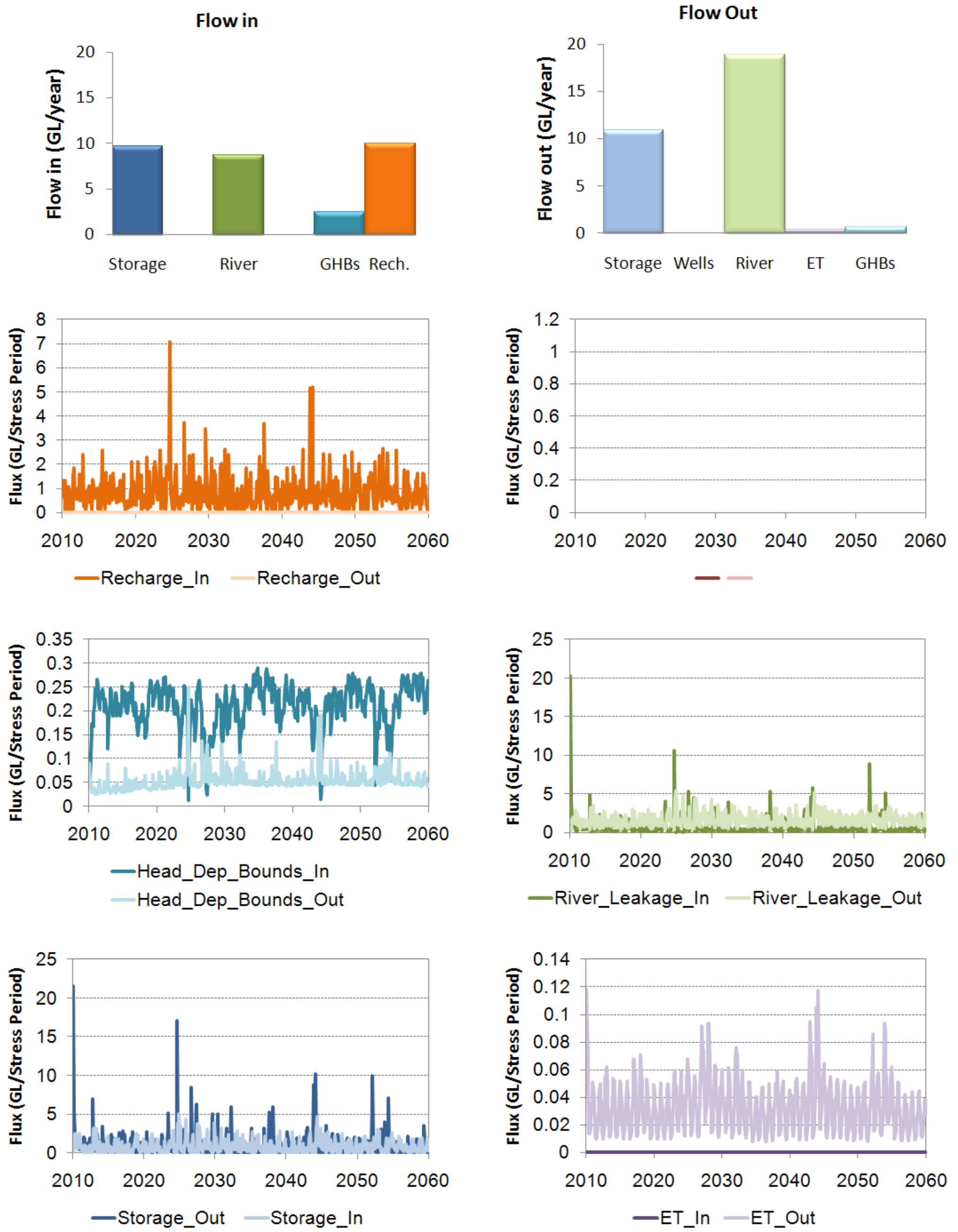

Scenario 4b

Mass Balance Summary

FLOW IN	Storage		River_Leakage		GHBs	Recharge	Total IN
(GL/year)	9.9		14.8		2.6	10.0	37.3
FLOW OUT	Storage	Wells	River_Leaka	ET	GHBs		Total Out
(GL/year)	10.5	11.3	14.7	0.4	0.5		37.3

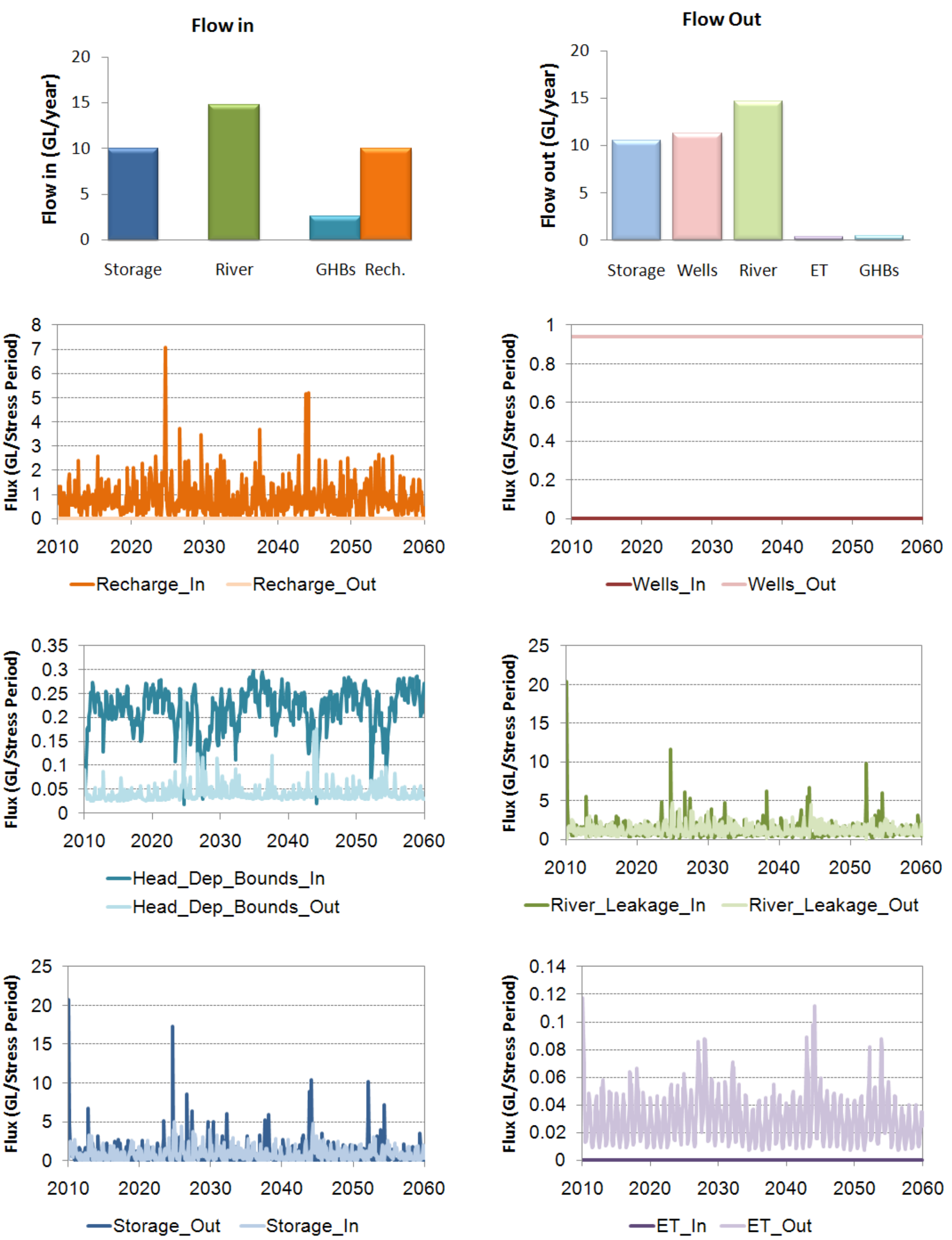

Scenario 4c

Mass Balance Summary

FLOW IN	Storage		River_Leakage		GHBs	Recharge	Total IN
(GL/year)	10.2		18.7		2.6	10.0	41.5
FLOW OUT	Storage	Wells	River_Leaka	ET	GHBs		Total Out
(GL/year)	10.4	16.7	13.7	0.4	0.4		41.5

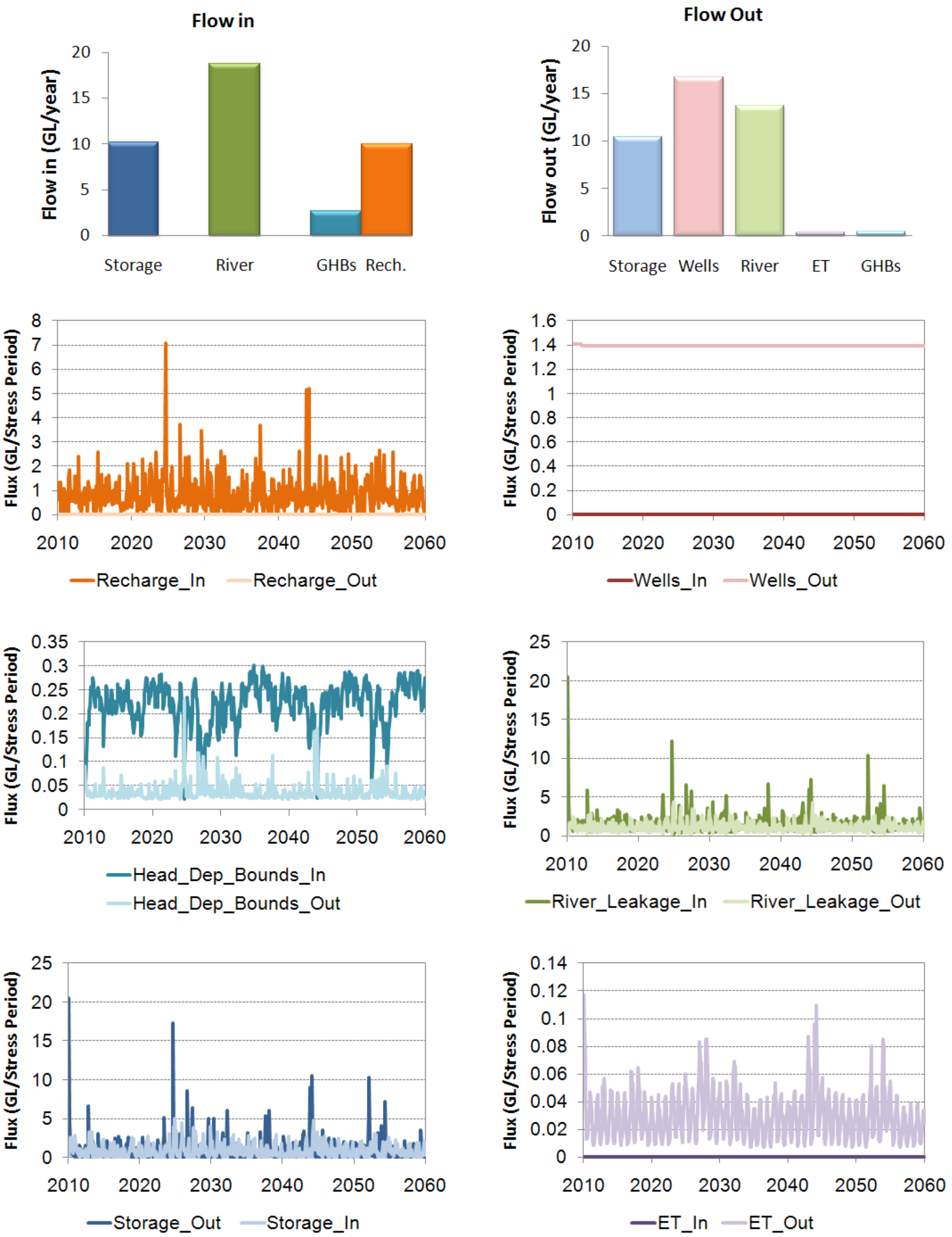

Scenario 4d

Mass Balance Summary

FLOW IN	Storage		River_Leakage		GHBs	Recharge	Total IN
(GL/year)	11.2		28.9		2.9	10.0	52.9
FLOW OUT	Storage	Wells	River_Leaka	ET	GHBs		Total Out
(GL/year)	10.6	29.7	11.9	0.3	0.3		52.9

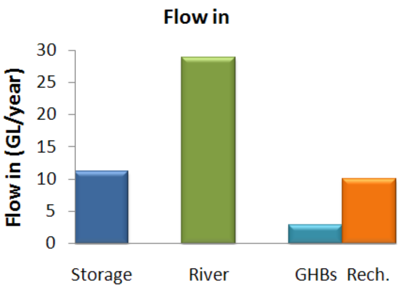

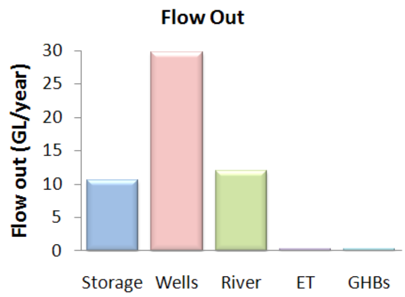

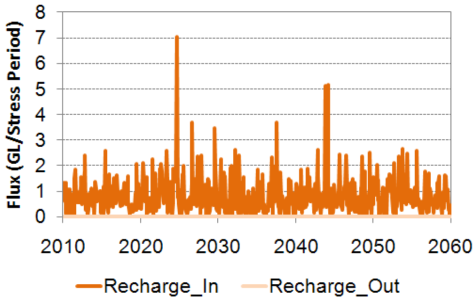

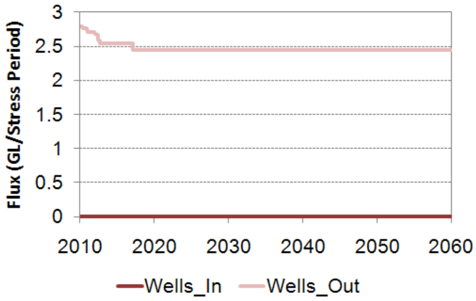

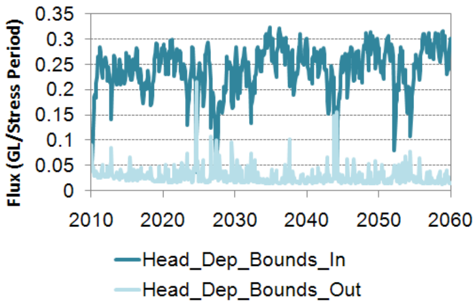

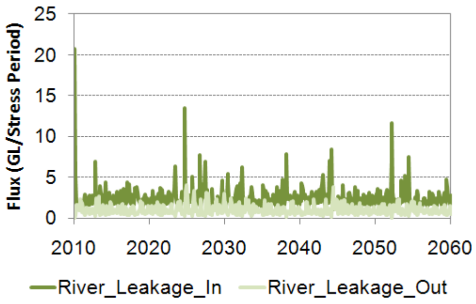

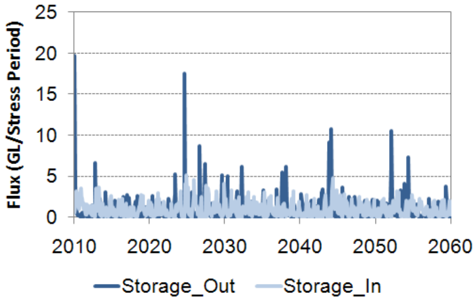

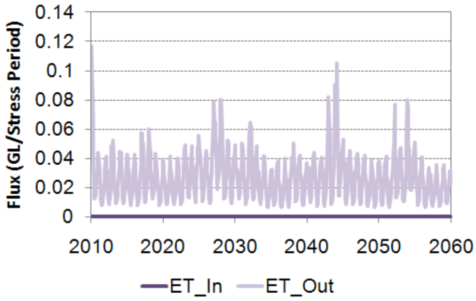

Appendix E Mass Balance

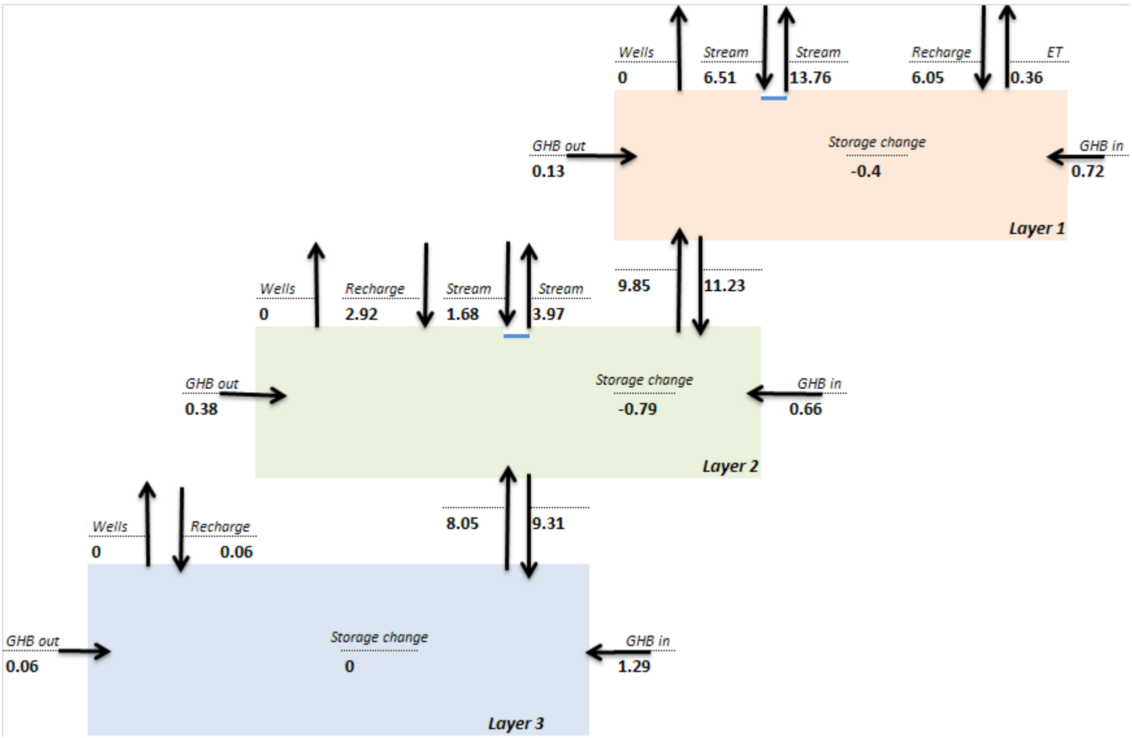

Scenario 1a

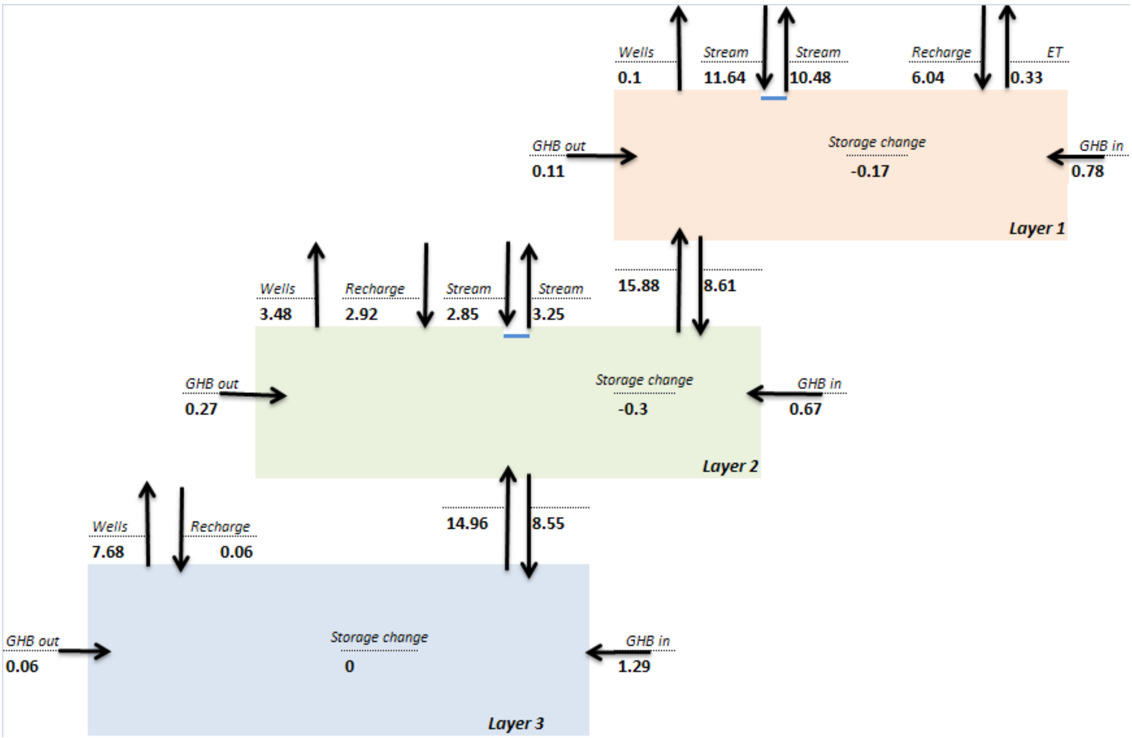

<u>*Scenario 1b*</u>

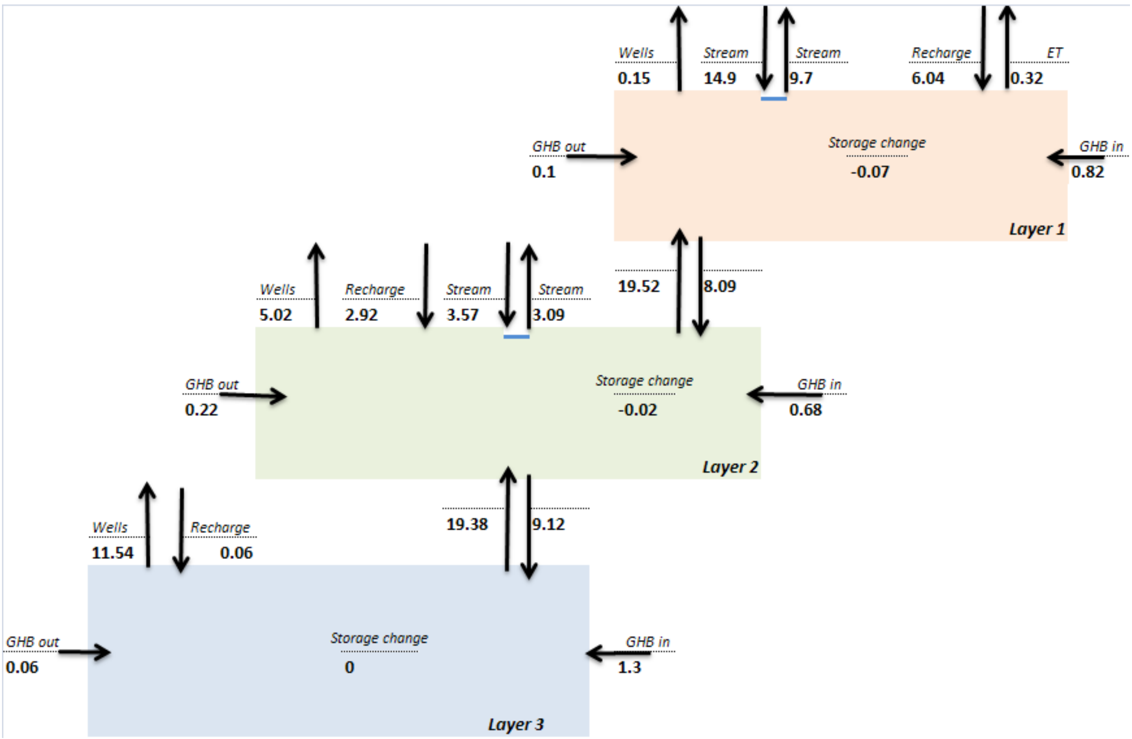

<u>*Scenario 1c*</u>

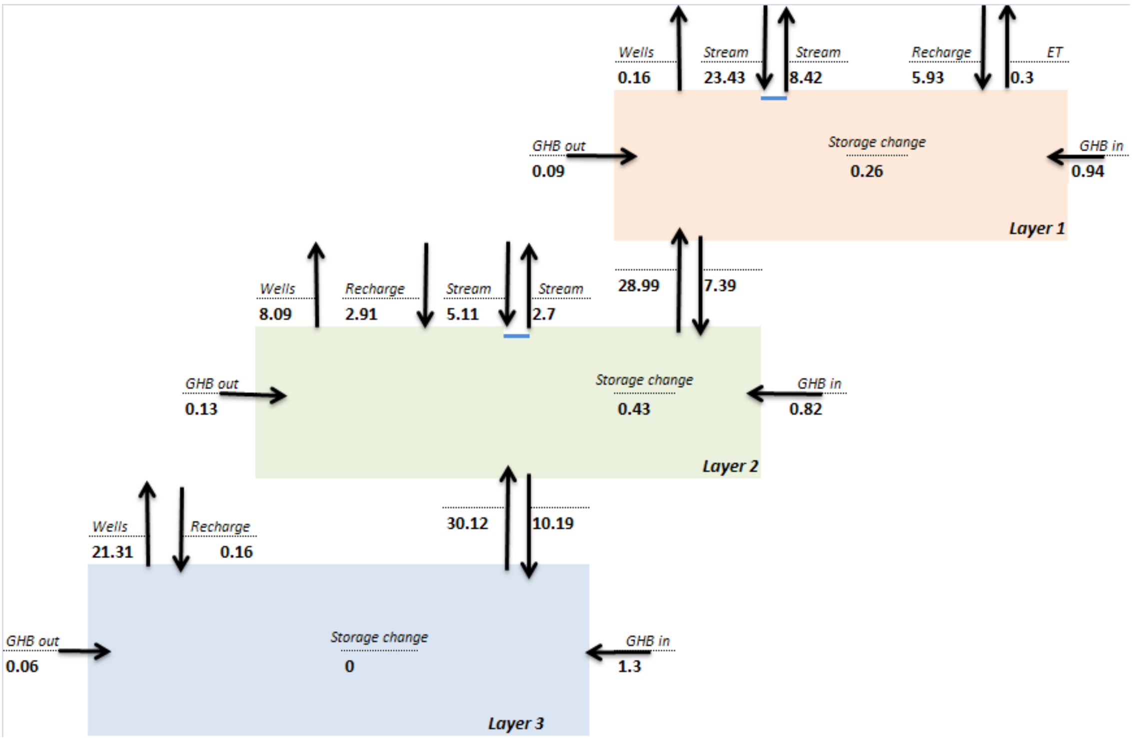

Scenario 1d

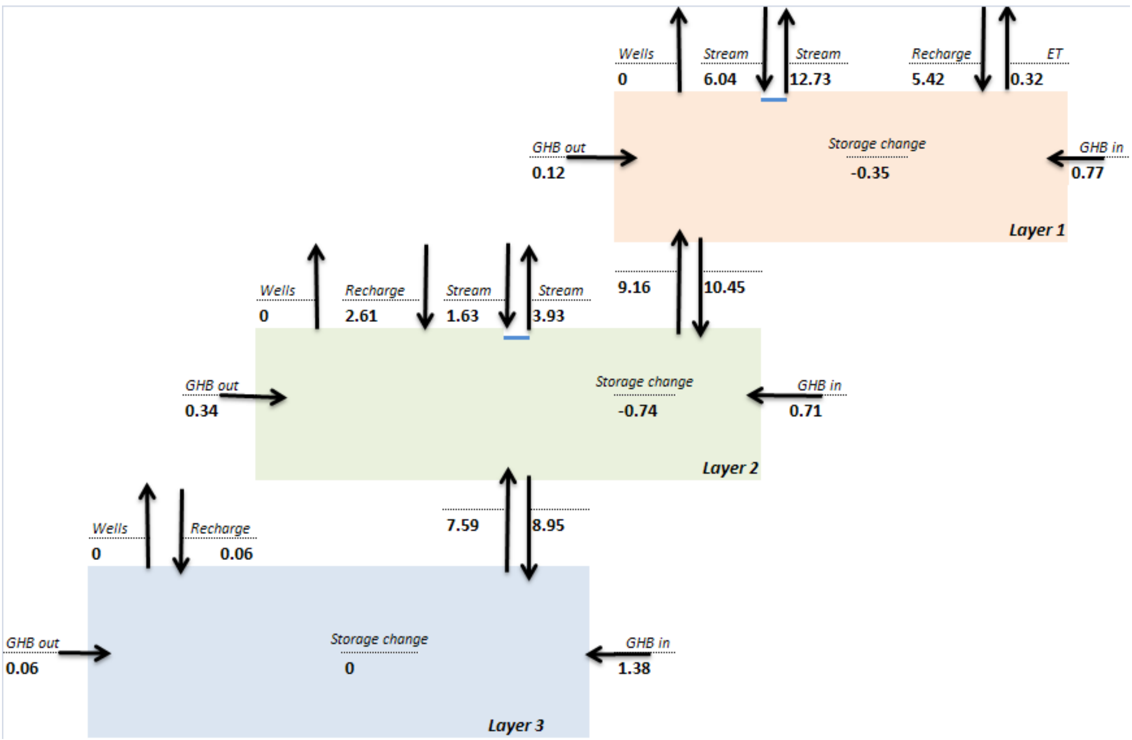

Scenario 2a

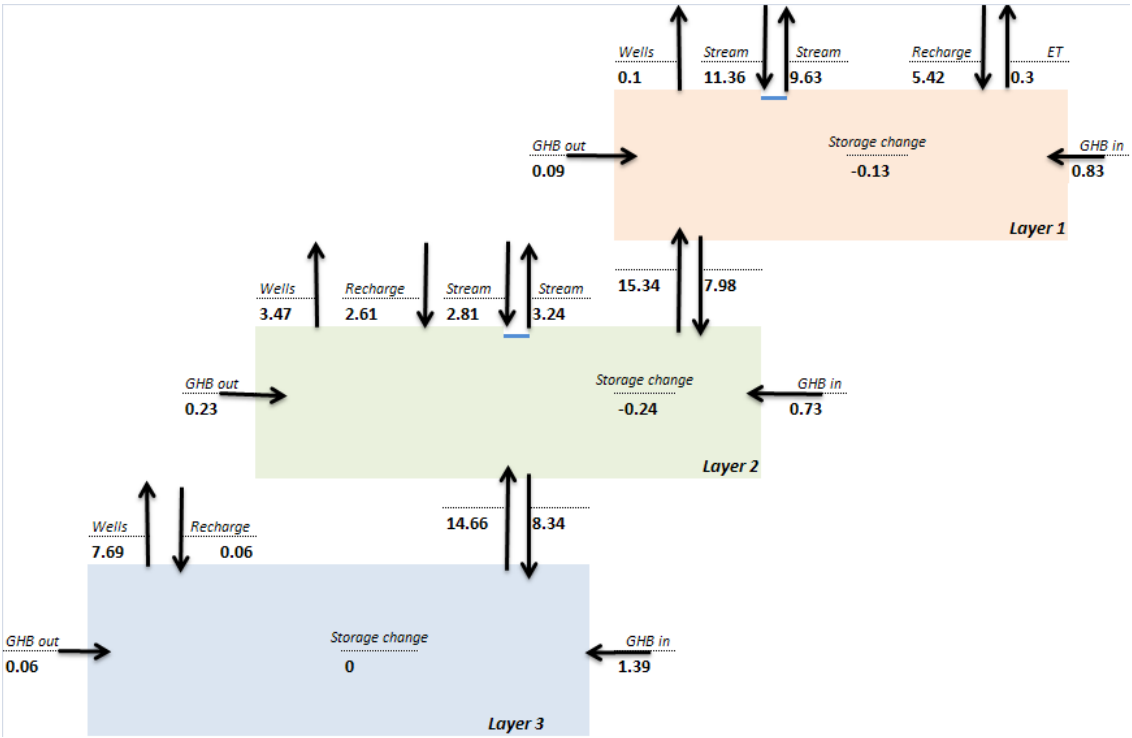

Scenario 2b

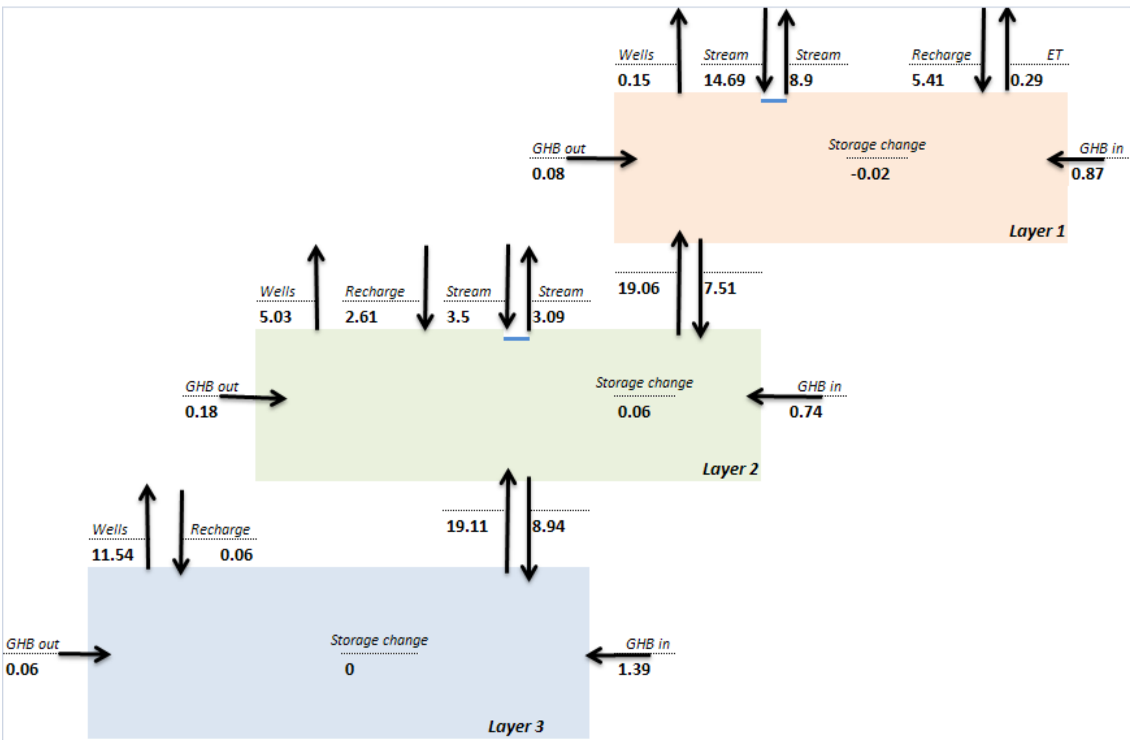

Scenario 2c

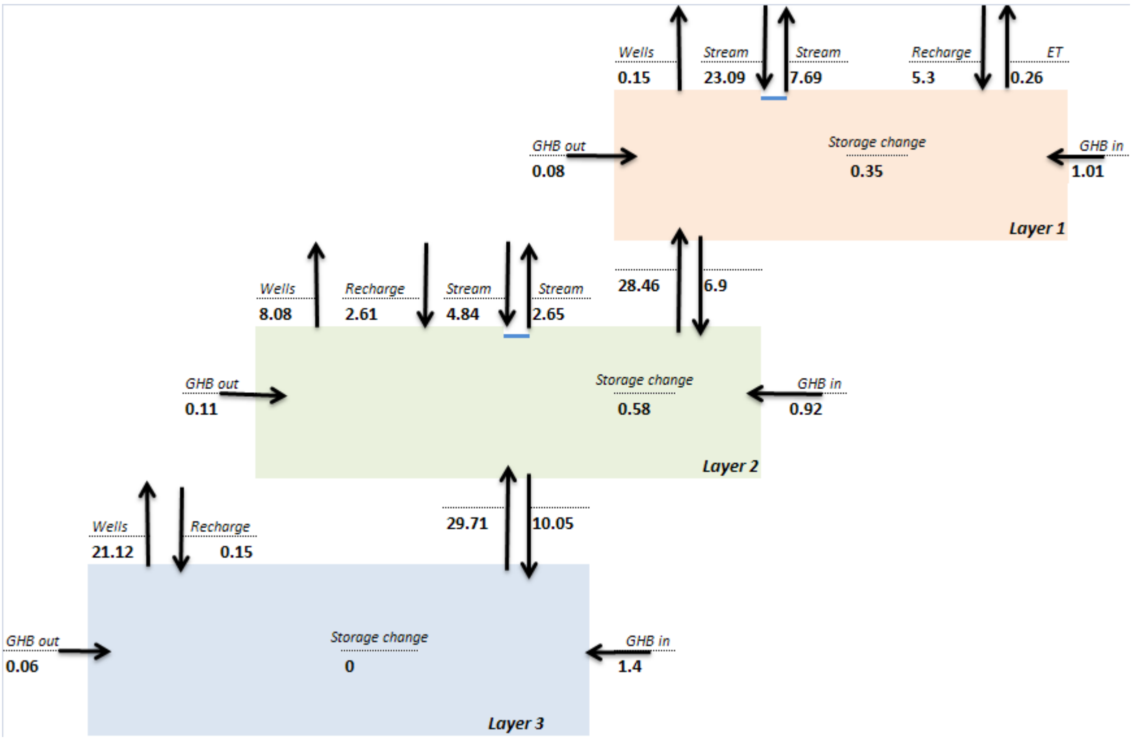

Scenario 2d

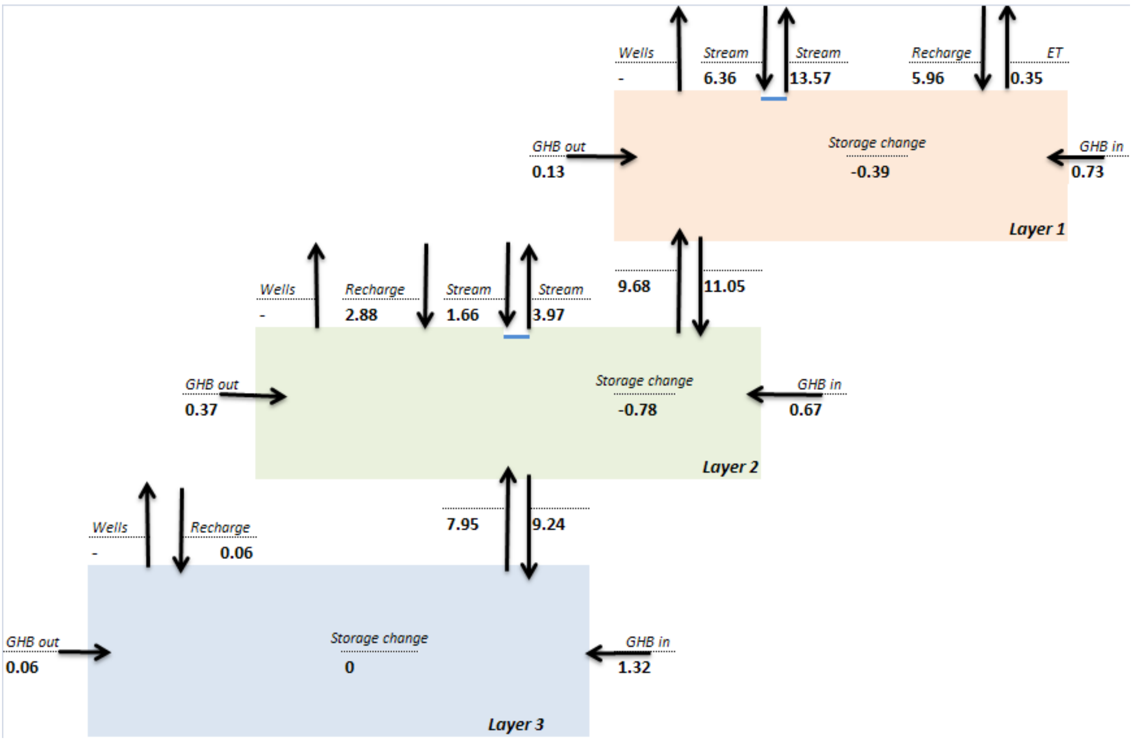

Scenario 3a

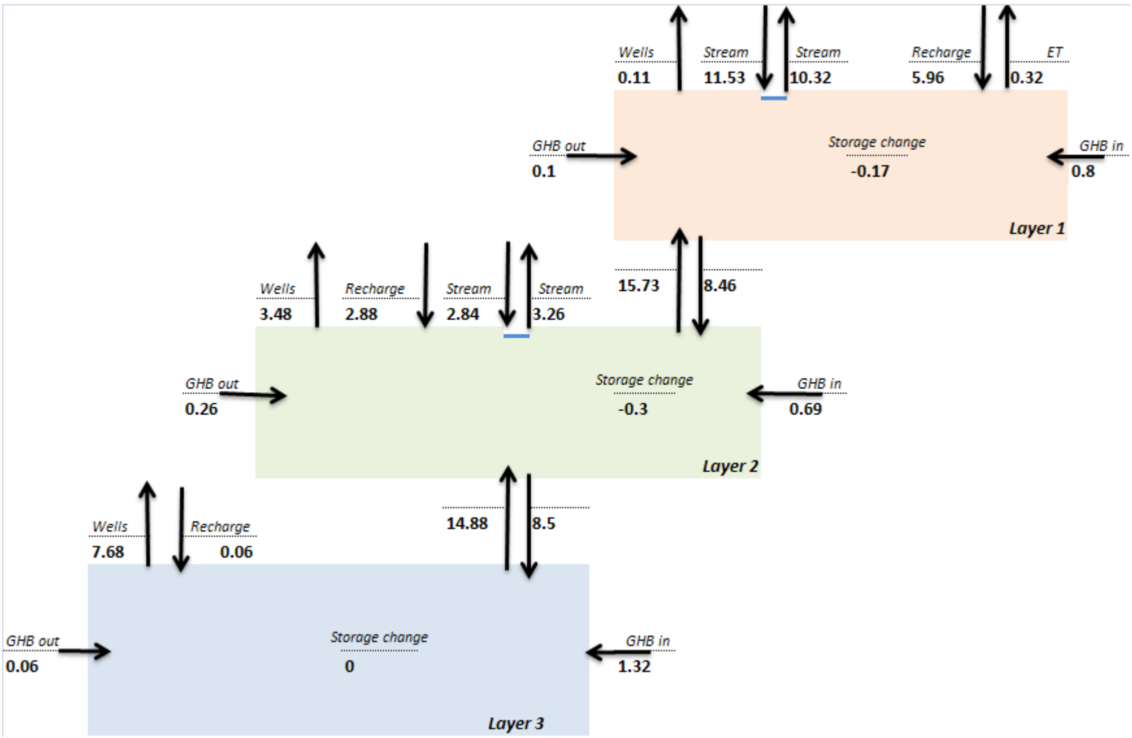

Scenario 3b

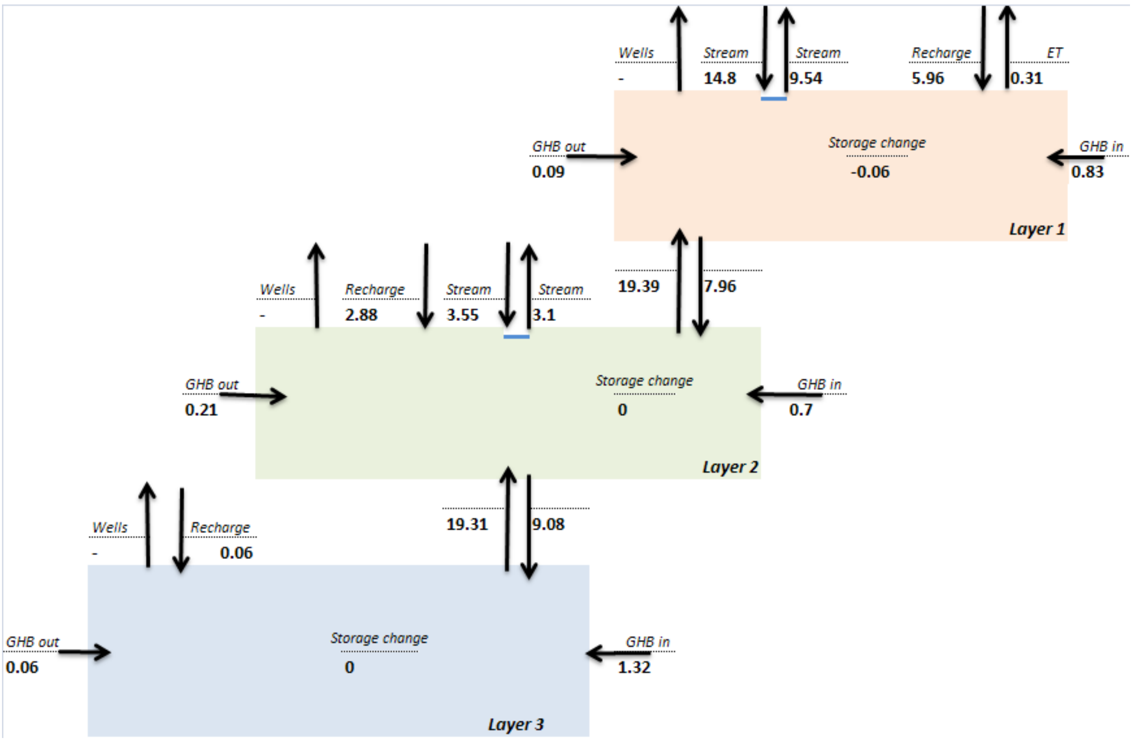

Scenario 3c

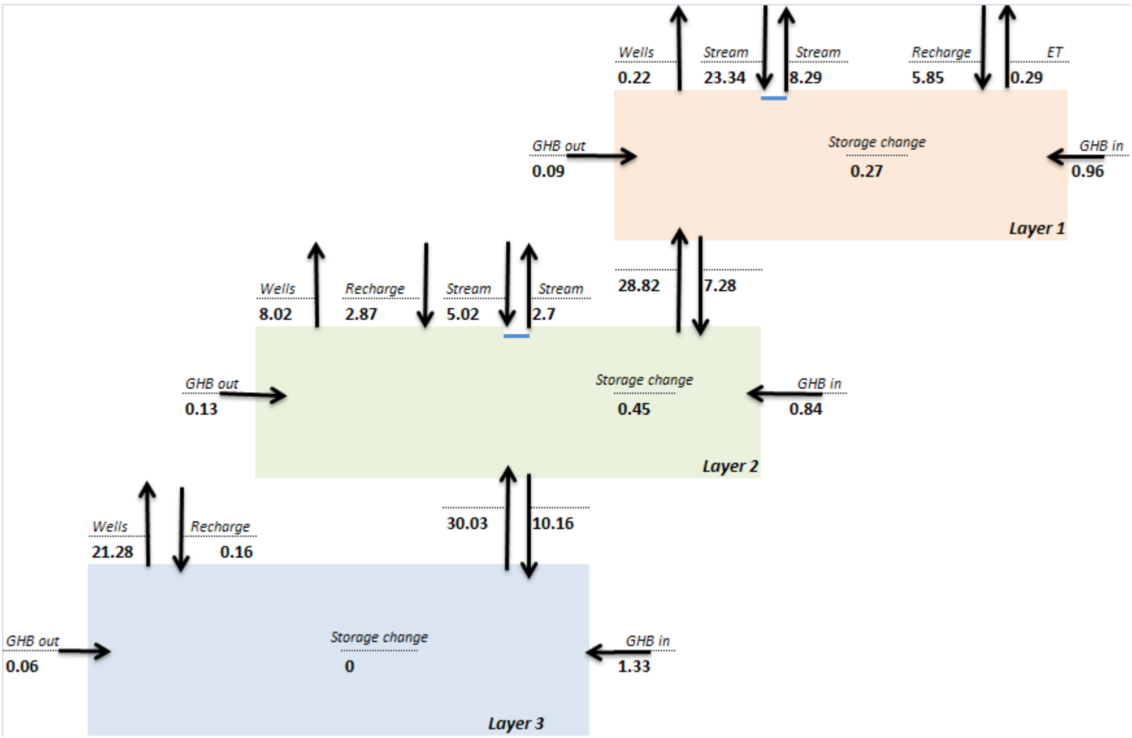

Scenario 3d

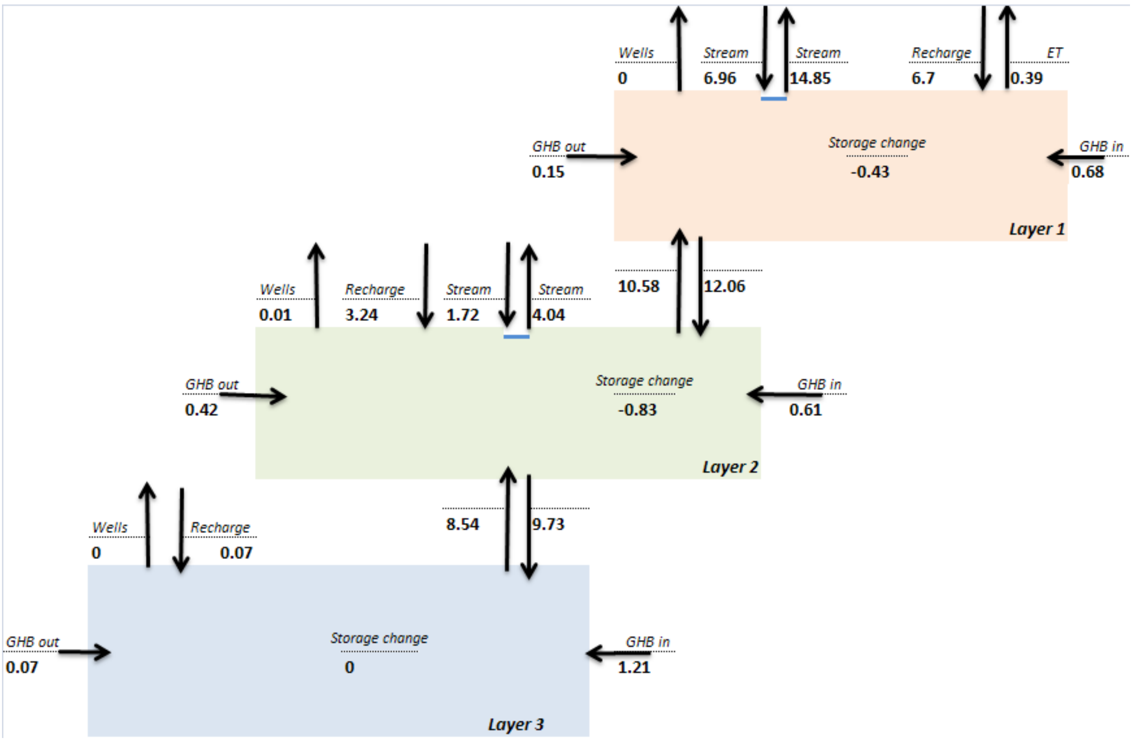

Scenario 4a

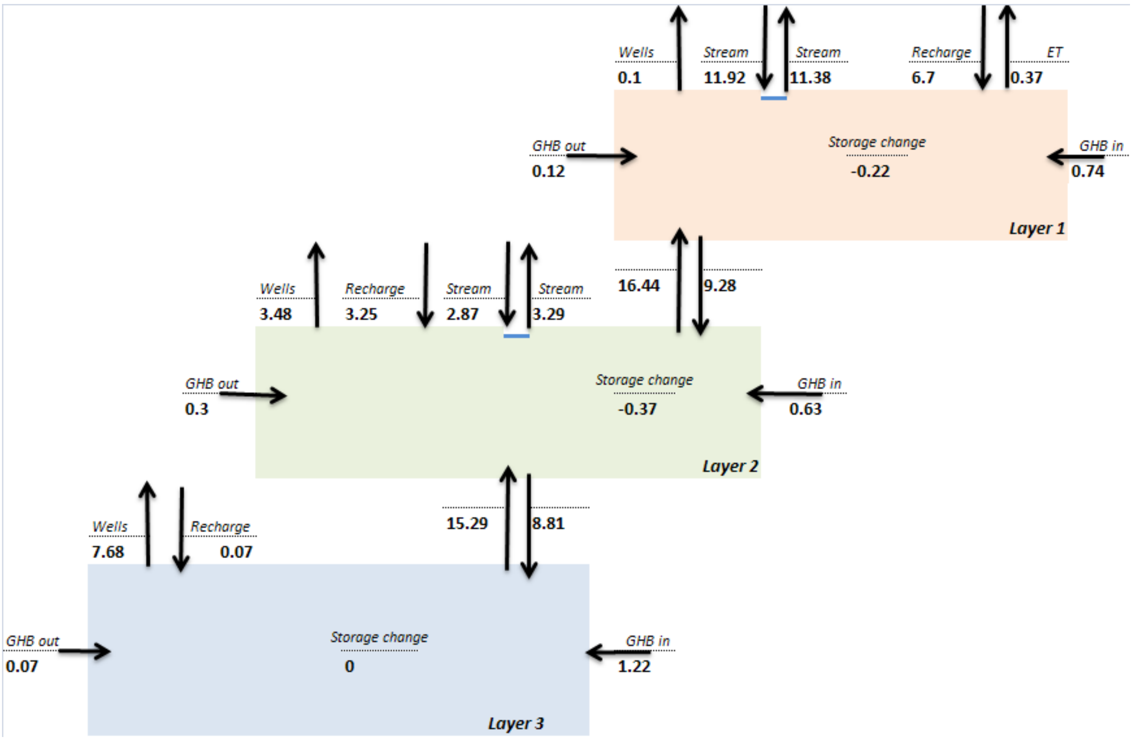

Scenario 4b

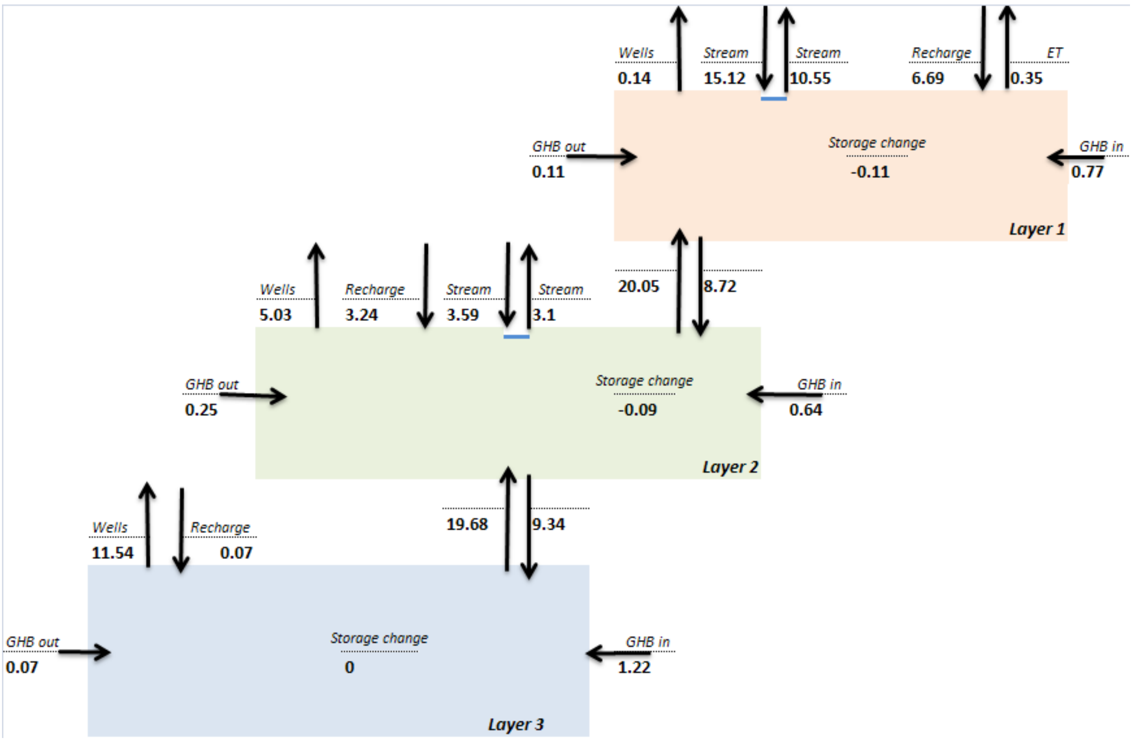

Scenario 4c

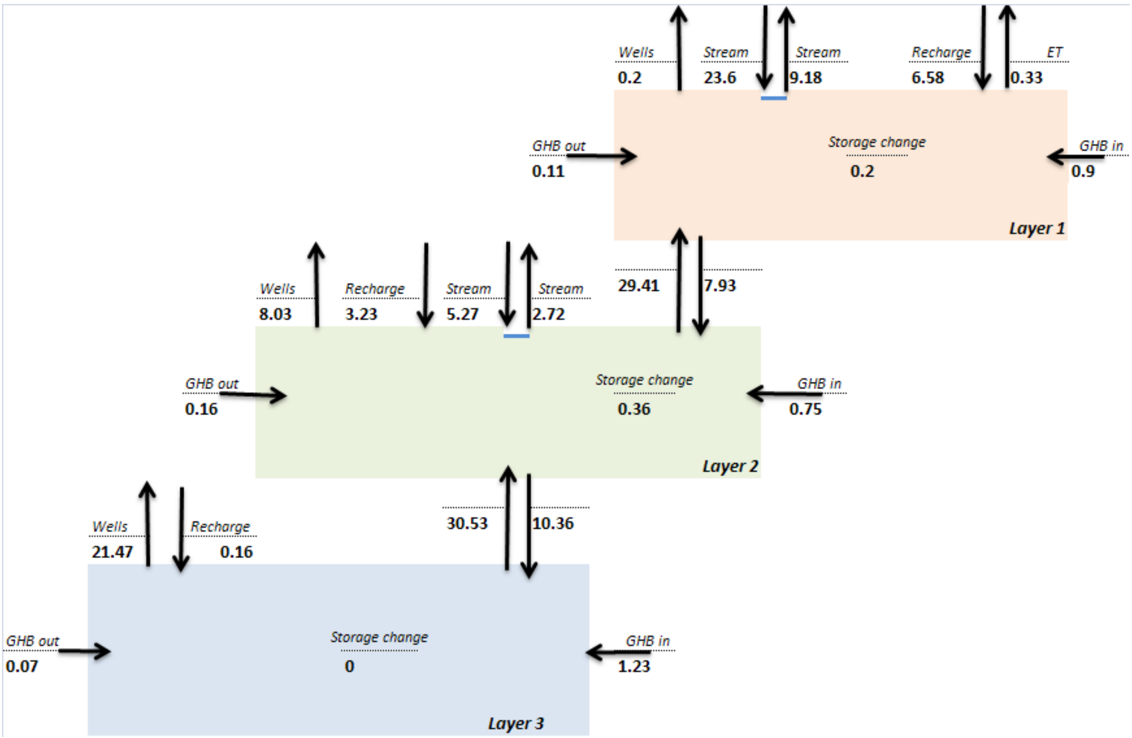
Wells
0.2
Stream
23.6
Stream
9.18
Recharge
6.58
ET
0.33
GHB out
0.11
Storage change
0.2
GHB in
0.9
Layer 1
29.41
7.93
Wells
8.03
Recharge
3.23
Stream
5.27
Stream
2.72
GHB out
0.16
Storage change
0.36
GHB in
0.75
Layer 2
30.53
10.36
Wells
21.47
Recharge
0.16
GHB out
0.07
Storage change
0
GHB in
1.23
Layer 3

Scenario 4d

Appendix F Climatic scenarios 2, 3 and 4 (declined with all pumping scenarios a, b, c, d)

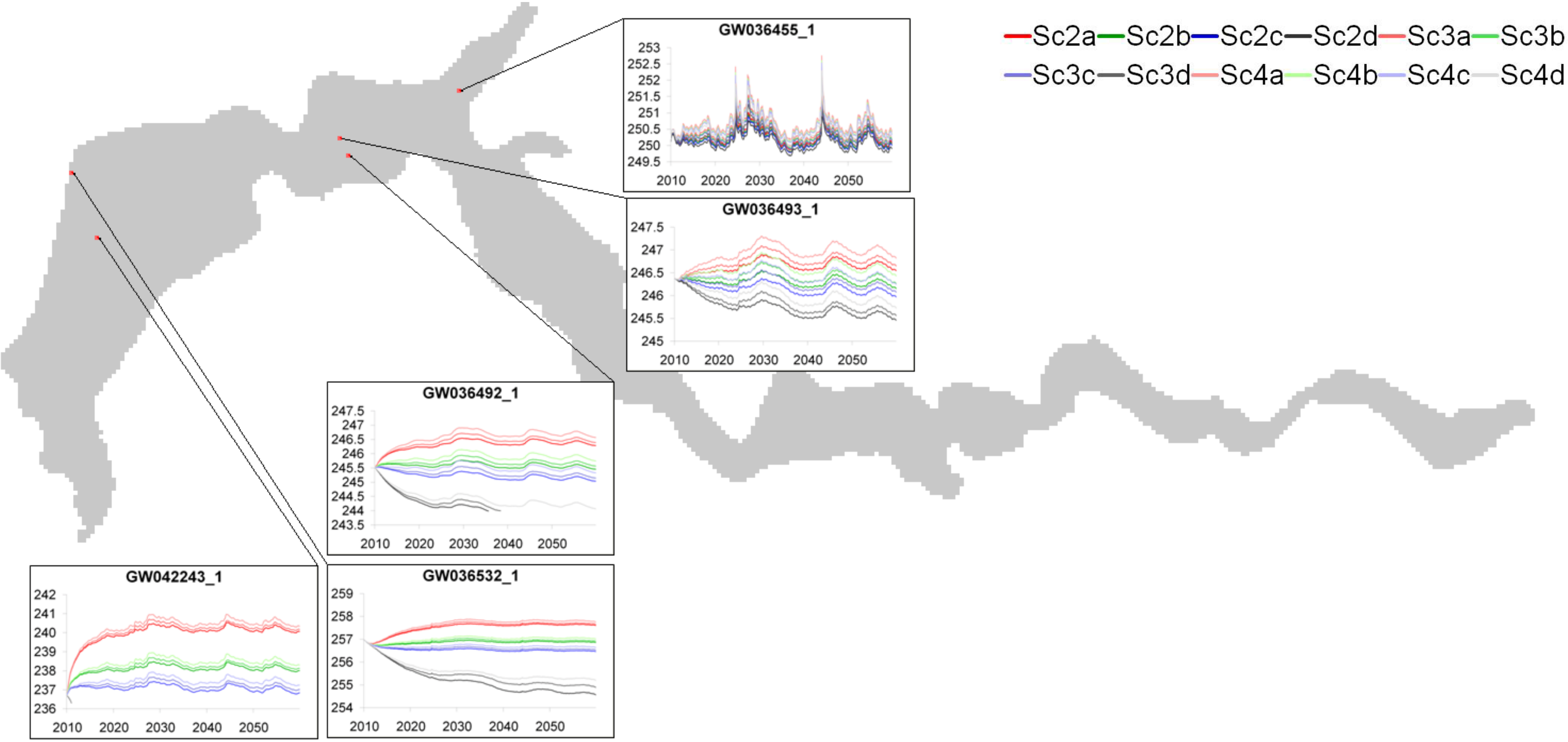

Figure 60 Hydrographs in layer 1 for scenario 2a to 3d

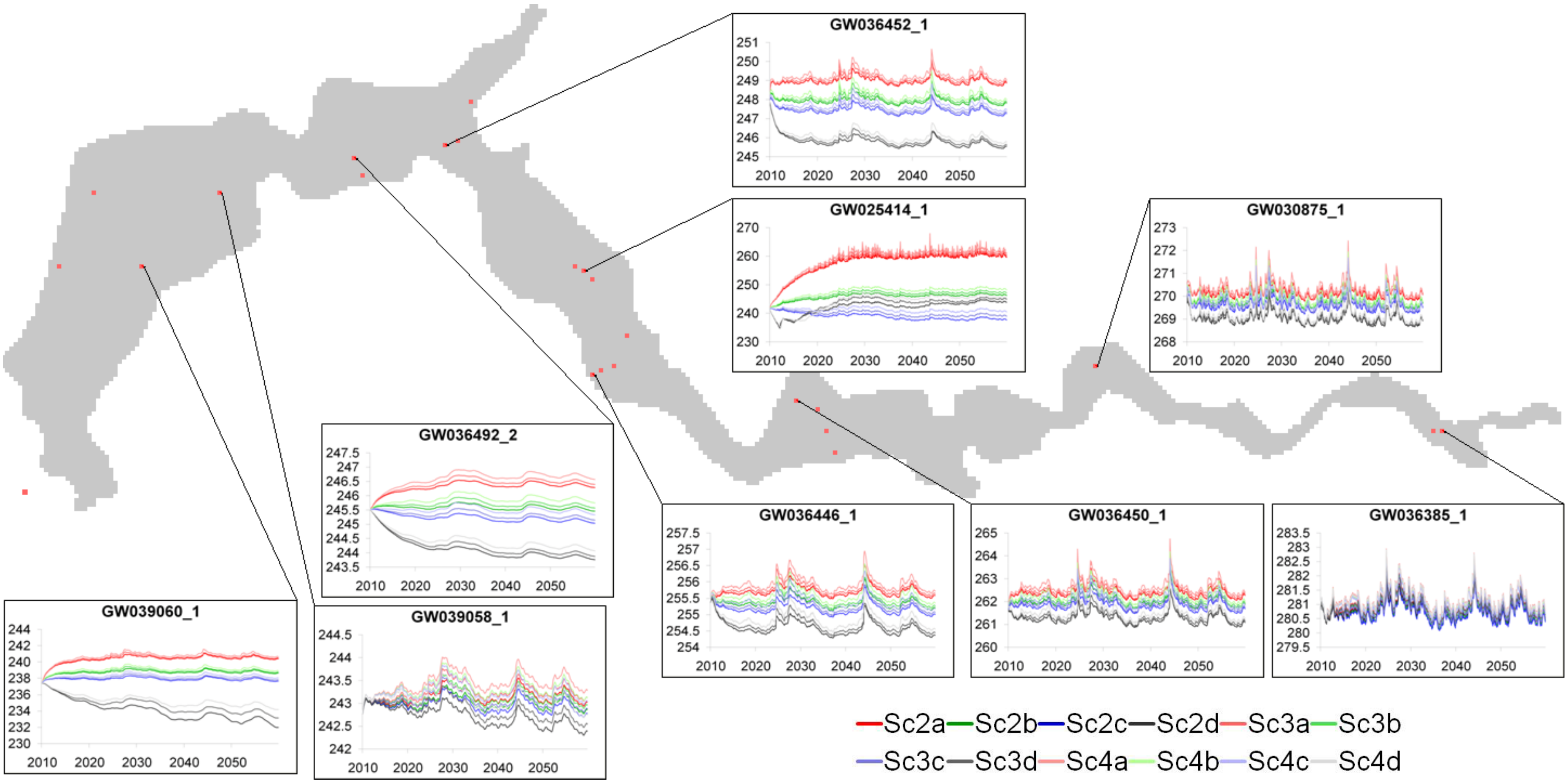

▪ **Figure 61 selection of representative Hydrographs in layer 2 for scenario 2a to 3d**

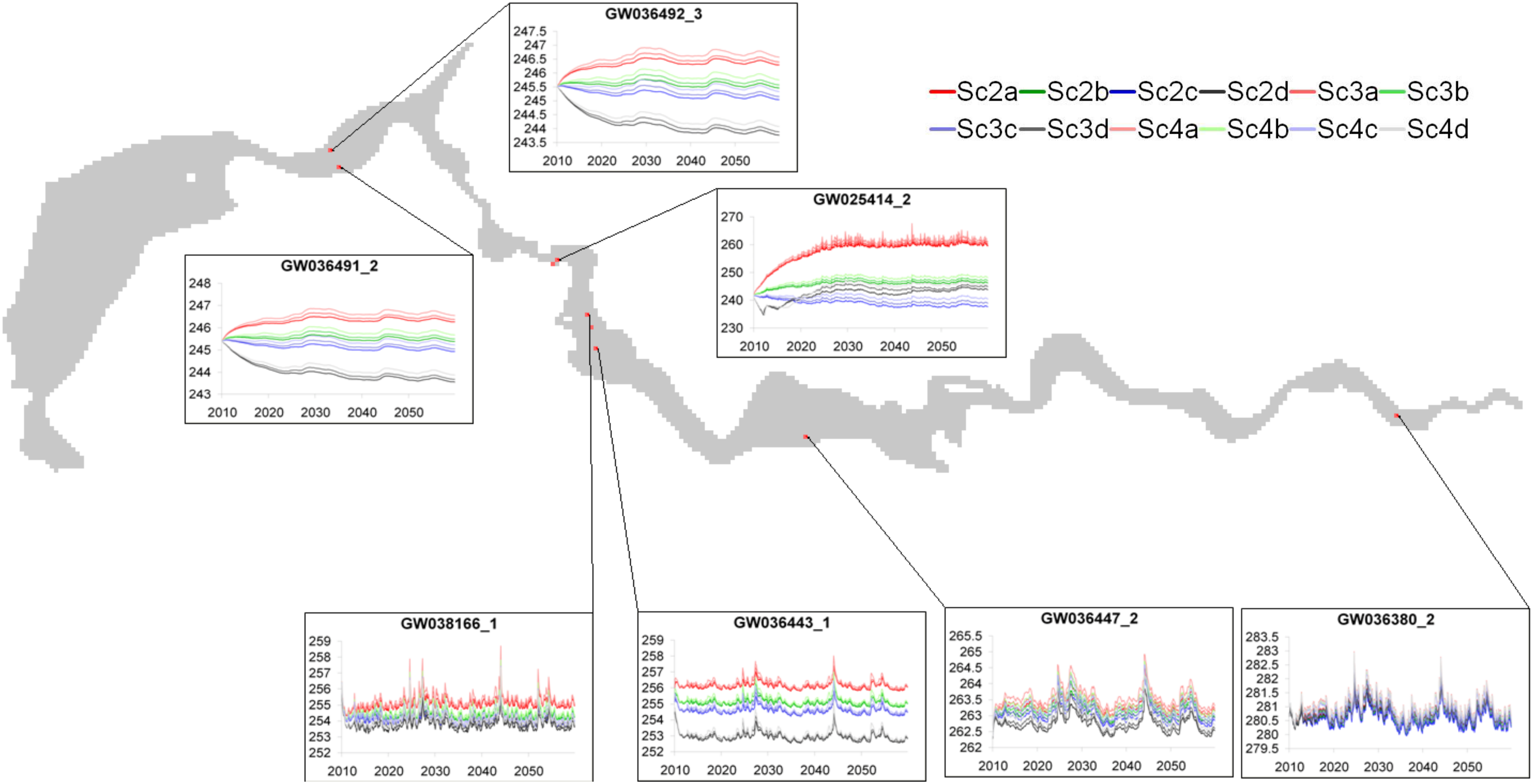

▪ **Figure 62 Hydrographs in layer 3 for scenario 2a to 3d**